University of Alberta

In vivo gene delivery with non-viral carriers

by

Laura Cary Rose

A thesis submitted to the Faculty of Graduate Studies and Research
in partial fulfillment of the requirements for the degree of

Doctor of Philosophy

in

Department of Biomedical Engineering

Spring 2014
Edmonton, Alberta

Abstract

Gene delivery is an emerging therapy for treatment of many different diseases and conditions, with the first therapy recently approved for clinical use. This thesis investigates non-viral carriers for gene delivery for bone regeneration, with an emphasis on the mechanisms of plasmid DNA (pDNA) delivery and methods to improve transfection. Polyethylenimine (PEI, 2 kDa) modified with linoleic acid (PEI-LA) was found to give transfection rates comparable to viral vectors both *in vitro* and *in vivo*. The PEI-LA/pDNA complexes were found to display a decreased transfection efficiency over time, but a gelatin coating was found to prevent this loss of transfection. The gelatin-coated particles also led to increased transfection *in vivo*, allowing lower doses of pDNA to be used. Finally, we developed a novel quantitative PCR (qPCR) method to detect pDNA bound in a polymer complex such that the pharmacokinetics could be investigated. The pDNA delivered without a polymeric carrier was degraded very rapidly, while pDNA from PEI and PEI-LA complexes were detectable for two and four weeks respectively. For polymeric complexes, the qPCR method was in good agreement with studies tracking fluorescently labelled pDNA. Similar to *in vitro* results, PEI complexes gave no gene expression while PEI-LA complexes gave gene expression for at least four weeks. Although no bone regeneration was observed following delivery of complexes, these studies provide crucial information on the non-viral gene delivery *in vivo*.

Acknowledgements

I would like to acknowledge funding by a Banting & Best doctoral research award from the Canadian Institutes of Health Research, the President's Prize of Distinction, a scholarship from Alberta Innovates Health Solutions (formerly Alberta Heritage Foundation for Medical Research), a Queen Elizabeth II master's level scholarhips, 75th Anniversary Faculty of Medicine & Dentistry scholarship, and trainee scholarships from the Skeletal Regenerative Medicine Team.

I also would like to acknowledge the contributions of co-authors in journal publications. Members of the Rancourt lab (Dr Derrick Rancourt, Dr Roman Krawetz, and Poh Lee) provided embryonic stem cell cultures and training for Chapter 3. Ross Fitzsimmons also assisted in this chapter by helping with RNA extractions. Cezary Kuckarski provided technical support with animal studies including animal care and anaesthesia for Chapters 4, 5, and 6. Dr Hamid Montazeri identified kinase targets to allow siRNA testing in Chapter 5, and Parvin Mahdipoor assisted with DNA and RNA extractions and loading qPCR plates for Chapter 6.

In addition to my co-authors, I would like to thank my lab mates and fellow researchers including Xiaoyue Lin and Cezary Kucharski for cell culture, Vanessa Incani and Guiling Wang for polymer synthesis, Charlie Hsu and Ross Fitzsimmons for plasmid construction, summer students Michael Leung and Michael Hogarth for binding and dissociation studies, high school

student Jocelyn Marsh for preliminary stability studies, Troy Locke for advice with qPCR of polymer-bound plasmid DNA, Dr Hamid Montazeri for help with phamarcokinetics studies, and of course partner-in-crime Breanne Landry for general mischief.

I would also like to thank Dr Hasan Uludag for his guidance and patience in the past five years; I appreciate the opportunity and support, and am grateful to have learned as much as I did. Finally, I would like to thank all my family and friends for their encouragement, entertainment, and enthusiasm.

Table of Contents

LIST OF TABLES

LIST OF FIGURES

CHAPTER 1

CHAPTER 3

CHAPTER 4

CHAPTER 4-Continued

CHAPTER 5

CHAPTER 6

APPENDICES

APPENDICES-Continued

LIST OF ABBREVIATIONS

Name	Abbreviation
Abundant in neuroepithelial area	ANA
Adeno-associated virus	AAV
Adenovirus	AV
Alkaline phosphatase	ALP
Analysis of variance	ANOVA
Basic fibroblast growth factor	bFGF
Beta-glycerol phosphate	B-GFP
Bone marrow stromal cell	BMSC
Bone morphogenetic proteins	BMP
Bone morphogenetic protein receptor	BMPR
C-X-C chemokine receptor type 4	CXCR4
Calcium/phosphate	CaP
Casein kinase-2 interacting protein-1	Plekho1
Complimentary DNA	cDNA
Connexin 43	Cx43
Constitutively active form of activin receptor-like kinase 6	caALK6
Core binding factor alpha1 subunit protein	Cbfa1
Cycle threshold	C_T
Cytosine-guanine dinucleotides	CpG
Deoxyribonucleic acid	DNA
Dexamethasone	DEX
Dickkopf-related protein 1	DKK1
3-(4,5-dimethylthiazol-2-yl)-2,5-diphenyltetrazolium bromide	MTT
Dioleoyl trimethylammonium propane	DOTAP
Dulbecco's Modified Eagle's Media	DMEM
Embryoid body	EB
Embryonic stem cell	ES cell
Enzyme-linked immunosorbant assay	ELISA
Extracellular signal regulated kinases	ERK
Fetal bovine serum	FBS
Fibroblast growth factor	FGF
Fibroblast growth factor receptor	FGFR
Focal adhesion kinase	FAK
Forkhead box protein O1	FoxO1
Four and half lim protein-2	FHL2
Glyceraldehye 3-phosphate dehydrogenase	GAPDH
Green fluorescent protein	GFP
Guanine nucleotide-binding protein alpha	GNAS1
Hank's balanced salt solution	HBSS

Histonedeacetylase 5	HDAC5
Homeobox-containing protein C8	HOXC8
Human embryonic stem cells	hES
Human foreskin fibroblasts	HFF
Human parathyroid hormone 1-34	hPTH1-34
Hydroxyapatite	HA
Insulin-like growth factor	IGF
Interleukin-2	IL-2
Interleukin-6	IL-6
Internal Standard	IS
Intramuscular	IM
Janus kinase-signal transducer and activator	JAK/STAT
Kinesin spindle protein	KSP
Leukemia inhibitory factor	LIF
LIM mineralization protein	LMP
Linear PEI	l-PEI
Linoleic acid	LA
Mesenchymal stem cell	MSC
Messenger RNA	mRNA
Micro RNA	miRNA
Moloney murine leukemia virus	M-MLV
Mouse embryonic fibroblasts	MEF
Mouse embryonic bodies	mEB
Mouse embryonic stem cells	mES
NEL-like 1	Nell1
Oligonucleotides	ODN
Osteocalcin	OCN
Osteogenic Protein-1	OP-1
p-nitrophenol phosphate	p-NPP
Pachyonychia congenita	PC
Peroxisome proliferator-activated receptor gamma	PPARϒ
Phenylmethanesulphonylfluoride	PMSF
Phycoerythrin	PE
Plaque-forming units	PFU
Plasmid DNA	pDNA
Platelet-derived growth factor (PDGF)	PDGF
Polyethyleneglycol	PEG
Polyethyleneglycol-aspartate-diethylenetriamine	PEG-b-(Asp-[DET])
Polyethylenimine	PEI
Poly(lactic-co-glycolic acid)	PLGA
Poly(propylene fumarate)	PFF
Prolyl hydroxylase domain-containing protein 2	PDH2
Protein related to DNA and cerberus	PRDC
Retrovirus	RV

Rho and Rho-associated protein kinase	ROCK
Ribonucleic acid	RNA
RNA integrity number	RIN
RNA interference	RNAi
Runt-related transcription factor 2	Runx2
Severe combined immunodeficiency	SCID
Signal transducer and activator of transcription 3	STAT3
Small interfering RNA	siRNA
Stage-specific embryonic antigen-1	SSEA-1
Standard deviation	SD
Sodium Chloride	NaCl
Subcutaneous	SC
Transforming growth factor beta	TGF- β
Triacrylate/amine polycationic polymer	TAPP
Tumor necrosis factor-alpha	TNF-α
Vascular endothelial growth factor	VEGF

1 Realizing the potential of gene-based molecular therapies in bone repair

New medicines and delivery strategies

A version this chapter was published in: L Rose, H Uludag. Journal of Bone and Mineral Research 2013;28(11):2245-62.

1.1 CLINICAL NEED FOR NEW BONE REGENERATION STRATEGIES

Up to 20% of fractures are hampered by impaired healing that requires additional intervention [162]. Nearly 2.2 million bone grafts are performed worldwide on an annual basis [51]. The economic impact of non-unions is enormous, with the cost of spinal fusions alone reaching $20 billion annually [131]. The gold standard for repair of large segmental defects remains autologous grafts. Here, bone is harvested from a non-weight bearing site, usually the iliac crest, and used to repair the defect. Bone grafts, however, are limited in several aspects, including potency of the grafts and the physiological detriment due to harvest surgery. Harvesting bone from a second site not only increases the surgical duration and risk of infection, but also compromises the integrity of harvest site, while there is no guarantee of sufficient bone quality or quantity. Allografts are alternatively employed, where donor tissue is used to repair the defect, but the risk of disease transmission is always a concern. Allografts are extensively processed to reduce this risk, but osteopotency of the graft could be decreased in this way as well. The American Association of Tissue Banks is working to develop standard protocols for harvest and sterilization process, but quality of grafts remains variable [30]. Demineralized bone matrix derived from decalcified bone can similarly act as a substitute, but its potency is variable and depends on the processing conditions.

Osteogenic proteins are frequently employed to render osteoconductive biomaterials, such as hydroxyapatite or collagen,

osteoinductive, and successfully turn these implants into *de novo* inducers bone formation. The most widely employed proteins are the Bone Morphogenetic Protein (BMPs). First discovered by Marshall Urist, BMPs are mophogens that can induce ectopic bone formation by causing stem cells to differentiate into osteoblasts [158], but can also act as a chemotactic agent to recruit cells at femtomolar concentrations [45]. Because of their potent bone induction properties, BMP-7 (also known as Osteogenic Protein-1, OP-1) has been approved for Humanitarian Device Exemption for spinal fusions and BMP-2 has been approved for clinical use in select indications, including spinal fusions, oral/maxillofacial applications, and orthopaedic trauma [53,107]. In these therapies, collagenous materials are loaded with BMP-2 (INFUSE® Bone Graft) or BMP-7 (OP-1® Bone Grafts) and implanted to induce local bone formation, where the outcomes were found to be comparable to those of autologous bone graft. Despite the initial success rate, protein therapies have not become a common place in part due to the expense of large amount of BMPs needed in these implants. Recent studies have raised safety concerns with protein therapies [20,22,34], including osteolysis, ectopic bone growth, wound complications, and urogenital events [22]. The full extent and frequency of complications associated with rhBMPs is still under investigation. The reasons for this are currently unclear, but may be associated with the exceedingly high protein concentrations required to maintain a therapeutic response in light of fast clearance and short half-life of recombinant proteins *in vivo*. Approximately 1.5 mg/cc of BMP-2 [107] or

0.9 mg/cc of OP-1 [47] are required for treatment, both of which are much higher than ~ng/mL levels of endogenous proteins in bone. Extended release formulations are being explored to overcome these barriers [175], but development of alternative approaches is critical to stimulate local bone regeneration.

Regeneration strategies have sought to restore osteogenic activity at the injury site by replacing or augmenting one or more constituents, typically in the framework of fracture repair [106]. The platelets at the fracture site release proteins such as platelet-derived growth factor (PDGF), transforming growth factor-β (TGF β) proteins including BMPs, insulin-like growth factor (IGF), vascular endothelial growth factor (VEGF), and fibroblast growth factors (FGF) [8,18,84,143,157] to recruit inflammatory cells, fibroblasts, mesenchymal stem cells and pre-osteoblasts for repair initiation. These cells lay down connective tissue to form a soft callus with extensive blood vessels, which hardens either through endochondral ossification, where a cartilage template calcifies, or through intramembranous ossification where osteoblasts lay down new bone tissue directly. The hard callus will undergo further remodelling to strengthen the deposited bone and establish the physiological contours. Failure at any point during this complex process will result in non-union. The complex and intertwined signalling events guiding bone formation are executed by many different proteins, many of which are investigated for bone regeneration [77]. Synthetic scaffolds have been used to provide a hospitable environment for new bone formation. Scaffolds have

been constructed from collagen and hydroxyapatite (HA), the main organic and inorganic component of bone, respectively. Such scaffolds, however, are incapable of inducing osteogenesis on their own, and require osteogenic proteins to make them osteoinductive [1]. This limits successful use of osteoconductive scaffolds to smaller defects where extensive regeneration is not required and minimal mechanical support is needed. Cell-based therapies have been explored where osteogenic cell lineages are transplanted, usually on a biomaterial scaffold, to induce bone formation. The transplanted cells can deposit an extra-cellular matrix directly and secrete the growth factors needed to further recruit cells to the site. Mesenchymal stem cells have been extensively studied for this purpose because of both their wide differentiation potential and long life-span, as well as their ability to home to bone marrow [112]. Even cell-based therapies, however, are not always robust enough with native cells and cells need to be frequently genetically modified to express osteogenic factors for improved potency. Cells can be transduced using viruses or transfected with non-viral methods to express therapeutic genes, thereby serving as delivery agents.

Cell-based therapies for bone regeneration are hindered by several drawbacks. The patient's own cells would be the most favourable option to circumvent any potential immune response. The expansion of host cells, however, would greatly increase the cost of the therapy. The long culture period required to obtain the number of cells for success would inevitably delay the treatment. Equally undesirable is the decrease in differentiation

and proliferative potential of cells during the long culture period [79], which can lead to drastic decreases in the amount of *in vivo* bone formation after transplantation [12]. For these reasons, reprogramming or trans-differentiating host cells directly at the local site is appealing for functional bone regeneration [72]. It is possible to achieve cellular transformation by manipulating genetic networks, where transforming agents are coded from exogenous DNAs or regulatory pathways are altered for a desired cellular transformation. This approach bypasses the need to produce large amounts of recombinant protein in an industrial setting, as well as eliminating the issues complicating cellular harvest, expansion and transplantation.

1.2 POSSIBILITY OF CLINICAL THERAPIES BASED ON GENETIC ELEMENTS

Both positive and negative regulation of gene expression has been explored as the basis of a therapeutic modality (***Figure 1-1***). Positive gene expression involves introduction of DNA coding for a therapeutic gene and *in situ* expression of proteins by host cells to by-pass the need for recombinant protein administration. This type of gene delivery has proven especially promising for monogenic disorders such as haemophilia, where replacement of clotting factor is required regularly to prevent spontaneous bleeding. Adeno-associated viruses delivering human factor IX, for example, were recently found to be effective in either decreasing or obviating the need for

protein injections for at least 6-16 months [119]. Particularly in light of safety concerns with high-dose protein therapies, gene delivery has been proposed to deliver proteins at more physiological levels [43,82]. Gene therapy is particularly amenable to bone regeneration because of the fact that a single gene, such as tissue-inducing BMPs, could induce a functional bone tissue. Genetic elements can also be employed to negatively regulate expression of proteins that inhibit osteogenesis. RNAs that prevent translation by RNA interference (RNAi) mechanism can silence specific protein expression. The specificity of protein knockdown allows treatment of diseases previously lacking any therapy, such as the inherited disorder pachyonychia congenita (PC) [89]. A recent clinical trial used short interfering RNA (siRNA) against a mutant form of keratin that causes calluses, which greatly limit patient's mobility. Injection of siRNA led to a decrease in the calluses, compared to a vehicle control, providing evidence for RNAi based approaches to modulate composition of tissues in a clinical setting. The dose of siRNA in each injection ranged from 0.1 to 17 mg, which is not an exuberant amount for clinical use. RNAi can be implemented with either exogenous agents, such as siRNA and oligonucleotides (ODN), or directly implemented by a plasmid for endogenous processing. Although RNAi-mediated therapies for bone regeneration are still at an early research stage, they hold untapped promise for their ability to inhibit specific pathways, as well as avoiding off-target effects that plague small molecule

inhibitors. With recent identification of proteins that impede bone formation, the scope of RNAi-based therapies is bound to increase in the future.

The current challenge in bringing a gene-based therapy to a clinical trial remains the safe and effective delivery of nucleic acids. Viruses have served well in preclinical models to demonstrate the feasibility of specific gene-based therapies, where a range of potential agents was shown to be capable to achieving bone repair (***Table 1***). Viruses, however, are associated with risk of immune response, inflammation, and insertional mutagenesis [156], which were evident even in some pre-clinical studies [75]. Since there are only a handful of effective non-viral carriers, use of viruses continues to dominate clinical attempts of gene delivery. As of 2012, 67% of all gene therapy trials used viral carriers, with nearly 20% employing retroviruses [50], and these numbers have not changed significantly in recent years [37,38]. Even though there are currently no approved gene delivery therapies for osteogenesis in clinical use, the promise of gene delivery has stimulated extensive explorations of various delivery approaches, in particular development of safer non-viral carriers in light of safety concerns associated with viruses.

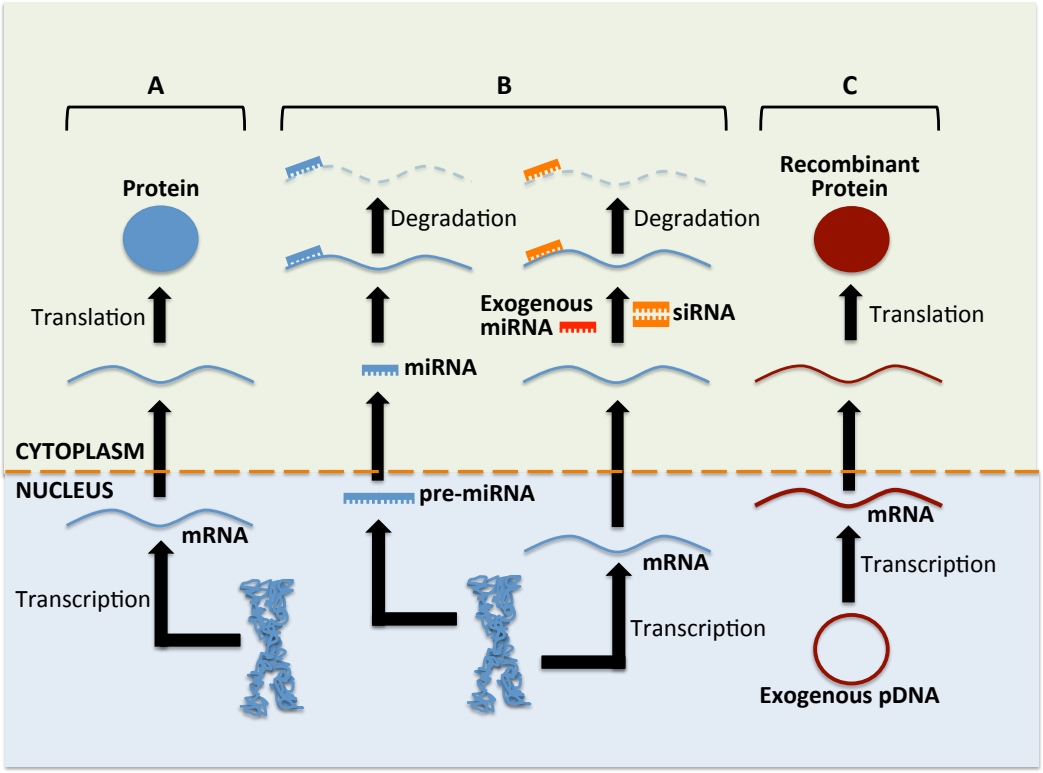

Figure 1-1: Schematic of gene-based therapies. The central dogma of molecular biology is shown in pathway **A**, where DNA is transcribed into mRNA in the nucleus and proteins are translated from mRNA in the cytoplasm. Pathway **B** shows regulation of protein translation through RNAi. Endogenous miRNA, exogenous miRNA, or synthetic siRNAs can bind mRNA and induce degradation of mRNA, which can be employed to target inhibitors of osteogenesis. Pathway **C** shows production of recombinant proteins, where exogenous DNA introduced into cells is employed to produce recombinant proteins capable of stimulating osteogenesis.

1.3 pDNA DELIVERY FOR BONE INDUCTION AND FUNCTIONAL OUTCOMES

While viral delivery has established the feasibility of gene delivery for bone repair (***Table 1-1, Figure 1-2***, Kimelman-Bleich et al [82]), a close inspection of the studies have raised questions about the actual effectiveness of viral delivery in a realistic setting. A particular issue is the impact of immune status of the animals on the outcome of therapy. Many viral carriers employed to induce bone formation show an attenuated response [5] or are ineffective in animals with intact immune systems [6,70,74,93,94,123-125,149]. Immunosuppression of normal animals can restore the efficacy of viral therapy [73], but this would be undesirable (perhaps unacceptable) in a clinical setting. The impact of immune response may depend on animal model, virus type, or the transgene employed, since there are reports of successful bone induction in both immune-competent and immune-compromised animals [70,74,93-95,159]. Even if a suitable combination of carrier and transgene could be found, clinical risks of viral gene delivery have to be mitigated; non-integrating, short-acting viral expression systems (such as adenoviral vectors) might be preferable over integrating, long-acting vectors in this regard. Only a handful of studies employed 'integrating' viruses to-date (***Table 1***), which recognizes the preference of practitioners in the field. Non-viral methods, including use of naked pDNA and physical delivery methods, may alternatively be more appealing to induce bone repair since the simpler mechanism of delivery may reduce long-term

complications of the intervention. A summary of preclinical studies on non-viral pDNA delivery is included in ***Figure 1-3***, with study details outlined in ***Table 2***.

Gene	Site	Carrier	Outcome
BMP2	Ectopic	AV	Gene delivery to quadriceps led to bone in athymic mice [93] but not in normal immunocompetent mice [74]
			Bone formation in calf muscle of rats only with immunosuppression [73]
			AV delivered in a collagen sponge to calf muscle led to bone in immunocompetent rats, but not when AV particles were injected without the sponge [149]
			Bone formation in the calf muscle of rats was observed only with immunosuppression [123-125]
			Bone induction in quadriceps was stronger in athymic nude rats compared to immunocompetent rats [5]
			AV delivery to soleus muscle of rats resulted in bone only when ischemic degeneration was induced via muscle grafting. Bone was not observed without grafting [52]
		AAV	Bone induction via endochondral ossification was observed in hindlimb muscle of immunocompetent rats [26,27]
			Viral particles delivered on hydroxyapatite scaffold to the back muscles of immunocompetent rats led to bone formation [118]
			Bone formation in thigh muscle after delivery of a tetracycline-sensitive expression system was observed in mice only when a tetracycline analogue was administered [48]
	Orthotopic	AV	Increased regeneration in a mandibular distraction osteogenesis model in rats [10]
			Increased bone regeneration in an osteoporotic fracture model in tibia of sheep [39]
			Bone formation or increased regeneration was observed in several defect models, including a critical-sized mandibular defect [6], critical-sized nasal defect in athymic nude mice [99], rib defect in horses [68], metatarsal defect in horses [67], and femoral critical-sized defect in rats [13]
			Injected AVs led to partial regeneration of a critical-size calvarial defects in rats, with a more vigorous response when particles were delivered in a gelatin scaffold [61]
			Healing of iliac crest critical-size defects in sheep was delayed compared to no treatment when viral particles were injected to injury site [40]
			Bone formation was observed in a dental model in immunocompetent dogs [103]
			Enhanced cartilage and subchondral bone was observed in femur condyle defect in immunocompetent ponies [110]

			Delaying administration of viral particles improved healing of femur critical-sized defects in rats [14]
		AAV	Bone formation in femur defects in immunocompromised rats, but addition of human mesenchymal stem cells did not improve the outcome [36]
BMP4	Ectopic	AV	Bone induction in hindlimb muscle [25], calf muscle [70], and quadriceps [74] of athymic nude rats
			Bone formation in the thigh muscle was observed in athymic nude rats, but not in immunocompetent rats [93]
	Ectopic	AAV	Bone formation in hindlimb muscle of immunocompetent rats [102]
	Orthotopic	AV	Enhanced bone formation around implants in femur defects in ovariectomized rabbits [88]
		RV	Increased callus size and enhanced healing in a femur fracture model in immunocompetent rats [138]
BMP6	Ectopic	AV	Bone formation in quadriceps in athymic nude mice [74], in thigh muscle of various immunocompetent rat strains [93,94], and in calf muscle of nude athymic rats [70]
	Orthotopic	AV	Enhanced cartilage and subchondral bone formation in a femur condyle defect model in immunocompetent ponies [110]
BMP7	Ectopic	AV	Bone formation in quadriceps of athymic nude mice [74] and thigh muscle of athymic nude rats [93], but not in thigh muscle of immunocompetent rats [93]
	Orthotopic	AV	Better osseointegration of dental implants by enhanced aveolar bone formation in immunocompetent rats [35]
			Bone regeneration in calvarial defect in mice when viral particles were delivered in a silk fibroin scaffold [178]
BMP9	Ectopic	AV	Bone formation in quadriceps in athymic nude mice [74] and rats [95,159], and thigh muscle of immunocompetent mice [93] and rat strains [94,95,159]
	Orthotopic	AV	Regeneration in critical-size mandibular defect [6] and healing of spinal arthrodesis model in athymic nude mice [55]
TGFβ	Orthotopic	AV	Increased epiphyseal thickness was observed after injection of viral particles into the humerus of rats [108]
VEGF	Orthotopic	AV	Viral particles injected into muscle surrounding a femur defect in immunocompetent rats led to faster healing and repair [155]
			No bone formation in a dental implant model in immunocompetent dogs [103]
PDGF	Orthotopic	AV	Enhanced aveolar bone repair and regeneration in periodontal lesions [71] and alveolar ridge

			defects [23] in immunocompetent rats
LMP1	Orthotopic	RV	Improved regeneration and healing in femur fractures in immunocompetent rats [152]
Cbfa1	Orthotopic	AV	Robust bone regeneration in an idiopathic osteonecrosis model in rats [139]
Nell1	Orthotopic	AV	Viral particles in demineralized bone matrix enhanced spinal fusion in immunocompetent rats [100]

Table 1-1: Summary of *in vivo* studies employing viral gene delivery for bone induction. Abbreviations: AV: adenovirus, AAV: adeno-associated virus, RV: retrovirus, BMP: bone morphogenetic protein, TGFβ: transforming growth factor-β, VEGF: vascular endothelial growth factor, PDGF: platelet derived growth factor, LMP1: LIM mineralization protein 1, Cbfa1: core binding factor alpha1 subunit protein (Runx2), Nell1: NEL-like 1.

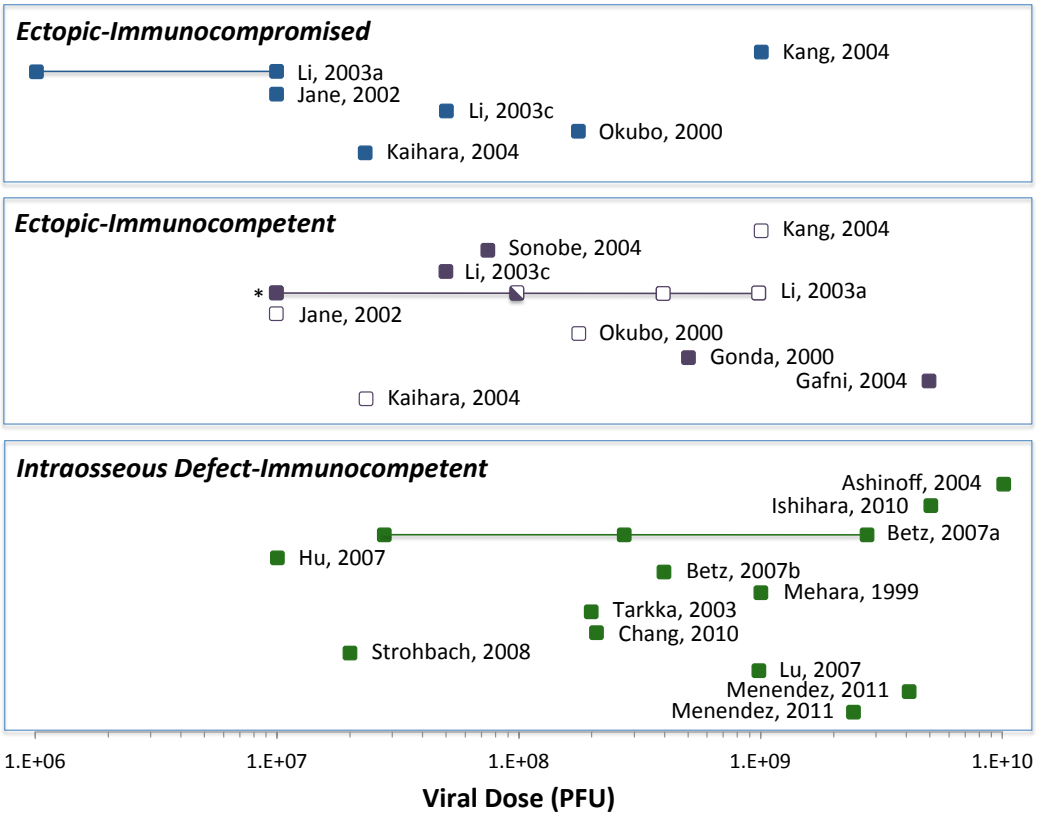

Figure 1-2: Summary of viral doses employed in bone induction studies. The summary shows viral doses for ectopic implantation in immunocompromised animals, ectopic implantation in immunocompetent animals, and intraosseous defect in immunocompetent animals. The viral dose is given as plaque forming units (PFU) per implant. Open squares (□) indicate studies with no bone formation, whereas closed squares (n) indicate successful bone formation. Connected squares indicate the range of doses employed in the study. In the case of Li 2003a (*), the studies employed only one dose for each of 5 different BMPs and are not indicative of any dose response, only the differences in BMP potency.

1.3.1 DELIVERY OF NAKED pDNA WITHOUT A CARRIER

The simplest approach to pDNA delivery is the administration of pDNA alone without a carrier to aid with intracellular uptake. With injections of 500 μg of BMP-2 plasmid into mouse gastrocnemius muscle [128], bone formation was induced as measured by histology and radiographs. However, bone induction was obtained only when the pDNA dose was divided into 2 to 8 smaller doses of 250-62.5 μg delivered over 2 to 8 days. A single injection of the full 500-μg dose was not sufficient to induce bone formation. This may suggest that the pDNA without a carrier does not sufficiently sustain protein expression for a prolonged time. In a separate study [19], pDNA delivered with or without a collagen solution led to small amounts of bone formation in a rat spinal fusion model, which was only histologically observed. A high pDNA dose (500 μg) was needed for this purpose, indicating that this method was also not very efficient. The specific role of the collagen in improving pDNA delivery is unknown, but it is likely that it helps to retain the pDNA at the injection site longer, rather than facilitating intracellular uptake/trafficking.

Other studies have delivered naked pDNA on biomaterial scaffolds. BMP-4 plasmid (500-1000 ug) delivered on a collagen scaffold in a rat critical femur model [44] led to bridging of the defect after 9 weeks, compared to the fibrous tissue seen in control animals with collagen sponges alone. A combination of a PTH1-34 and BMP-4 plasmid led to accelerated healing such that the bone defect was bridged in 4 weeks. A similar collagen sponge

containing 100 or 1000 mg of VEGF plasmid increased angiogenesis, leading to bone formation in a rat critical-sized effect [49]. Delivery of a PTH1-34 plasmid on a collagen sponge implanted at a beagle tibial defect model was successful without the use of a carrier [17]. Bone formation at the critical-size defect increased by 25% after 4 weeks with 40 mg, but 100 mg pDNA was required for union of the defect within 6 weeks. These studies indicate that although pDNA without any carrier can induce the desired response, exorbitant amounts of pDNA may be required for significant bone induction, making this approach not clinically feasible.

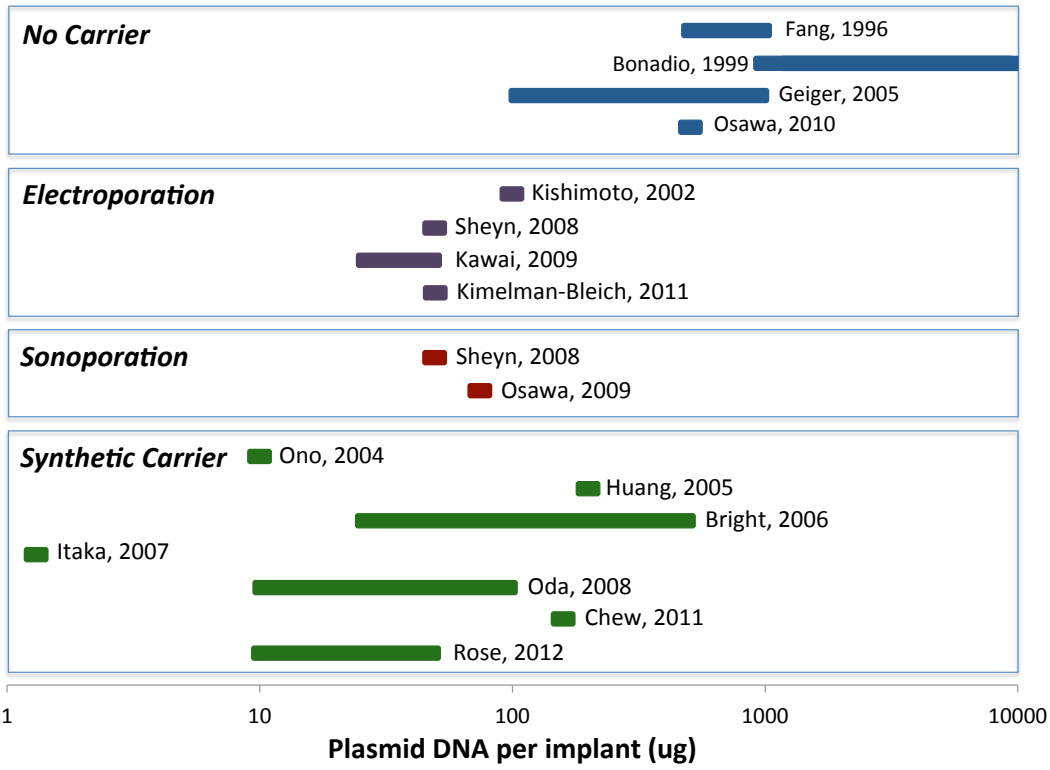

Figure 1-3: Amount of pDNA used in bone induction studies involving non-viral gene delivery. The graph summarizes the range of pDNA doses used in osteogenesis studies, which were classified based on the type of non-viral gene delivery: (i) no carrier (naked pDNA), (ii) electroporation, (iii) sonoporation, or (iv) synthetic carriers. Experimental details of each study are described in **Table 2**.

Reference	Gene	Scaffold	Model	Outcome
No Carrier				
Fang (1996)	BMP-4, hPTH1-34	Collagen	Rat femur-critical defect	Bone formation and gap healing after 9 weeks with BMP-4; the combination of BMP-4 and hPTH1-43 was more potent than individual factors, with boney bridging after 4 weeks.
Bonadio (1999)	hPTH1-34	Collagen	Beagle tibia-critical defect	Although some regeneration was seen after 4 weeks with 40 mg of pDNA, 100 mg was required for major regeneration after 6 weeks.
Geiger (2005)	VEGF	Collagen	Rat cranium-critical defect	The defect was bridged after 6 weeks
Osawa (2010)	BMP-2	No scaffold	Mouse radius-critical defect	Bone formation was detected after 3 weeks, but only when multiple injections were given
Electroporation				
Kishimoto (2002)	BMP-4	No scaffold	Mouse SC implantation	Bone formation after 2-4 weeks of BMP-4 electroporation, but dystrophic calcification in all groups receiving electroporation
Kawai (2009)	BMP-2/7	No scaffold	Mouse IM injection	Bone formation was observed after 10 days
Sheyn (2009)	BMP-9	No scaffold	Mouse IM injection	Bone formation after 5 weeks of electroporation
Kimelman-Bleich (2011)	BMP-9	Collagen	Mouse radius-critical defect	Critical-sized defect was bridged with electroporation of BMP-9 after 5 weeks
Sonoporation				
Sheyn (2009)	BMP-9	No scaffold	Mouse IM injection	Sonoporation led to bone formation to a lesser extent than electroporation
Osawa (2009)	BMP-2	No scaffold	Mouse IM injection	Bone was observed with 7 cycles of injection/sonoporation after 3 weeks
Synthetic Carrier				
Ono (2004)	BMP-2	HA	Rabbit cranium-critical defect	SuperFect™ mediated gene delivery led to bridging of the critical defect, but the new bone was outside the scaffold
Huang (2005)	BMP-2	PLGA	Rat cranium-critical defect	Limited bone formation was observed with 25 kDa PEI delivery after 15 weeks
Bright (2006)	BMP-7	No scaffold, Collagen	Rat spinal-fusion	Limited bone formation was observed histologically when pDNA was delivered with cross-linked collagen
Itaka (2007)	Runx2 and caALK6	Ca/P cement	Mouse cranium-critical defect	A novel polymeric carrier, composed of block co-polymers of polyethyleneglycol-aspartate-diethylenetriamine. led to bone formation

				at four weeks
Oda (2009)	BMP-2	HA Fiber	Rat SC implantation	Bone formation was observed after 4 weeks with calcium phosphate
Chew (2011)	BMP-2	PFF	Rat cranium-critical defect	No bone formation was observed with triacrylate/amine polycationic polymer (TAPP) as a gene carrier
Rose (2012)	BMP-2	Gelatin	Rat SC implantation	2 kDa polyethylenimine modified with linoleic acid (PEI-LA) gene delivery led to extensive tissue induction, but no bone formation

Table 1-2: Details of studies described in Figure 1-3. SC: subcutaneous. IM: intramuscular. HA: hydroxyapatite, PFF: poly(propylene fumarate), PLGA: poly(lactic-co-glycolic acid).

1.3.2 PHYSICAL DELIVERY METHODS

Both sonoporation and electroporation have been employed to increase intracellular uptake of naked pDNA delivered without a carrier. Sonoporation uses microbubbles that collapse, compromising plasma membrane integrity to allow pDNA passage into the cell [167]. Sonoporation with 75 μg of BMP-2 plasmid in microbubbles led to radiographic bone formation in a mouse intramuscular model, although pDNA without sonoporation also led to some ectopic bone in this study [127]. Multiple cycles of injections and sonoporations during a 3-week study period was required to induce bone [127]. A comparison of electroporation and sonoporation with BMP-9 plasmid for ectopic bone formation in a mouse intramuscular model found that the volume of bone formed was ~30 fold higher with sonoporation as compared to electroporation [146]. Electroporation similarly allows cellular internalization of pDNA after plasma membrane integrity is compromised by electrical pulses, allowing diffusion of large charged molecules that would not normally pass through cell membranes [141]. Electroporation of 25-50 μg BMP-2/7 plasmid was shown to yield radiopaque bone in a rat intramuscular model [76]. A similar system was also effective for intraosseous application, where electroporation with 50 μg of BMP-9 plasmid induced bone formation in a critical-size defect in a mouse radius [81]. No bone formation was evident with osteogenic or control pDNA without electroporation. The use of only 50 μg pDNA to heal a defect with electroporation represents ~10-fold decrease in the pDNA dose needed

for naked pDNA delivery, where ~500 μg pDNA was needed for bone formation. This is a significant improvement. A separate study also demonstrated osteogenesis in an ectopic model following electroporation of 100 μg of BMP-4 plasmid, but this study also found dystrophic calcification in all electroporation groups including no pDNA (saline controls) and control pDNA [83]. This excessive tissue damage is worrisome, particularly if such a physical intervention is applied at a site that is already injured. It must be noted that in preclinical models, the surrounding tissue is relatively thin and the bone tissue is easily accessible. The thick tissues surrounding human bones may greatly limit the ability of percutaneously applied electroporation or sonoporation to perturb cellular membranes *in situ* and internalize therapeutic pDNA. Further refining of both sonoporation and electroporation is required to minimize non-specific effects, while achieving effective pDNA expression.

1.3.3 DELIVERY WITH SYNTHETIC CARRIERS

Synthetic carriers are intended to facilitate intracellular uptake of pDNA without non-specific membrane disruptions induced by electroporation and sonoporation. Since unmethylated CpG motifs on naked pDNA can be recognized by Toll-like Receptor-9 [56], and stimulate an immune response, synthetic carriers can also mask the immunogenic CpG motifs [86], as long as they remain non-immunogenic themselves. The broadly-effective carrier, branched 25 kDa polyethylenimine (PEI25) has

been employed to deliver osteogenic genes for bone formation. PEI25 complexes containing 200 μg of BMP-4 plasmid were delivered in a poly(lactic-*co*-glycolic) acid (PLGA) implant for regeneration of a rat critical-size skull defect [64]. Bone formation was observed around defect edges with BMP-4/PEI25 complexes after 8 weeks, whereas naked pDNA and scaffolds alone gave no bone formation. Bone formation being limited to the edge of implants may in part be due to the toxicity of PEI25. Although the amount of implanted polymer was not provided, this is likely to be in excess of 32 μg (polymer:pDNA ratios are typically >1.0 with synthetic carriers). We previously found that relatively small amounts of PEI25 (16-32 μg) was sufficient to inhibit BMP-2 (protein) induced bone formation at ectopic sites [175], so that the excess PEI25 in the above study might have limited a robust bone tissue formation

A more biocompatible carrier is low molecular weight (2 kDa) PEI modified with linoleic acid [120]. Although this carrier yielded the same recombinant protein expression rate as viral vectors (based on *in vitro* assessment), no bone formation was observed with 10-50 μg of BMP-2 plasmid at subcutaneous sites in rats [135]. The same outcome was observed with the PEI25 carrier as well. This may be in part due to insufficient transgene expression (i.e., dose and/or duration) at this site. Alternatively, the nature of implanted scaffold (i.e., Gelfoam™) may not be sufficiently supportive of osteoinduction at the ectopic site, although it was effective for an AV-mediated bone induction in a skull defect in rats [61]. Another study

employed a rat critical-size skull defect and delivered 160 μg of BMP-2 plasmid [29] by using a triacrylate/amine polycationic polymer (TAPP) for delivery. The resulting particles were incorporated into gelatin microspheres and implanted in a poly(propylene fumarate) scaffold. Despite the large amount of implanted pDNA, gene delivery had no effect on bone formation. The reasons for this are unclear, but given that the TAPP polymeric carrier only led to a small increase in transfection compared to free pDNA *in vitro* [29], the low efficiency of the carrier may be responsible for this outcome.

When 50-100 μg of BMP-2 plasmid condensed with calcium phosphates were implanted in HA scaffolds, radiopaque masses were seen at the subcutaneous implant site after 4 weeks [122]. A lower (10 μg) plasmid dose was also effective, but required 12 weeks to show radiopaque (calcified) tissue. HA may prove to be a more optimal scaffold for bone applications as the scaffold itself induced formation of calcified tissue in this study. HA scaffolds containing 10 μg of BMP-2 plasmid in cationic liposomes (SuperFect™) were also employed for bone repair in an intraosseous model [126]. The amount of pDNA to be delivered was limited by the toxicity of the carrier, as noted by the investigators in this study. The defect containing BMP-2 liposomes was bridged after 6 weeks, however most of the new bone was formed on the periphery of the scaffold with little bone tissue penetrating the scaffold. This pattern of tissue induction is bound to compromise the mechanical properties of the new bone. Longer-term studies might prove otherwise but low potency of the delivery systems and/or sub-

optimal scaffolds might have hindered a robust response. Finally, a unique study employed only 1.3 μg of pDNA expressing both runt-related transcription factor 2 (Runx2) and constitutively active form of activin receptor-like kinase 6 (caALK6) [69], both of which act as intracellular mediators of osteogenesis. pDNA was condensed by a novel carrier consisting of block co-polymers of polyethyleneglycol-aspartate-diethylenetriamine. Complexes were mixed into a calcium phosphate cement to fill the cranial defect. Unlike polymeric PEI25 or liposomal Fugene™ that led to no regeneration, this novel carrier led to histologically-observed bone covering approximately half of the original defect site after 4 weeks. This is a noteworthy result since the dose of the pDNA employed was significantly lower than any other studies reported. The aspartic acid residues in the polymer are expected to enhance the affinity of pDNA complexes to the employed calcium/phosphate scaffold, better localizing the pDNA to the defect site. The use of calcium/phosphate cement might have been also a direct contributing factor since such a mineral is noted to stimulate endogenous mineralization [121], but whether it also supports enhanced transgene expression *per se* remains to be investigated.

A

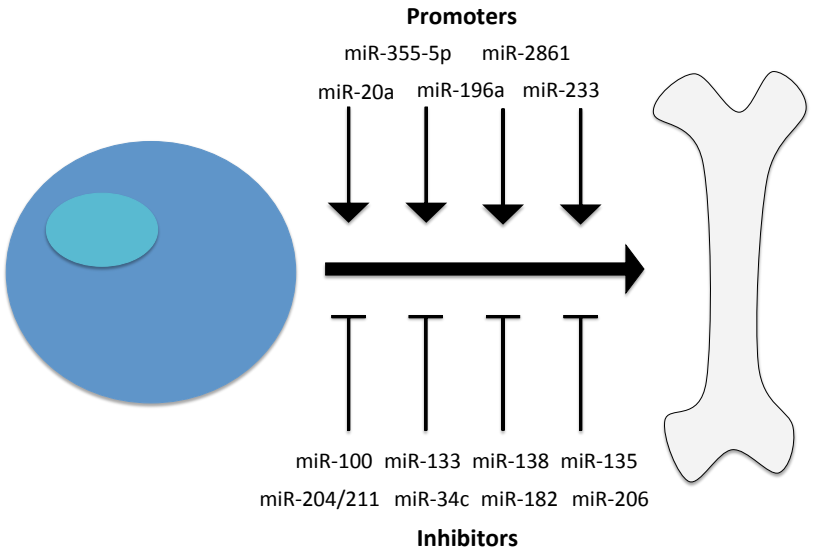

B

miRNA	Role in or Link to Human Disease	Pathway or Mechanism	Reference
miR-20a	Expression of miR-20a promotes osteogenic differentiation	Inhibits PPARY, Bambi, and Crim1, antagonists of BMP/Runx2 signalling	[174]
miR-34c	Overexpression of miR-34c into osteoblasts leads to defective mineralization and osteoporosis	miR-34c decreases Notch signalling	[11]
miR-100	Overexpression of miR-100 inhibits osteogenic differentiation of hADSC, whereas knockdown enhanced osteogenesis	miR inhibits BMPR2 expression	[171]
miR-133	Overexpression of miR-133 inhibits expression of osteogenic genes	miR-133 targets Runx2	[97]
miR-135	Overexpression of miR-135 inhibits expression of osteogenic genes	miR-135 targets Smad5	[97]
miR-138	Inhibition of miR-138 induces bone formation	miR-138 inhibits ERK pathway by targeting FAK	[42]
miR-155	Mice without miR-155 did not develop collagen-induced arthritis.	miR-155 is involved in innate and adaptive immunity	[15]
miR-182	Osteogenesis and bone formation inhibited by overexpression of miR-182	miR-182 inhibits FoxO1	[78]
miR-196a	hADSC osteogenesis was inhibited by knockdown and enhanced by overexpression of miR-196a	miR-196a down regulates the HOXC8	[80]
miR-204/211	miR-204 expression stimulates adipocyte differentiation from bone marrow stromal cells	miR-204 decreases expression of osteogenic Runx2 expression	[63]

miR-206	Osteogenesis is inhibited by over-expression and induced by knockdown of miR-206	miR-206 decreases Cx43 expression	[66]
miR-233	Overexpression prevents osteoclastogenesis	Unknown	[153]
miR-355-5p	Delivery of miR-355-5p increases expression of osteogenic genes	Inhibits DKK, an antagonist of Wnt signalling	[173]
miR-2861	Mutation in miRNA linked to osteoporosis. Knockdown inhibits bone formation, whereas overexpression increases osteogenesis.	The miRNA represses HDAC5, which enhances Runx2 degradation	[92]

Figure 1-4: A. miRNA identified to promote or inhibit bone regeneration. A miRNA whose expression leads to osteogenesis (or depletion hinders osteogenesis) was categorized as a promoter of bone regeneration. In contrast, a miRNA whose expression impedes bone formation was categorized as an inhibitor of bone regeneration. **B. List of miRNAs with potential for bone regeneration and their reported mechanisms of action.** Abbreviations used are peroxisome proliferator-activated receptor gamma (PPARY), bone morphogenetic proteins receptor II (BMPR2), Extracellular signal-regulated kinases (ERK), Focal adhesion kinase (FAK), forkhead box protein O1 (FoxO1), Homeobox-containing protein C8 (HOXC8), Connexin 43 (Cx43), Dickkopf-related protein 1 (DKK1), Histonedeacetylase 5 (HDAC5).

1.4 BONE INDUCTION BY RNA INTERFERENCE

Small, drug-like inhibitors are being investigated as a means to overcome negative regulators of osteogenesis. Examples of such inhibitors include (i) the small GTPase Rho and Rho-associated protein kinase (ROCK) inhibitor Y27632, which enhanced BMP-2 (protein) induced bone formation subcutaneously [168], histone deacetylase inhibitor Trichostatin A, which altered expression of Runx2 in adipose-derived stem cells [62], CXCR4 inhibitor AMD3100 [101], whose activity is mediated by Signal Transducer and Activator of Transcription 3 (STAT3) signalling, and the cGMP-dependent phospodiesterase-5 inhibitor Sildenafil, whose stimulatory activity on bone regeneration was demonstrated in a mouse fracture model [57]. Unlike the synthetic entities, however, inhibitory RNAs in the form of microRNAs (miRNA) and small interfering RNAs (siRNA) are more appropriate (i.e., physiological) means to alter gene expression. miRNAs are ~22 nucleotide-long, endogenously expressed mediators regulating protein translation. These single stranded oligomers bind to RNA-Induced Silencing Complex (RISC), which then binds target mRNA at the 3' untranslated region (URT) to reduce or inhibit the translation. miRNA with exact complementary sequences may result in cleavage of the bound mRNA, whereas base mismatches likely lead to translational repression [54]. The miRNA have recently been shown to regulate lineage commitment of many cell types, including osteogenic commitment of mesenchymal stem cells [164] and C2C12 myoblasts [97]. The miRNAs can act as negative regulators of

osteogenesis [11,42,63,66,171,174] or as promoters of osteoblast differentiation [80,92,153,173]. A summary of miRNAs recently linked to osteogenesis and their mechanism of action can be found in ***Figure 1-4***. Pro-osteogenic miRNAs can act through up-regulating Wnt [173] and BMP/Runx2 [174] signalling, or other means. In addition to their role in lineage commitments, miRNA alterations are implicated in musculoskeletal diseases. Mutations in miR-2861, a positive regulator of bone formation, are associated with Type 1 osteoporosis in adolescents due to functional loss of miR-2861 [92]. In contrast, mice lacking miR-155 do not develop collagen-induced arthritis, and had reduced bone destruction due to diminished osteoclastic activity [15]. Currently, there are no published studies that have investigated direct delivery of miRNA for bone induction in an animal model. Human mesenchymal stem cells, however, transfected with miR-138 or antimiR-138 expression systems, were explored for enhanced osteogenesis; when seeded on a HA/calcium-phosphate scaffold and implanted subcutaneously in SCID mice, miR-138 modified cells decreased ectopic bone formation by ~80%, while anti-miR-138 more than doubled the ectopic bone formation compared to a control miRNA [42]. miR-138 inhibited osteogenesis through extracellular signal-receptor kinase (ERK) via focal adhesion protein (FAK), although the precise signalling pathway is still unclear. Presumably the obtained effect was due to re-programming of transplanted pluripotent cells, altering the osteogenic differentiation of grafted cells. Direct delivery of miRNA to re-program host cells, instead of

delivery via cell transplantation, is likely going to be more clinically relevant, due to previously discussed difficulties encountered with relying on host cells for therapy.

The siRNA have been alternatively employed to selectively silence protein expression in support of osteogenesis. siRNAs are synthetic nucleic acids (19-23 base pairs) but can be introduced into the cell to silence gene expression through naturally occurring RNAi pathways [148]. Double-stranded siRNA contains a passenger strand and a guiding strand, which are incorporated into the RISC complex. The passenger strand is then released to allow the guiding RNA strand remaining in RISC to bind with complementary mRNA. Once bound, RISC cleaves the target mRNA, preventing translation of the target protein. The guiding strand and RISC combination is not altered during this process, and is able to continue cleaving other mRNA targets. siRNA-mediated down-regulation of STAT3 [90], Abundant in Neuroepithelial Area (ANA) [115], Hoxc8 [179], Protein related to DAN and cerberus (PRDC) [65], Noggin [105,154], Notch [170], zinc finger Zfp467 [169], guanine nucleotide-binding protein alpha (GNAS1) [134], prolyl hydroxylase domain-containing protein 2 (PHD2) [134] have been all shown to enhance osteogenic activity of various cell types *in vitro*. siRNA has been additionally investigated as a supplement to protein delivery, where siRNA against Noggin have been deployed in support of BMP-induced osteogenesis [105,154]. In one study, the muscle surrounding the implantation site was primed for osteogenesis through injection and electroporation of Noggin

siRNA, after which a collagen sponge containing 5 μg of BMP-2 was implanted. A small increase in BMD was observed with Noggin siRNA [154]. A subsequent study found similar results when Noggin siRNA was delivered alongside BMP-2 in a synthetic scaffold [105]. For these studies, we estimate that 10-16 μg of siRNA was delivered in each implant, which is practical for clinical scale up. These *in vivo* studies were in line with the reported effect of Noggin on osteogenesis from some *in vitro* studies, but there are also conflicting reports on Noggin effect on BMP-2-induced osteogenic differentiation. siRNA-mediated Noggin suppression in human bone marrow-derived stem cells reduced expression of osteoblastic gene and *in vitro* calcification in our hands [24], unlike its well-known effect on rodent cells and in animal models as articulated above. Others also noted that a stimulatory role of Noggin protein on osteogenesis of human mesenchymal stem cells under a variety of inducing conditions [133]. Such a contradictory Noggin effect is concerning and calls for better understanding of the reasons behind this observation. In addition to species effects, pharmacokinetics differences as well as non-specific effects of delivery could account for such differences. Inherent differences in cell populations, such as the activity of osteogenesis-related intracellular pathways and/or receptor repertories, could be another reason, as well as differences in culture conditions, especially choice of osteogenic supplements used to treat the cells.

The delivery of siRNA alone has been attempted in animal models (***Table 3***). In a ground-breaking study, an siRNA against Plekho1 (casein

kinase-2 interacting protein-1) was delivered systemically using a novel carrier consisting of the cationic lipid dioleoyl trimethylammonium propane (DOTAP) with six repeat of a tripeptide aspartate-serine-serine [172]. The peptide, due to its inherent binding capacity to bone mineral, was able to target siRNA to bone surfaces, and decrease accumulation of siRNA in kidney and liver. Peptide-modified liposomes containing the Pleckho1 siRNA led to an increase in bone mineral density, compared to un-modified liposomes or free siRNA, over the course of 9 weeks. Bone mineral density returned to normal levels in ovariectomized rats upon delivery of Pleckho1 siRNA in peptide-modified liposomes over a 13-week period. Based on an average mass of 300 g, each rat probably received ~1 mg of siRNA. siRNA has been employed locally to enhance bone formation, where delivery of siRNA alone was investigated to induce osteogenesis. Silk fibroin-chitosan scaffolds were loaded with siRNA against GNAS1, PDH2, or a combination of siRNAs against both targets, and were implanted intramuscularly [134]. No specific carrier for siRNA was employed, and it was unclear how much siRNA was delivered to the implant site. An *in vitro* model used mesenchymal stem cells seeded onto the scaffolds and the commercial reagent siPort™ Amine siRNA, and showed minimal changes in osteogenic gene expression. In agreement with *in vitro* data, minimal increases in bone formation (compared to scaffold alone) were observed *in vivo* after delivery of GNAS1 or PDH2 siRNA.

These studies, however, require better controls to confirm the efficacy of RNAi-mediated bone induction. Of foremost importance is the

inclusion of scrambled (control) siRNA in studies that would not result in knockdown of any protein. With systemic delivery of ~1 mg of Pleckho1 siRNA, off-target effects could be potentially exacerbated [113], leading to immune responses, knockdown of non-specific mRNA and unpredictable cellular toxicities. The lack of other controls, such as siRNA delivery with unmodified (i.e., non bone-seeking) carriers, make it difficult to evaluate the specificity of both molecular action and tissue targeting. Scrambled siRNA was also omitted from local (electroporation) delivery studies [134,154], which is known to cause tissue damage and dystrophic calcification [83]; employing relevant control siRNAs is the only way to rule out such effects. It is important to note that local siRNA delivery still required the presence of osteogenic protein (2.5-5 μg per defect in the employed models) to induce bone formation and delivery of Noggin siRNA alone would have led to minimal, if any, calcification at intramuscular sites [154]. Given that Noggin siRNA led to slight enhancement of BMP-2 induced bone formation in employed models (we estimate a 'savings' of ~20% of implanted BMP dose), selection of targets more potent than Noggin will be needed to significantly reduce and/or obviate the recombinant protein.

siRNA Target	Carrier	Amount	Model	Reference
Plekho1	Novel carrier of DOTAP with six repeats of aspartate, serine, serine.	1 mg (est.)	Mouse, systemic delivery targeting to bone surfaces	[172]
GNAS PDH2	Naked siRNA with silk fibroin-chitosan scaffold	Unknown	Sheep, intramuscular implantation	[134]
Noggin	Electroporation	10-16 μg	Mouse, intramuscular implantation of collagen sponge containing 5 μg of BMP-2 after injection and electroporation of siRNA	[154]
Noggin	No carrier	10-16 μg	Mouse, intramuscular of novel scaffold (poly-D,L lactic acid-co-dioxanone-co-polyethyleneglycol hydrogel) containing 2.5 μg of BMP-2 and siRNA	[105]

Table 1-3: *In vivo* studies using siRNA-mediated RNAi for osteogenesis.

1.5 PHARMACOKINETICS AND PHARMACODYNAMICS OF GENE DELIVERY

Although the studies outlined above clearly establish the feasibility of non-viral delivery in osteogenesis, the obtained therapeutic responses remain inefficient based on the amount of pDNA required to achieve functional bone formation; i.e., significant defect bridging was observed with only large (1 to 100 mg) quantities of pDNA [17,44]. Based on the estimated volume of the defect, the concentration of pDNA required for efficacy borders that of protein in clinical therapies (0.9-1.5 mg/cc). The main premise behind gene delivery was to reduce the amount of exogenous agent so as to minimize possible complications. The need for more effective synthetic carriers calls for a better understand the pharmacokinetics and pharmacodynamics issues surrounding gene medicines, which underlie their efficiency. This is crucial to accurately assess efficacy, dose response, and safety. The pharmacodynamics of pDNA and siRNA differ from small molecule drugs because of number of processing steps required to obtain the bioactive molecule, and the specificity of intracellular compartment to which the nucleic acid must be delivered. As outlined above, nucleic acids without any carrier yields very low or undetectable levels of transfection *in vivo* [135]. In the context of pDNA, the production of a therapeutic protein is the desired end result, so that pDNA must be internalized by the cells, dissociated from the carrier, and trafficked to nucleus for transcription. On the other hand, microRNA and siRNA must be internalized and dissociate

from its carrier in cytoplasm to achieve the desired silencing. A closer inspection of pDNA (and siRNA) pharmacokinetics and pharmacodynamics will help better understand and improve gene delivery of bone diseases; however, these considerations are different from systemic attempts at gene delivery [129] since transfection, protein secretion and tissue induction are all occurring locally in the case of bone repair.

1.5.1 *IN SITU* PHARMACOKINETICS OF pDNA

As in protein therapeutics, a critical issue with gene medicines is the local residence time of delivered pDNA (although similar issues are pertinent with microRNA and siRNA delivery, we will restrict this discussion to pDNA since no information exists on the latter reagents). One would expect *in situ* retention of pDNA to allow a high level of cellular uptake at the local site, but release from scaffold (or extracellular matrices) to be equally important as well for free (un-sequestered) availability of pDNA to invading and surrounding cells. This issue can be addressed by following the fate of labelled (^{32}P or fluorophore) pDNA or by amplification of unlabeled pDNA via PCR reaction. The impact of a scaffold is expected to be greatest in its ability to retain the pDNA. In studies where the pDNA was administered freely in a collagen scaffold [17], pDNA was shown to remain at boney defect sites for 6 weeks, with significant loss from 2 to 6 weeks (kinetics not quantitated). While significant reduction in transgene expression was evident during healing period [81], which is desirable for transient tissue induction such as

bone regeneration, whether this decrease is due to physical loss of pDNA, pDNA degradation or transcriptional silencing is not known. Carrier-to-carrier differences in functional bone induction, for example (PEG)-b-(Asp-[DET]) vs. l-PEI vs. Fugene6 [69], were evident when complexes were delivered within the same scaffold, but whether pDNA pharmacokinetics or cell uptake was the underlying reason for this difference is not known. The carriers, by converting long, string-like pDNA into charged nanoparticles, can obviously affect local pDNA pharmacokinetics. With the choice of appropriate polymeric carrier, pDNA complexes can display a sustained release if the interactions with a scaffold are controlled [29], making it possible to release the pDNA over a period of 3-4 weeks that represent a suitable time-frame for healing in preclinical models. However, not all such attempts resulted in robust bone formation. In one study, PEI25 carrier was beneficial when pDNA was delivered in scaffolds in a cranial defect site [64]. The PEI25 presumably improved the local retention of pDNA or facilitated intracellular uptake of exogenous pDNA. However, other studies using sustained release formulations [29] or a carrier functional *in vitro* (N,N,N-trimethyl chitosan; 91) did not result in improved bone formation in a similar intracranial defect site. It remains to be seen whether the scaffold effects (chemical composition, physical architecture controlling cell invasion, degradation products, etc.) contributed to these conflicting results [29,64]. Fundamental studies on pDNA pharmacokinetics are still needed to better reveal the underlying basis of these observations. Particular areas of desired investigations include (i)

long-term pharmacokinetics of pDNA (i.e., duration exceeding one month even if improved analytical techniques might be needed for accurate assessment of low levels of pDNA *in situ*), (ii) relating pDNA pharmacokinetics to gene expression (i.e., whether the presence of pDNA corresponds to transcriptionally active therapeutic genes), (iii) pharmacokinetics of various carriers with special emphasis on comparing free versus bound (either to a synthetic carrier or scaffold itself) pDNA among carriers, and (iv) effect of release rate of pDNA (or its complexes) on bone formation.

1.5.2 DURATION OF TRANSGENE EXPRESSION

The durations of protein expression from reported studies are summarized in ***Figure 1-5*** to compare the ability of viral and non-viral carriers to sustain exogenous gene expression. Certain AAVs led to detectable levels of proteins for at least 8 weeks [26,27,102,118], although other viruses showed a much shorter duration of protein expression. Non-viral carriers showed similar lengths of detectable protein levels on average, but fewer studies reported extended (>6 weeks) protein delivery. For small animal models, the 3-4 weeks of gene expression observed with the majority of viral and non-viral studies are likely sufficient for bone formation, but a more sustained protein expression will be probably needed for clinical studies. Although exuberant amounts of naked pDNA can also lead to protein expression for 2-4 weeks [17,44], the mRNA and pDNA can be sometimes

detected for much longer [17], suggesting active repression of protein translation. Electroporation similarly led to detectable protein levels for 2-3 weeks [81, 83,128,146], while sonoporation gace detectable proteins for nearly 3 weeks [146]. It was interesting to note that therapeutic proteins were present at comparable durations whether physical methods of delivery or synthetic carriers were employed. These two distinct approaches have been traditionally usually pursued on their own and it is likely that combining synthetic carriers with physical delivery will lead to enhanced (additive or synergistic) protein expression.

A more direct measure of delivery efficiency is the amount of recombinant protein produced, since increased protein secretion is generally expected to correlate with the repair response (note that a non-linear dose-effect relationship was noted for some non-viral systems [116]). Reporter genes, such as fluorescent proteins GFP or DsRed, are frequently employed as surrogate markers of protein expression due to the convenience of fluorescence detection technology, and especially the retention of reporter proteins inside the cells, which is paramount to localize gene expression patterns and to assess the extent of modified cell population. However, this analysis is a poor substitute for protein secretion rates that directly affect the outcomes. Exogenous proteins and growth factors can be detected in preclinical models through immunohistochemistry, but this provides at best a semi-quantitative assessment of production. Quantitative assays such as ELISA might be more useful provided full recovery of the secreted protein

from the physiological milieu is attained. We observed a maximal BMP-2 secretion rate of ~0.3 ng/implant/day (based on *ex vivo* measurement of BMP-2 secretion from recovered implants) with the polymeric carrier linoleic acid-substituted PEI [135]. An independent study reported BMP-2 secretion rate of ~0.1 ng BMP-2/implant/day with *ex vivo* AV transduction of fat pads, which was sufficient for healing in a critical-size femur defect. Similarly, 0.25 ng BMP-2/clot/day was produced by chondrocyte clots transduced *ex vivo* with a retrovirus for repair of an osteochondral defect [166]. Higher secretion rates (1-5 ng/24 hr for BMP-2 [103] and BMP-7 [177]) were reported with another AV system that were used for transfecting human bone marrow stromal cells for intraosseous implantation. Based on these limited studies, it appears that BMP production rates remain relatively similar with these diverse delivery systems. The absolute level of protein secretion (~ng/day) appears to be significantly lower than protein amounts used in equivalent preclinical studies (>1 mg/implant), suggesting that proteins endogenously produced at repair sites are more potent in inducing new tissue. Further studies to correlate actual protein production rates to obtained responses will better reveal the efficiency of delivery systems at the fundamental level.

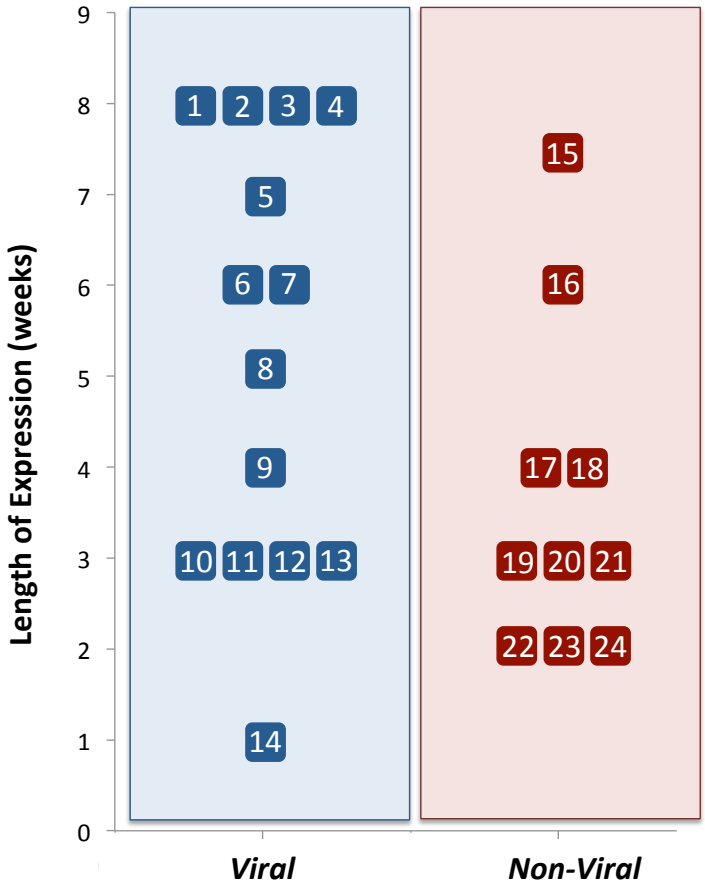

1	Chen, 2003	**9**	Rundle, 2003	**17**	Itaka, 2007
2	Chen, 2004	**10**	Jin, 2004	**18**	Fang, 1996
3	Nasu, 2009	**11**	Kaihara, 2004	**19**	Sheyn, 2008
4	Luk, 2003	**12**	Gafni, 2004	**20**	Osawa, 2012
5	Mehara, 1999	**13**	Strohbach, 2008	**21**	Ono, 2004
6	Lu, 2007	**14**	Okubo, 2001a	**22**	Kishimoto, 2002
7	Ishihara, 2010	**15**	Bright, 2006	**23**	Kimelman, 2011
8	Eggermann, 2006a	**16**	Bonadio, 1999	**24**	Sheyn, 2008

Figure 1-5: Comparison of duration of gene expression in viral and non-viral studies. The numbers indicate the specific study shown on the Table on the right. The length of expression was determined by how long the recombinant protein was detected. In some cases, however, the studies did not include sufficient time points to inspect the loss of expression and may therefore underestimate the expression length.

1.5.3 STABILITY OF GENE DELIVERY SYSTEMS

Unlike viral delivery systems (with molecularly defined structure and size), non-viral systems comprise of free molecules (microscopic size pDNA) or nucleic acid/carrier nanoparticles that are heterogeneous and range in size from ~100 nm (typical of polyplexes) to >1 mm (typical of liposomes). The stability of gene delivery systems is frequently reported in terms of their physicochemical features (e.g., size or zeta-potential), with several studies investigating methods to stabilize the formulations for pharmaceutical use. For example, polyplexes stored at body [109] and room temperature [28,58,145] both exhibited a time-dependent decline in transfection efficiency. Lowering the storage temperature [28,58,145] and lyophilisation [28,33] can decrease loss of activity, but these measures are not useful to maintain transfection efficiency once implanted *in vivo*. In case of systemic delivery, size stability is an important factor, as complexes must be able to travel unobstructed through capillary beds, but such stringent size requirements are likely not necessary for local delivery, provided that the size does not impact cell uptake and transgene expression. In some cases, the strategies employed to ensure a size-stable complex (e.g., PEG addition) compromise its *in vivo* transfection efficiency [111] or increased its susceptibility to nucleases [132]. Physicochemical parameters, furthermore, are not accurate representations of how the transfection ability of the complexes changes over time. The authors recently investigated this issue (see ***Figure 1-6A;*** 136), and found that the loss in transfection efficiency is

both immediate (i.e. within hours) and large, with up to a 90% loss compared to freshly made complexes after a 24 hour exposure to body temperature. Not all systems display such a drastic change and some carriers can better retain the activity in short duration studies (***Figure 1-6B***). This reduction in transfection efficiency is ignored in development of gene delivery systems and must be considered during development due to its obvious impact in bone regeneration; the therapeutic agents do not immediately come in contact with target cells and must remain 'active' in days to weeks needed for the infiltration of osteogenic cells into a repair site. The *in vitro* studies where complexes are added to cell culture media for immediate contact with cells might be misleading in this regard.

Stability is especially crucial for gene delivery systems that employ scaffolds to deliver the nucleic acids complexes. Even AV systems display a loss of activity with storage at 4 ^{o}C (e.g., ~85% loss with lyophilisation after one month, and no infectious viral particles were detected after two weeks in PBS; [61]). These rates of loss are expected to be accelerated at the physiological temperature, with a one log reduction in viral infectivity observed after storage in buffer for 4 hours at 37 ^{o}C [31]. Various methods to stabilize viral particles during freezing and lyophilisation have been investigated [31,32], but few have investigated stabilization techniques at physiological temperature. In light of the dearth of publications reporting on this topic, studies investigating complex stability and methods to stabilize

transfection efficiency are needed to ensure that non-viral delivery systems are as effective as possible.

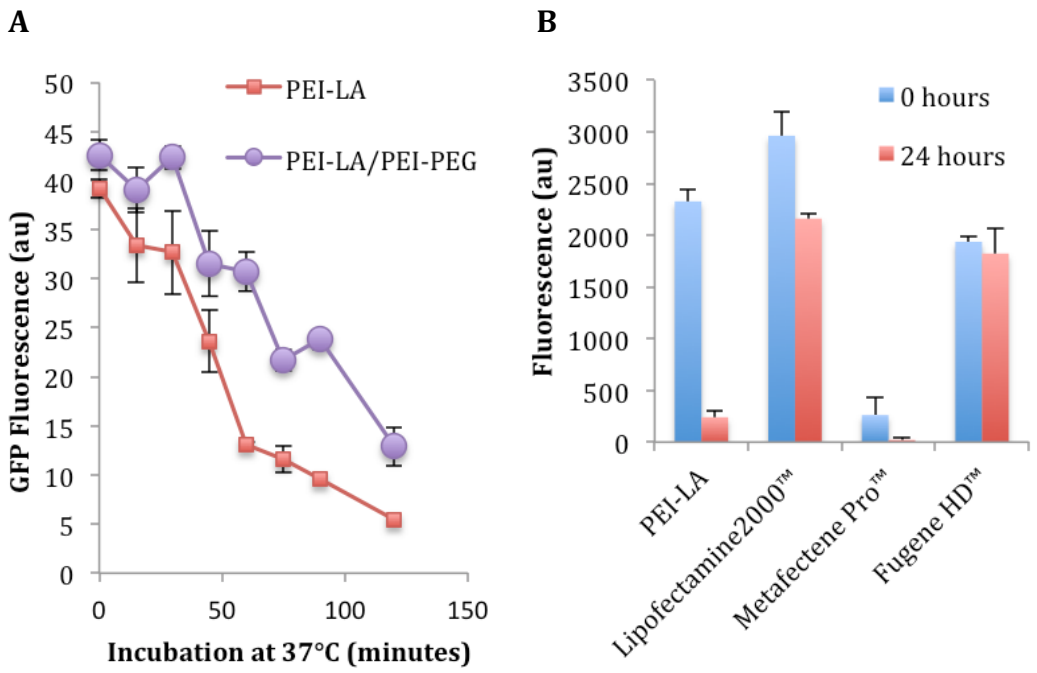

Figure 1-6: Changes in transfection efficiency during incubations at body temperature. Complexes made of plasmid DNA and either 2 kDa polyethylenemine modified with linoleic acid (PEI-LA) or a mixture of PEI-LA and PEI modified with polyethyleneglycol (PEI-PEG) show a steady decrease in transfection efficiency when exposed to 37 °C (**A**) prior to addition to 293T cell culture. Note that even PEI-LA/PEI-PEG, which maintain a constant size during this period, also show a decline similar to PEI-LA and PEI-LA/PEI complexes, both of which show a steady increase in size during this time (data not shown). Incubation of commercially available reagents led to minimal changes for Fugene HD™, while PEI-LA, Lipofectamine2000™, and Metafectene Pro™ all led to decreases in transfection efficiency (**B**).

1.5.4 SCAFFOLDS IN GENE DELIVERY

As in protein (BMP-2 and BMP-7) therapy, a scaffold is going to be indispensible in gene-based bone repair. The scaffold is envisioned to control three aspects of bone repair; (i) by its inherent ability to present a substrate for cell attachment, differentiation as well as mineralization, a scaffold can directly modulate osteogenic activity *in situ* [59]; (ii) by its ability to interact with delivery systems (both viral and non-viral), a scaffold can control the local pharmacokinetics of therapeutic agent and its availability to invading cells, and; (iii) by sequestering the protein product secreted, a scaffold can localize the bioactive protein for cellular differentiation, or control its release for chemotactic activity. Bone induction studies using gene therapy indicated relatively fast (1-2 weeks) bone formation with both viral and non-viral delivery irrespective of the anatomical site (***Figure 1-7***), so that a prolonged release system might not be necessary in these cases. Some studies indicated bone induction after 8 weeks, so that a more prolonged release might be needed in these cases. Clinical studies with humans are expected to mimic the latter scenario, so that prolonged release systems are likely going to be needed. Controlling the structural features of scaffolds [46], or degradation rate of biodegradable scaffolds [85] are obvious means to control the pDNA release. However, such systems remain to be tested for bone repair, and relationship between pDNA release rates and osteogenic potency remains to be established.

Beyond non-viral systems, scaffolds have been also used to deliver BMP-2 expressing AVs to successfully regenerate bone defects around dental implants [103]. Based on *in vitro* studies, scaffolds were even shown to allow improved viral-mediated transfection as compared to 'free' virus in solution [147]. Presumably, the scaffold slows the release from the administration site, prolonging transfection ability while providing a template for regeneration. The release from the scaffold is expected to be relatively rapid, with a typical half-life of 24 hrs [147], but it was possible to control the release rate by controlling the surface features of scaffolds. Fibronectin, for example, was shown to slow the release of an AV from a PLGA scaffold, while not influencing the release of a lentivirus. A diverse range of scaffolds was compatible with bone regeneration induced by AV delivery, for example collagen/chitosan composites [176,177] and silk fibroin scaffolds [178]. Scaffolds made from HA, however, did not show efficacious delivery of a BMP-7 AV in a subcutaneous implant model [142], unlike the experience with such scaffolds in non-viral delivery. It is likely that subcutaneous site was sub-optimal for evaluating such a deliver system, since others had shown the HA scaffolds to be compatible with AV delivery for BMP-2 expression [61]. The bone induction capability of the AV was even improved as compared to freely administered AVs in the latter case. This highlights the need to employ scaffolds even for viral delivery systems, but it is likely that scaffolds will require tailoring for particular delivery systems, and a 'universal' scaffold serving all delivery systems is not imaginable to us.

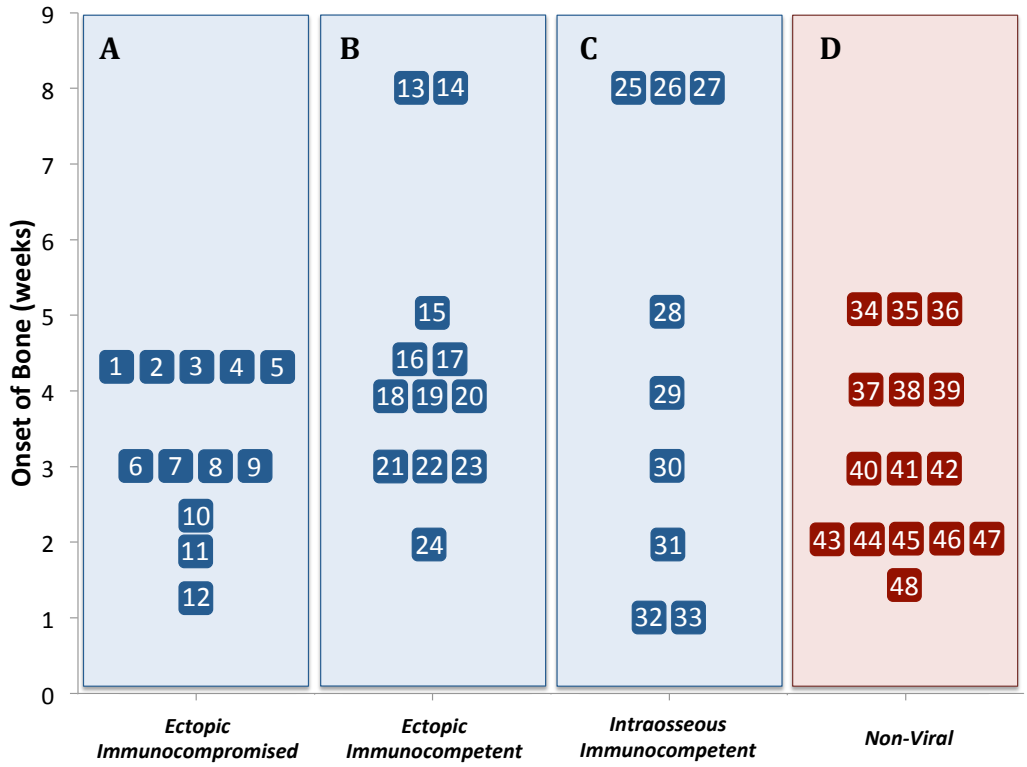

1	Li, 2003a	**17**	Li, 2003a	**33**	Ashinoff, 2004
2	Li, 2003a	**18**	Gafni, 2004	**34**	Sheyn, 2008
3	Li, 2003a	**19**	Nasu, 2009	**35**	Kimelman, 2011
4	Li, 2003a	**20**	Gonda, 2000	**36**	Sheyn, 2008
5	Li, 2003a	**21**	Varady, 2001	**37**	Itaka, 2007
6	Jane, 2002	**22**	Jane, 2002	**38**	Oda, 2008
7	Okubo, 2000	**23**	Chen, 2003	**39**	Fang, 1996
8	Chen, 2002	**24**	Sonobe, 2004	**40**	Geiger, 2005
9	Kaihara, 2004	**25**	Egermann, 2006b	**41**	Ono, 2004
10	Alden, 1999	**26**	Betz, 2007a	**42**	Huang, 2005
11	Okubo, 2001a	**27**	Betz, 2007b	**43**	Osawa, 2009
12	Li, 2003c	**28**	Hu, 2007	**44**	Kishimoto, 2002
13	Chen, 2004	**29**	Ishihara, 2008	**45**	Osawa, 2010
14	Luk, 2003	**30**	Ishihara, 2008	**46**	Bright, 2006
15	Kang, 2004	**31**	Rundle, 2003	**47**	Bonadio, 1999
16	Li, 2003a	**32**	Tarkka, 2003	**48**	Kawai, 2009

Figure 1-7: Onset of bone formation with gene-based therapeutics. For studies involving viral delivery, the onset of bone formation is categorized into ectopic implantations in immunocompromised animals (**A**), ectopic implantations in immunocompetent animals (**B**), and intraosseous defects in

immunocompetent animals (**C**). Studies involving non-viral delivery (**D**) are in immunocompetent animals. In some studies, a limited number of time-points were investigated such that some points may overestimate the time for onset of bone formation. The Table below summarizes the specific studies involved in this analysis.

1.6 PERSPECTIVE

Delivery of nucleic acid-based therapeutic agents for bone regeneration is an attractive option, but many obstacles remain for a successful clinical therapy. Although bone induction has been observed with small amounts of pDNA [69], clinically significant results such as bridging of critical-size defects remain challenging without employing large amounts of pDNA. Developing more effective gene delivery strategies will aid in this goal, but this requires a better understanding of not only the pharmacokinetics of delivery formulations but also the pharmacodynamics of transgene expression both in the form of protein production and resultant tissue response. Since the success of a delivery system ultimately depends on the amount of protein produced at the local site, further examination and quantitation of recombinant protein expression is needed. Many studies use indirect measures to gauge transfection efficiencies, such as mRNA expression or biological changes known to be associated with the transgene. The presence of pDNA or mRNA may suggest production of the protein therapeutic, but both have been shown to persist longer than the protein itself [17]. Biological changes, such as extent of angiogenesis or newly induced bone, are highly dependent on surrounding environment, and can significantly miss-judge protein expression depending on the preclinical model.

The microenvironment at the repair site is obviously different from a prototypical cell culture environment; there is no guarantee that the effective

carriers (and delivery formulations) optimized *in vitro* will be most effective for *in vivo* use. Comparison of *in vivo* gene delivery efficiencies of different carriers is crucial for continued advancement of gene-based therapies. Transfections in monolayer culture may not realistically represent the efficiency of a delivery system, but transfection in three-dimensional scaffolds may better mimic the events at repair sites. However, clearance of delivery systems *in vivo* (i.e., release from scaffold and subsequent transport away from the site by diffusion and/or vascular system) is difficult to reproduce in any culture system, and may be the primary reason for failure of gene delivery *in vivo*. The risks associated with virus-based gene delivery systems have been recognized and resulted in many exclusion criteria in clinics for patients' own safety. For example, because AV can be associated with liver toxicity, patients with impaired liver function are not well-suited for viral therapy. Immunodeficient patients or patients with viral infections such as hepatitis possess similar grounds for exclusion. The non-viral pDNA-based delivery is not as limiting, but transfection efficiency of naked pDNA is likely going to be very low (based on data from preclinical models) and the amount of administered pDNA accordingly high. Development of efficient and safe synthetic carriers will obviate the shortcomings of viral systems and naked pDNA delivery.

The miRNA and siRNA based approaches have untapped potential at this stage, but require a more thorough understanding of effective molecular pathways during healing to identify the appropriate and effective targets.

They face similar delivery challenges with respect to development of carriers that are effective *in vivo*. With siRNA, effective carriers have been intensely explored in cancer therapeutics field [7], but this expertise remains to be translated into bone therapeutics. It is likely that some of the effective carriers used for anti-cancer therapy will be effective in delivering siRNA to stimulate bone repair. Delivering microRNAs or oligonucleotides capable of modulating intracellular microRNAs is at infancy, with no animal studies reported to-date. As a starting point, carriers employed in pDNA delivery may be employed for RNAi molecules, since our experience indicate that carriers effective for pDNA are also effective in siRNA delivery. Whether that holds true for microRNA or oligonucleotides is unknown at this stage; differences in the way oligonucleotides interact with synthetic carriers are known [140,144], which suggest that optimal delivery formulations might need to be tailored for each class of nucleic acids. Non-specific physical methods (electroporation and sonoporation) might provide more effective delivery initially in the absence of experience with synthetic carriers.

Finally, identifying the most potent gene or gene combinations is paramount for clinical translation. Although BMP-2 and BMP-7 (OP-1) are the only proteins used for clinical bone regeneration, and may represent the initial choice for gene delivery, more potent proteins were recently identified that may allow for a greater response with lower amounts [4]. Due to crucial role of vascularization in new bone formation, angiogenic proteins can enhance bone formation [21]. In particular, Vascular Endothelial Growth

Factor (VEGF) [151] and bFGF [60,117] have been shown to be beneficial on their own for osteogenesis, and in combinations with BMPs [130,165]. Angiogenic genes have been delivered in clinical studies, but not in the context of bone regeneration. VEGF expressing AVs have been delivered for treatment of coronary heart diseases [41] and end stage renal disease [2], while pDNA expressing VEGF have been injected for treatment of diabetic neuropathy [160], critical limb ischemia [161]. pDNA expression bFGF has similarly been used for no-option coronary disease [9]. The effect(s) of osteogenic-angiogenic combinations, however, might be closely linked to the delivery mode; while BMP-2 gene delivery benefited from VEGF protein co-delivery (in the form of accelerated bone deposition), delivering VEGF gene along with BMP-2 gene did not offer an obvious benefit in a canine dental implant model [103]. Slower expression of VEGF (compared to readily available protein) presumably did not provide a robust angiogenic activity in that study. A combination of AV-based BMP-7 and PDGF-B (as a mitogen) expression systems, on the other hand, was found to provide a synergistic activity in the same animal model, enhancing bone deposition around dental implants [177], clearly highlighting the importance of the gene combinations chosen. Other proteins associated with canonical osteogenic pathways, such as BMP-6 [150], BMP-9 [104] and Wnt [114], have been investigated for regenerative therapy, but their gene delivery remains to be explored in detail. Four and half lim protein-2 (FHL2) and Lim mineralization proteins 1 and 3 (LMP 1 and LMP3) are recently investigated proteins that were shown

to induce bone regeneration [87,163]. LMP-1 and LMP-3 can also act synergistically with BMPs [16,98]. NEL-like molecule-1 (Nell-1) is another molecule under investigation for its osteogenic properties in repair of large segmental defects [96,100,152]. Nell-1 was shown to be as effective as BMP-2 in repair of critical-size defect [3], and also work synergistically with BMPs [4] that are endogenously expressed at the defect site. These proteins and, their combinations, are expected to provide further leads in aiding or even replacing BMPs in functional bone regeneration.

1.7 REFERENCES

1. Abarrategi A, Moreno-Vicente C, Martinez-Vasquez FJ, Civantos A, Ramos V, Sanz-Casado JV, Martinez-Corria R, Perera FH, Mulero F, Miranda P, Lopez-Lacomba JL. Biological properties of solid free form designed ceramic scaffolds with BMP-2: in vitro and in vivo evaluation. PLoS One 2012;7(3):e34117.
2. Adenovirus vascular endothelial growth factor (VEGF) therapy in vascular access-Novel trinam again control evidence (AdV-VANTAGE) (2012) from US National Institutes of Health http://clinicaltrials.gov/ct2/show/NCT00895479?term=VEGF+gene+therapy&rank=24 Accessed on October 8, 2012.
3. Aghaloo T, Cowan CM, Chou YF, Zhang X, Lee H, Miao S, Hong N, Kuroda S, Wu B, Ting K, Soo C. Nell-1-induced bone regeneration in calvarial defects. Am J Pathol 2006;169(3):903-15.
4. Aghaloo T, Cowan CM, Chou YF, Zhang X, Freymiller E, Soo C, Wu B, Ting K, Zhang Z. Effect of NELL1 and bone morphogenetic protein-2 on calvarial bone regeneration. J Oral Maxillofac Surg 2010;68(2):300-8.

5. Alden T, Pittman D, Hankins F, Beres E, Engh J, Das S, Hudson S, Kerns K, Kallmes D, Helm G. In vivo endochondral bone formation using a bone morphogenetic protein 2 adenoviral vector. Hum Gene Ther 1999;10(13):2245-53.
6. Alden T, Beres E, Laurent J, Engh J, Das S, London S, Jane J, Hudson S, Helm G. The use of bone morphogenetic protein gene therapy in craniofacial bone repair. J Craniofac Surg 2000;11(1): 24-30.
7. Aliabadi HM, Landry B, Sun C, Tang T Uludag H. Supramolecular assemblies in functional siRNA delivery: where do we stand? Biomaterials 2012;33(8):2546-69.
8. Andrew J, Hoyland J, Andrew S, Freemont A, Marsh D. Demonstration of TGF-beta 1 mRNA by in situ hybridization in normal human fracture healing. Calcif Tissue Int 1993;52(2):74-78.
9. Angiogenesis using VEGF-A165/bFGF plasmid delivered percutaneously in no-option CAD patients; A controlled trial (VIF-CAD) (2012) from the US National Institutes of Health < http://clinicaltrials.gov/ct2/show/NCT00620217?term=bFGF+gene+therapy&rank=1>. Accessed October 8, 2012.
10. Ashinoff R, Cetrulo C, Galiano R, Dobryansky M, Bhatt K, Ceradini D, Michaels J, McCarthy J, Gurtner G. Bone morphogenic protein-2 gene therapy for mandibular distraction osteogenesis. Ann Plast Surg 2004;52(6):585-90.
11. Bae Y, Yang T, Zeng HC, Campeau PM, Chen Y, Bertin T, Dawson BC, Munivez E, Tao J, Lee BH. miRNA-34c regulates Notch signalling during bone development. Hum Mol Genet 2012;21(13):2991-3000.
12. Banfi A, Muraglia A, Dozin B, Mastrogiacomo M, Cancedda R, Quarto R. Proliferation kinetics and differentiation potential of ex vivo expanded human bone marrow stromal cells: implications for their use in cell therapy. Exp Hematol 2000;28(6):707-6.

13. Betz V, Betz O, Glatt V, Gerstenfeld L, Einhorn T, Bouxsein M, Vrahas M, Evans C. Healing of segmental bone defects by direct percutaneous gene delivery: effect of vector dose. Hum Gene Ther 2007a;18(10):907-15.
14. Betz O, Betz V, Nazarian A, Egermann M, Gerstenfeld L, Einhorn T, Vrahas M, Bouxsein M, Evans C. Delayed administration of adenoviral BMP-2 vector improves the formation of bone in osseous defects. Gene Therapy 2007b; 14:1039-1044.
15. Bluml S, Bonelli M, Niederreiter B, Puchner A, Layr G, Hayer S, Koenders MI, van den Berg WB, Smolen J, Redlich K. Essential role of microRNA-155 in the pathogenesis of autoimmune arthritis in mice. Arthritis Rheum 2011;63(5):1281-8.
16. Boden SD, Liu Y, Hair GA, Helms JA, Hu D, Racine M, Nanes MS, Titus L. LMP-1, a LIM-domain protein, mediates BMP-6 effects on bone formation. Endocrinology 1998;139(12):5125-34.
17. Bonadio J, Smiley E, Patil P, Goldstein S. Localized, direct plasmid gene delivery in vivo: prolonged therapy results in reproducible tissue regeneration. Nature Medicine 1999;5(7):753-759.
18. Bourque W, Gross M, Hall B. Expression of four growth factors during fracture repair. Int J Dev Biol 1993;37:573-579.
19. Bright C, Park YS, Sieber AN, Kostuik JP, Leong KW. In vivo evaluation of plasmid DNA encoding OP-1 protein for spine fusion. Spine 2006;31:2163.
20. Cahill K, Chi J, Day A, Claus E. Prevalence, complications, and hospitals charges associated with use of Bone Morphogenetic Proteins in spinal fusion procedures. JAMA 2009;302(1):58-66.
21. Carano R, Filvaroff E. Angiogenesis and bone repair. Drug Delivery Today 2003;8(21):980-989.
22. Carragee EJ, Hurwitz EL, Weiner BK. A critical review of recombinant human bone morphogenetic protein-2 trials in spinal surgery: emerging safety concerns and lessons learned. Spine J 2011;11(6):471-91.

23. Chang P, Seol Y, Cirelly J, Pellegrini G, Jin Q, Franco L, Goldstein S, Chandler L, Sosnowski B, Giannobile. PDGF-B gene therapy accelerates bone engineering and oral implant osseointegration. Gene Ther 2010;17(1):95-104.
24. Chen C, Uludag H, Wang Z, Jiang H. Noggin suppression decreases BMP-2-induced osteogenesis of human bone marrow-derived mesenchymal stem cells in vitro. J Cell Biochem 2012;113(12):3672-80.
25. Chen Y, Cheung K, Kung H, Leong J, Lu W, Luk K. In vivo new bone formation by direct transfer of adenoviral-mediated bone morphogenetic protein-4 gene. Biochem Biophys Res Commun 2002;298(1):121-127.
26. Chen Y, Luk K, Cheung K, Xu R, Lin M, Lu W, Leong J, Kung H. Gene therapy for new bone formation using adeno-associated viral bone morphogenetic protein-2 vectors. Gene Therapy 2003;10:1345-1353.
27. Chen Y, Luk K, Cheung K, Lu A, An X, Ng S, Lin M, Kung H. Combination of adeno-associated virus and adenovirus vectors expressing bone morphogenetic protein-2 produces enhanced osteogenic activity in immunocompetent rats. Biochem Biophys Res Commun 2004;317(3):675-81.
28. Cherng JY, Talsma H, Crommelin DJ, Hennink WE. Long term stability of poly((2-dimethylamino)ethyl methacrylate)-based gene delivery systems. Pharm Res 1999;16(9):1417-23.
29. Chew SA, Kretlow JD, Spicer PP, Edwards AW, Baggett LS, TAbata Y, Kasper FK, Mikos AG. Delivery of plasmid DNA encoding bone morphogenetic protein-2 with a biodegradable branched polycationic polymer in a critical-size rat defect model. Tissue Eng Part A 2011;17(5-6):751-63.
30. Cook E, Cook J. Bone graft substitutes and allografts for reconstruction of the foot and ankle. Clin Podiatr Med Surg 2009;26:589-605.
31. Croyle MA, Roessler BJ, Davidson BL, Hilfinger JM, Amidon GL. Factors that influence stability of recombinant adenoviral preparations for human gene therapy. Pharm Dev Technol 1998;3(3):373-83.

32. Croyle MA, Cheng X, Wilson JM. Development of formulations that enhance physical stability of viral vectors for gene therapy. Gene Ther 2001;8(17):1281-1290.
33. Del Pozo-Rodriguez A, Solinis MA, Gascon AR, Pedraz JL. Short- and long-term stability study of lyophilized solid lipid nanoparticles for gene therapy. Eur J Pharm Biopharm 2009;71:181-189.
34. Dmitriev AE, Lehman RA Jr, Symes AJ. Bone morphogenetic protein-2 and spinal arthrodesis: the basic science perspective on protein interaction with the nervous system. Spine J. 2011;11(6):500-5.
35. Dunn C, Jin Q, Taba M, Franceschi R, Bruce Rutherford R, Giannnobile W. BMP gene delivery for alveolar bone engineering at dental implant defects. Mol Ther 2005;11(2):294-9.
36. Dupont KM, Boerckel JD, Stevens HY, Diab T, Kolambkar YM, Takahata M, Schwarz EM, Guldberg RE. Synthetic scaffold coating with adeno-associated virus encoding BMP2 to promote endogenous bone repair. Cell Tissue Res 2012; 347(3):575-88.
37. Edelstein M, Abedi M, Wixon J. Gene therapy clinical trials worldwide to 2007-an update. J Gene Med 2007;9(10):833-842.
38. Edelstein ML, Abedi MR, Wixon J, Edelstein RM. Gene therapy clinical trials worldwide 1989-2004-an overview. J Gene Med 2004; 6(6):597-602.
39. Egermann M, Baltzer A, Adamaszek S, Evans C, Robbins P, Schneider E, Lill C. Direct adenoviral transfer of bone morphogenetic protein-2 cDNA enhances fracture healing in osteoporotic sheep. Hum Gene Ther 2006a;17(5):507-17.
40. Egermann M, Lill C, Griesbeck K, Evans C, Robbins P, Schneider E, Baltzer A. Effect of BMP-2 gene transfer on bone healing in sheep. Gene Ther 2006b;13(17):1290-9.
41. Endocardial Vascular Endothelial Growth Factor-D (VEGF-D) gene therapy for treatment of sever coronary heart disease (KAT301) (2012) from the US National Institutes of Health

http://clinicaltrials.gov/ct2/show/NCT01002430?term=VEGF+gene+therapy&rank=4 Accessed October 8, 2012.

42. Eskildsen T, Taipaleenmaki H, Stenvang J, Abdallah BM, Ditzel N, Nossent AY, Bak M, Kauppinen S, Kassam M. MicroRNA-138 regulates osteogenic differentiation of human stromal (mesenchymal) stem cells in vivo. Proc Natl Acad Sci USA 2011;108(15):6139-44.
43. Evans CH. Gene delivery to bone. Adv Drug Deliv Rev 2012;64(12):1331-40.
44. Fang J, Zhu YY, Smiley E, Bonadio J, Rouleau J, Goldstein S, McCauley L, Davidson B, Roessler B. Stimulation of new bone formation by direct transfer of osteogenic plasmid genes. Proc Natl Acad Sci USA 1996;93:5753.
45. Feidler J, Roderer G, Gunther K, Brenner R. BMP-2, BMP-4 and PDGF-bb stimulate chemotactic migration of primary human mesenchymal progenitor cells. J Cell Biochem 2002;87(3):305-12.Fink D, DeLuca N, Yamada M, Wolfe D, Glorioso J. Design and application of HSV vectors for neuroprotection. Gene Ther. 2000;7(2):115-9.
46. Fischer W, Quadir MA, Barnard A, Smith DK, Haag R. Controlled release of DNA from photoresponsive hyperbranched polyglycerols with oligoamine shells. Macromol Biosci 2011;11(12):1736-46.
47. Friedlaender G, Perry C, Cole JD, Cook S, Cierny G, Muscheler G, Zych G, Calhoun J, LaForte A, Yin S. Osteogenic protein-1 (bone morphogenetic protein-7) in the treatment of tibial nonunions. J Bone Joint Surg Am 2001;83-A Suppl 1:S151-158.
48. Gafni Y, Pelled G, Zilberman Y, Turgeman G, Apparailly F, Yotvat H, Galun E, Gazit Z, Jorgensen C, Gazit D. Gene therapy platform for bone regeneration using an exogenously regulated, AAV-2-based gene expression system. Mol Ther 2004;9(4):587-95.
49. Geiger F, Betram H, Berger I, Lorenz H, Wall O, Eckhardt C, Simank HG, Richter W. Vascular endothelial growth factor gene-activated matrix

(VEGF165-GAM) enhances osteogenesis and engiogenesis in large segmental bone defects. J Bone Miner Res 2005;20:2028.

50. Gene therapy clinical trials worldwide. J Gene Med 2012. < http://www.abedia.com/wiley/vectors.php> Accessed on October 10, 2012
51. Giannoudis P, Dinopoulos H, Tsiridis E. Bone substitutes: an update. Injury 2005;36S:S20-27.
52. Gonda K, Nakaoka T, Yoshimura K, Otawara-Hamamoto Y, Harrii K. Heterotopic ossification of degenerating rat skeletal muscle induced by adeno-virus mediated transfer of bone morphogenetic protein-2 gene. J Bone Miner Res 2000;15(6):1056-65.
53. Govender S, Csimma C, Genant HK, Valentin-Opran A. Recombinant human bone morphogenetic protein-2 for treatment of open tibial fractures. J Bone Joint Surg Am 2002;84(12):2123-2134.
54. Guo H, Ingolia NT, Weissman JS, Bartel DP. Mammalian microRNAs predominantly act to decrease target mRNA levels. Nature 2010;466(7308):835-40.
55. Helm G, Alden T, Beres E, Hudson S, Das S, Engh J, Pittman D, Kern K, Kallmes D. Use of bone morphogenetic protein-9 gene therapy to induce spinal arthrodesis in the rodent. J Neurosurg 2000;92(2S):191-6.
56. Hemmi H, Takeuchi O, Kawai T, Kaisho T, Sat S, Sanjo H, Matsumoto M, Hoshino K, Wagner H, Takeda K, Akira S. A Toll-like receptor recognizes bacterial DNA. Nature 2000;408:740-745.
57. Histing T, Marciniak K, Scheuer C, Garcia P, Holstein JH, Klein M, Matthys R, Pohlemann T, Menger MD. Sildenafil accelerates fracture healing in mice. J Orthop Res 2011;29(6):867-73.
58. Hobel S, Prinz R, Malek A, Urban-Klein B, Sitterberg J, Bakowsky U, Czubayko F, Aigner A. Polyethylenimine PEI F25-LMW allows the long-term storage of frozen complexes as fully active reagents in siRNA-mediated gene targeting and DNA delivery. Eur J Pharm Biopharm 2008;70:29-41.

59. Holzwarth JM, Ma PX. Biomimetic nanofibrous scaffolds for bone tissue engineering. Biomaterials 2011; 32(36):9622-9.
60. Hong KS, Kim EC, Bang SH, Chung CH, Lee YI, Hyun JK, Lee HH, Jang JH, Kim TI, Kim HW. Bone regeneration by bioactive hybrid membrance containing FGF2 within rat calvarium. J Biomed Mat Res 2010; 94A(4):1187-1194.
61. Hu WW, Wang Z, Hollister SJ, Krebsbach PH. Localized viral vector delivery to enhance in situ regeneration gene therapy. Gene Ther 2007;12(11):891-901.
62. Hu X, Zhang X, Dai L, Zhu J, Jia Z, Wang W, Zhou C, Ao Y. Histone deacetylase inhibitor trichostatin A promotes osteogenic differentiation of adipose-derived stem cells by altering the epigenetic modifications on Runx2 promoter in a BMP signalling-dependent manner. Stem Cells Dev 2013;22(2):248-55.
63. Huang J, Zhao L, Xing L, Chen D. MicroRNA-204 regulates Runx2 protein expression and mesenchymal progenitor cell differentiation. Stem Cells 2010;28(2):357-64.
64. Huang YC, Simmons C, Kaigler D, Rice KG, Mooney DJ. Bone regeneration in a rat cranial defect with delivery of PEI-condensed plasmid DNA encoding for bone morphogenetic protein-4 (BMP-4). Gene Therapy 2005; 12:418.
65. Ideno H, Takanabe R, Shimada A, Imaizumi K, Araki R, Abe M, Nifuji A. Protein related to DAN and cerberus (PRDC) inhibits osteoblastic differentiation and its suppression promotes osteogenesis in vitro. Exp Cell Res 2009;315(3):474-84.
66. Inose H, Ochi H, Kimura A, Fujita K, Sato S, Iwasaki M, Sunamura S, Takeuchi Y, Fukumoto S, Saito K, Nakamura T, Siomi H, Ito H, Arai Y, Shinomiya K, Takeda S. A microRNA regulatory mechanism of osteoblast differentiation. Proc Natl Acad Sci USA 2009;106(49):20794-9.
67. Ishihara A, Shields K, Litsky A, Mattoon J, Weisbrode S, Bartlett J, Bertone A. Osteogenic gene regulation and relative acceleration of healing by

adenoviral-mediated transfer of human BMP-2 or -6 in equine osteotomy and ostectomy models. J Orthop Res 2008;26(6):764-71.

68. Ishihara A, Zekas L, Weisbrode S, Bertone A. Comparative efficacy of dermal fibroblast-mediated and direct adenoviral bone morphogenetic protein-2 gene therapy for bone regeneration in an equine rib model. Gene Ther 2010;17(6):733-44.
69. Itaka K, Ohba S, Miyata K, Kawaguchi H, Nakamura K, Takato T, Chung U, Kataoka K. Bone regeneration by regulated in vivo gene transfer using biocompatible polyplex nanomicelles. Molecular Therapy 2007;15(9):1655.
70. Jane J, Dunford B, Kron A, Pittman D, Sasaki T, Li J, Li H, Alden T, Dayoub H, Hankins G, Kallmes D, Helm G. Ectopic osteogenesis using adenoviral bone morphogenetic protein (BMP)-4 and BMP-6 gene transfer. Mol Ther 2002;6(4):464-70.
71. Jin Q, Anusaksathien O, Webb S, Printz M, Giannobile W. Engineering of tooth-supporting structures by delivery of PDGF gene therapy vectors. Mol Ther 2004;9:519-526.
72. Jopling C, Boue S, Izpisua Belmonte JC. Dedifferentiation, transdifferentiation and reprogramming: three routes to regeneration. Nat Rev Mol Cell Biol. 2011, 12(2):79-89.
73. Kaihara S, Dessho K, Okubo Y, Sonobe J, Kawai M, IIzuka T. Simple and effective osteoinductive gene therapy by local injection of a bone morphogenetic protein-2-expressing recombinant adenoviral vector and FK506 in rats. Gene Therapy 2004;11:439-447.
74. Kang Q, Sun M, Cheng H, Peng Y, Montag A, Deyrup A, Jiang W, Luu H, Luo J, Szatkowski J, Vanichakarn P, Park J, Li Y, Haydon R, He T. Characterization of the distinct orthotopic bone formting activity of 14 BMPs using recombinant adenovirus-mediated gene delivery. Gene Ther 2004;11(17):1312-20.

75. Kass-Eisler A, Leinwand L, Gall J, Bloom B, Falck-Pedersen E. Circumventing the immune response to adenovirus-mediated gene therapy. Gene Ther 1996;3(2):154-62.
76. Kawai M, Maruyama H, Bessho K, Yamamoto H, Miyazaki J, Yamamoto T. Simple strategy for bone regeneration with a BMP-2/7 gene expression cassette vector. Biochem Biophys Res Commun 2009;390(3):1012-7.
77. Khosla S, Westendorf JJ, Oursler MJ. Building bone to reverse osteoporosis and repair fractures. J Clin Invest. 2008, 118(2):421-8.
78. Kim KM, Park SJ, Jung SH, Kim EJ, Jogeswar G, Ajita J, Rhee Y, Kim CH, Lim SK. miR-182 is a negative regulator or osteoblast proliferation, differentiation, and skeletogenesis through targeting FoxO1. J Bone Miner Res 2012;27(8):1669-79.
79. Kim M, Kim C, Choi YS, Kim M, Park C, Suh Y. Age-related alterations in mesenchymal stem cells related to shift in differentiation from osteogenic to adipogenic potential: implication to age-associated bone diseases and defects. Mech Ageing Dev 2012;133(5):215-25.
80. Kim YJ, Bae SW, Yu SS, Bae YC, Jung JS. miRNA-196a regulates proliferation and osteogenic differentiation in mesenchymal stem cells derived from human adipose tissue. J Bone Miner Res 2009;24(5):816-25.
81. Kimelman-Bleich N, Pelled G, Zilberman Y, Kallai I, Mizrahi O, Tawackoli W, Gazit Z, Gazit D. Targeted gene-and-host progenitor cell therapy for nonunion bone fracture repair. Mol Ther 2011;19(1):53-9.
82. Kimelman Bleich N, Kallai I, Lieberman JR, Schawrz EM, Pelled G, Gazit D. Gene therapy approaches to regenerating bone. Adv Drug Deliv Rev 2012;64(12):1320-30.
83. Kishimoto K, Watanabe Y, Nakamura H, Kokubun S. Ectopic bone formation by electroporatic transfer of bone morphogenetic protein-4 gene. Bone 2002;31(2):340-347.
84. Kloen P, Lauzier D, Hamdy RC. Co-expression of BMPs and BMP-inhibitors in human fractures and non-unions. Bone 2012;51(1):59-68.

85. Kolk A, Haczek C, Koch C, Vogt S, Kullmer Pautke C, Deppe H, Plank C. A strategy to establish a gene-activated matrix on titanium using gene vectors protected in a polylactide coating. Biomaterials 2011;32(28):6850-9.
86. Krieg A. CpG Motifs in bacterial DNA and their immune effects. Annu Rev Immunol 2002;20:709-760.
87. Lai CF, Bai S, Uthgenannt BA, Halstead LR, McLoughlin P, Schafer BW, Chu PH, Chen J, Otey CA, Cao X, Cheng SL. Four and half lim protein 2 (FHL2) stimulates osteoblast differentiation. J Bone Miner Res 2006;21(1):17-28.
88. Lai YL, Kuo NC, Hsiao WK, Yew TL, Lee SY, Chen HL. Intramarrow bone morphogenetic protein 4 gene delivery enhances early implant stability in femurs of ovariectomized rabbits. J Periodontol 2011;82(7):1043-50.
89. Leachman SA, Hickerson RP, Schwartz ME, Bullough EE, Hutcherson SL, Boucher KM, Hansen CD, Eliason MJ, Srivatsa GS, Kornbrust DJ, Smith FJ, McLean WI, Milstone LM, Kaspar RL. First-in-human mutation-targeted siRNA phase 1b trial of an inherited skin disorder. Mol Ther 2010;18(2):442-6.
90. Levy O, Ruvinov E, Reem T, Granot Y, Cohen S. Highly efficient osteogenic differentiation of human mesenchymal stem cells by eradication of STAT3 signaling. Int J Biochem Cell Biol 2010;42(11):1823-30.
91. Li D, Wang W, Guo R, Qi YY, Gou ZR, Gao CY. Restoration of rat calvarial defects by poly(lactide-co-glycoled)/hydroxyapatite scaffolds loaded with bone mesenchymal stem cells and DNA complexes. Chin Sci Bull 2012;57:435-444.
92. Li H, Xie H, Liu W, Hu R, Huang B, Tan YF, Liao EY, Kang X, Sheng ZF, Zhou HD, Wu XP, Luo XH. A novel microRNA targeting HDAC5 regulates osteoblast differentiation in mice and contributes to primary osteoporosis in humans. J Clin Invest 2009;119(12):3666-3677
93. Li J, Li H, Sasaki T, Holman D, Beres B, Dumont J, Pittman D, Hankins G, Helm G. Osteogenic potential of five different recombinant human bone

morphogenetic protein adenoviral vectors in rat. Gene Therapy 2003a;10:1735-1743.

94. Li J, Dunford B, Holman D, Beres B, Pittman D, Hankins G, Helm G. Rat strain differences in the ectopic osteogenic potential of recombinant human BMP adenoviruses. Mol Ther 2003b; 8(5):822-9.
95. Li J, Hankins G, Kao C, Li H, Kammauff J, Helm G. Osteogenesis in rats induced by a novel recombinant helper-dependent bone morphogenetic protein-9 (BMP-9) adenovirus. J Gene Med 2003c; 5(9):748-56.
96. Li W, Zawa JN, Siu RK, Lee M, Aghaloo T, Zhang X, Wu BM, Gertzman AA, ting K, Soo C. Nell-1 enhances bone regeneration in a rat critical-sized remoral defect model. Plast Reconstr Surg 2011;127(2):580-87.
97. Li Z, Hassan MQ, Volinia S, van Wijnen AJ, Stein JL, Croce CM, Lian JB, Stein GS. A microRNA signature for a BMP2-induced osteoblast lineage commitment program. Proc Natil Acad Sci USA 2008;105(37):13906-11.
98. Lin Z, Rios HF, Park CH, Taut AD, Jin Q, Sugai JV, Robbins PD, Giannobile WV. LIM domain protein-3 (LMP3) cooperates with BMP7 to promote tissue regeneration by ligament progenitor cells. Gene Ther 2012. doi: 10.1038/gt.2011.203
99. Lindsey W. Osseous tissue engineering with gene therapy for facial bone reconstruction. Laryngoscope 2001;111(7):1128-36.
100. Lu SS, Zhang X, Soo C, Hsu T, Napoli A, Aghaloo T, Wu B, Tsou P, Ting K, Wang J. The osteoinductive properties of Nell-1 in a rat spinal fusion model. Spine J 2007;7(1):50-60.
101. Luan J, Cui Y, Zhang Y, Zhou X, Zhang G, Han J. Effect of CXCR4 inhibitor AMD100 on alkaline phosphatase activity and mineralization in osteoblastic MC3T3-E1 cells. Biosci Trend 2012;6(2):63-9.
102. Luk K, Chen Y, Cheung K, Kung H, Lu W, Leong J. Adeno-associated virus-mediated bone morphogenetic protein-4 gene therapy for in vivo bone formation. Biochem Biophys Res Commun 2003;308(3):636-45.
103. Luo T, Zhang W, Shi B, Cheng X, Zhang Y. Enhanced bone regeneration around dental implant with bone morphogenetic protein 2 gene and

vascular endothelial growth factor protein delivery. Clin Oral Implants Res 2012;23(4):467-73.

104. Luther G, Wagner ER, Zhu G, Kang Q, Luo Q, Lamplot J, Bi Y, Luo X, Luo J, Teven C, Shi Q, Kim SH, Gao JL, Huang E, Yang K, Rames R, Liu X, Li M, Hu N, Liu H, Su Y, Chen L, He BC, Zuo GW, Deng ZL, reid RR, Luu HH, Haydon RC, He TC. BMP-9 induced osteogenic differentiation of mesenchymal stem cells: molecular mechanism and therapeutic potential. Curr Gene Ther 2011;11(3):229-40.
105. Manaka T, Suzuki A, Takayama K, Imai Y, Nakamura H, Takaoka K. Local delivery of siRNA using biodegradable polymer application to enhance BMP-induced bone formation. Biomaterials 2011;32(36):9642-8.
106. Marsh D, Li G. The biology of fracture healing: optimising outcome. British Medical Bulletin 1999;55(4):856-869.
107. McKay W, Peckham S, Badura J. A comprehensive review of recombinant human bone morphogenetic protein-2 (INFUSE® Bone Graft). International Orthopaedics 2007;31:729-734.
108. Mehara B, Saadeh P, Steinbrech D, Dudziak M, Spector J, Greenwald J, Gittes G, Longaker M. Adenovirus-mediated gene therapy of osteoblasts in vitro and in vivo. J Bone Miner Res 1999;14(8):1290-301.
109. Meilander NJ, Pasumarthy MK, Kowalczyk, Cooper MJ, Bellamkonda RV. Sustained release of plasmid DNA using lipid microtubules and agarose hydrogels. J Control Release 2003;88(2):321-31.
110. Menendez MI, Clark DJ, Carlton M, Flanigan DC, Jia G, Sammet S, Weisbrode SE, Knopp MV, Bertone AL. Direct delayed human adenoviral BMP-2 or BMP-6 gene therapy for bone and cartilage regeneration in a pony osteochondral model. Osteoarthritis Cartilage 2011;19(8):1066-75.
111. Merdan T, Kunath K, Petersen H, Bakowsky U, Voigt KH, Kopecek J, Kissel T. PEGylation of poly(ethylene imine) affects stability of complex with plasmid DNA under in vivo conditions in a dose-dependent manner after intravenous injection into mice. Bioconjugate Chem 2005;16:785-792.

112. Meyerrose T, Olson S, Pontow S, Kalomoiris S, Jung Y, Annett G, Bauer G, Nolta JA. Mesenchymal stem cells for the sustained in vivo delivery of bioactive factors. Adv Drug Deliv Rev 2010;62(12):1167-1174.
113. Miele E, Spinelli GP, Miele E, Fabrizio E, Ferretti E, Tomao S, Gulino A. Nanoparticle-based delivery of small interfering RNA: Challenges for cancer therapy. Int J Nanomedicine 2012;7:3637-57.
114. Minear S, Leucht P, Jiang J, Liu B, Zeng A, Fuerer C, Nusse R, Helms JA. Wnt proteins promote bone regeneration. Sci Transl Med. 2010, 2(29):29ra30.
115. Miyai K, Yoneda M, Hasegawa U, Toita S, Izu Y, Hemmi H, Hayata T, Ezura Y, Mizutani S, Miyazono K, Akiyoshi, Yamamoto T, Noda M. ANA deficiency enhances bone morphogenetic protein-induced ectopic bone formation via transcriptional events. J Biol Chem 2009;284(16):10953-600.
116. Moriguchi R, Kogure K, Iwasa A, Akita H, Harashima H. Non-linear pharmacodynamics in a non-viral gene delivery system: positive non-linear relationship between dose and transfection efficiency. J Control Release 2006;110(3):605-9.
117. Nakamura T, Hanada K, Tamura M, Shibanushi T, Nigi H, Tagawa M, Fukumoto S, Matsumoto T. Stimulation of endosteal bone formation by systemic injections of recombinant basic fibroblast growth factor in rats. Endocrinology 1995;136:1276-1284.
118. Nasu T, Ito H, Tsutsumi R, Kitaori T, Takemoto M, Schwarz E, Nakamura T. Biological activation of bone-related biomaterials by recombinant adeno-associated virus vector. J Orthop Res 2009;27(9):1162-8.
119. Nathwani AC, Tuddenham EG, Rangarajan S, Rosales C, McIntosh J, Linch DC, Chowdary P, Riddell A, Pie AJ, Harrington C, O/Beirne J, Smith K, Pasi J, Glader B, Rustagi P, Ng CY, Kay MA, Zhou J, Spence Y, Morton CL, Allay J, Coleman J, Sleep S, Cunningham JM, Srivasta D, Basner-Tschakarjan E, Mingozzi F, High KA, Gray JT, Reiss UM, Nienhuis AW, Davidoff AM.

Adenovirus-associated virus-vector-mediated gene transfer in haemophilia B. N Engl J Med 2011;365(25):2357-65.

120. Neamnark A, Suwantong O, Bahadur R, Hsu C, Supaphol P, Uludag H. Aliphatic lipid substitution on 2 kDa polyethylenimine improves plasmid delivery and transgene expression. Mol Pharm 2009;6(6):1798-815.
121. Nejadnik MR, Mikos AG, Jansen JA, Leewenburgh SC. Facilitating the mineralization of oligo(poly(ethylene glycol) fumarate) hydrogel by incorporation of hydroxyapatite nanoparticles. J Biomed Mater Res A 2012;100(5):1316-23.
122. Oda M, Kuroda S, Kondo H, Kasugai S. Hydroxyapatite fiber material with BMP-2 gene induces ectopic bone formation. J Biomed Mat Res Part B 2009;90(1): 101.
123. Okubo Y, Bessho K, Fujimura K, Iizuka T, Miyatake S. Osteoinduction by bone morphogenetic protein-2 via adenoviral vector under transient immunosuppression. Biochem Biophys Res Commun 2000;267(1):382-7.
124. Okubo Y, Bessho K, Fujimura K, Kaihara S, Iizuka T, Miyatake S. The time course study of osteoinduction by bone morphogenetic protein-2 via adenoviral vector. Life Sci 2001a;70:325-336.
125. Okubo Y, Bessho K, Fujimura K, Iizuka T, Miyatake S. In vitro and in vivo studies of a bone morphogenetic protein-2 expressing adenoviral vector. J Bone Joint Surg Am 2001b;83-A:S99-104.
126. Ono I, Yamashita T, Jin HY, Ito Y, Hamada H, Akasaka Y, Nakasu M, Ogawa T, Jombow K. Combination of porous hydroxyapatite and cationic liposomes as a vector for BMP-2 gene therapy. Biomaterials 2004;25:4709-4718.
127. Osawa K, Okubo Y, Nakao K, Koyama N, Bessho K. Osteoinduction by microbubble-enhanced transcutaneous sonoporation of human bone morphogenetic protein-2. J Gene Med. 2009;11(7):633-41.
128. Osawa K, Okubo Y, Nakao K, Koyama N, Bessho K. Osteoinduction by repeat plasmid injection of human bone morphogenetic protein-2. J Gene Med 2010;12(12):937-44.

129. Parra-Guillen ZP, Gonzalez-Aseguinolaza G, Berraondo P, Troconiz IF. Gene Therapy: a pharmacokinetic/pharmacodynamics modelling overview. Pharm Res 2010;27(8):1487-97.
130. Patel ZS, Young S, Tabata Y, Jansen JA, Wong ME, Mikos AG. Dual delivery of an angiogenic and an osteogenic growth fractor for bone regeneration in a critical size defect model. Bone 2008;43(5):931-40.
131. Porter J, Ruckh T, Popat K. Bone tissue engineering: a review in bone biomimetics and drug delivery strategies. Biotechol Prog 2009;25(6):1539-1560.
132. Remaut K, Lucas B, RAemdonck K, Braeckmans K, Demeester J, De Smedt SC. Protection of oligonucleotides against enzymatic degradation by PEGylated and NonPEGylated branched polyethyleneimine. Biomacromolecules 2007;8:1333-1340.
133. Rifas L. The role of noggin in human mesenchymal stem cell differentiation. J Cell Biochem 2007;100)4):824-34.
134. Rios CN, Skoracki RJ, Mathur AB. GNAS1 and PHD2 short-interfering RNA support bone regeneration in vitro and in an in vivo sheep model. Clin Orthop Relat Res 2012;470(9):2541-53.
135. Rose L, Kucharski C, Uludag H. Protein expression following non-viral delivery of plasmid DNA coding for basic FGF and BMP-2 in a rat ectopic model. Biomaterials 2012;33(11):3363-74.
136. Rose L, Kucharski C, Aliabadi HM, Uludag H. Gelatin coatings to stabilize the transfection ability of nucleic acid polyplexes. Acta Biomaterialia 2013;9(7):7429-38.
137. Rujitanaroj PO, Jao B, Yang J, Wang F, Anderson JM, Wang J, Chew SY. Controlling fibrous capsule formation through long-term down-regulation of collagen type I (COL1A1) expression by nanofiber-mediated siRNA gene silencing. Acta Biomater 2013;9(1):4513-24.
138. Rundle C, Miyakoshi N, Kasukawa Y, Chen S, Sheng M, Wergedal J, Lau K, Baylink D. In vivo bone formation in fracture repair induced by direct

retroviral-based gene therapy with bone morphogenetic protein-4. Bone 2003;32(6):591-601.

139. Sakai S, Tamura M, Mishima H, Kojima H, Uemura T. Bone regeneration induced by adenoviral vectors carrying til-1/Cbfa1 genes implanted with biodegradable porous materials in animal models of osteonecrosis of the femoral head. J Tissue Eng Regen Med 2008;2(2-3):164-7.
140. Salcher EE, Kos P, Frohlich T, Badgujar N, Scheible M, Wagner E. Sequence-defined four-arm oligo(ehtanamino)amides for pDNA and siRNA delivery: impact of building blocks on efficacy. J Control Release 2012;164(3):380-6.
141. Satkauskas S, Ruzgys P, Venslauskas MS. Towards the mechanisms for efficient gene transfer into cells and tissues by means of cell electroporation. Expert Opin Biol Ther 2012;12(3):275-86.
142. Schek RM, Wilke EN, Hollister SJ, Krebsbach PH. Combined use of designed scaffolds and adenoviral gene therapy for skeletal tissue engineering. Biomaterials 2006;27(7):1160-6.
143. Schmid G, Kobayashi C, Sandell L, Ornitz D. Fibroblast growth factor expression during skeletal fracture healing in mice. Dev Dyn 2009; 238(3):766-774.
144. Scholz C, Wagner E. Therapeutic plasmid DNA versus siRNA delivery: common and different tasks for synthetic carriers. J Control Release 2012;161(2):554-65.
145. Sharma VK, Thomas M, Klibanov AM. Mechanistic studies on aggregation of polyethylenimine-DNA complexes and its prevention. Biotech Bioeng 2005;90(5):614-620.
146. Sheyn D, Kimelman-Bleich N, Pelled G, Zilberman Y, Gazit D, Gazit Z.: Ultrasound-based nonviral gene delivery induces bone formation in vivo. Gene Ther. 2008;15(4):257-66.
147. Shin S, Salvay DM, Shea LD. Lentivirus delivery by adsorption to tissue engineering scaffolds. J Biomed Mater Res A 2010;93(4):1252-9.

148. Singh S, Narang AS, Mahato RI. Subcellular fate and off-target effects of siRNA, shRNA, and miRNA. Pharm Res 2011;28(12):2296-3015.
149. Sonobe J, OkuboY, Kaihara S, Miyatake S, Bessho K. Osteoinduction by bone morphogenetic protein 2-expressing adenoviral vector: application of biomaterial to mask the host immune response. Hum Gene Ther 2004;15:659-668.
150. Soran Z, Aydin RS, Gumusderelioglu M. Chitosan scaffolds with BMP-6 loaded alginate microspheres for periodontal tissue engineering. J Microencapsul 2012;29(8):770-80.
151. Street J, Bao M, deGuzman L, Bunting S, Peale F, Ferrara N, Stelnmetz H, Hoeffel J, Cleland J, Daugherty A, van Bruggen N, Redmond H, Carano R, Filvaroff E. Vascular endothelial growth factor stimulates bone repair by promoting angiogenesis and bone turnover. PNAS 2002;99(15):9656-9661.
152. Strohbach C, Rundle C, Wergedal J, Chen S, Linkhart T, Lau K, Strong D. LMP-1 retroviral gene therapy influences osteoblast differentiation and fracture repair: a preliminary study. Calcif Tissue Int 2008;83(3):202-11.
153. Sugatani T, Hruska KA. MicroRNA-233 is a key factor in osteoclast differentiation. J Cell Biochem 2007;101(4):996-9.
154. Takayama K, Suzuki A, Manaka T, Taguchi S, Hashimoto Y, Imai Y, Wakitani S, Takaoka K. RNA interference for noggin enhances the biological activity of bone morphogenetic proteins in vivo and in vitro. J Bone Miner Metab 2009;27(4):402-11.
155. Tarkka T, Sipola A, Jamsa T, Soini Y, Yla-Herttuala S, Tuukkanen J, Hautala T. Adenoviral VEGF-A gene transfer induces angiogenesis and promotes bone formation in healing osseous tissues. J Gene Med 2003;5(7):560-6.
156. Trobridge G. Genotoxicity of retroviral hemaotopoietic stem cell gene therapy. Expert Opin Biol Ther 2011;11(5):581-93.
157. Uchida S, Sakai A, Kudo H, Otomo H, Watanuki M, Tanaka M, Nagashima M, Nakamura T. Vascular endothelial growth factor is expressed along

with its receptors during the healing process of bone and bone marrow after drill-hole injury in rats. Bone 2003;32:491-501.

158. Urist M. Bone formation by autoinduction. Science 1956;150:893-899
159. Varady P, Li J, Cunningham M, Beres E, Das S, Engh J, Alden T, Pittman D, Kerns K, Kallmes D, Helm G. Morphologic analysis of BMP-9 gene therapy-induced osteogenesis. Hum Gene Ther 2001;12(6):697-710.
160. VEGF gene transfer for diabetic neuropathy (2012) from US National Institutes of Health. http://clinicaltrials.gov/ct2/show/NCT00056290?term=VEGF+gene+therapy&rank=6 Accessed on October 8, 2012.
161. VEGF gene transfer for critical limb ischemia (2012) from US National Institutes of Health. http://clinicaltrials.gov/ct2/show/NCT00304837?term=VEGF+gene+therapy&rank=7 Accessed on October 8, 2012.
162. Verettas D, Galanis B, Kazakos K, Hatziyiannakis A, Kotsios E. Fractures of the proximal part of the femur in patients under 50 years of age. Injury 2002;33:41-51.
163. Viggeswarapu M, Boden SD, Liu Y, Hair GA, Louis-Ugbo J, Murakami H, Kim HS, Mayr MT, Hutton W, Titus L. Adenoviral delivery of LIM mineralization protein-1 induces new-bone formation in vitro and in vivo. J Bone Joint Surg Am 2001;83-A(3):364-76.
164. Vimalraj S, Selvamurugan N. MicroRNAs: Synthesis, gene regulation and osteoblast. Curr Issues Mol Biol 2012;15(1):7-18.
165. Visser R, Arrabal PM, Santos-Ruiz L, Becerra J, Cifuentes M. Basic fibroblast growth factor enhances the osteogenic differentiation induces by bone morphogenetic protein-6 in vitro and in vivo. Cytokine 2012;58(1):27-33.
166. Vogt S, Wexel G, Tischer T, Schillinger U, Ueblacker P, Wagner B, Hensler D, Willisch J, Geis C, Wubbenhorst D, Aigner J, Gerg M, Kruger A, Salzma G, Martinek V, Anton M, Plank C, Imhoff A, Gansbacher B. The influence

of the stable expression of BMP2 in fibrin clots on the remodeling and repair of osteochondral defects. Biomaterials 2009;30(12):2385-2392

167. Yoon CS, Park JH. Ultrasound-mediated gene delivery. Expert Opin Drug Deliv 2010;7(3):321-30.
168. Yoshikawa H, Yoshioka K, Nakase T, Itoh K. Stimulation of ectopic bone formation in response to BMP-2 by Pho kiaase inhibitor: a pilot study. Clin Orthop Relat Res 2009;467(12):3087-95.
169. You L, Pan L, Chen L, Chen JY, Zhang X, Lv Z, Fu D. Suppression of zinc finger protein 467 alleviates osteoporosis through promoting differentiation of adipose derived stem cells to osteoblasts. J Trans Med 2012;10:11
170. Zanotti S, Smerdel-Ramoya A, Stadmeyer L, Durant D, Radtke F, Canalis E. Notch inhibits osteoblast differentiation and causes osteopenia. Endocrinology 2008;149(8):3890-9.
171. Zeng Y, Qu X, Li H, Huang S, Wang S, Xu Q, Lin R, Han Q, Li J, Zhao RC. MicroRNA-100 regulates osteogenic differentiation of human adipose-derived mesenchymal stem cells by targeting BMPR2. FEBS Lett 2012;586(16):2375-81.
172. Zhang G, Guo B, Wu H, Tang T, Zhang BT, Zheng L, He Y, Yang Z, Pan X, Chow H, To K, Li Y, Li D, Wang X, Wang Y, Lee K, Hou Z, Dong N, Li G, Leung K, Hung L, He F, Zhang L, Qin L. A delivery system targeting bone formation surfaces to facilitate RNAi-based anabolic therapy. Nat Med. 2012, 18(2):307-14.
173. Zhang J, Tu Q, Bonewald LF, He X, Stein G, Lian J, Chen J. Effects of miR-335-5p in modulating osteogenic differentiation by specifically downregulating Wnt antagonist DKK1. J Bone Miner Res 2011;26(8):1953-63.
174. Zhang JF, Fu WM, He ML, Xie WD, Lv Q, Wan G, Li G, Wang H, Lu G, Hu X, Jiang S, Li JN, Lin MC, Zhang YO, Kung HF. MiRNA-20A promoted osteogenic differentiation of human mesenchymal stem cells by co-regulating BMP signalling. RNA Biol 2011;8(5):829-38.

175. Zhang S, Doschak M, Uludag H. Pharmacokinetics and bone formation by BMP-2 entrapped in polyethylenimine-coated albumin nanoparticle. Biomaterials 2009;30:5143-5155.
176. Zhang Y, Song J, Shi B, Wang Y, Chen X, Huang C, Yang X, Xu D, Cheng X, Chen X. Combination of scaffold and adenovirus vectors expressing bone morphogenetic protein-7 for alveolar bone regeneration at dental implant defects. Biomaterials 2007;28(31):4635-42.
177. Zhang Y, Shi B, Li C, Wang Y, Chen Y, Zhang W, Luo T, Cheng X. The synergistic bone-forming effects of combinations of growth factors expressed by adenovirus vectors on chitosan/collagen scaffolds. J Control Release 2009;136(3):172-8.
178. Zhang Y, Wu C, Luo T, Li S, Cheng X, Miron RJ. Synthesis and inflammatory response of a novel silk fibroin scaffold containing BMP7 adenovirus for bone regeneration. Bone 2012;51(4):704-13.
179. Zheng YJ, Chung HJ, Min H, Kang M, Kim SH, Gadi J, Kim MH. In vitro osteoblast differentiation is negatively regulated by Hoxc8. Appl Biochem Biotechnol 2010;160(3):891-900.

2 Scope

The work contained in this thesis reflects a series of studies on non-viral gene delivery for the purpose of bone regeneration and addresses some of the issues discussed in the introductory chapter. The third chapter investigated exposure of embryonic stem cells to exogenous bFGF and BMP-2 to determine the extent of osteogenic response. This work was primarily undertaken as a preparation for gene delivery experiments in these cells. To gauge the effectiveness of bFGF or BMP-2 transfection, the response of embryonic stem cell culture to bFGF or BMP-2 needed to be determined. Based on a limited effect of exogenous bFGF, gene delivery studies to the embryonic stem cells were not pursued further.

Since the ultimate objective of the thesis is bone formation in a pre-clinical model, the fourth chapter presents a series of studies on *in vivo* gene delivery. Although the success of bone formation following gene delivery is discussed, the primary objective of this chapter was to examine *in vivo* transgene expression following non-viral delivery of bFGF and BMP-2 expression systems. As discussed in Chapter 1, a major drawback of the development of non-viral carriers is the lack of studies that quantify transgene expression, and so that the studies in this chapter was conducted to address this problem and provide a benchmark in the field.

The fifth chapter investigated a previously under-studied characteristic of non-viral complexes, namely stability of complexes, which

has implications for *in vivo* gene delivery. This chapter demonstrated that the functionality of the complexes changes during incubation at the physiological temperature, losing a high percentage of their transfection ability. A simple solution was presented to preserve the functionality of complexes, including in an *in vivo* model, and is demonstrated to prevent similar losses in transfection ability in siRNA.

The sixth chapter investigated the mechanics of *in vivo* gene delivery to improve our understanding of what happens after the complexes are delivered *in vivo*. This is especially crucial since we were not able to obtain bone formation after gene delivery in the previous chapters, and so we sought to better understand the pharmacokinetics of pDNA on the implant, along with mRNA expression. This chapter included a method development to allow detection of total implanted plasmid DNA, including both naked and polymer-bound. A comparison of the improved gene carrier, linoleic acid substituted 2 kDa PEI (PEI-LA), was conducted to that of its native counterpart (2 kDa PEI) based on this fundamental perspective.

Finally, we discuss the impact of these studies on the advancement of the gene delivery field as well as comparing our outcomes with those from other groups. We conclude the thesis with an overview of directions for future studies to address questions that have arisen from the current research, as well as further improve our proposed gene delivery system for therapeutic purposes.

3 Effect of basic fibroblast growth factor on mouse embryonic stem cells during osteogenic differentiation

A version of this chapter was published in: L Rose, R Fitzsimmons, P Lee, R Krawetz, D Rancourt, H Uludağ. J Tiss Eng Regen Med 2013;7(5):371-82.

3.1 INTRODUCTION

Embryonic stem (ES) cells are derived from the inner cell mass of the blastocyst [8]. These cells are identified by their pluripotency and unlimited self-renewal properties. These characteristics make ES cells promising as a cell source for tissue engineering and regenerative medicine, as adult stem cells are restricted with respect to lineage commitment and expansion potential. The pluripotency of ES allows differentiation of the cells into any tissue in the body under the appropriate culture conditions. Their self-renewal capabilities make it possible to attain large cell numbers in culture necessary for clinical transplantation. The ES cells are being particularly investigated as a source of osteoblasts for bone regeneration, after being treated with osteogenic supplements in culture [12]. Among the osteogenic supplements, basic fibroblast growth factor (bFGF) is well known to play a central role in the culture of adult stem cell populations, since it facilitates ex vivo bone marrow stromal cell (BMSC) expansion [27]. The BMSCs contain a population of mesenchymal stem cells (MSCs; multipotent stem cells), which bridge the transition from pluripotent ES cells to fully differentiated osteoblasts. Exposure to bFGF positively selects for mesenchymal cell progenitors in adult cell populations [2, 16] and stimulates bone formation and repair in vivo when the protein is administered in animal models [17, 20]. Therefore, bFGF could be an important supplement for the cultivation of ES cells as well when they are expanded for osteogenic tissue repair.

In initial studies, mouse ES (mES) cells were cultured on a feeder layer

to prevent spontaneous differentiation. Leukemia inhibitory factor (LIF) produced by the feeder cells was found to be critical for maintaining pluripotency [24, 29]. In mES cells, the activity of LIF is mediated by activation of the Janus kinase–signal transducer and activator (JAK/STAT) pathway via the gp130 receptor. In contrast, treatment with LIF was not sufficient for human ES (hES) cell pluripotency or self-renewal. Unlike mES cells, hES cells did not express the receptor gp130 to allow LIF binding and STAT3 activation [11, 25]. The mitogen bFGF was then explored in hES cell culture and this growth factor appeared to significantly influence the self-renewal of hES cells [1]. Elevated bFGF concentrations (~100 ng/ml) were able to maintain cell numbers and surface markers when undifferentiated hES cells were maintained on MatrigelTM, with similar efficiency to that of feeder cell-conditioned medium [15, 30]. Some non-human primate [9] and rabbit ES cells [10] also benefited from bFGF supplementation during their culture; however, it is not clear whether the observed bFGF influences are universal, given the interspecies differences in the signalling pathways responsible for self-renewal and pluripotency [18]. There have been no systematic investigations of the effect of bFGF on mES cells, despite the fact that FGF receptors 1–4 (FGFR1–4) were shown to be upregulated during osteogenic differentiation of mES cells and that blocking the signalling activity of the FGFRs reduced the proliferation of mES cells [21]. This study was conducted to explore the role of bFGF supplementation during mES cell expansion and differentiation toward the osteogenic lineage. The mES cells

present fewer technical difficulties during cultivation than hES cells, and they are an important model for studying embryonic development, given the difficulties in employing human tissues for this purpose. The availability of numerous mouse models of bone diseases makes it possible to utilize mES cells in animal models of bone repair. Hence, in this study, we set out to: (a) explore the influence of bFGF on maintenance cultures of mES cells; and (b) determine the potential of bFGF in directing mES cells toward an osteogenic lineage during spontaneous and BMP-induced differentiation.

3.2 MATERIALS & METHODS

3.2.1 *Materials*

D3 mES cells were obtained from American Type Culture Collection (Rockville, MD, USA). ESGRO was obtained from Millipore (Temecula, CA, USA), trypan blue solution from MP Biomedicals (Solon, OH, USA) and CyQuant DNA kit from Molecular Probes (Eugene, OR, USA). Mitomycin-C, HCl and sulphuric acid were obtained from Fisher (Fairlawn, NJ, USA). bFGF was obtained from R&D Systems (Minneapolis, MN, USA); its bioactivity is confirmed as we routinely use it for culture and expansion of human adult bone marrow stromal cells. Fetal bovine serum (FBS), Dulbecco's modified Eagle's medium (DMEM) high-glucose medium with L-glutamine, penicillin/streptomycin and b-mercaptoethanol were all from Invitrogen (Grand Island, NY, USA). Gelatin, p-nitrophenol phosphate (p-NPP), ascorbic acid, b-glycerol phosphate, calcium standards, o-cresolphthalein, 2-amino-2-

methyl-propan-1-ol and 8-hydroxyquinoline were all purchased from Sigma (St Louis, MO, USA). Phycoerythrin (PE)-conjugated mouse anti-human/mouse stage-specific embryonic antigen-1 (SSEA-1) was purchased from Stemgent (San Diego, CA, USA). The RNeasy kit was purchased from Qiagen (Missassauga, ON, USA) and the RNA 6000 Nano Chip kit was from Agilent (Santa Clara, CA, USA). M-MLV reverse transcriptase and random primers were from Invitrogen (Carlsbad, CA, USA). Oligos (dT18) and real-time PCR primers were purchased from Fermentas (Burlington, ON, Canada) and IDT (San Diego, CA, USA), respectively. The Escherichia coli-derived BMP-2 used in this study was kindly provided by Dr W. Sebald (University of Würzburg).

3.2.2 Methods

3.2.2.1 Cell culture

The stock cultures of D3 embryonic stem cells were co-culturedwith Mitomycin C-arrested human foreskin fibroblasts (HFFs) or mouse embryonic fibroblast (MEF) feeder cells on gelatin-coated plates to maintain pluripotency and a normal karyotype [19]. Cells were grown in basal medium with 1000 U/ml ESGRO, which contains LIF. Basal medium was composed of high-glucose DMEM with L-glutamine and 15% ES-qualified FBS, 0.1 mM non-essentialamino acids, 50 U/ml each of penicillin and streptomycin and 100mm b-mercaptoethanol. In order to investigate the effect of growth factors on mES cells, basal medium was supplemented with exogenous bFGF

or BMP-2 in the specified groups. The medium was changed daily and the cells were passaged every 2–3days. Feeder cells were removed just prior to experiments during a 30 min incubation on gelatin to selectively plate feeders.

3.2.2.2 Effect of exogenous bFGF on pluripotent mES cells

Maintenance mES cells were grown on MEF feeders for one passage prior to experiments. Feeder cells were removed from the cultures and mES cells were seeded in 24-well gelatin-coated plates in basal medium with combinations of bFGF (0–40ng/ml) and LIF (1000 U/ml). Medium was changed daily and cultures were subcultured every 3 days, as dictated by the density of the 0 ng/ml bFGF with LIF group. At each passage, the remaining cells were taken for live cell counts and for alkaline phosphatase (ALP) activity, as an indicator of pluripotency. Trypan blue was used as an exclusion agent for live cell counts in order to identify dead cells. Alkaline phosphatase (ALP) activity was determined as previously described (Clements et al., 2009). In brief, cell cultures assessed for ALP activity were washed with HBSS and incubated in ALP buffer (0.5 M 2-amino-2-methylpropan-1-ol, 0.1% v/v Triton-X, pH 10.5) at room temperature for 2h to lyse cells. Phosphatase substrate p-NPP was added to the lysate in 96-well plates to give a concentration of 1mg/ml. Kinetic ALP activity was attained from the maximum slope of eight absorbance readings (at 405 nm), 90 s apart. ALP activity was normalized to DNA content in each sample.

3.2.2.3 Embryoid body formation and differentiation

Embryoid body (EB) formation and differentiation was induced via hanging drop culture, as described previously [33]. After the removal of feeder cells, mES cells were counted, resuspended in medium and hanging drops (750 cells/drop) were made on the inner sides of the lids of tissue culture plates containing 3ml sterile PBS. On day 3, aggregates were transferred to bacteriological Petri dishes in 10ml medium. On day 5, EBs were transferred to 48-well tissue culture plates with medium containing 0 or 1000 U/ml LIF and bFGF concentrations of 0, 2, 10 and 40ng/ml. The medium was changed as needed, typically at 2–3 day intervals.

3.2.2.4 Effect of exogenous bFGF during early differentiation

To determine the effect of bFGF during EB formation, ES cells were exposed to bFGF (0–40 ng/ml), with and without LIF, in basal medium from day 0 to day 15. At days 5, 10 and 15, EBs cultures were harvested to assay for DNA content, ALP activity and SSEA-1 staining. Cultures for DNA content and ALP activity were washed with HBSS and incubated at 37 °C in ALP buffer for 2 h. Cultures for SSEA-1 staining were trypsinized, resuspended in 50 mL HBSS, and incubated for 1h on ice with 10 mL PE- anti-mouse/human SSEA-1. After washing with HBSS, cells were analysed by flow cytometry at the FL2 channel (Quanta; Beckman Coulter), with unstained cells set to 1% as a background control.

3.2.2.5 Osteogenic differentiation of mES cells

Osteogenic differentiation was induced by treatment with osteogenic factors at day 5, after plating EBs in 48-well plates. EBs were grown in basal medium with 50mg/ml ascorbic acid and combinations of 10 mM b-glycerol phosphate, 1 mM dexamethasone, 10 ng/ml bFGF and 500 ng/ml BMP-2. At days 15 and 25, cultures were harvested to assay for DNA content, ALP activity and extracellular calcium content. For alizarin red staining, the EBs were transferred to glass coverslips and incubated with medium (in six-well plates) containing the indicated supplements (see **Figure 3-8B**). Alizarin red staining was performed according to Zur Nieden et al. [33] on days 15 and 25.

3.2.2.6 DNA content, calcium deposition and ALP activity assays

The cultures were washed with HBSS and incubated with ALP buffer. After incubation, the plates were washed with HBSS and the extracellular matrix was dissolved in 0.5 N HCl. A 500 ml solution of 2-amino-2-methyl-propan-1-ol (1.5% v/v) and o-cresolphthalein (37mM) was mixed with 100 ml 8-hydroxyquinoline (28 mM) and sulphuric acid (0.5% v/v) in 48-well plates containing of 20ml of sample. The absorbance was determined at 570 nm and compared against calcium standards. Kinetic ALP activity was measured as described above and DNA content was quantified using a CyQUANT assay kit.

3.2.2.7Real-time polymerase chain reaction (PCR)

RNA was harvested from osteogenic cultures on day 14, after treatment with medium containing ascorbic acid (50 mg/ml), bFGF (0 or 10 ng/ml) and BMP-2 (0 or 500 ng/ml) in 24-well plates. Cultures were washed with HBSS and then RNA was extracted with an RNeasy Kit, according to the manufacturer's instructions. The obtained RNA concentration was measured with a GE NanoVue spectrophotometer; RNA quality was determined with an RNA 6000 Nano Chip Kit. All but one RNA sample (6.1) had RNA integrity numbers (RIN) 7.2. From each sample, 150ng RNA was reverse-transcribed using M-MLV reverse transcriptase, following the manufacturer's instructions, in a reaction volume of 20 mL. In addition to random primers, oligos (dT18) were used to synthesize cDNA template. Primer sets (***Table 3-1***) were validated by ensuring equal PCR efficiencies between endogenous control GAPDH and the gene of interest over a five-fold change in template cDNA concentration (not shown). The stability of the GAPDH endogenous control was confirmed by ensuring similar cycle threshold (CT) values from different biological replicates of all four treatment groups. SYBR green dye, which binds double-stranded DNA, was used to monitor real-time reaction products on a 7500 Fast Real-Time PCR System (Applied Biosystems). From the 20 mL reverse-transcription reactions, 1 out of 10 dilutions were made for template in real-time PCR. The 10 mL real-time reaction mixture consisted of 2.5 mL cDNA template, 2.5 mL 3.2 mM primers and 5 mL 2x master mix containing SYBR green dye, dNTPs and salts. Reaction mixtures

were heated to 95 °C for 2 min before going through 40 cycles of a denaturation step (15 s at 95 °C) and an annealing/elongation step (60 s at 60 °C), during which SYBR green fluorescence data were collected. A ΔΔCT analysis was used to determine differences in gene expression, as compared to no treatment controls. GAPDH was employed as an endogenous control, to which the CT of the gene of interest was normalized. Changes in gene expression were determined by normalizing the differences in cycle threshold (ΔCT) to spontaneous differentiation (no treatment) controls. RNA from three biological replicates was pooled and run in triplicate to screen for changes in gene expression. Any changes from the no treatment control were verified in three independent biological replicates, with each real-time reaction performed in triplicate.

3.2.2.8Statistical analysis

For all results, except EB formation for osteogenic differentiation, error bars represent the standard deviation (SD) of results in triplicate. Error bars in osteogenic differentiation experiments (ALP activity, DNA and calcium content) represent SD for groups with five or six replicates. To determine significant changes due to bFGF treatment, one-way analysis of variance (ANOVA) was employed, followed by Dunnett's test, which compares all treatment groups to a single control.

Table 3-1 – Real time PCR primers

Primer Set	Marker	Direction	Primer Sequence (5' to 3')
1	ALP	Forward	GGCCAGCAGGTTTCTCTCTTG
		Reverse	GCAGGGTCTGGAGAATATATTTGG
2	Cbfa1/Runx2	Forward	GCCGGGAATGATGAGAACTACT
		Reverse	AGATCGTTGAACCTGGCTACTTG
3	CD29	Forward	CCAGGGCTGGTTATACAGAATCA
		Reverse	CCACATACATCACTGGGAATTCC
4	CD105	Forward	CCTCCCAGTGGAGACTTCAGAT
		Reverse	AGTGCCGTGTCTTTCTGTAATCC
5	Col-1a1	Forward	CCCTGCCTGCTTCGTGTAAA
		Reverse	TTGGGTTGTTCGTCTGTTTCC
6	FGFR1	Forward	TGAGCTTGGCTTCCTATAGTTTTTC
		Reverse	GCAGAATTGAGTTGCCAAGTTG
7	GAPDH	Forward	ATGTGTCCGTCGTGGATCTGA
		Reverse	CCTGCTTCACCACCTTCTTGA
8	OCN	Forward	CGGCCCTGAGTCTGACAAAG
		Reverse	AGGTAGCGCCGGAGTCTGTT
9	OP	Forward	AGGCATTCTCGGAGGAAACC
		Reverse	CAAACAGGCAAAAGCAAATCAC
10	Sca-1	Forward	CAAGGTGGGAGTAGTGTGTGAAAT
		Reverse	GCCCTAGAGAGGATTAGAGCACCTA
11	SSEA-1	Forward	AGCTGTGACTAACATTGCCTCATT
		Reverse	GAAACCCTGTCTGAAAAACCAAA

3.3 RESULTS

3.3.1 Effect of exogenous bFGF on pluripotent mES cell cultures

To investigate the bFGF response of mES cells, the cells were cultured with 0, 2, 10 and 40 ng/ml bFGF with (1000 U/ml) and without LIF. Cell numbers and ALP activity were used as measures of self-renewal and pluripotency. ALP is a membrane-bound enzyme that exhibits biphasic behaviour. It is expressed on the surface of pluripotent undifferentiated ES cells and disappears as cells begin to differentiate. If cells are directed toward an osteogenic lineage, its expression is upregulated as cells mature into osteoblasts. For clarity, activity associated with undifferentiated ES cells is here denoted as ALP_{Embryo}, while activity associated with osteo- genic differentiation is denoted as ALP_{Osteo}. The 0ng/ml bFGF with 1000 U/ml LIF group served as the control, as this condition mimicked the maintenance cultures of mES cells, and the visual cell density of this group was used as an indicator of the timing of cell passaging. mES cells at each passage were counted and cell numbers in treatment groups were expressed relative to the control group.

In the absence of LIF, mES cells showed a rapid decrease in cell numbers with cell passage and cell viability was essentially lost at the second passage under the feeder-free conditions (**Figure 3-1**). In the presence of LIF, bFGF resulted in a slow decrease in cell numbers over the five passages, as compared to the maintenance conditions. There was no evidence of a dose–response relationship in relative cell numbers within the employed bFGF

concentrations. The control group itself also showed a decrease in cell numbers over the study period (**Figure 3-1**, insert).

Similar to the changes in cell numbers, the ALP_{Embryo} activity was decreased in the absence of LIF but remained constant with LIF (**Figure 3-2A**). However, specific ALP_{Embryo} activity (ALP_{Embryo} activity/cell) remained relatively constant relative to the maintenance condition (**Figure 3-2B**). There was no effect of bFGF on the ALP_{Embryo} activity under the conditions of this experiment.

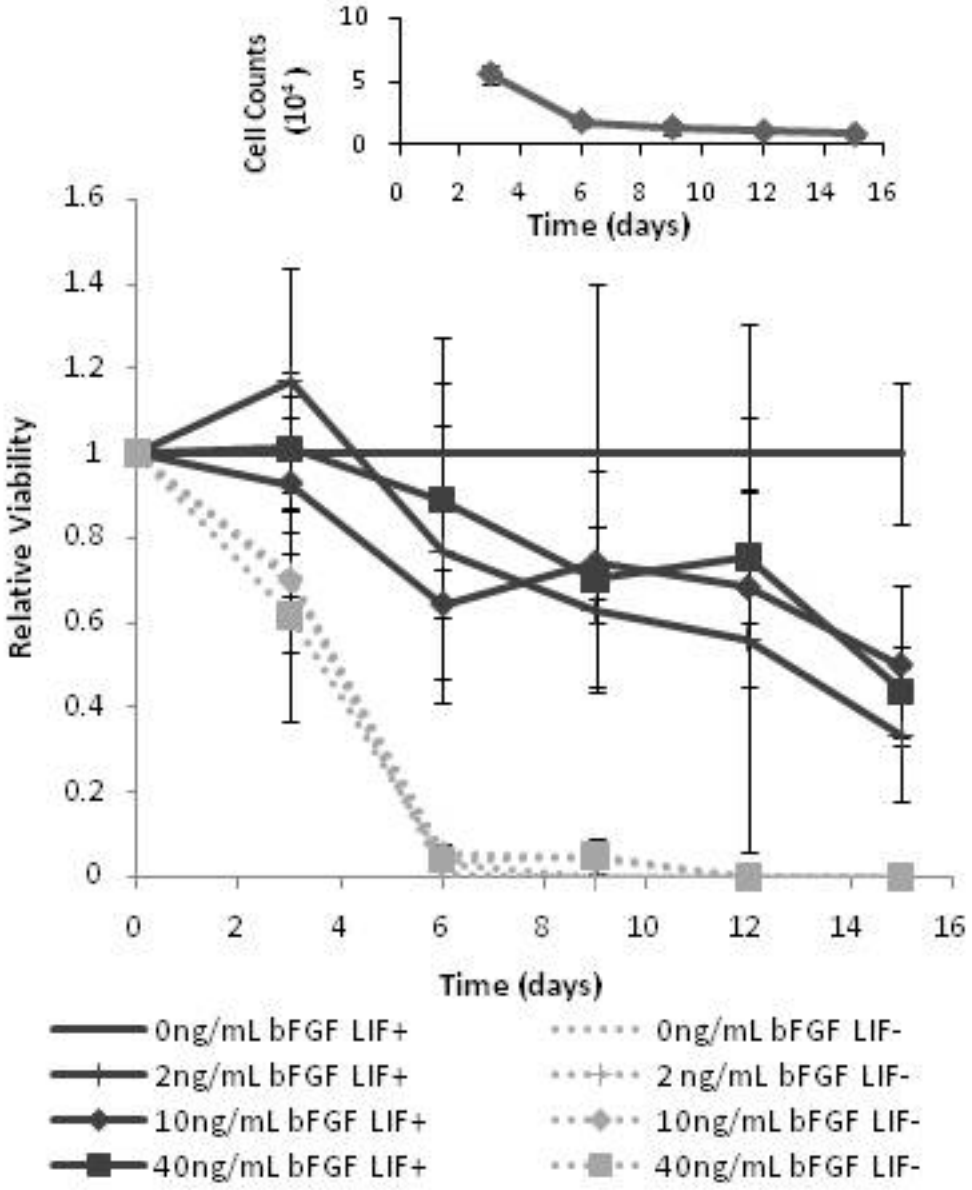

Figure 3-1 - ***Effect of bFGF on Self-Renewal during Maintenance Conditions*****.** Relative cell counts for mESC treated with 0, 2, 10 and 40 ng/mL bFGF in the absence and presence (1000 U/mL) of LIF. The cell counts were normalized relative to the maintenance conditions (i.e., 0 ng/mL bFGF and 1000 U/mL LIF). Note that there was a gradual reduction of mESC counts in the absence of LIF irrespective of the bFGF concentration in the medium. There was also a gradual reduction of relative cell counts in the presence of

bFGF (2-40 ng/mL) as compared to the maintanence conditions. Insert: cell numbers of cultures grown under maintenance conditions (0 ng/mL bFGF and 1000 U/mL LIF).

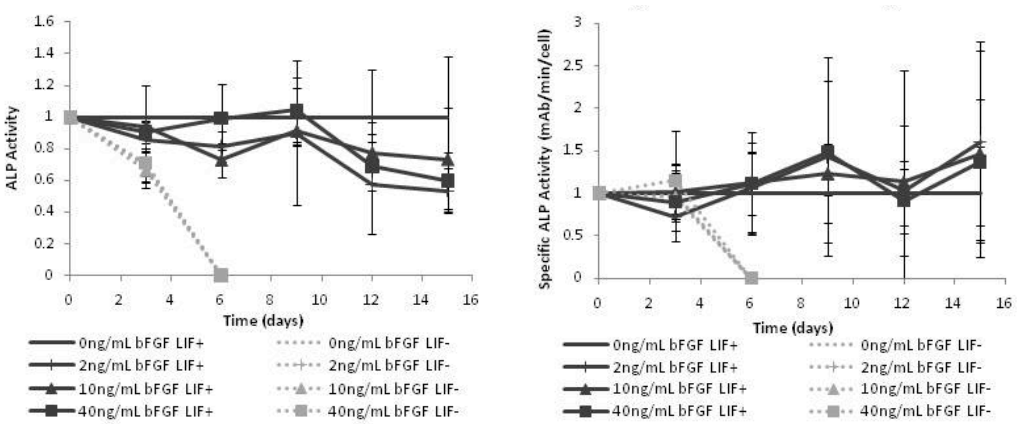

Figure 3-2 - *Effect of bFGF on ALP Activity during Maintenance Conditions*. ALP Activity for mESC treated with 0, 2, 10 and 40 ng/mL bFGF in the absence and presence (1000 U/mL) of LIF. ALP activity (**2A**) was normalized to the maintenance conditions of 0 ng/mL bFGF with LIF. Specific ALP (**2B**) activity (mAb/min/µg of DNA) was normalized to the maintenance conditions of 0 ng/mL bFGF with LIF.

3.3.2 Effect of bFGF during EB formation and early phase of differentiation

To investigate the effects of bFGF during spontaneous differentiation in high-density cultures, EBs were grown in basal medium containing 0–40 ng/ml bFGF with (1000 U/ml) and without LIF from hanging drop formation. The EBs in 48-well plates were harvested on days 5, 10 and 15 to assay for DNA content, ALP_{Embryo} activity and SSEA-1 expression. DNA content was used as an indicator of cell number, since it was not possible to obtain accurate cell counts, due to technical difficulties in dissociating EBs into uniform cell suspensions. At day 5, there were no significant differences in DNA content among the study groups without or with LIF (**Figure 3-3A** and **B**, respectively). Proliferation in subsequent days was evident in EBs even in the absence of LIF (**Figure 3-3A**), which was unlike the monolayer cultures (see **Figure 3-1**). At day 10 in the absence of LIF, significant increase in DNA content was obtained when mES cells were cultured with 40 ng/ml bFGF ($p < 0.01$ vs 0 ng/mlbFGF). Similarly, at day 15 a significant increase in DNA content was obtained at 2 and 10ng/ml bFGF ($p<0.05$ and $p<0.01$ vs 0ng/ml bFGF). In the presence of LIF (**Figure 3-3B**), there were no significant differences in DNA content among the study group.

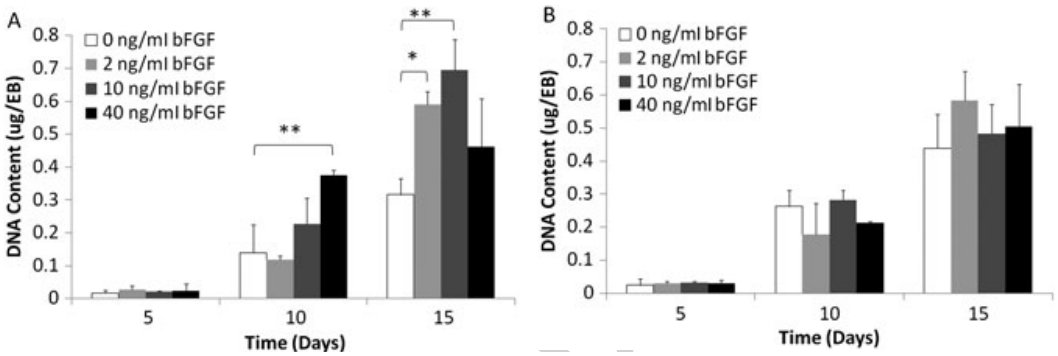

Figure 3-3 - *DNA Content of EB during Early Phase of Differentiation*. DNA content of EBs harvested on Day 5, 10 or 15. Cultures were grown in basal media containing 0, 2, 10 or 40 ng/mL bFGF with (1000 U/mL; B) and without LIF (A) from hanging drop formation at Day 0. Treatment groups were compared to the negative control of 0 ng/mL bFGF at each timepoint. (* $p<0.05$ and ** $p<0.01$).

The specific ALP_{Embryo} activity did not vary significantly among the study groups (Figure 4). A drop in the specific ALP_{Embryo} activity was evident for some of the mES cells cultured without LIF (**Figure 3-4A**), but bFGF did not have a stimulatory or inhibitory effect on this activity at different time points. In the presence of LIF (**Figure 3-4B**), an upward trend in the specific ALP_{Embryo} activity was apparent, but bFGF did not influence the specific ALP_{Embryo} activity under these conditions either.

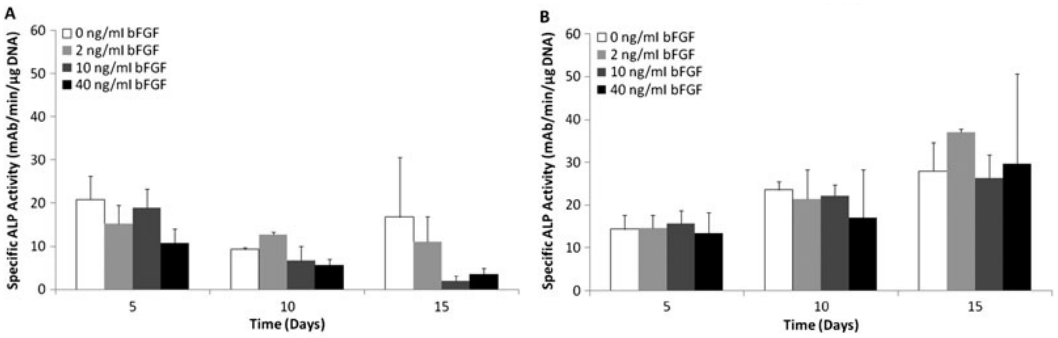

Figure 3-4 - *ALP Activity of EB during Early Phase of Differentiation*. ALP activity (mAb/min) of EB normalized to the amount of DNA in each sample. Cultures were grown in basal media containing 0, 2, 10 or 40 ng/mL bFGF with (1000 U/mL; B) and without LIF (A) from hanging drop formation at Day 0. Treatment groups were compared to the negative control of 0 ng/mL bFGF each timepoint.

Flow cytometry was used to detect SSEA-1 positive cells as a function of time. Sufficient cells were not collected on day 5 to obtain an accurate assessment of SSEA-1, but there were no apparent differences among the study groups, as judged by the average fluorescence of the sample (data not shown). On day 10 (**Figure 3-5**), all four groups treated with LIF showed significant SSEA-1-positive cells ($p < 0.01$ for 0, 2 and 40 ng/ml bFGF and $p < 0.05$ for 10 ng/ml bFGF vs without LIF). On day 15, the level of SSEA-1 expression was significantly reduced as compared to the day 10 levels, and only the cells treated with 10ng/ml bFGF and LIF showed significant ($p < 0.01$) variation in SSEA-1-positive cells compared to LIF treatment alone (0ng/ml bFGF). Addition of bFGF did not prevent the reduction in the levels of SSEA-1-positive cells from day 10 to day 15.

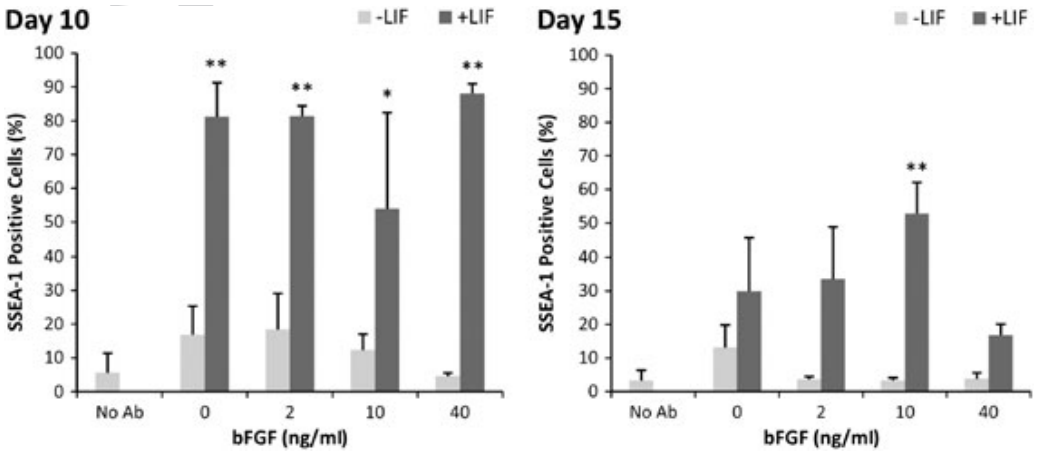

Figure 3-5 - *SSEA-1 Staining of EB during Early Phase of Differentiation*. Flow cytometry analysis of cells stained with PE-anti-SSEA-1 at 10 and 15 days after hanging drop formation. Cultures were grown in basal media containing 0, 2, 10 or 40 ng/mL bFGF with (1000 U/mL) and without LIF from hanging drop formation at Day 0. Treatment groups were compared to the negative control of 0 ng/mL bFGF without LIF at each timepoint. (* $p<0.05$ and ** $p<0.01$).

3.3.3 Effect of bFGF during osteogenic differentiation of mES cell cultures

To investigate the effect of bFGF during osteogenic differ- entiation, EBs were treated with different combinations of osteogenic supplements (b-GP, DEX and BMP-2) in basal medium containing ascorbic acid but without LIF. The EB grown in each combination was exposed to either 0 or10ng/ml bFGF. This concentration of bFGF was chosen based on the increases in DNA content found when mES cells were cultured without LIF during early differentiation. The EBs in 48-well dishes were harvested on days 15 and 25 to assay for the DNA content, ALP_{Osteo} activity and calcification. The addition of exogenous bFGF did not result in significant increase in DNA content at day 15 (**Figure 3-6**).

EBs treated with BMP-2 alone showed a significant increase ($p < 0.05$) in DNA content, along with the EBs treated with b-GP/bFGF and b-GP/DEX/bFGF ($p < 0.01$). At day 25, only the DEX/BMP-2/bFGF group showed a significant ($p < 0.05$) increase over control without bFGF, indicating no clear effect of bFGF supplementation on the DNA content under osteogenic stimulation.

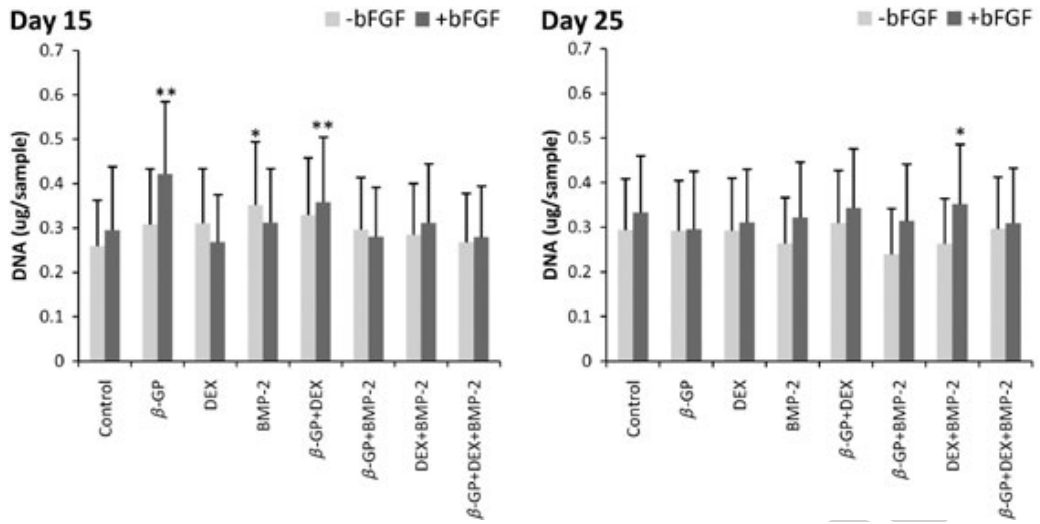

Figure 3-6 - *DNA Content of EB during Osteogenic Differentiation*. DNA content of EB exposed to ascorbic acid-containing basal media with combinations of osteogenic supplements β-GP, DEX, BMP-2 and bFGF. EB in 48-well plates were harvested on Day 15 and 25 after hanging drop formation. Significantly different groups vs control (-bFGF) are indicated (* $p<0.05$, ** $p<0.01$).

None of the specific ALP_{Osteo} values were significantly different among the study groups on day 15 (**Figure 3-7**). This was the case in the absence or presence of bFGF. However, on day 25, EBs treated with BMP-2 ($p < 0.05$), DEX/BMP-2 ($p < 0.01$) and b-GP/DEX/BMP-2 ($p < 0.05$) showed significant increases in specific ALP_{Osteo} activity as compared to the control EBs (EBs treated with no osteogenic supplements and no bFGF). In the presence of bFGF, these groups did not lead to a significant increase in specific ALP_{Osteo} activity, indicating the ability of bFGF to down-regulate induced ALP activity. Accordingly, there were no differences in the specific ALP_{Osteo} activity among the treatment groups.

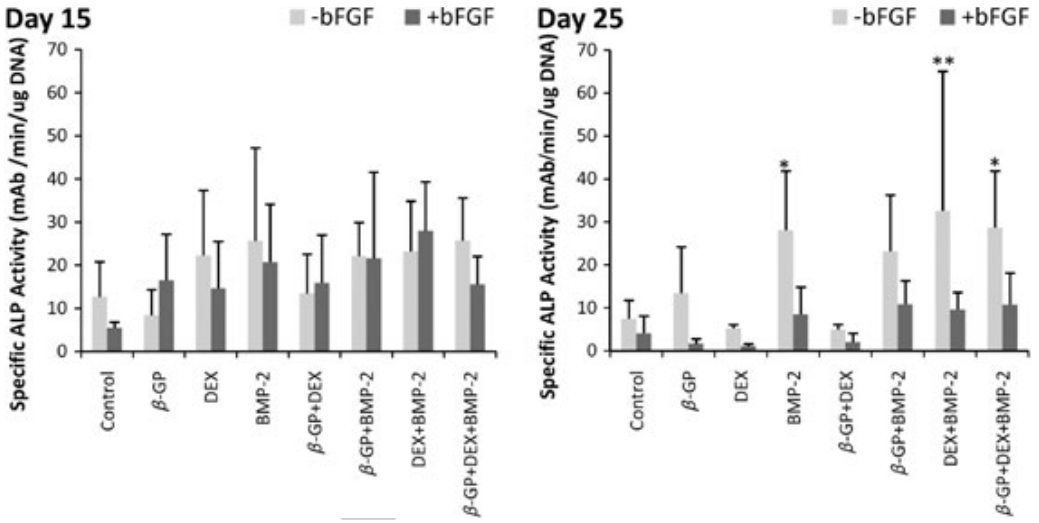

Figure 3-7 - *ALP Activity of EB during Osteogenic Differentiation*. ALP activity, normalized to DNA content, of EB exposed to ascorbic acid-containing basal media with combinations of osteogenic supplements β-GP, DEX, BMP-2 and bFGF. EB in 48-well plates were harvested at Day 15 and 25 after hanging drop formation. (* $p<0.05$, ** $p<0.01$).

The EBs treated with b-GP/BMP-2 and b-GP/DEX/BMP-2/ bFGF (**Figure 3-8A**) showed significant ($p < 0.01$) calcium deposition on day 15, but the calcium deposition with EBs treated with b-GP/DEX was not significant. The latter group again did not give significant calcium accumulation on day 25 compared to the control EBs (EBs treated with no osteogenic supplements and no bFGF). However, the EB cells treated with b-GP/BMP-2, b-GP/BMP-2/bFGF, b-GP/ DEX/BMP-2 and b-GP/DEX/BMP-2/bFGF combinations all showed significant calcium deposition ($p < 0.01$). The presence of the bFGF in these groups did not alter the level of calcium deposition. Consistent with the biochemical calcium assay, alizarin red staining indicated significant mineralization in EB cultures, which generally increased from day 15 to day 25 (**Figure 3-8B**).

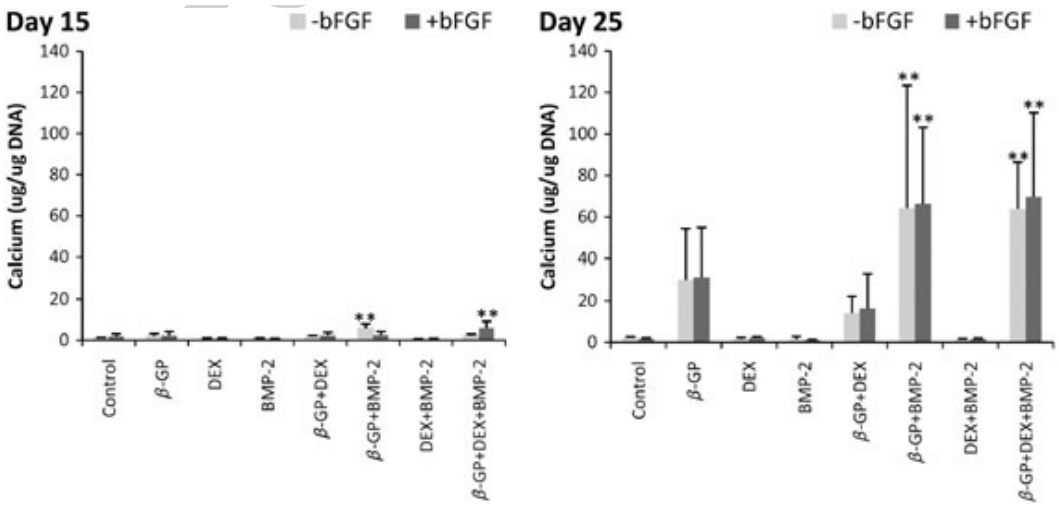

Figure 3-8 - *Extra-Cellular Matrix Calcification of EB during Osteogenic Differentiation*. (A) Calcium content of EBs following exposure to osteogenic supplements. EBs were grown in basal medium, which contained ascorbic acid, with combinations of b-GP, DEX, BMP-2 and bFGF. Basal medium alone served as a control. Cultures were harvested at day 15 or 25 and assessed for calcification. Calcium content of the cultures was normalized to DNA content. Significant differences from control medium without bFGF are indicated; $p < 0.05$, $**p < 0.01$. (B) Representative alizarin red-stained EBs, which were cultured in the presence of the indicated supplements. EB cultures stained after day 15 (left) and day 25 (right) are shown. Note that the pictures are intended as a qualitative measure of calcification in EB cultures and should not be used for quantitative purposes to compare different groups

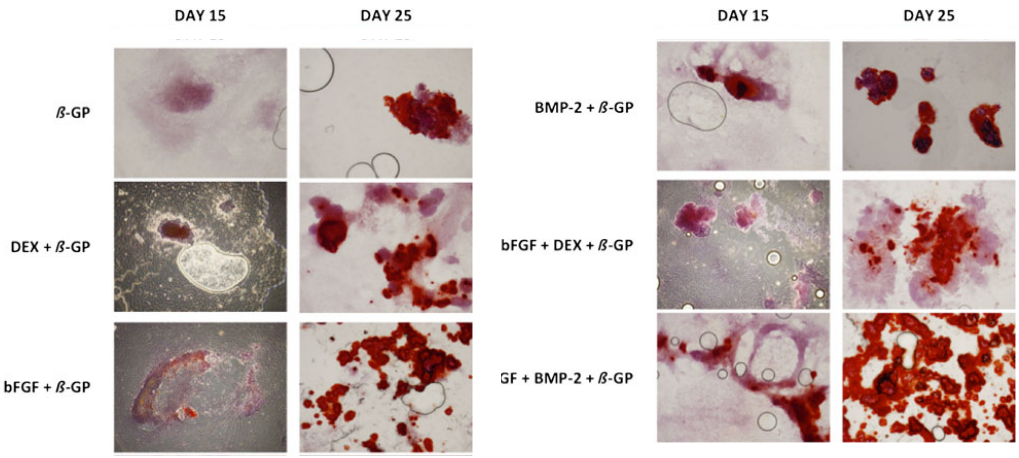

Figure 3-8 – continued.

3.3.4 Effect of bFGF on gene expression during osteogenic differentiation

Changes in gene expression with exposure to bFGF during osteogenic differentiation were investigated using real-time PCR. The EBs were treated with bFGF (10 ng/ml), BMP-2 (500 ng/ml) and a combination of bFGF and BMP-2 (10 and 500 ng/ml, respectively), and RNA was harvested from cultures on day 14 or 21 for cDNA templates. Untreated mEB served as a control in the PCR analysis. Osteogenesis- associated genes analyzed included runt- related transcription factor 2 (Runx2), osteocalcin (OCN), osteopontin, collagen and ALP. Markers associ- ated with ES cell pluripotency (SSEA-1), mesenchymal stem cells (CD105, CD29, Sca1) and haematopoetic stem cells (Sca1) were also included.

The ALP mRNA was found to increase 1.8–2.2-fold at days 14 and 21 after BMP-2 treatment of EBs (**Figure 3-9**). However, the combination of

bFGF and BMP-2 led to a decrease in ALP expression at day 21, similar to the results from the enzyme activity assay, where the addition of bFGF during osteogenic differentiation led to a decrease in ALP activity.

The bFGF treatment resulted in a ~2.5-fold increase in Sca1 (a marker present on both mesenchymal and haematopoetic stem cells) expression on day 14 as compared to no treatment. In combination with BMP-2, a ~5.2-fold increase in Sca1 expression was observed. A small increase in Sca-1 expression (~1.5-fold) was evident at day 21 with bFGF treatment.

On day 14, an increase in OCN expression was observed following exposure to BMP-2 (2.2-fold); however the combination of BMP-2 and bFGF led to an even higher (6.7-fold) OCN levels over BMP-2 alone (**Figure 3-9**). A similar trend was observed on day 21.

At day 14, a significant (1.9-fold) increase in Runx2 over no treatment was observed when EBs were exposed to a combination of BMP-2 and bFGF, but not BMP-2 or bFGF alone. No changes in Runx2 were seen at day 21 for all groups.

PCR analysis for SSEA-1 expression indicated no increase in expression following the addition of bFGF (not shown) on day 14 or 21, confirming the flow cytometry results. The other molecular markers (CD29, CD105, Cpl-1a1, FGFR1 and OP) were not significantly changed (not shown) from the no treatment group under the investigated conditions.

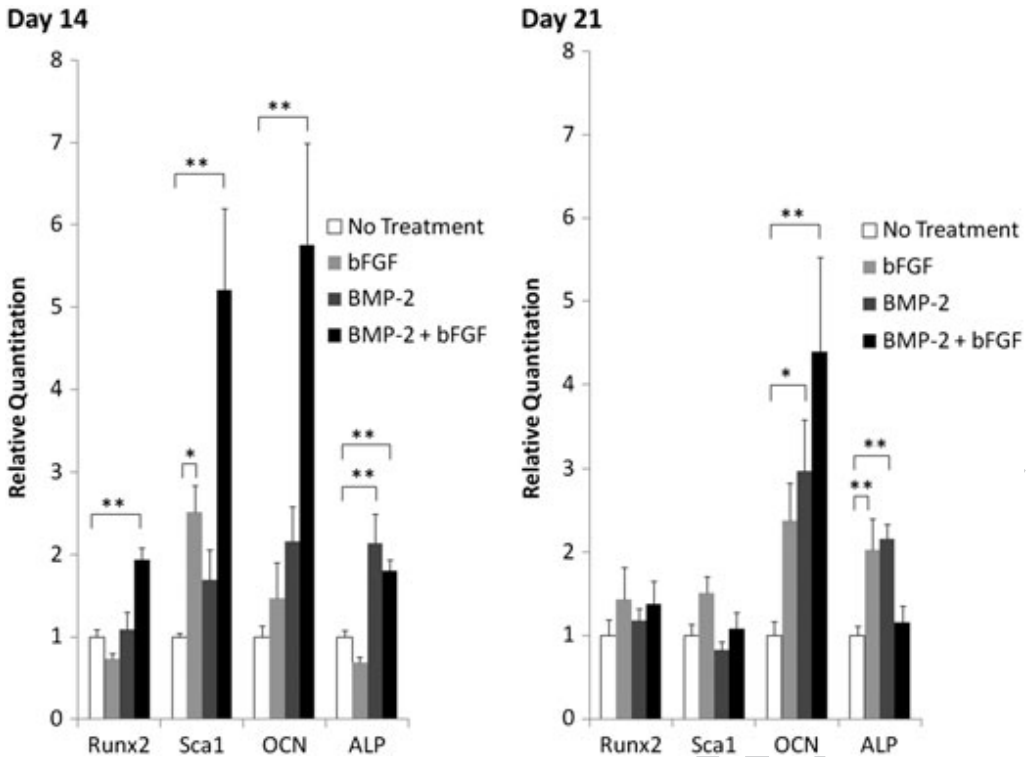

Figure 3-9. - *Changes in gene expression during osteogenic differentiation.* Quantitative PCR results showing gene expression of ALP, Sca-1 and OCN (osteocalcin) during BMP-2-induced osteogenic differentiation. Cells were exposed to either BMP-2 alone or a combination of BMP-2 and bFGF. Basal medium without BMP-2 or bFGF served as a control. Cells were harvested at days 14 and 21 and a ΔΔCT analysis was used to evaluate changes in expression of target genes, using GADPH as an endogenous control. Expression in the bFGF, BMP-2 and BMP-2 + bFGF treatment groups were $^{**}p < 0.01$

3.4 DISCUSSION

The mechanism of bFGF-mediated feeder-free culture has not been uncovered, but bFGF is proposed to interfere with bone morphogenetic protein (BMP) signalling, associated with unconditioned medium, that causes differentiation of hES cells [31]. Although bFGF is routinely used in the culture of pluripotent hES cells, the effects of bFGF on mES cell cultures is not known. Based on the experience with hES cells and human/mouse BMSCs [13, 28], we expected bFGF to enhance survival and proliferation of the cells and, therefore, facilitate the expansion of these cells. In addition, we were interested to determine whether bFGF could enhance BMP-2 mediated osteogenic differentiation. An understanding of how mES cells respond to these commonly used growth factors would greatly enhance our understanding of stem cells, which would further facilitate the use of stem cells that are vitally needed for regenerative medicine approaches. We conducted the current study to explore the beneficial effect, if any, of bFGF mES cell expansion and osteogenic differentiation. The effects of exogenous bFGF on D3 mES cells were investigated in three different environments: during maintenance conditions, at an early stage of spontaneous differentiation (in high-density EB formation) and during osteogenic differentiation. The feeder-independent nature of the D3 line allowed feeder-free conditions (i.e. on gelatin-coated plates) during experiments, so that only the effects of exogenous growth factor were observed. This prevented any synergistic effects from combinations of bFGF and other growth factors

produced by the feeder layers.

Under the maintenance conditions with regular passaging, bFGF did not sustain self-renewal capabilities of mES cells in the absence of LIF and it was no substitute for LIF in prolonging self-renewal. In combination with LIF, there was a slight decrease in the number of cells after five passages with bFGF compared to basal conditions (with LIF) in the absence of bFGF. However, the specific ALP_{Embryo} activity of bFGF-treated mES cells was unaffected, indicating that the addition of bFGF did not appear to result in differentiation and maintained pluripotency.

Since self-renewal was not supported in cultures without LIF, the effect of bFGF alone on pluripotency could not be assessed under maintenance conditions. To investigate the effect of bFGF on mES differentiation, EBs were formed via hanging drops in medium, since the cells were previously cultivated without LIF under these conditions [33]. This was shown to be the case here as well. Under these conditions and in the absence of LIF, bFGF treatment did stimulate proliferation in EBs under certain concentrations, suggesting that a careful optimization might be necessary to obtain this beneficial effect of bFGF on EBs. When mES cells are cultured in tissue-engineering scaffolds it is likely that EB formation will occur more readily, due to the confined spaces of the scaffolds, and our results indicate that bFGF may help in mEB cell expansion under these conditions. The bFGF did not stimulate cell proliferation in the presence of LIF, since the cells displayed a more robust proliferation under this condition.

Based on the chances in ALP_{Embryo} of the EBs treated with LIF, the cytokine was found to be beneficial to maintaining the pluripotency of the mES cells, even in EBs. A similar conclusion was reached based on SSEA-1 expression, which is present in undifferentiated cells and disappears as ES cells undergo differentiation. Although not statistically significant, the addition of bFGF appeared to cause a larger decrease in ALP_{Embryo} activity compared in the absence of LIF. Taking these factors together, bFGF did not appear to adversely affect the pluripotency of mES in EBs. Although different signaling pathways are employed to maintain pluripotency in mouse and human ES cells, some of these differences may be attributed to ES cells derived from different temporal origins [3]. Regardless, bFGF pluripotency and self-renewal pathways do not appear to be present in mES cells, given the unresponsiveness of mES cells to the exogenous bFGF.

The effects of bFGF during osteogenic differentiation were subsequently investigated. The EBs were exposed to all combinations of b-GP, DEX and BMP-2 in order to induce osteogenic differentiation, and cultured with and without bFGF to investigate the changes in osteogenic differentiation. The success of these treatments in inducing osteoblast characteristics was assessed by alizarin red staining [4], ALP_{Osteo} levels [26], formation of discrete mineralized nodules [4, 6] and expression of osteogenic lineage-specific genes [33]. In our differentiation experiments, it is possible that the ALP_{Osteo} activity at day 15 was not entirely due to induction of the osteogenic pathway, but ALP_{Osteo} activity at day 25 was most likely due to the

presence of osteoblast-like cells. Some markers of pluripotency, such as Oct3/4, remain strong for at least 7days after the removal of LIF, but markers associated with the primitive endoderm have been found to increase at day 6 [26], suggesting that the molecular pathways involved in differentiation are activated relatively early.

The presence of bFGF did not consistently lead to an increase in DNA content during the imposed osteogenic differentiation (days 15–25). However, bFGF did appear to have negative effects on specific ALP_{Osteo} activity. EBs grown with BMP-2, DEX/BMP-2 or b-GP/DEX/BMP-2 all showed significantly higher ALP_{Osteo} activity but the addition of bFGF to these combinations resulted in significant decreases in specific ALP_{Osteo} activity. Although we were not able to show significant ALP_{Osteo} activity with our AA/b-GP/DEX positive control, a similar bFGF-dependent inhibition of ALP_{Osteo} activity [5, 27] was seen in adult BMSCs grown in osteogenic medium containing AA/b-GP/DEX. Others reported conflicting results on the effect of bFGF on osteogensis of human BMSC, including ALP activity (reviewed in Clements et al., [5]), this despite the fact that bFGF administration in rat and mouse models resulted in a stimulation of bone formation [7, 20]. The decreased ALP_{Osteo} activity observed with bFGF did not necessarily correlate with decreased calcium deposition, as the combinations of b-GP/BMP-2 and b-GP/BMP-2/DEX that gave significant calcification showed no change upon addition of bFGF. b-GP/BMP-2 and b-GP/BMP-2/DEX/bFGF appeared to have accelerated calcification, and these two

groups were the only ones that had significant calcium deposition on day 15. Nevertheless, all BMP-2-containing groups gave increased calcification by mES cells in EBs, consistent with the expected activity of this well-established osteogenic protein [14].

Addition of b-GP was essential for calcification; the combination of DEX/BMP-2 led to significantly higher specific ALP_{Osteo} activity in EBs, but required the addition of b-GP for the formation of any significant calcification (also seen in alizarin red-stained EBs). It must be noted, however, that although not statistically significant, the addition of b-GP alone resulted in some calcification. It is possible that DEX and BMP-2 are required to induce osteo-specific markers, whereas b-GP may result in spontaneous calcium precipitation on its own [23].

In order to determine the effects of bFGF on osteogenic lineage specific gene expression, quantitative PCR was used to analyse changes in gene expression following EBs formation and treatment with BMP-2 and bFGF. Changes in ALP gene expression correlated well with the changes in enzymatic (colorimetric) ALP activity. Osteocalcin was upregulated when the cells were treated with BMP-2 (consistent with a previous report on mES [22], and was even further increased with a combination of bFGF and BMP-2 treatments, along with Runx2. This confirmed that the cells did undergo osteogenic differentiation with BMP-2 and, based on this marker alone, bFGF did stimulate osteogenic differentiation. Further evidence to suggest that bFGF may alter the differentiation process was the expression profile of Sca-

1 at day 14, a marker present in both mesenchymal and haematopoetic stem cells [32]. The addition of bFGF to the culture medium caused an increase in Sca-1 at day 14, which indicated expansion of the mesenchymal/haematopoetic stem cells that was consistent with the loss of pluripotency marker SSEA-1 expression. The disappearance of Sca-1 at day 21 was most likely due to further differentiation, and decrease in mesenchymal stem cells in the obtained cell population. This Sca-1 upregulation indicated that bFGF increased the population of mesenchymal-like cells, in agreement with previous results obtained from BMSCs [2, 16]. To fully assess osteogenic differentiation in mES cells, more characterization will be needed for changes in the markers of pluripotency (e.g. Oct4, SOX2, etc.) to better realize the potential of teratoma formation, if the osteogenic differentiation mES cells are used for transplantation. The chances of teratoma formation are likely to be diminished if the pluripotency markers are decreased as a result of osteogenic differentiation. Future studies should elucidate such changes.

3.5 CONCLUSIONS

We conclude that, despite the known mitogenicity of bFGF, we have not observed any consistent increase in cell numbers or DNA content of mES cells during regular maintenance conditions in monolayers. LIF was indispensable under these conditions. The bFGF on its own (i.e. without LIF) did stimulate cell proliferation without causing osteogenic differentiation in

high-density EB cultures. These results pointed to significant differences between human and mouse bFGF-dependent pluripotency and self-renewal pathways. During differentiation under the influence of osteogenic supplements, the addition of bFGF prevented the increase in ALP_{Osteo} activity of EBs exposed to osteogenic factors, which was reminiscent of the behaviour of adult BMSCs exposed to bFGF. Upregulation of Sca-1 and osteogenesis-related genes suggested that bFGF may enhance the population of mesenchymal stem cells and lead to osteogenic differentiation under these conditions. We conclude that, while LIF was indispensable for long-term survival, bFGF could be useful in expansion of stem cells in EBs cultures and can further support BMP-2-induced osteogenesis at the gene level.

3.6 REFERENCES

1. Amit M, Carpenter M, Inokuma M, Chiu CP, Harris C, Waknitz M, *et al*. Clonally derived human embryonic stem cell lines maintain pluripotency and proliferative potential for prolonged periods of culture. Dev Biol 2000;227(2):271-8.
2. Bianchi G, Banfi A, Mastrogiacomo M, Notaro R., Luzzatto L., Cancedda R., *et al*. Ex vivo enrichment of mesenchymal cell progenitors by fibroblast growth factor 2. Exp Cell Res 2003;287(1):98-105.
3. Brons IGM, Smithers LE, Trotter M, Rugg-Gunn P, Sun B, Chuvada de Sousa Lopes SM, *et al*. Derivation of pluripotent epiblast stem cells from mammalian embryos. Nature Letters 2007;448(7150):191-5.
4. Buttery LDK, Bourne S, Xynos JD, Wood H, Hughes FJ, Hughes SPF, *et al*. Differentiation of osteoblasts and in vitro bone formation from murine embryonic stem cells. Tissue Eng 2001;7(1):89-9.
5. Clements BA, Hsu C, Kucharski C, Lin X, Rose L, Uludag H. Non-viral delivery of basic fibroblast growth factor gene to bone marrow stromal cells. Clin Orthop Relat Res 2009;467(12):3129-37.
6. Duplomb L, Dagouassat M, Jourdon P, Heymann D. Differentiation of osteoblasts from mouse embryonic stem cells without generation of embryoid body. In Vitro Cell Dev Biol Anim 2007;43(1):21-4.
7. Dunstan CR, Boyce R, Boyce BF Garrett IR, Izbicka E, Burgess WH, *et al*. Systemic administration of acidic fibro- blast growth factor (FGF-1) prevents bone loss and increases new bone formation in ovariectomized rats. J Bone Min Res 1999;14(6): 953–959.
8. Evans M, Kaufman M. Establishment in culture of pluripotential cells from mouse embryos. Nature 1981;292)5819:154-6.

9. Furuya M, Yasuchika K, Mizutani K, Yoshimura Y, Nakatsuji N, Suemori H. Electroporation of cynomolgus monkey embryonic stem cells. Genesis 2003;37(4):180-7.

10. Honda A, Hirose M, Ogura A. Basic FGF and Activin/Nodal but not LIF signalling sustain undifferentiated status of rabbit embryonic stem cells. Exp Cell Res 2009;315(12):2033-42.

11. Humphrey R, Beattie G, Lopez A, Bucay N, King C, Firpo M, *et al*. Maintenance of pluripotency in human embryonic stem cells is STAT3 independent. Stem Cells 2004;22(4):522-30.

12. Jukes JM, van Blitterswijk CA, de Boer J. Skeletal tissue engineering using embryonic stem cells. J Tissue Eng Regen Med 2010;4(3):165-80.

13. Jung S, Sen A, Rosenberg L, Behie LA. Identification of growth and attachment factors for the serum-free isolation and expansion of human mesenchymal stromal cells. Cytotherapy 2010;12(5):637-57.

14. Lecanda F, Avioli LV, Cheng SL. Regulation of bone matrix protein expression and induction of differentiation of human osteoblasts and human bone marrow stromal cells by bone morphogenetic protein-2. J Cell Biochem 1997;67(1):386-96.

15. Levenstein M, Ludwig T, Xu RH, Llanas R, Vanderheuval-Kramer K, Manning D, *et al*. Basic fibroblast growth factor support of human embryonic stem cell self-renewal. Stem Cells 2006;24(3):568-74.

16. Maegawa N, Kawamura K, Hirose M, Yajima H, Takakura Y, Ohgushi H. Enhancement of ostoblastic differentiation of mesenchymal stromal cells cultured by selective combination of bone morphogenetic protein-2 (BMP-2) and fibroblast growth factor-2 (FGF-2). J Tissue Eng Regen Med 2007;1(4):306-13.

17. Martin I, Muraglia A, Campanile G, Cancedda R, Quarto R. Fibroblast growth factor-2 supports ex vivo expansion and maintenance of

osteogenic precursors form human bone marrow. Endocrinology 1997;138(10):4456-62.

18. Martins-Taylor K, Xu RH. Determinants of pluripotency: from avian, rodents, to primates. J Cell Biochem 2010;109(1):16-25.

19. Meng GL, Zur Nieden N, Liu SY, Cormier JT, Kallos MS, Rancourt DE. Properties of murine embryonic stem cells maintained on human foreskin fibroblasts without LIF. Mol Reprod Dev 2008;75(4):614-22.

20. Nagai H, Tsukuda R, Mayahara H. Effects of basic fibroblast growth factor (bFGF) on bone formation in growing rats. Bone 1995;16(3):367-73.

21. Ng KW, Speicher T, Dombrowski C, Helledie T, Haupt L, Nurcombe V, *et al*. Osteogenic differentiation of murine embryonic stem cells is mediated by fibroblast growth factor receptors. Stem Cells Dev 2007;16(2):305-18.

22. Ohba S, Nakajima K, Komiyama Y, Kugimiya F, Igawa K, Itaka K, *et al*. A novel osteogenic helioxanthin-derivative acts in a BMP-dependent manner. Biochem Biophys Res Commun 2007;357(4):854-60.

23. Roach HI. Induction of normal and dystrophic mineralization by glycerophosphates in long-term bone organ culture. Calcif Tissue Int 1992;50(6):553-63.

24. Smith A, Heath J, Donaldson D, Wong G, Moreau J, Stahl M, *et al*. Inhibition of pluripotential embryonic stem cell differentiation by purified polypeptides. Nature 1988;336(6200):688-90.

25. Thomson JA, Itskovits-Eldor J, Shapiro S, Waknitz M, Swiergiel J, Marshall V, *et al*. Embryonic stem cell lines derived from human blastocysts. Science 1998;282(5391):1145-7.

26. Toumadjie A, Kusumoto KI, Parton A, Mericko P, Dowell L, Ma G, *et al*. Pluripotent differentiation in vitro of murine ES-D3 embyronic stem cells. In Vitro Cell Dev Biol Anim 2003;39(10):449-53.

27. Varkey M, Kucharski C, Haque T, Sebald W., Uludağ H. In vitro osteogenic response of rate bone marrow stromal cells to bFGF and BMP-2 treatments. Clin Orthop Relat Res 2006;443:113-23.

28. Wang L, Huang Y, Pan K, Jiang X, Liu C. Osteogenic responses to different concentrations/ratios of BMP-2 and bFGF in bone formation. Ann Biomedl Eng 2010;38(1):77-87.

29. Williams RL, Hilton D, Pease S, Willson T, Stewart C, Gearing D, *et al*. Myeloid leukaemia inhibitory factor maintains the development potential of embryonic stem cells. Nature 1988;336(6200):684-7.

30. Xu C, Rosler E, Jiang J, Lebkowski JS, Gold JD, O'Sullivan C, *et al*. Basic fibroblast growth factor supports undifferentiated human embryonic stem cell growth without conditioned medium. Stem Cells 2005;23(3):315-32.

31. Xu RH, Peck RM, Li DS, Feng X, Ludwig T, Thomson JA. Basic FGF and suppression of BMP signalling sustain undifferentiated proliferation of human ES cells. Nat Methods 2005;2(3):185-90.

32. Zhu H, Guo ZK, Jiang XX, Li H, Wang XY, Yao HY, *et al*. A protocol for isolation and culture of mesenchymal stem cells from mouse compact bone. Nature Protocols 2010;5(3):550-60.

33. Zur Nieden N, Kempka G, Ahr HJ. In vitro differentiation of embryonic stem cells into mineralized osteoblasts. Differentiation 2003;71(1)18-27.

4 Protein expression following non-viral delivery of plasmid DNA coding for basic FGF and BMP-2 in a rat ectopic model

A version of this chapter was published in: L Rose, C Kucharski, H Uludag. Biomaterials 2012;33(11):3363-74.

4.1 INTRODUCTION

Fracture healing is a complex process governed by the expression of multiple growth factors that control cell recruitment, soft callus formation, angiogenesis, callus mineralization, and bone remodelling. Failure of these coordinated processes can lead to non-union, which requires additional intervention and surgical procedures. In non-unions incapable of healing, a stimulation *de novo* bone formation is required for clinical success. Synthetic scaffolds containing recombinant human growth factors, such as bone morphogenetic proteins (BMP), provide a bioactive material that can induce bone formation at repair sites [53]. Collagen-based scaffolds with BMP-2 and BMP-7 (also known as Osteogenic Protein-1) are currently clinically approved for a range of orthopaedic applications, including spinal fusion, oral/maxillofacial applications and orthopaedic trauma [33][18]. Due to short half-life of proteins *in situ*, however, excessive amounts of recombinant proteins are required to maintain concentrations within a therapeutic range for sufficiently long duration for stimulation of bone formation; for example, ~1.5 mg/cc of BMP-2 [33] and ~0.9 mg/cc of BMP-7 (estimate) [14] are needed to treat tibial trauma. This is despite that the fact that natural levels of the proteins are in the ng/mL to mg/mL range. Large doses of recombinant proteins and the resulting expense of treatment may limit widespread use of protein therapies, and may also contribute to inflammation and higher rates of complication compared to an autologous bone graft [9]. Gene delivery for local production of growth factor offers a

solution to the limitations of the protein therapy. Direct administration of genes in a host is preferred due its convenience, possibility of immediate intervention with the trauma and the lower cost compared to costly cell culture-based therapies, where the desired genes are delivered via *ex vivo* modification of host cells. Viral delivery vectors have dominated the gene delivery approach for bone diseases, but they are generally more successful in immune-compromised animals with lower success rates in normal animals [54]. Clinical translation of viral vectors is also questionable due to safety concerns associated with viruses [52]. Non-viral vectors are, therefore, actively investigated for delivering therapeutic genes from plasmid DNA based expression systems in stimulating bone formation [5]. Plasmid DNA is attractive for driving expression of osteogenic proteins since it does not integrate into host genome and sustains transient gene expression that is sufficient (and desirable) in the case of bone regeneration.

Direct gene delivery for bone regeneration has been attempted by administration of plasmid DNA without the use of a DNA-binding carrier [12][7][17][8], and by electroporation without a carrier [27][47][29]. Such approaches are not likely to translate into a clinical setting due to low efficacy of transfection in the absence of a carrier or invasive treatment in the case of electroporation. In one study, BMP-4 plasmid complexed with 25 kDa polyethylenimine (PEI25) gave minimal bone formation in a rat skull defect, while naked BMP-4 plasmid showed no regeneration without a carrier [22]. It is estimated that >200 μg of PEI25 was used to be used in this study. PEI25

is exceptionally cytotoxic both *in vitro* [4] and *in vivo* [4][44], and considering that 16-32 μg PEI25 interfered with bone induction activity of BMP-2 [60], significant toxicity must have arisen and possibly impeded bone induction. The lack of histological analysis did not confirm if the bone deposition was indeed from the transfected cells. In a separate study, SuperFect™ (a cationic liposome) was employed to condense and deliver a BMP-2 plasmid in a hydroxyapatite scaffold in a rabbit skull defect [41]. After 3 weeks, implants with BMP-2 plasmid showed signs of new bone formation and, by 9 weeks, half of the defect was penetrated with new bone. Some bone formation was also observed when the BMP-2 plasmid/liposomes were administered to the site without a scaffold. HA fibers, however, showed radiopaque regions in μ-CT analysis, suggesting that the HA scaffold itself may induce calcification in the absence of gene expression [37]. Finally, Itaka et al. employed 1.3 μg of plasmid DNA and showed successful bone repair in a mouse skull defect [23]. A block polymer of PEG-aspartate-diethylenetriamine was used to deliver runt-related transcription factor 2 (Runx2) and activin receptor-like kinase 6 (caALK6) genes, both intracellular mediators involved in osteogenic differentiation. These are unique genes since they are not extracellularly acting proteins on stem cells, but rather intracellularly active proteins that will transform the transfected cells, rather than by acting on neighboring cells. Bone formation was observed histologically after 4 weeks covering ~50% of the defect.

While bone formation has been observed in some studies, there has been no assessment of recombinant protein expression *in situ*, a parameter that is crucial in the success of bone regeneration. With implantation of recombinant proteins, several studies have reported clear dose-response relationships [18][6], which helped to refine the devices for a robust bone induction. With non-viral gene delivery, no information is available about the local production rates of the therapeutic proteins. The confirmation of gene expression *in situ* is critical in order to validate the delivered therapeutic effect as well as to better predict the magnitude of the observed bone induction. It is also impossible to evaluate the *in vivo* utility of gene carriers without assessing gene expression directly; while some reagents are effective *in vitro* [28], their performance was found to be limited *in vivo* [23], and no information is available for the underlying reason(s) for this observation. Assessing the levels of secreted therapeutic proteins quantitatively will help advance the non-viral gene delivery approach.

This study was performed in order to assess expression of therapeutic proteins after non-viral delivery of the expression vectors with polymeric carriers. The genes delivered for this study were BMP-2 and basic Fibroblast Growth Factor (bFGF), coding for two proteins that were shown to stimulate bone formation on their own [58][26] and in combination with each other [57][2]. The polymeric carriers chosen were (i) PEI25, a gold standard for *in vitro* gene delivery and a carrier previously used for gene delivery in a skull defect, and (ii) a linoleic acid-substituted 2 kDa PEI (PEI-LA), which was

developed in the authors' lab as a less toxic substitute for PEI25 [36]. By using a convenient and well-characterized animal model, i.e., rat subcutaneous implant model [60], we report protein expression levels following *in vivo* implantation of BMP-2 and bFGF expression vectors.

4.2 MATERIALS AND METHODS

4.2.1 Materials

Dulbecco's Modified Eagle Medium (DMEM) cell culture media, trypsin (0.05%, w/v), penicillin/streptomycin (10,000 U/mL/10,000 mg/mL), and DNAse/RNAse free water were purchased from Invitrogen (Grand Island NY). Fetal bovine serum was from PAA Laboratories Inc. (Etobicoke, ON) and Hank's Balanced Salt Solution (HBSS) was from BioWhittaker (Walkersville, MD). Absorbable gelatin (Gelfoam™) and collagen (Helistat™) sponges were from Pharmacia & Upjohn (Kalamazoo, MI) and Medtronic (Memphis, TN), respectively. The 2 kDa (PEI2) and 25 kDa PEI (PEI25) were from Sigma (St Louis, MO) and it was used without further purification. The human bFGF enzyme-linked immunosorbant assay (ELISA) was purchased from R & D Systems (Minneapolis, MN) and the BMP-2 ELISA was from Peprotech (Rocky Hill, NJ). Shandon cryomatrix was from Thermo Scientific (Pittsburgh, PA) and cryomolds were from Electron Microscope Services (Hatfield, PA). The pEGFP-N2 plasmid was purchased from BD Biosciences, while the gWIZ-GFP and gWIZ plasmids were purchased from Aldevron (Fargo, ND). The pIRES-AcGFP plasmid was purchased from Clonetech (Palo Alto, CA). The BMP2-

pCMV6-XL4 plasmid was from Origene (Rockville, MD). T4 DNA Ligase and restriction enzymes NheI, SacII, BglII and EcoRI were purchased from New England Biolabs (Ipswich, MA). A 2 kDa PEI modified with linoleic acid (PEI-LA) was prepared as previously described [36]. The extent of lipid modification was 1.2 linoleic acids per PEI molecule for the polymer used in this study.

4.2.2 bFGF and BMP-2 plasmid construction

Plasmids expressing the growth factors bFGF or BMP-2 were constructed in house (**Figure 3-1**). The pIRES-AcGFP vector contains an internal ribosome entry site (IRES) allowing simultaneous transcription of separate mRNAs for the growth factor (i.e., bFGF or BMP-2) and the *Aequorea coerulescens* GFP. The construction of the bFGF expressing plasmid was described elsewhere [11] and will not be repeated here. The resulting plasmid is 5764 base pairs and is referred to as bFGF-IRES-AcGFP. For the BMP-2 expression plasmid, the cDNA coding for growth factor was excised from the plasmid BMP2-pCMV6-XL4 with NheI and SacII restriction enzymes, and ligated with T4 DNA Ligase into NheI/SacII sites on the pIRES-AcGFP plasmid. BMP-2 gene insertion was confirmed by restriction mapping and sequencing. The resulting plasmid was sequenced at Molecular Biology Services Unit at the University of Alberta (Edmonton, AB) to confirm insertion of the BMP-2 gene. This plasmid is 7027 base pairs and referred to as BMP2-IRES-AcGFP. Analysis of bFGF or BMP-2 expression was determined

by using bFGF or BMP-2 specific ELISAs, while the expression of GFP was assessed by flow cytometry.

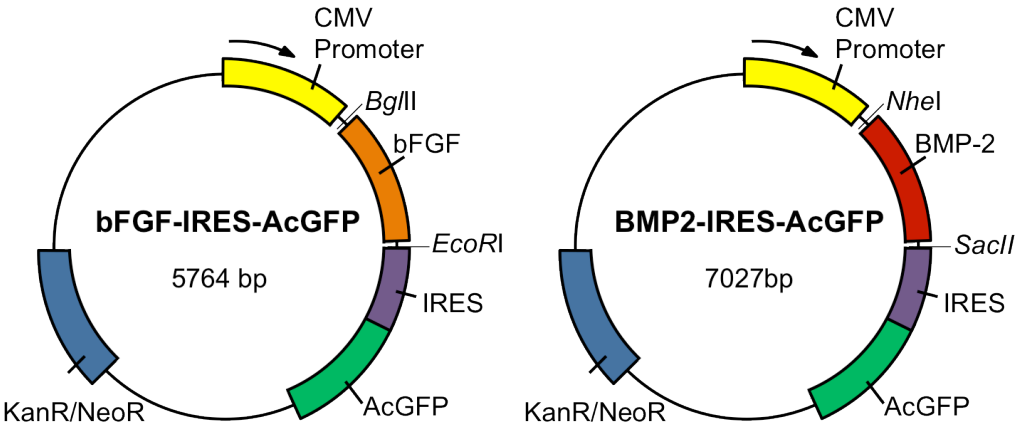

Figure 4-1 – ***Maps bFGF-IRES-AcGFP and BMP2-IRES-AcGFP plasmids used in this study.*** The bFGF and BMP-2 coding regions were ligated into the pIRES-AcGFP plasmid to construct the bFGF-IRES-AcGFP and BMP2-IRES-AcGFP plasmids, respectively.

4.2.3 Preparation of DNA/polymer complexes

The plasmid DNAs and polymers were dissolved in DNAse/RNAse free water at 0.4 mg/mL and 1 mg/mL, respectively. The DNA solutions were diluted in 150 mM NaCl, and then the desired polymer solutions (PEI25 or PEI2-LA) were added to the plasmid solutions. After gently vortexing, the solutions were allowed to incubate for 30 minutes at room temperature. Saline (150 mM NaCl) alone was used for no treatment groups, and complexes prepared with the blank gWIZ plasmid were used as treatment controls. The polymer/plasmid weight ratio was controlled during complex

formation and specified in the appropriate experiments below. The weight ratio was 5/2 for PEI25 and 10/2 for PEI-LA. These optimized ratios were chosen based on previous studies, and showed complete polymer binding to plasmid [36], with excess polymer remaining in complex solution. For *in vitro* studies, plasmid concentration in culture media is provided as nanogram of plasmid per millilitre of tissue culture media, whereas the amount of plasmid added per sponge is provided for *in vivo* studies.

4.2.4 In vitro transfection studies

The functionality and protein secretion rates from the constructed plasmids were evaluated in the immortal 293T cell line *in vitro*. For assessment of GFP expression, cells were seeded in 24-well plates either onto the tissue culture wells (2D monolayer culture) or onto absorbable gelatin sponges (0.75 cm x 0.75 cm; 3D culture) in media containing 10% FBS and 1% penicillin/streptomycin. PEI-LA/gWIZ-GFP (10/2 w/w ratio) or control PEI-LA/gWIZ (10/2 w/w ratio) complexes were added to the cells either during seeding or the day after seeding. The final DNA concentration was 2 µg/mL in the media. After 24 hours exposure, the complex-containing media was removed and replaced with fresh media. The GFP expression of cultures was measured *in situ* with a fluorescent plate reader and the cells were imaged with an FSX 100 Olympus fluorescence microscope. On Day 6, cells were trypsinized and fixed in 3.7% formalin for flow cytometry analysis as previously described [36]. The cells not treated with DNA or polymers were

also analyzed by flow cytometry and used to set a background level to designate 1% GFP positive population.

To investigate protein secretion from bFGF and BMP-2 plasmids, bFGF-IRES-AcGFP and BMP2-IRES-AcGFP plasmids were used to form complexes with PEI-LA (10/2 w/w). The blank gWIZ plasmid was used as a negative control. The complexes were added to the cells for 24 hours, after which the medium was replaced with fresh medium. After three days of protein accumulation, media were collected and frozen at -20°C until further use. The cells were then washed with HBSS, trypsinized and viable cells were counted using Trypan Blue exclusion and a haemocytometer. Collected media was assessed for bFGF or BMP-2 secretion by using ELISA protocols according to the manufacturer suggestions (details not provided). The protein secretion rates were normalized with the cell counts and duration of secretion to provide protein secretion in ng protein/10^6 cells/day.

4.2.5 In vivo assessment of transgene expression

4.2.5.1. *Animal implantation procedures*

Four to six-weeks old female Sprague-Dawley rats were purchased from Biosciences (Edmonton, Alberta) and kept in standard laboratory conditions (23 °C; 12 h of light/dark cycle). Rats were kept 2-3 per cage with free access to water and a commercial rat chow. All procedures involving the rats were pre-approved by the Animal Welfare Committee at the University of Alberta (Edmonton, Alberta). Rats were anaesthetised with isofluorane and small bi-lateral ventral incisions were made with blunt-ended surgical scissors to

create subcutaneous pouches. One scaffold was inserted into each pouch, and the pouches were closed with wound clips. Each rat received two scaffolds, duplicates of the same type. For scaffold preparation, absorbable gelatin or collagen sponge (1 cm x 1 cm) were soaked with complexes for 15 minutes before implantation. The polymer/DNA complexes had been incubated for 15 minutes before addition to sponges so that the total complex incubation time was 30 minutes. At pre-determined time points (see Figure Legends), the rats were sacrificed by CO_2 asphyxiation to recover the scaffolds. Scaffolds were retrieved and used for (i) histological processing, (ii) lysis or (iii) *ex vivo* culture for GFP and recombinant bFGF and BMP-2 expression.

4.2.5.2. In vivo GFP expression

The scaffolds were analyzed for GFP expression by using flow cytometry, a fluorescent plate reader and histology. Complexes were prepared with the polymers PEI25 and PEI-LA, and the plasmid pEGFP-N2 and control gWiz, at the polymer:DNA ratios of 5:2 and 10:2, respectively (w/w), and loaded onto absorbable collagen or gelatin sponges with a total amount of 100 or 50 μg of plasmid DNA, respectively. From each group, 6 full scaffolds were washed in HBSS, trypsinized and the recovered cells were fixed in 3.7% formalin. Cells were analyzed for GFP expression using flow cytometry. The remaining three scaffolds were cut into equal pieces. One portion of the scaffold was put into a black 96-well plate containing HBSS. The fluorescence of the plate was read with an excitation and emission wavelengths of 485 and 527 nm respectively.

Scaffolds for histology were placed in tissue section holders and embedded in Shandon Cryomatrix. The scaffolds were frozen at -20°C and then sliced to obtain tissue sections. Slices were stained with a commercial reagent containing a nucleus stain and imaged with an FSX 100 fluorescent microscope (Olympus).

4.2.5.3. bFGF and BMP-2 Expression

Recombinant growth factor production was evaluated either by immediate lysis of the scaffolds after recovery or following an *ex vivo* culture period. Complexes for implantation were made with either PEI25 or PEI-LA and plasmid DNA at a ratio of 5:2 and 10:2 respectively (w/w). Absorbable gelatin or collagen sponges (1 cm x 1 cm) were loaded with complexes containing 10 µg or 50 µg of plasmid DNA (see Figure legends). Following a 1, 2 or 5 week implantation, scaffolds were harvested and cut into small pieces in a lysis buffer (pH 8) containing 50 mM Tris-HCl, 150 mM NaCl, 1% Tween 20, 1% protease inhibitor. Samples were vortexed to enable complete cell lysis. The supernatant was evaluated with bFGF or BMP-2 ELISA. To determine *ex vivo* protein production, scaffolds containing were harvested in a sterile environment after a 1 week implantation and transferred to 24-well plates containing 1mL of DMEM with 10% FBS and 1% P/S. Sponges were cultured *ex vivo* for a total of 5 days and media was changed on day 3. The supernatant was evaluated with bFGF or BMP-2 ELISA. Alternatively, complexes containing 10 µg of BMP2-IRES-AcGFP plasmid were implanted in

gelatin scaffolds for 1, 2 or 3 weeks before a 5 day *ex vivo* culture to determine GFP expression with a fluorescent plate reader and BMP-2 expression with an ELISA.

4.2.6 Statistical analysis

The data was summarized with mean of the measured parameters with error bars representing one standard deviation. Results were analyzed with an analysis of variance (ANOVA) followed by the Dunnett multiple comparison post-hoc test. For *in vivo* studies that had non-Gaussian distribution, the Kruskal-Wallis test, the non-parametric ANOVA, was employed followed by Dunn's multiple comparison tests. The level of significance was set at $p<0.05$.

4.3 RESULTS

4.3.1 *Comparison of GFP expression in monolayer and sponge cultures in vitro*

We first evaluated the ability of complexes to transfect cells either in 2D monolayer cultures or 3D sponge cultures, which is more representative of *in vivo* transfection. The GFP expression by the transfected 293T cells is summarized in **Figure 4-2**. Low levels of fluorescence were found in the No Treatment and control PEI-LA/gWIZ groups irrespective of whether the cells were grown on tissue culture plastic or in Gelfoam sponges (**Figure 4-2A**). Generally, cells grown in gelatin sponges had higher auto-fluorescence values than the cells on a monolayer (1.4-1.8 vs. 0.1-0.2 au, respectively) for control

groups, possibly reflecting the presence of residual media in sponges during the fluorescence measurements. A significantly elevated GFP fluorescence was observed in all groups treated with PEI-LA/gWIZ-GFP complexes. Adding the complexes during cell seeding or 24 hours following cell seeding was equally effective for GFP expression. For the latter group, GFP expression was also evident when the cells were examined with a fluorescent microscope (**Figure 4-3**). No Treatment and control PEI-LA/gWIZ treated groups showed no fluorescence under the microscope (not shown).

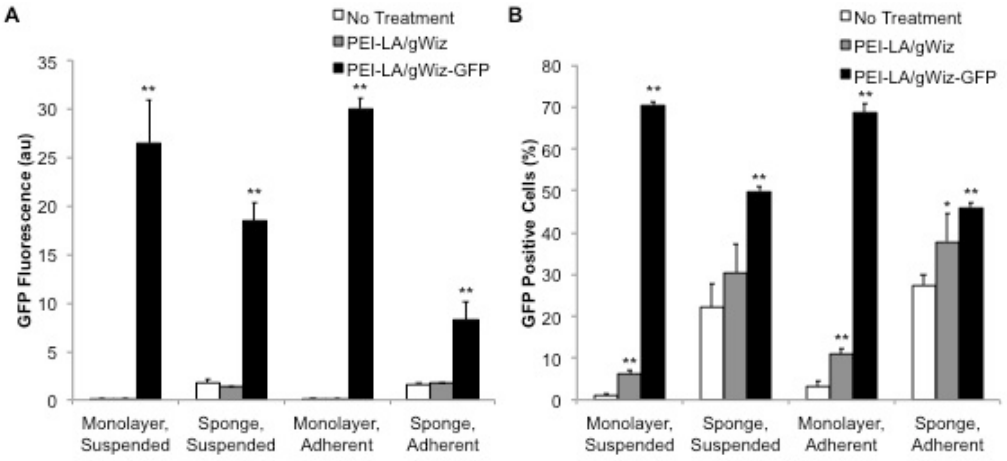

Figure 4-2 - ***GFP Expression following delivery of PEI-LA complexes.*** Cells were grown on tissue culture plates as a monolayer or in gelatin sponges. Complexes were added either during seeding (suspended) or one day after cell seeding and attachment (adherent). 293T cells were evaluated for GFP expression 6 days after exposure to the PEI-LA/gWiz-GFP complexes. The GFP fluorescence was assessed by either a fluorescent plate reader to obtain total GFP fluorescence (**A**) or flow cytometry to obtain percentage of GFP-positive cells (**B**).

The data from the flow cytometric analysis is summarized in **Figure 4-2B**. For cells grown as a monolayer, exposure to control PEI-LA/gWIZ complexes did not lead to a change in GFP expression. However, cells treated with PEI-LA/gWIZ-GFP complexes gave ~70% GFP-positive population with no clear difference between cells exposed to complexes while seeding or after 24 hours of attachment. Subtracting the background of control PEI-LA/gWIZ group, 64±1% of cells were GFP-positive when complexes were added to suspended cells while adherent cells gave 58±2% GFP-positive cell population. For cells grown in sponges, large increases (22-27%) in GFP-positive cells were observed in No Treatment groups. This increase was likely a consequence of the excessive trypsinization required to recover the cells from the sponges. Subtracting the background of PEI-LA/gWIZ group from the PEI-LA/gWIZ-GFP group, cells from the sponges were ~19% and ~8% GFP positive for suspended and adherent groups, respectively.

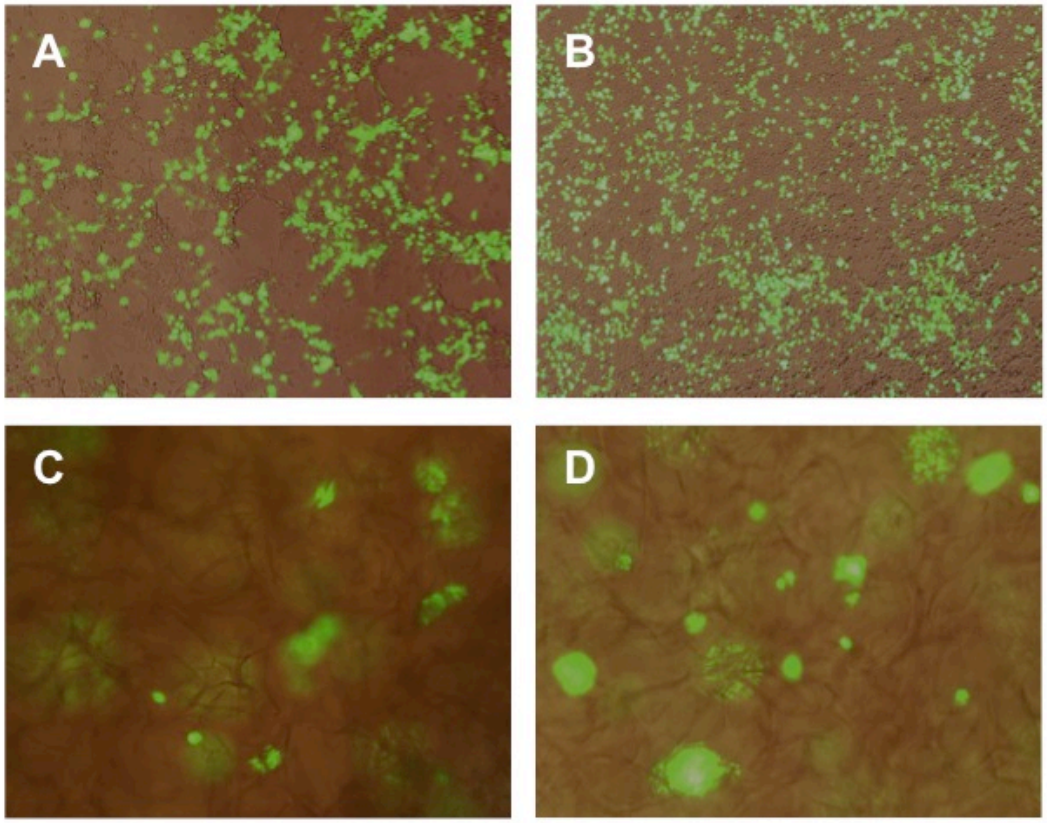

Figure 4-3 – ***Microscopic images of cells following delivery of PEI-LA complexes.*** Cells were grown as a monolater on tissue culture plates (**A,B**) or in gelatin sponges (**C,D**). PEI-LA/gWiz-GFP complexes were added to cells during seeding (**A,C**) or 24 hours after cell seeding (**B,D**). Microscopic images were taken 6 days after incubation with the complexes.

4.3.2 *Growth factor secretion from monolayer and sponge cultures in vitro*

To confirm growth factor expression, 293-T cells were exposed to PEI-LA/bFGF-IRES-AcGFP complexes to determine bFGF production rates. As before, cells were grown as a monolayer and in sponges, and the complexes were added to suspended or adherent cells (**Figure 4-4A**). Suspended cells grown in a monolayer produced ~2.5 ng of bFGF/well. Suspended and adherent sponge cultures along with monolayer adherent cultures all produced ~3.5 ng bFGF/well. No bFGF was detected in monolayer cultures when cells were untreated or treated with blank PEI-LA/gWIZ complexes. Small amount of bFGF (<0.3 ng/well) were detected in controls from cells in sponges, which was hypothesized to be due to cross-reactivity of scaffold components with the bFGF ELISA. Complete extraction of the cells from the sponge cultures was not possible, so that bFGF secretion rates could not be normalized to cell numbers. In a subsequent study, protein secretion rates from monolayer culture were investigated from cells treated with PEI-LA/bFGF-IRES-AcGFP and PEI-LA/BMP2-IRES-AcGFP complexes. Relatively large amounts of BMP-2 and bFGF secretion rates were evident: ~13 ng BMP-2 and ~3.5 ng bFGF per 10^6 cells/day (**Figure 4-4B**). No BMP-2 or bFGF was detected in the No Treatment and PEI-LA/gWIZ control groups.

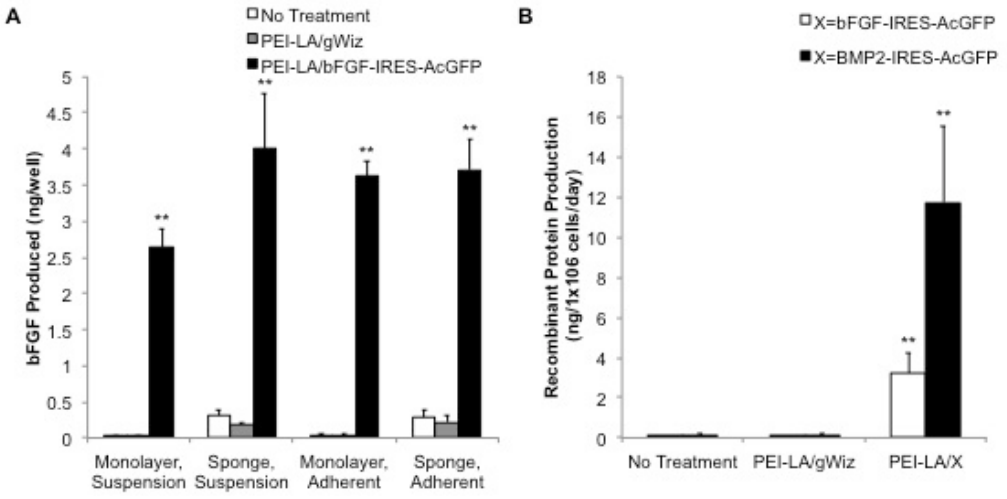

Figure 4-4 – *Recombinant growth factor production in 293T cells.* (**A**) PEI-LA/bFGF-IRES-AcGFP and PEI-LA/gWiz complexes were added to 293-T cells grown as a monolayer and in gelatin sponges. Complexes were added either during seeding (suspended) or one day after cell seeding and attachment (adherent). Media was assayed for bFGF production 3 days later and results are summarized as ng protein secreted per well. (**B**) Specific protein secretion rates from monolayer cultures for bFGF and BMP-2 expression vectors. Media was assayed for protein production 3 days later and results are summarized as ng protein secreted per 10^6 cells per day.

4.3.3 *GFP transfection in scaffolds after implantation*

Transgene expression *in vivo* was first investigated by delivering the GFP-expression vector pEGFP-N2, soaked in collagen (**Figure 4-5A**) and gelatin sponges (**Figure 4-5B**). Collagen scaffolds were first tested using the PEI25 carrier. The sponges showed extensive host cell infiltration around the scaffolds, whose outline was visible by the faint background fluorescence of the collagen implant. With PEI25/pEGFP-N2 complexes, localized regions of strongly fluorescent GFP-positive cells were observed unlike the sponges with blank PEI25/gWIZ complexes.

Gelatin scaffolds was then evaluated for GFP expression by implanting the plasmid DNA either naked (i.e. without a carrier) or in complexes (**Figure 4-5B**). The bFGF-IRES-AcGFP plasmid was also delivered in addition to the pEGFP-N2 plasmid to ensure that the obtained results were not specific to one type of expression vector. Similar to collagen sponges, no GFP expression was obtained in the case of naked (i.e., without a carrier) pEGFP-N2 or bFGF-IRES-AcGFP delivery. No GFP expression was observed with PEI25/pEGFP-N2 or PEI25/bFGF-IRES-AcGFP complexes either. GFP expression was, however, observed in patches when PEI-LA was used to deliver pEGFP-N2 and bFGF-IRES-AcGFP plasmids. There was no apparent difference in GFP expression between the two plasmids in this set of implants. The PEI25 and PEI-LA complexes containing gWIZ complexes did not give any GFP expression (data not shown), as expected.

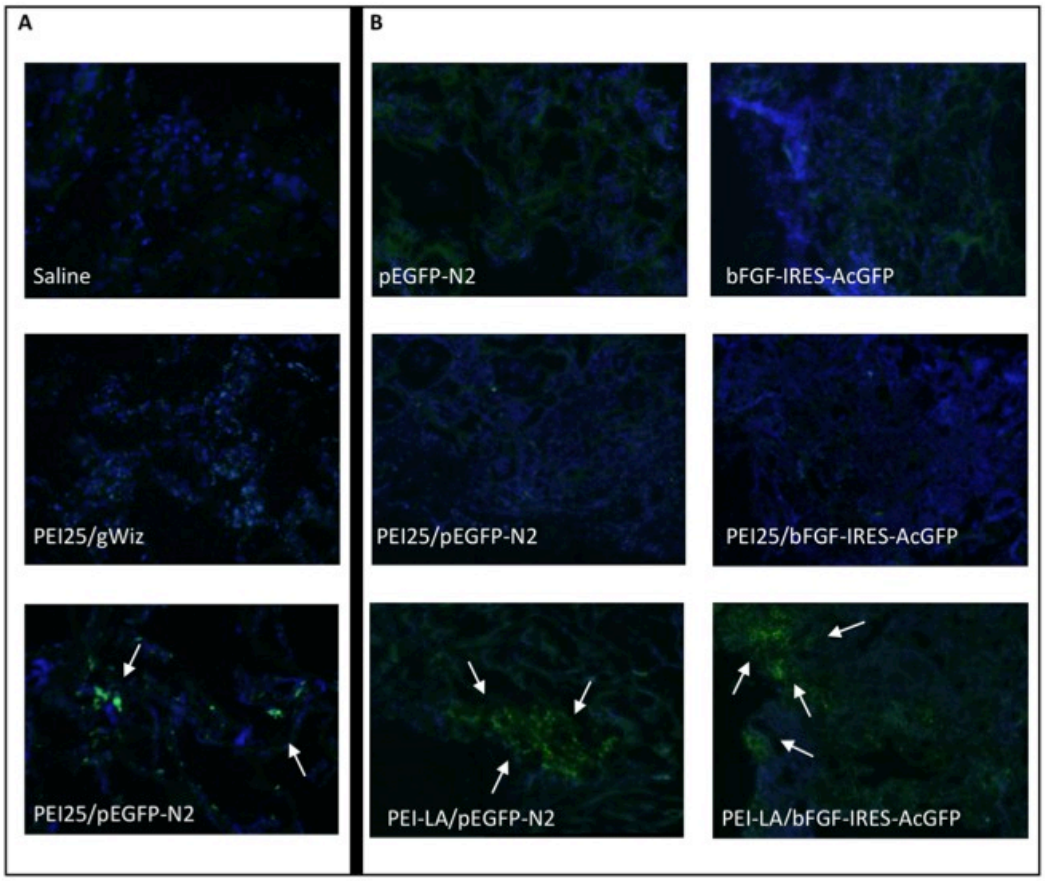

Figure 4-5 – *Histology of polymer/pDNA-loaded sponges following recovery from subcutaneous implantation*. Collagen scaffolds were implanted for 8 days (**A**), and gelatin scaffolds for 14 days (**B**). The plasmids or polymer/plasmid complexes delivered in each scaffold is indicated on each image. Arrows indicate GFP positive regions. The plasmids in the absence of a carrier did not give any GFP-positive cells. With collagen sponges, PEI25 was effective for GFP expression, but not with gelatin sponges, where only PLL-LA was effective in supporting the trangene (GFP) expression. Note that the scaffolds themselves showed low levels of diffuse autofluorescence.

4.3.4 bFGF and BMP-2 secretion from implanted scaffolds

4.3.4.1 In vivo protein secretion from implanted scaffolds

To evaluate bFGF and BMP-2 secretion *in vivo*, gelatin sponges were implanted with gWIZ, bFGF-IRES-AcGFP and BMP-2-IRES-AcGFP complexes prepared with PEI25 and PEI-LA. An obvious difference between the implants containing the bFGF and BMP-2 expression vectors and the control gWIZ vector was the difference in tissue organization around the scaffolds and new blood vessel formation at the time of explantation (**Appendix A**). Gelfoam sponges containing PEI25/gWIZ and PEI-LA/gWIZ complexes showed little integration with the surrounding tissue with no evidence of visual angiogenesis (**Appendix A**). Little or no effort was required to extricate these sponges from their subcutaneous sites. However, sponges with polymer complexes containing bFGF-IRES-AcGFP and BMP2-IRES-AcGFP were well integrated with the surrounding tissue (**Appendix A**). These implants were surrounded by soft tissue to such an extent that surgical scissors were required to fully excise the implanted sponges. Additionally, hematomas were observed within these sponges.

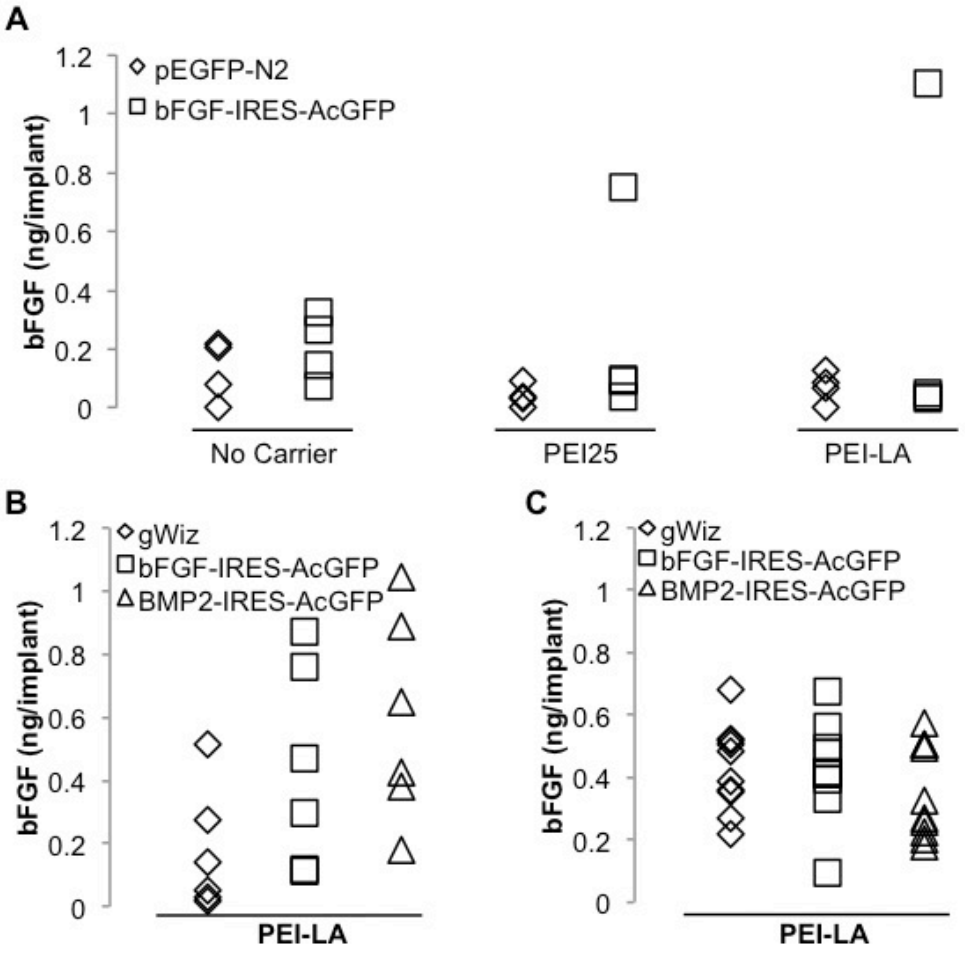

Figure 4-6 – ***In situ detection of recombinant bFGF in sponges following subcutaneous implantation.*** (**A**) For implants recovered after 1 week, gelatin sponges were loaded with plasmids pEGFP-N2 and bFGF-IRES-AcGFP without any carriers or with PEI25 and PEI-LA complexes. For implants recovered after 2 (**B**) and 5 weeks (**C**), gelatin sponges were loaded with PEI-LA complexes of gWIZ, bFGF-IRES-AcGFP and BMP2-IRES-AcGFP. The weight ratios of polymer/plasmid were 5/2 and 10/2 for PEI25 and PEI-LA, respectively. The lysates from the recovered implants were assayed for bFGF production.

To determine whether recombinant growth factors were being expressed, explanted sponges were lysed and the lysates were analysed by ELISAs. The bFGF amount in scaffolds implanted for 1, 2 or 5 weeks is shown in **Figure 4-6**. The bFGF amounts were minimal (0-0.2 ng/implant) for implants containing bFGF-IRES-AcGFP and pEGFP-N2 plasmids alone (i.e., without a carrier) after a 1-week implantation (**Figure 4-6A**). There were no changes in bFGF levels for PEI25/pEGFP-N2 and PEI-LA/pEGFP-N2. For the polymer/bFGF-IRES-AcGFP complexes, one implant in both PEI25 and PEI-LA groups (out of 6 implants) showed increased bFGF concentration (0.8 and 1.1 ng/implant, respectively), but the mean differences in these groups were not significantly different from the control group. The bFGF expression after 2 weeks of implantation is shown in **Figure 4-6B** for PEI2-LA complexes. For these implants, complexes with BMP2-IRES-AcGFP plasmid were also implanted to ensure there was no ELISA cross-reactivity between the two recombinant proteins. After 2 weeks, the range of bFGF detected was 0 to 0.5 ng/implant in the control group, and there was no significant increase in bFGF secretion with PEI-LA/bFGF-IRES-AcGFP and PEI-LA/BMP2-IRES-AcGFP complexes. Similar results were observed for groups following a 5 week implantation with a range of 0.1-0.7 ng/implant for the three groups (**Figure 4-6C**).

Similarly, BMP-2 expression was evaluated in scaffold (**Figure 4-7**). No BMP-2 was detected in the No Treatment group after a 1 week of implantation (**Figure 4-7A**). Up to 1.1 ng/implant was detected when the

BMP2-IRES-AcGFP plasmid alone (without a carrier) was delivered after one week. No BMP-2 was detected when the BMP-2 plasmid was delivered with PEI25; however, there was up to 1.2 ng BMP-2/implant when the plasmid was delivered by PEI-LA (not significantly different from no carrier group). At 2 and 5 weeks, BMP-2 protein was detected following delivery of both PEI-LA/bFGF-IRES-AcGFP and PEI-LA/BMP2-IRES-AcGFP complexes (**Figure 4-7B, 4-7C**). At 5 weeks, BMP-2 protein was detected in implants receiving PEI-LA/gWIZ, PEI-LA/bFGF-IRES-AcGFP, and PEI-LA/BMP2-IRES-AcGFP, which ranged from 0 to 3.5 ng/implant with no apparent differences among the study groups (**Figure 4-7C**).

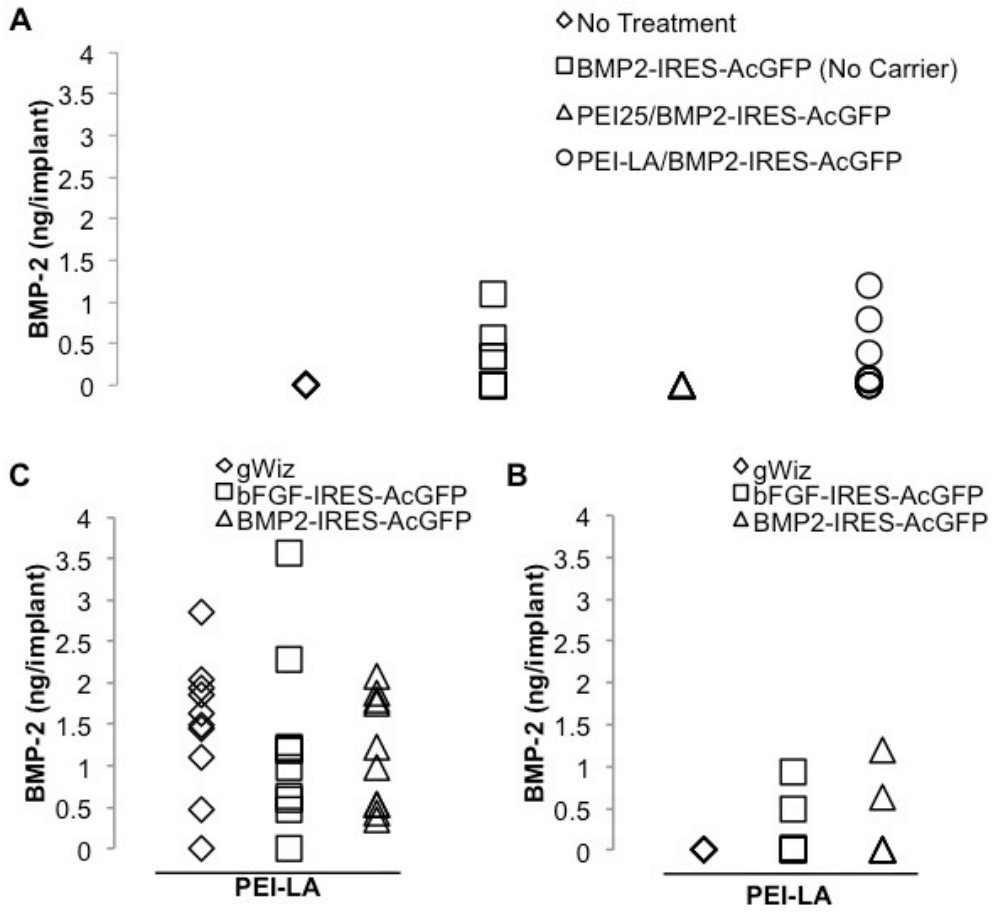

Figure 4-7 – ***In situ detection of recombinant BMP-2 in sponges following subcutaneous implantation.*** (**A**) For implants recovered after 1 week, gelatin sponges were loaded with saline (no treatment), BMP2-IRES-AcGFP without any carrier or BMP2-IRES-AcGFP complexed with PEI25 and PEI-LA. For implants recovered after 2 (**B**) and 5 weeks (**C**), gelatin sponges were loaded with PEI-LA complexes of gWIZ, bFGF-IRES-AcGFP and BMP2-IRES-AcGFP. The weight ratios of polymer/plasmid were 5/2 and 10/2 for PEI25 and PEI-LA, respectively. The lysates from the recovered implants were assayed for BMP-2 production.

4.3.4.2 Ex vivo protein secretion

Given the difficulty in detecting bFGF and BMP-2 proteins in scaffolds, we cultured the explanted scaffolds *ex vivo* for up to five days and assayed the media for protein secretion. It was hypothesized that (i) the secreted proteins did not have a chance to accumulate in implants, and/or (ii) supernatant from *ex vivo* culture would show less background than lysate from the scaffolds, so that the secreted proteins would be more easily detected in this way. A preliminary study was performed to determine whether explanted scaffolds would survive *ex vivo* culture long enough to produce recombinant growth factor. The implants received BMP2-IRES-AcGFP plasmid (10 mg/implant) without a carrier, or as complexes with PEI-LA and PEI25, and recovered after 1, 2 and 3 weeks. The GFP fluorescence in the implants receiving complexes was significantly higher than the implants receiving the plasmid without any carrier, especially for implants recovered after 2 and 3 weeks ($p<0.01$; **Figure 4-8A**). No significant BMP-2 secretion was detected following *ex vivo* culture (**Figure 4-8B**), although several PEI-LA explants showed increased BMP-2 expression on week one and two.

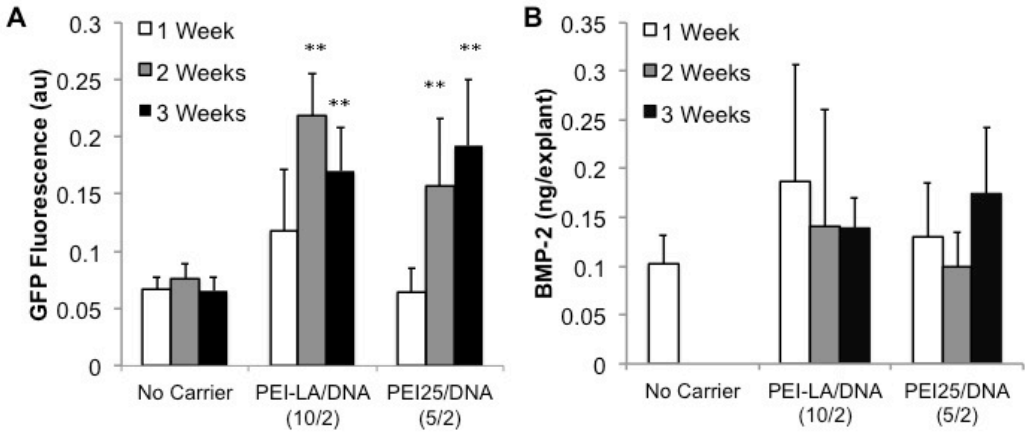

Figure 4-8 – ***Assessment of GFP (A) and BMP-2 (B) expression in gelatin sponges following ex vivo culture*****.** Gelatin sponges were loaded with BMP2-IRES-AcGCP plasmid (10 mg) without a carrier or as complexes with PEI-LA (10/2 w/w) and PEI25 complexes (5/2 w/w). The implants were harvested after 1, 2 and 3 weeks. The GFP expression was assessed by recovering the cells in implants and measuring GFP fluorescence in a plate reader, which BMP-2 in the supernatants was detected by ELISA

A similar study was repeated by implanting the BMP-2 expression vector by using gelatin and collagen scaffolds, but a significantly higher dose (50 mg) of plasmid was used. The implants received either gWIZ or BMP2-IRES-AcGFP complexes of PEI-LA. Following 1 week of implantation, *ex vivo* BMP-2 secretion rates were summarized in **Figure 4-9**. Compared to PEI-LA/gWIZ controls, sponges with PEI-LA/BMP2-IRES-AcGFP complexes showed increased BMP-2 secretion during day 0-3 post explantation (**Figure 4-9A**; $p<0.01$ and $p<0.05$ for collagen and gelatin sponges, respectively). The net BMP-2 secretion rates on Day 0-3 from the collagen and gelatin sponges (i.e., difference between average secretion from PEI-LA/BMP2-IRES-AcGFP complexes minus average secretion from PEI-LA/gWIZ complexes) were ~0.12 and 0.28 ng/implant/day, respectively. Similar net secretion rates of 0.16 and 0.30 were obtained for collagen and gelatin implants, respectively, on Day 4-5 (**Figure 4-9B**), although this difference was not significantly different at this time point.

A similar study was conducted for assessment of bFGF secretion as well, by using bFGF-IRES-AcGPF plasmid delivered without a carrier or as complexed with PEI-LA. No bFGF was detected from the delivery of naked bFGF-IRES-AcGFP plasmid while PEI-LA complexes gave a net bFGF secretion rate that was lower than the BMP-2 secretion rate (<0.08 ng/implant/day). The difference between the two groups was not significant ($p>0.05$; not shown).

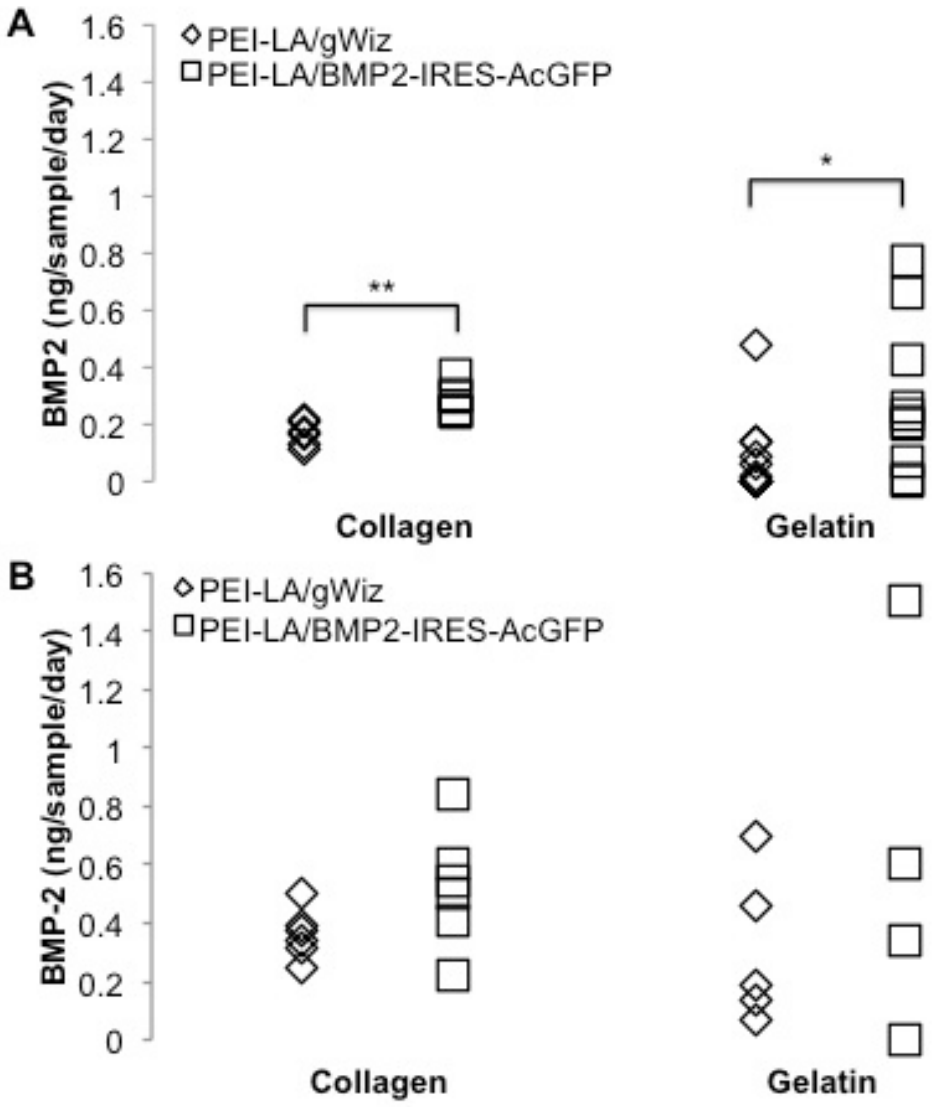

Figure 4-9 – ***Recombinant human BMP-2 secretion in collagen and gelatin sponges following ex vivo culture.*** Absorbable collagen or gelatin sponges were loaded with polymer/pDNA complexes by using gWIZ and BMP2-IRES-AcGFP plasmids and PEI-LA polymer. Following subcutaneous implantation for 1 week, sponges were cultured ex vivo, and the media assayed for BMP-2 secretion between day 0-3 (**A**) and day 4-5 (**B**). * $p<0.05$, ** $p<0.01$.

4.4 DISCUSSION

Direct gene delivery offers an exciting strategy for bone regeneration and repair. *In vivo* gene delivery, however, requires confirmation of effective gene expression *in situ*, as the success of many carriers *in vitro* does not readily translate to success in an animal model. Recombinant protein expression *in situ* allows direct estimation of gene delivery efficiency, and provides a method for comparing the effectiveness of carriers intended for direct gene delivery. This study reports on the feasibility of assessing transgene expression and compares *in vivo* performance of two polymeric systems, namely PEI-LA and PEI25. The latter is the 'gold standard' for *in vitro* transfection studies, where it provides a cost-effective, albeit relatively cytotoxic [34], reagent for routine cell modification. PEI25 serves as a routine reference for *in vitro* transfection studies, and it is one of the two polymers used for non-viral gene delivery in bone regeneration (as stated in Introduction). Our previous studies showed that local concentration of PEI25 was critical when it was used in nanoparticulate formulations for BMP-2 protein delivery; measures to reduce its toxicity was needed to sustain a robust bone induction *in vivo*. The PEI-LA, on the other hand, was derived from a non-toxic PEI molecule (2 kDa PEI), which was lipid-substituted for better packaging of nucleic acids and improved interaction with cellular membranes necessary for cellular delivery. Using the reporter protein GFP, PEI-LA was shown to give superior transgene expression compared to PEI25

in primary bone marrow stromal cells from rats *in vitro* [21], but with less toxicity displayed on the highly sensitive primary cells.

The *in vitro* efficiency of PEI-LA was first investigated with 293T cells and by using the vectors specifically designed for growth factor expression. Standard transfection protocols reported in the literature typically expose monolayer cells to complexes in media on the day after seeding, whereas direct *in vivo* gene delivery involves host cells infiltrating the complex-loaded sponge and internalizing the complexes as they penetrate into the sponge. A variety of host cells are expected to invade the sponge at ectopic sites [42], but the specific phenotype conducive for complex uptake and expression remains elusive. To account for this important difference, the ability to transfect both adherent cells and suspended cells, which may better represent cell invasion into the scaffold, were investigated. Gene delivery with gelatin scaffolds was assessed to ensure that there was no unintended interaction between the complex and sponge components that might have prevented transfection. Extensive GFP expression was seen in 293-T cells exposed to PEI-LA complexes in the sponge, which was also confirmed by the bFGF expression and secretion into the culture supernatants. These results indicated that gene delivery was successful in sponges and there were no major differences between the ability of cells getting transfected as a monolayer or in three-dimensional sponge culture. A comparison between the bFGF and BMP-2 expression vectors showed that the BMP-2 vector gave better protein expression/secretion than the bFGF plasmid (~3-fold better),

based on results with monolayer cultures. The difference between bFGF and BMP-2 expression may be due to differences in mRNA stability, as bFGF mRNA contain an antisense transcript used to regulate expression [35].

The recombinant protein production obtained with PEI-LA mediated delivery (3.5-13 ng/10^6 cells/day) was similar to *in vitro* reported rates with 293-T cells using PEI25 and Lipofectamine2000™ (estimated at 30 ng/10^6 cells/day) [11], and using adenovirus vectors (15 ng/10^6 cells/day) [16]. Higher (~10-fold) expression was observed with an integrating retroviral transduction system on a murine chondrogenic cell line [55]. In primary fibroblasts transfected with PEI25 [32] or nucleofection [61], chondrocytes transfected with Fugene™ 6 [46], and bone marrow stromal cells transfected with Lipofectamine or PEI [11], similar production rates was obtained compared to fibroblasts transduced with an adenovirus of <1 ng/10^6 cells/day [50]. Others reported much higher protein secretion rates (10-100 fold) for retrovirus transduction of chondrocytes [55], and adenovirus transduction of mesenchymal stem cells [51] and gingival fibroblasts [48]. Therefore, non-viral carriers, including PEI-LA, seem to match some of the 'lower-performing' viral vectors for *in vitro* transfection, but exuberant secretion rates, which might be needed for some applications, seem to be obtained with only certain viral vectors.

The ultimate test of a delivery system, however, is its *in vivo* performance and viral vectors show a well-documented decrease in efficiency in component animal models due to immune system interference.

The gene delivery was attenuated [1] or ineffective in immune-competent animals [25][31][49][24] with viral vectors. Immune suppression can restore efficiency [38][39], but such treatment makes clinical translation of these viral systems unlikely. On the other hand, non-viral carriers are not expected to be affected by the immune response to the same extent. Not all non-viral carriers are an appropriate choice for use *in vivo*, however, and they are greatly limited by their toxicities. Both PEI25 [4] and SuperFect™ [41] were limited by high toxicity. Similar to PEI25, no more than 40 μg SuperFect™ could be employed without concerns of toxicity, which limited the amount of plasmid administered to 10 μg [41]. Although increased bone formation was observed with SuperFect™, new bone was formed mostly on the underside of the implant without infiltrating into HA scaffolds in that study. Similar bone formation patterns were observed with PEI25 as well [22], where new bone was primarily found in the periphery of cranial defects. The pattern of tissue regeneration in these models may suggest that the recombinant BMPs are expressed at a low dose, and therefore acting as a chemotactic agent [13], instead of a morphogen [53]. While chemotactic effects would lead to tissue induction, higher doses would be needed for tissue calcification to fully heal critical sized defects [18].

Bone regeneration is affected by a myriad of factors including the species, immune status, defect model, type of implant scaffold, and the choice of therapeutic protein and, hence, comparisons among different gene delivery studies in animal models are difficult. Recombinant protein

expression *in situ* is potentially a better parameter for delivery system development and optimization. Several studies have investigated non-viral gene delivery for bone regeneration but none have quantified recombinant protein production. We readily detected GFP expression with as little as 10 μg plasmid DNA delivered with the PEI-LA; however, expression of recombinant BMP-2 was not as clear at this plasmid dose. This may be due to differences in localization of the gene product: GFP is retained within the transfected cells, while the growth factors such as BMP-2 are mostly secreted and diffuse away from the implants. Although providing no therapeutic effect, GFP allows for facile detection of successful gene delivery. At this plasmid dose, the effectiveness of PEI-LA was equivalent to PEI25 for GFP expression (**Figure 4-8**). At the higher dose of 50 μg, PEI-LA outperformed PEI25, based on histological assessment of GFP expression (**Figure 4-5**). This may be a manifestation of the cytotoxicity of PEI25 at the higher dose.

Several studies have investigated delivery of naked plasmid DNA for bone regeneration but few have directly compared delivery of naked to polymer-mediated delivery. Higher amounts of plasmid were generally required for bone regeneration with naked plasmid. No bone formation was observed with 100 μg of BMP-4 plasmid delivered intramuscularly [29], whereas minimal bone formation was detected with 200 μg of BMP-4 plasmid in a cranial defect site [22] or 500 μg of BMP-7 plasmid in a collagen solution [8]. Bone formation was observed with 100 μg of VEGF plasmid in a radial critical defect model [17], 500 μg to 1 mg of BMP-4 and hPTH1-34

plasmids in a femur critical sized defect [12], and 40 mg of h-PTH1-34 plasmid in a tibia critical model defect [7]. Lower doses of plasmid have led to bone formation when combined with a polymeric carrier. Bone formation was observed when PEI25 delivered 200 μg of BMP-2 plasmid in cranial defect [22]. Similarly, 10 μg of BMP-2 plasmid delivered by SuperFect™ in cranial critical defect [41] or by calcium phosphate in subcutaneous model [37] led to bone formation. The smallest amount of plasmid DNA that led to bone formation was 1.3 μg of plasmid DNA coding for Runx2 and caALK6 that was delivered with a novel polymer in a rat cranial defect model [23]. Some of these studies included histological assessment to confirm efficacy, although these studies provided no quantitative expression data and not all included a control plasmid to account for un-specific effects. Unmethylated plasmid DNA produced by bacteria can induce immune responses [59][19]. Methylated DNA can attenuate immune response [10] to extend transgene expression [45], but it can still induce immune activation and contribute to osteogenesis. Cytokines produced by monocytes can stimulate an osteogenic response from bone marrow stromal cells, including increased BMP-2 and Runx2 production [40]. Such immune regulated changes in osteogenesis highlight the need to confirm recombinant protein expression and compare bone formation against appropriate controls including non-expressing plasmids.

At the plasmid dose employed in this study, a polymeric carrier was required for transgene expression. Clear detection of recombinant proteins

was successful only in an *ex vivo* culture model with the 50 μg plasmid implant dose; high background in control implants made detection of proteins in scaffold difficult when we attempted to extract the proteins from implants. It is possible that intracellular proteins released by the lysis buffer and/or extracellular proteins deposited in implants, including chromogenic components of vascular system (such as red blood cells), were the reasons for this background. Even in the *ex vivo* secretion model, significant increases in recombinant protein secretion were observed for only the BMP-2 (**Figure 4-9**), and not the bFGF (not shown), which most likely reflected differences in the expression rates between the two plasmids, as observed *in vitro*. In addition to the recombinant protein, collagen and gelatin scaffolds were compared for delivery of gene complexes. Collagen sponges are used for delivery of BMP-2 for bone regeneration [33][18][60], whereas gelatin (i.e., denatured collagen) sponges are primarily used as a hemostatic agent. Gelatin sponges have been investigated to deliver proteins for bone regeneration, [56][15], so that the use of gelatin was not likely an impediment for bone regeneration. Although the details of fabrication (e.g., crosslinking reactions) for these two sponges are not readily known, we wanted to use both sponges to make sure that the nature of a scaffold did not bias the obtained results. Higher BMP-2 expression (~0.3 ng/implant/day) was observed on gelatin sponges compared to collagen sponges (~0.1 ng/sample/day). The reasons for this difference is not obvious at this time, but differences in the recombinant protein expression relay the importance

of selecting not only appropriate gene carriers, but also appropriate scaffolds. To compare the rate of PEI-LA-mediated gene expression, an independent study reported BMP-2 secretion rate of 0.1 ng BMP-2/implant/day [30] with *ex vivo* adenovirus transduction of fat pads, and was accompanied by robust bone regeneration and healing of a critical-sized femur defect. Similarly, 0.25 ng BMP-2/clot/day was produced by chondrocyte clots transduced *ex vivo* with a retrovirus for repair of an osteochondral defect [3]. Both of these studies were conducted at a bony site and they were able to demonstrate a stimulation of bone formation in the employed model. Based on release rates alone, it is likely that the non-viral approach reported here should be also suitable for these models.

We were not able to see any osteogenic transformation at the subcutaneous implant site employed for this study. BMP-2, but not bFGF, usually provides a robust bone induction at this site when a sufficiently high dose of protein (>1 mg/implant) is administered ectopically. With our system, we exposed to local site at most ~10 ng BMP-2 during 1-2 weeks of implantation period, which is below the dose needed to sustain an osteogenic effect at an ectopic site. The small amounts of BMP-2 produced with PEI-LA gene delivery, however, might be sufficient to produce bone formation in a bone defect model, which has a greater osteogenic capacity than an ectopic site [43]. It might be possible to add supplementary factors to attract a robust population of target cells (e.g., by using SDF-1 for BMP-2 responsive, CXCR4-positive stem cells, [20]), where sub-optimal doses of osteogenic proteins

was sufficient to induce effective osteoinduction. Future studies using orthopaedic sites will provide a better indication if the non-viral gene expression levels reported in this study will translate into new bone induction.

4.5 CONCLUSIONS

Recombinant protein expression was determined *in vitro* and, more importantly, *in vivo* using a rat subcutaneous implant model. Despite being expressed from the same plasmid vector, BMP-2 expression was found to be higher than the bFGF in 293-T cells *in vitro* and after implantation *in vivo*. GFP was readily detected histologically *in vivo* with as little as 10 μg of plasmid, and was detected macroscopically for up to 3 weeks after implantation when delivered with PEI-LA. High background in controls prevented clear detection of secreted proteins in implants but, by using an *ex vivo* culture method, implants receiving the plasmid complexes with polymeric carriers were shown to secrete significant amount of recombinant proteins. Compared to *in vitro* studies, where ~2 mg/mL DNA concentrations were sufficient to provide readily detectable proteins secretion, larger amounts of plasmid DNA (50 mg/implant) were required to observe significant increases in BMP-2 secretion. Furthermore, scaffolds delivering complexes influenced recombinant protein production: more BMP-2 was produced from PEI-LA/plasmid complexes delivered on a gelatin scaffold than a collagen scaffold. Taken together, our studies indicate that PEI-LA was

an effective *in vivo* gene delivery carrier and yields BMP-2 production rates similar to viral gene delivery reported in the literature. Given the perceived notion that viral vectors are generally more effective, it is particularly important to investigate recombinant protein production for non-viral carriers in situ for better assessment of their clinical potential.

4.6 REFERENCES

1. Alden T, Pittman D, Hankins F, Beres E, Engh J, Das S, et al. In vivo endochondral bone formation using a bone morphogenetic protein 2 adenoviral vector. Hum Gene Ther 1999;10(13):2245–53.
2. Akita S, Fukui M, Nakagawa H, Fugii T, Akino K. Cranial bone defect healing is accelerated by mesenchymal stem cells induced by coadministration of bone morphogenetic protein-2 and basic fibroblast growth factor. Wound Repair Regen 2004;12(2):252-9.
3. Betz O, Betz V, Abdulazim A, Penzkofer R, Schmitt B, Schroder C, et al. The repair of critical-sized bone defects using expedited autologous BMP-2 gene activated fat implants. Tiss Eng Part A 2010;16(3):1093-1101.
4. Beyerle A, Irmler M, Beckers J, Kissel T, Stoeger T. Toxicity pathway focused gene expression profiling of PEI-based polymers for pulmonary applications. Mol Pharm 2010;7(3):727-37.
5. Bleiziffer O, Eriksson E, Yao F, Horch R, Kneser U. Gene transfer strategies in tissue engineering. J Cell Mol Med 2007;11(2):206-23.
6. Boerckel J, Kolambkar Y, Dupont K, Uhrig B, Phelps E, Stevens H, et al. Effects of protein dose and delivery system on BMP-2 mediate bone regeneration. Biomaterials 2011;32(22):5241-5251.
7. Bonadio J, Smiley E, Patil P, Goldstein S. Localized, direct plasmid gene delivery in vivo: prolonged therapy results in reproducible tissue regeneration. Nature Medicine 1999;5(7):753-759.
8. Bright C, Park YS, Sieber AN, Kostuik JP, Leong KW. In vivo evaluation of plasmid DNA encoding OP-1 protein for spine fusion. Spine 2006;31:2163.
9. Cahill K, Chi J, Day A, Claus E. Prevalence, complications, and hospitals charges associated with use of Bone Morphogenetic Proteins in spinal fusion procedures. JAMA 2009;302(1):58–66.

10. Chen Y, Lenert P, Weeratna R, McCluskie M, Wu T, Davis H, et al. Identification of methylated CpG motifs as inhibitors of the immune stimulatory CpG motifs. Gene Ther 2001;8(13):1024-32.
11. Clement B, Hsu C, Kucharski C, Lin X, Rose L, Uludag H. Nonviral delivery of basic fibroblast growth factor gene to bone marrow stromal cells. Clin Orthop Relat Res 2009;467(12):1329-37.
12. Fang J, Zhu YY, Smiley E, Bonadio J, Rouleau J, Goldstein S, et al. Stimulation of new bone formation by direct transfer of osteogenic plasmid genes. Proc Natl Acad Sci USA 1996;93:5753.
13. Fiedler J, Roderer G, Gunther K, Brenner R. BMP-2, BMP-4, and PDGF-bb stimulate chemotactic migration of primary human mesenchymal progenitor cells. J Cell Biochem 2002;87(3):305-312.
14. Friedlaender G, Perry C, Cole JD, Cook S, Cierny G, Muscheler G, et al. Osteogenic protein-1 (bone morphogenetic protein-7) in the treatment of tibial non-unions. J Bone Joint Surg Am 2001;83-A Suppl 1:S151-158.
15. Fujita N, Matsushita T, Ishida K, Sasaki K, Kubo S, Matsumoto T, et al. An analysis of bone regeneration at a segmental bone defect by controlled release of bone morphogenetic protein 2 from a biodegradable sponge composed of gelatin and tricalcium phosphate. J Tissue Eng Regen Med 2011;doi10.1002/term432.
16. Garcia-Martinez C, Opolon P, TrochonV, Chianale C, Musset K, Lu H, et al. Angiogenesis induced in muscle by a recombinant adenovirus expressing functional isoforms of basic fibroblast growth factor. Gene Ther 1999;6(7):1210-21.
17. Geiger F, Betram H, Berger I, Lorenz H, Wall O, Eckhardt C, et al. Vascular endothelial growth factor gene-activated matrix (VEGF165-GAM) enhances osteogenesis and engiogenesis in large segmental bone defects. J Bone Miner Res 2005;20:2028.
18. Govender S, Csimma C, Genant HK, Valentin-Opran A. Recombinant human bone morphogenetic protein-2 for treatment of open tibial fractures. J Bone Joint Surg Am 2002;84(12): 2123–2134.

19. Hartmann G, Krieg A. CpG DNA and LPS induce distinct patterns of activation in human monocytes. Gene Ther 1999;6(5):893-903.
20. Higashino K, Viggeswarapu M, Bargouti M, Liu H, Titus L, Boden S. Stromal cell-derived factor-1 potentiates bone morphogenetic protein-2 induced bone formation. Tissue Eng Part A 2011;17(3-4):523-30.
21. Hsu C, Hendzel M, Uludag H. Improved transfection efficiency of an aliphatic lipid substituted 2 kDa polyethylenimine is attributed to enhanced nuclear associated and uptake in rate bone marrow stromal cells. J Gene Med 2011;31(1):46-59.
22. Huang YC, Simmons C, Kaigler D, Rice KG, Mooney DJ. Bone regeneration in a rat cranial defect with delivery of PEI-condensed plasmid DNA encoding for bone morphogenetic protein-4 (BMP-4). Gene Therapy 2005; 12:418.
23. Itaka K, Ohba S, Miyata K, Kawaguchi H, Nakamura K, Takato T, et al. Bone regeneration by regulated in vivo gene transfer using biocompatible polyplex nanomicelles. Molecular Therapy 2007;15(9):1655.
24. Jane J, Dunford B, Kron A, Pittman D, Sasaki T, Li J, et al. Ectopic osteogenesis using adenoviral bone morphogenetic protein (BMP)-4 and BMP-6 gene transfer. Mol Ther 2002;6(4):464–70.
25. Kang Q, Sun M, Cheng H, Peng Y, Montag A, Deyrup A, et al. Characterization of the distinct orthotopic bone formting activity of 14 BMPs using recombinant adenovirus-mediated gene delivery. Gene Ther 2004;11(17):1312–20.
26. Kawaguchi H, Kurokawa T, Hanada K, Hiyama Y, Tamura M, Ogata E, et al. Stimulationof fracture repair by recombinant human basic fibroblast growth in normal and streptozocin-diabetic rats. Endocrinology 1994;135(2):774-81.
27. Kawai M, Maruyama H, Bessho K, Yamamoto H, Miyazaki J, Yamamoto T. Simple strategy for bone regeneration with a BMP-2/7 gene expression cassette vector. Biochem. Biophys. Res. Comm. (2009) 390: 1012-1017.

28. Kim SW, Ogawa T, Tabata Y, Nishimura I. Efficacy and cytotoxicity of cationic-agent- mediated nonviral gene transfer into osteoblasts. J Biomed. Mat. Res. (2004) 71: 308-315.
29. Kishimoto K, Watanabe Y, Nakamura H, Kokubun S. Ectopic bone formation by electroporatic transfer of bone morphogenetic protein-4 gene. Bone 2002;31(2):340-347.
30. Kohara H, Tabata Y. Enhancement of ectopic osteoid formation following the dual release of bone morphogenetic protein 2 and Wnt1 inducible signalling pathway protein 1 from gelatin sponges. Biomaterials 2011;32(24):5726-32.
31. Li J, Li H, Sasaki T, Holman D, Beres B, Dumont J, et al. Osteogenic potential of five different recombinant human bone morphogenetic protein adenoviral vectors in rat. Gene Therapy 2003;10:1735–1743.
32. Lim S, Liao IC, Leong K. Nonviral gene delivery from nonwoven fibrous scaffolds fabricated by interfacial complexation of polyelectrolytes. Mol Ther 2006;13(6):1163-1172.
33. McKay W, Peckham S, Badura J. A comprehensive review of recombinant human bone morphogenetic protein-2 (INFUSE® Bone Graft). International Orthopaedics 2007;31: 729–734.
34. Moghimi S, Symonds P, Murray J, Hunter A, Debska G, Szewczyk A. A two-stage poly(ethylenimine)-mediated cytotoxicity: implications for gene transfer/therapy. Mol Ther 2005;11(6):990-5.
35. Murphy P, Knee R. Identification and characterization of an antisense RNA transcript (gfg) from the human basic fibroblast growth factor gene. Mol Endocrinol 1994;8(7):852-9.
36. Neamnark A, Suwantong O, Remant Bahadur KC, Hsu C, Supaphol P, Uludag H. Aliphatic lipid substitution on 2 kDa polyethylenimine improves plasmid delivery and transgene expression. Mol Pharm 2009;6(6):1798-815.

37. Oda M, Kuroda S, Kondo H, Kasugai S. Hydroxyapatite fiber material with BMP-2 gene induces ectopic bone formation. J Biomed Mat Res Part B 2009;90(1):101.
38. Okubo Y, Bessho K, Fujimura K, Iizuka T, Miyatake S. Osteoinduction by bone morphogenetic protein-2 via adenoviral vector under transient immunosuppression. Biochem Biophys Res Commun 2000;267(1):382–7.
39. Okubo Y, Bessho K, Fujimura K, Iizuka T, Miyatake S. In vitro and in vivo studies of a bone morphogenetic protein-2 expressing adenoviral vector. J Bone Joint Surg Am 2001;83-A:S99-104.
40. Omar O, Graneli C, Ekstrom K, Karisson C, Johansson A, Lausmaa J, et al. The stimulation of an osteogenic response by classical monocyte activation. Biomaterials 2011;32(32):8190-8204.
41. Ono I, Yamashita T, Jin HY, Ito Y, Hamada H, Akasaka Y, et al. Combination of porous hydroxyapatite and cationic liposomes as a vector for BMP-2 gene therapy. Biomaterials 2004;25:4709–4718.
42. Otsuru S, Tamia K, Yamazaki T, Yoshikawa H, Kaneda Y. Circulating bone marrow-derived osteoblast progenitor cells are recruited to the bone-forming site by the CXCR4/stromal cell-derived factor-1 pathway. Stem Cells 2008;26(1):223-34.
43. Park J, Jung I, Yun J, Choi S, Cho K, Kim C. Induction of bone formation by Escherichia coli-expressed recombinant human bone morphogenetic protein-2 using block-type macroporous biphasic calcium phosphate in orthotopic and ectopic rat models. J Periodontal Res 2011;46(6):682-90.
44. Peng L, Gao Y, Xue Y, Huang S, Zhuo R. Cytotoxicity and in vivo tissue compatibility of poly(amidoamine) with pendant aminobutyl group as a gene delivery vector. Biomaterials 2010;31(16):4467-76.
45. Reyes-Sandoval A, Ertl H. CpG methylation of plasmid vector results in extended transgene product expression by circumventing induction of immune responses. Mol Ther 2004;9(2):249-61.

46. Schmal H, Melhorn AT, Zwingmann J, Muller C, Stark G, Sudkamp N. Stimulation of chondrocytes in vitro by transfer with plasmids coding for epidermal growth factor (hEGF) and basic fibroblast growth factor (bFGF). Cytotherapy 2005;7(3):292-300.
47. Sheyn D, Kimelman-Bleich N, Pelled G, Zilberman Y, Gazit D, Gazit Z. Ultrasound-based nonviral gene delivery induces bone formation in vivo. Gene Ther 2008;15:257-266.
48. Shin JH, Kim KH, Kim SH, Koo KT, Kim TI, Seol YJ, et al. Ex vivo bone morphogenetic protein-2 gene delivery using gingival fibroblasts promotes bone regeneration in rats. J Clin Per 2010;37(3):305-311.
49. Sonobe J, OkuboY, Kaihara S, Miyatake S, Bessho K. Osteoinduction by bone morphogenetic protein 2-expressing adenoviral vector: application of biomaterial to mask the host immune response. Hum Gene Ther 2004;15:659–668.
50. Spanholtz T, Theodorou P, Holzbach T, Wutzler S, Giunta R, Machens HG. Vascular endothelial growth factor ($VEGF^{165}$) plus basic fibroblast growth factor (bFGF) producing cells induce a mature and stable vascular network-a future therapy for ischemically challenged tissue. J Surg Res 2011;171:329-338.
51. Steinert A, Palmer G, Pilapil C, Noth U, Evans C, Ghivizzani S. Enhanced in vitro chondrogenesis of primary mesenchymal stem cells by combined gene transfer. Tiss Eng Part A 2008;15(5):1127-1139.
52. Trobridge G. Genotoxicity of retroviral hemaotopoietic stem cell gene therapy. Expert Opin Biol Ther 2011;11(5):581-93.
53. Urist M. Bone formation by autoinduction. Science 1956;150:893–899.
54. Varkey M, Gittens S, Uludag H. Growth factor delivery for bone tissue repair: an update. Expert Opin Drug Deliv 2004;1(1):19–36.
55. Vogt S, Ueblacker P, Geis C, Wagner B, Wexel G, Tischer T, et al. Efficient and stable gene transfer of growth factors in to chondrogenic cells and primary articular chondrocytes using a VSV.G pseudotyped retrovirus vector. Biomaterials 2008;29(9):1242-1249.

56. Vogt S, Wexel G, Tischer T, Schillinger U, Ueblacker P, Wagner B, et al. The influence of the stable expression of BMP2 in fibrin clots on the remodeling and repair of osteochondral defects. Biomaterials 2009;30(12):2385-2392
57. Wang L, Zou D, Zhang S, Zhao J, Pan K, Huang Y. Repair of defects around dental implants with bone morphogenetic protein/fibroblast growth factor-loaded porous calcium phosphate cement: a pilot study in a canine model. Clin Oral Implants Res 2011;22(2):173-81.
58. Yasko A, Lane J, Fellinger E, Rosen V, Wozney J, Wang E. The healing of segmental bone defects, including by recombinant human bone morphogenetic protein (rhBMP-2). A radiographic, histological, and biomechanical study in rats. J Bone Joint Surg Am 1992;74(5):659-70.
59. Yew N, Cheng S. Reducing the immunostimulatory activity of CpG-containing plasmid DNA vectors for non-viral gene therapy. Expert Opin Drug Deliv 2004;1(1):115-25.
60. Zhang S, Doschak M, Uludag H. Pharmacokinetics and bone formation by BMP-2 entrapped in polyethylenimine-coated albumin nanoparticle. Biomaterials 2009;30:5143–5155.
61. Zhang Z, Slobodianski A, Ito W, Arnold A, Nehlsen J, Weng S, et al. Enhanced collateral growth by double transplantation of gene-nucleofected fibroblasts in ischemic hindlimbs of rats. PLOS ONE 2011;6(4):e19192

5 Gelatin coating to stabilize the transfection ability of nucleic acid polyplexes

A version of this chapter was published in: L Rose, HM Aliabadi, H Uludag. Acta Biomaterialia 2013;9(7):7429-38

5.1 INTRODUCTION

Gene delivery is actively pursued for treatment of a myriad of diseases due to its potential to eradiate the underlying cause of pathology, rather than alleviating the disease symptoms that are often targeted with drug therapy. Viral gene carriers are highly effective at introducing transgenes into human cells and have been used extensively in cell culture for modification of a wide variety of cells. For *in vivo* gene delivery, however, viral carriers display reduced or abolished efficacy [11,15,22,29] in immune-competent animals. The use of immune suppressors can restore the efficacy of viral carriers [10,22], but this is undesirable in a clinical setting. Viral carriers are also associated with potentially lethal consequences such as insertional mutagenesis [13]. The poor safety profiles of viral carriers make non-viral carriers attractive alternatives for gene delivery. It has been well-established that plasmid DNA (pDNA) delivery without a carrier is inefficient and requires exuberant doses for transgene expression [1,8,7]. Amphiphilic polymers incorporating cationic and lipophilic domains can bind, condense and neutralize the anionic pDNA to facilitate transfer across hydrophobic cell membrane and increase the efficiency of gene delivery. When administered *in vivo*, the polymer/pDNA complexes are expected to remain stable and enable transfection, whether the complexes are administered freely or implanted along with biomaterial scaffolds. Encounter of complexes with cells is expected to take place anywhere from minutes to days and the complexes must remain active during this period for effective internalization and expression.

Time-dependent changes in the transfection ability of complexes were

investigated in aqueous solutions at room temperature and 4 °C [5,8,28], in frozen state at -20 °C and -80 °C, in liquid N_2 [8], or as lyophilized formulations up to 40 °C [5,6]. These studies were aimed at investigating the stability of the complexes *in vitro* as a pharmaceutical formulation. A loss of transfection ability has been routinely observed for complexes incubated at room temperature [5,8,28]. Lowering the temperature to 4 °C [5,28] slows the loss of function, while freezing below -20 °C [8] and lyophilisation [5,6] preserves the transfection ability for some complexes. Storage in low temperature or in lyophilized form, however, are not useful to predict the performance of complexes under realistic transfection conditions, where the complexes come in contact with high concentrations of endogenous molecules at 37 °C for a prolonged time. Strategies that control complex size have been investigated to stabilize the complexes; one commonly used strategy is modification of polymeric carriers with hydrophilic polyethyleneglycol (PEG) [16]. PEG, due to enhanced hydration and steric repulsion, maintains pDNA complexes separated, preventing their association and subsequent aggregation. PEG modifications have been used for polyethylenimine (PEI) based complexes, particularly smaller PEI complexes [24,26] that are prone to aggregation [16]. Despite good control over the particle size, the ability of PEG to preserve the transfection ability of the complexes over time was not investigated. Moreover, PEGylated PEI eradicated plasmid transfection efficiency *in vivo* [17], and increased degradation of short interfering RNA (siRNA) in PEG-containing complexes

[25], making this approach questionable for use in preserving complex stability.

In this study, we explored the stability of polymer complexes prepared with nucleic acids and confirmed a significant reduction in transfection ability of the complexes in as little as 24 hours after complexation. We then explored a method to preserve the transfection ability of the complexes and here report a simple approach to achieve this goal, based on gelatin coating of the complexes. An amphiphilic polymer, 2 kDa PEI modified with linoleic acid (PEI2-LA) previously described from our lab [19], was used as a prototypical polymeric carrier. This polymer was highly effective when the prepared pDNA and siRNA complexes were used immediately for transfection. We show the proposed gelatin-coating method is applicable for both pDNA and siRNA complexes and it improves the functional outcomes with both types of nucleic acids.

5.2 MATERIALS & METHODS

5.2.1 *Materials*

The DMEM medium, trypsin/EDTA, SYBR Green I, and penicillin-streptomycin solution (10000 U/mL-10000 μg/mL) were from Invitrogen (Grand Island, NY). Fetal bovine serum (FBS) was from PAA Laboratories Inc. (Etobicoke, ON) and Hank's Balanced Salt Solution (HBSS) was from BioWhittaker (Walkersville, MD). Absorbable gelatin sponges (Gelfoam) were

from Pharmacia & Upjohn (Kalamazoo, MI). An enzyme-linked immunosorbant assay (ELISA) to quantify Bone Morphogenetic Protein-2 (BMP-2) in tissue culture supernatants was purchased from Peprotech (Rocky Hill, NJ). The gWiz-GFP and gWiz plasmids were purchased from Aldevron (Fargo, ND). The pCAG-dsRed2 plasmid was purchased from Addgene (Cambridge, MA). Heparin sodium salt, Type A 300 bloom gelatin from pork skin (Catalogue No G1890), and thiazolyl blue tetrazolium bromide (MTT) was purchased from Sigma-Aldrich (St Louis, MO). The BMP-2 expressing plasmid BMP2-IRES-AcGFP was previously described [27]. The gWiz plasmid was labeled with the Cy3 fluorescent probe (gWIZ-Cy3) using Label-IT Tracker Kit from Mirus (Piscataway, NJ). All siRNAs (unlabeled scrambled, FAM-labeled scrambled, and KSP-specific siRNA) were obtained from Ambion (Austin, TX). The 2 kDa PEI (PEI2) modified with linoleic acid (PEI-LA) was prepared as described [19]. The extent of lipid modification was 1.2-1.6 linoleic acids per PEI. The 2 kDa PEI was also modified with polyethyleneglycol (PEI-PEG; ~5 PEG per PEI2), as previously described [33].

5.2.2 *Complex formation*

The desired polymers and pDNA (gWIZ, gWIZ-GFP or BMP2-IRES-AcGFP) were mixed together in saline (150 mM NaCl) for complexation. For example, 9 mL of 1 mg/mL of PEI-LA was added to 4.5 mL of 0.4 mg/mL of pDNA in 22.5 mL of saline. After 30 minutes, 264 mL of gelatin solution (0, 0.01, 0.1 and 1% in water) was added to the complexes and used either

immediately (no incubation) or incubated in the eppendorf tubes at 37 °C for a desired period before use. Where indicated, the complexes were also incubated for extended period for up to 48 hours up to 48 hours before addition to the cells. For complexes prepared with a combination of polymers (e.g., PEI-LA and PEI-PEG), the polymers were first mixed together before being added to pDNA in saline. For transfections in gelatin sponges, complexes were formed as usual, incubated for 15 minutes at room temperature, and then added onto the sponges for a further 15 minutes at room temperature, before the sponges are either incubated with cells or implanted. The weight ratio of polymer:pDNA in complexes was controlled at 5:1, and the concentration of pDNA during transfection was maintained at 2 μg pDNA/mL of media. The siRNA complexes were similarly prepared by replacing the pDNA with the desired siRNA. The polymer:siRNA weight ratio was 2:1 with a final siRNA concentration of 36 nM in cell culture media.

5.2.3 *Complex solubility, size, zeta-potential, and dissociation*

To assess solubility of complexes, polymer/pDNA complexes in saline were centrifuged at 13,000 rpm for 10 minutes. pDNA remaining in solution was measured at A_{260} (Nanovue) to determine its concentration, which was normalized against free pDNA (i.e., no polymers) in saline. The size and zeta-potential of polymer/pDNA complexes were evaluated using dynamic light scattering with the ZetaPlus-Zeta Potential Analyzer (Brookhaven Instrument Corporation) at room temperature. For size, complexes were measured over a period of 60 minutes at

room temperature. The size of each complex was taken as the average of four readings. For these experiments, 10 μg gWiz was mixed with 50 μg of polymer in saline for a polymer:pDNA weight ratio of 5:1. Particles were formed with PEI-LA alone, or mixtures of PEI-LA and unmodified PEI or PEI-PEG. For zeta-potential, complexes were made as usual in water with a polymer to pDNA weight ratio of 5:1 as well. Complexes were measured after with or without additional 24 hour incubation in either water or 0.1% gelatin. The viscosity of water was used for measurements, and the zeta-potential of each complex was taken as the average of 12 runs.

To assess dissociation, the complexes were exposed to heparin (0-12 μg/mL) for one hour at room temperature to induce dissociation. Free pDNA released from the complexes was measured by using SYBR Green I in black 96-well plates with a fluorescent plate reader (λ_{ex}: 485 nm, λ_{em}: 527 nm). Complex dissociation was calculated by dividing the amount of pDNA released at the specific heparin concentration by the total amount of pDNA released without complex incubation. Experiments were performed in triplicate.

5.2.4 *Cell culture*

The 293T cell line was used to assess pDNA delivery *in vitro*. Cells were grown in DMEM supplemented with 10% FBS and 1% penicillin/streptomycin in a humidified incubator (37 °C, 5% CO_2). The 293T cells were seeded either directly on tissue culture plates (monolayer) or on gelatin sponges. Monolayer cultures were seeded the day prior to complex exposure (100 μL complex/well in

triplicate), whereas complexes were loaded onto the sponge immediately before cell seeding. Cells were seeded to achieve ~60% confluency for monolayer studies in multiwall plates. Sponges were seeded at approximately three times the density of monolayer cultures to account for the three-dimensional nature of the sponge. The human breast cancer MDA-MB-435 cell line was used for siRNA studies. Cells were grown in RPMI media supplemented with 10% FBS and 1% penicillin/streptomycin under conditions described above. Cells were seeded as a monolayer in 24-well plates the day before siRNA complex exposure.

5.2.5 *Assessment of GFP and BMP-2 expression*

For analysis of GFP expression, 293T cells were exposed to the desired complexes for 24 hours, and then the media were changed to remove complexes. After 2 days, monolayer cultures were washed with HBSS, trypsinized to create a single-cell suspension, and fixed in 3.7% formalin in HBSS. Approximately 5000 cells per sample were analyzed for GFP expression with Beckman Coulter Cell Lab Quanta SC flow cytometer using a 488 nm laser for excitation and the FL1 channel for emission. The 'No Treatment' control group was set at 1% for GFP-positive cells as calibration. GFP expression in sponge culture was assessed with a fluorescent plate reader (λ_{ex}: 485 nm, λ_{em}: 527 nm), where the fluorescence of the 'No Treatment' group (sponges containing cells with no pDNA exposure) was subtracted from the fluorescence of the study groups. For analysis of BMP-2 expression, complexes containing BMP2-IRES-AcGFP were loaded onto gelatin sponges and the 293T cells were seeded onto the sponges. Every four days,

sponges were transferred to new 48-well plates in lieu of passaging and supernatants were collected to detect BMP-2 secretion using a commercial ELISA kit. Each transfection was performed in triplicate.

5.2.6 Uptake of pDNA and siRNA

For pDNA uptake, complexes were prepared as described in section 2.2 with gWiz-Cy3. The fluorescence of the complexes was measured at formation and after 24 hours at 37 °C to ensure that Cy3 signal did not change significantly by polymer binding, gelatin addition or extended incubation. The 293T cells were exposed to complexes for 24 hours and harvested for flow cytometry as described in section 2.5. The washing and trypsinization of cells was previously been found to effectively remove pDNA complexes that are absorbed to the surface but not internalized (Reimer, 1997). The Cy3 signal was measured in the FL2 channel, with background (un-treated cells) set at 1%. The gWiz-Cy3 without polymeric carrier was included with cells as a control. Similarly, uptake of siRNA complexes was measured in MDA-MB-435 cells using FAM-labelled siRNA. The fluorescence of complexes was measured at formation and after a 24 hours at 37 °C to ensure that FAM signal did not change significantly by polymer binding, gelatin addition or extended incubation. Complexes were prepared with FAM-labelled siRNA and incubated for 0 or 24 hour period at 37 °C. The siRNA-FAM complexes were then exposed to the MDA-MB-435 cells for 24 hours and similarly washed and trypsinized for flow cytometry. The FAM signal was measured in the FL1 channel, with background (un-treated cells) set at 1%. The

siRNA-FAM without polymeric carrier was included as a control. Each experiment was performed in triplicate.

5.2.7 KSP silencing with siRNA

The siRNA complexes were prepared with scrambled (control) or kinesin spindle protein (KSP) specific siRNAs, and additionally incubated in saline or gelatin (1, 0.1 and 0.01%) for 0 or 24 hours at 37 °C. Selective KSP inhibition results in cell death in acute myeloid leukemia cells [4], and silencing similarly results in apoptosis and loss of viability in breast cancer cells MDA-MB-435 (unpublished data). Complexes at 2:1 polymer:siRNA ratio were added to cells at 36 nM siRNA (in triplicate in 24-well plates), and the MTT assay was performed after 72 hours as described [19]. Cell viability after KSP silencing was normalized against control complexes and expressed as percent decrease in cell viability. Each experiment was performed in triplicate.

5.2.8 In vivo gene delivery

Gene delivery was assessed *in vivo* by expression of dsRed2 from the pCAG-dsRed2 plasmid [32] in a rat subcutaneous implantation model. All protocols involving rats were approved by the University of Alberta Animal Welfare Committee. Female Sprague-Dawley rats from Biosciences (Edmonton, Alberta) were kept under standard laboratory conditions (12 hour light/dark cycle) with free access to water and rat chow. Each rat received two sponges loaded with complexes (duplicates of the same group)

in bilateral ventral pouches. The PEI-LA/pDNA complexes were prepared in microcentrifuge tubes for 15 minutes, and then saline or 0.1% gelatin was added to the tubes. Complexes containing 10 mg of pDNA and 50 mg of PEI-LA in 150 mL were then loaded onto sponges for 15 minutes prior to implantation. At designated time points, rats were sacrificed via CO_2 asphyxiation and the sponges were harvested. Implants were imaged with the FujiFilm FLA-5000 scanner. Fluorescence of the implants was normalized against sponges containing only saline. Each study group contained four to five rats, giving 8-10 implants for assessment.

5.2.9 Statistical Analysis

Statistical tests were applied to determine significance of study results. For comparison between two groups, the results were analyzed with the Student's *t*-test. For comparisons among multiple groups, an Analysis of Variance (ANOVA) was performed. This was followed by a Dunnett test compared to a control group, as indicated in figure captions. The results of the *in vivo* study were found not to follow a normal distribution, so a Kruskal-Wallis test (non-parametric Analysis of Variance; ANOVA) was performed. The Dunn's Multiple Comparison Test was used to compare expression to controls, as described in the figure caption.

5.3 RESULTS

5.3.1 Complex solubility, size, and transfection ability

We first investigated aggregation of complexes after 30 minutes of complex formation by centrifugation to determine the amount of pDNA remaining in solution. The PEI-LA complexes formed visible aggregates (i.e., cloudy solution), leaving <10% of the original pDNA in solution after centrifugation (***Figure 5-1A***). Adding PEI2 to complexes up to 50% by polymer weight gave a similar result, with 10-15% of pDNA remaining in solution after centrifugation. The PEI-PEG containing complexes were more soluble with ~70% of pDNA remaining in solution at a 1:1 PEI-LA:PEI-PEG ratio. The size of the polymer/pDNA complexes followed a similar pattern (***Figure 5-1B***); both PEI-LA and PEI-LA/PEI complexes increased from ~380 nm after 5 minutes to ~1200 nm at 60 minutes, while, PEI-LA/PEI-PEG complexes remained at ~200 nm for the study duration.

The dissociation of complexes was investigated with heparin for complexes incubated up to 24 hours. Sigmoidal dissociation curves were observed for PEI-LA, PEI-LA/PEI, and PEI-LA/PEI-PEG complexes (***Figure 5-1C***) at the initial time point. However, after 24 hours, PEI-LA, PEI-LA/PEI, and PEI-LA/PEI-PEG complexes showed incomplete dissociation, where PEI-LA and PEI-LA/PEI complexes released <20% of pDNA, while PEI-LA/PEI-PEG complexes gave ~60% pDNA release. The pDNA complexes formed with the PEG-PEI gave the most robust dissociation at both time points, suggesting a weaker binding with this agent.

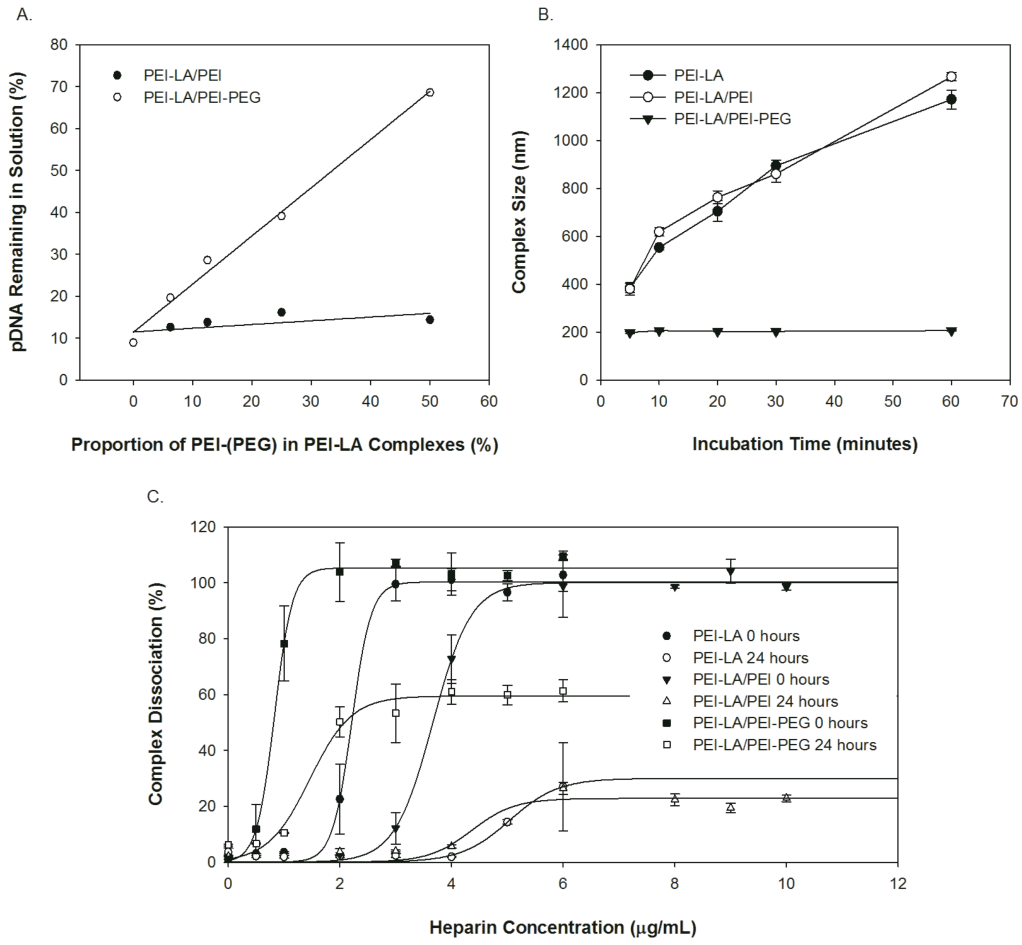

Figure 5-1: Effect of Incubation on Size, Solubility and Dissociation. (**A**) Changes in the solubility of PEI-LA complexes after 30 minutes of complexation. The complexes were formed with PEI-LA/PEI and PEI-LA/PEI-PEG mixtures where the percentages of PEI and PEI-PEG were varied between 0 and 50%. (**B**) Size of PEI-LA, PEI-LA/PEI and PEI-LA/PEI-PEG complexes during 60 minutes of complexation. Heparin dissociation of PEI-LA, PEI-LA/PEI, or PEI-LA/PEI-PEG complexes was assessed after 0 or 24 hours of incubation at 37 °C (**C**).

The transfection ability of complexes was investigated in 293T monolayers and in gelatin sponges, where the complexes were used either immediately following preparation or after 24 hours incubation at 37 °C. For fresh complexes, high levels of GFP expression were observed for all groups in both the monolayer (***Figure 5-2A***) and sponge cultures (***Figure 5-2B***). The proportion of GFP-positive cells ranged from 40 to 80% for saline-incubated complexes (not shown). In both monolayer and sponge cultures, the transfection efficiency decreased gradually when complexes were incubated for 24 hours before addition to the cells, until GFP fluorescence was only slightly high than the background when complexes were incubated for 48 hours prior to transfection. This trend was observed for all PEI-LA, PEI-LA/PEI and PEI-LA/PEI-PEG complexes ($p<0.01$). Similar decreases were observed even when complexes were incubated at room temperature or 4 °C although the lower temperature helped slow the decline in transfection efficiency (***Appendix B, Supplemental 5-1***). Incubating the complexes in tissue culture medium containing serum led to a slight improvement compared to media without serum, but ultimately also led to minimal transfection ability after 48 hours (***Appendix B, Supplemental 5-2***).

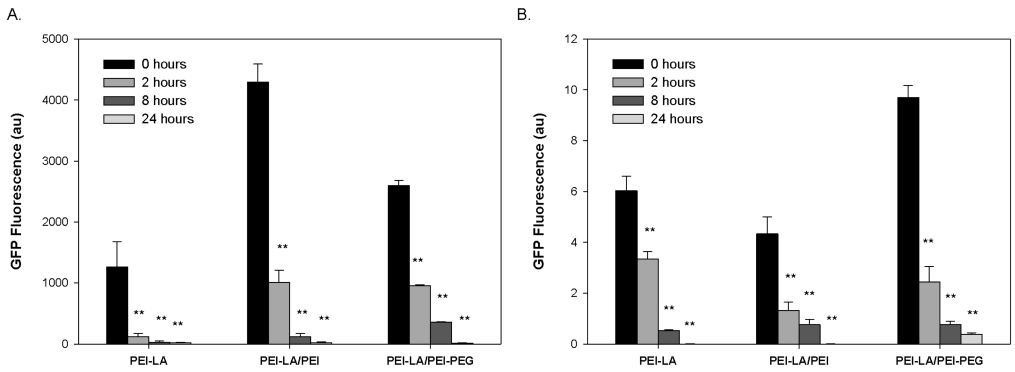

Figure 5-2: Change in Transfection Efficiency with Complex Incubation. Transfection efficiency of complexes containing gWiz-GFP was determined after incubation of complexes (37 °C) for 0, 2, 8 and 24 hours in 293T grown in monolayers (**A**) or sponge cultures (**B**). GFP expression was assessed two days afterwards by flow cytometry (**A**) or fluorescent plate reader (**B**). ** $p<0.01$ compared to 0 hours for each complex type.

5.3.2 Effect of gelatin on transfection efficiency during extended incubations

The prepared complexes were incubated with a variety of buffers for 8 hours to screen for formulations that retained the transfection efficiency. The buffers employed HBSS, HEPES, Tris, and phosphate buffers at a pH range of 5-8 did not alleviate the loss of transfection efficiency (not shown). Both D-glucose and gelatin were found to improve transfection, but 0.1% gelatin was the only formulation to improve transfection of both PEI-LA and PEI-LA/PEI (***Appendix B, Supplemental 5-3***). Dextrose was subsequently found to be insufficient for maintaining the transfection efficiency for longer periods (***Appendix B, Supplemental 5-4***). The addition of 0.01% to 1% gelatin to complexes during incubation at 37 °C allowed complexes to maintain their transfection efficiencies, unlike the control conditions (150 mM NaCl; ***Figure 5-3A, B, C***). Addition of gelatin coatings led to higher transfection for PEI-LA (***Figure 5-3A***) and PEI-LA/PEI (***Figure 5-3B***) when complexes were incubated for 24 or 48 hours compared to complexes made in saline ($p<0.05$-0.01), except for PEI-LA coated with 1% gelatin. For PEI-LA complexes incubated in gelatin, no change in transfection efficiency was observed after 24 hours but the transfection efficiency of PEI-LA decreased by ~50% after 48 hours. For PEI-LA/PEI complexes, no change in transfection efficiency was observed when complexes were incubated up to 48 hours. For both PEI-LA and PEI-LA/PEI complexes, gelatin concentrations between 0.01% and 1% were similarly effective. The PEI-LA/PEI-PEG complexes incubated in 1% gelatin showed no

improvement over saline incubation (***Figure 5-3C***), whereas 0.01% gelatin improved the transfection with increasing incubation time.

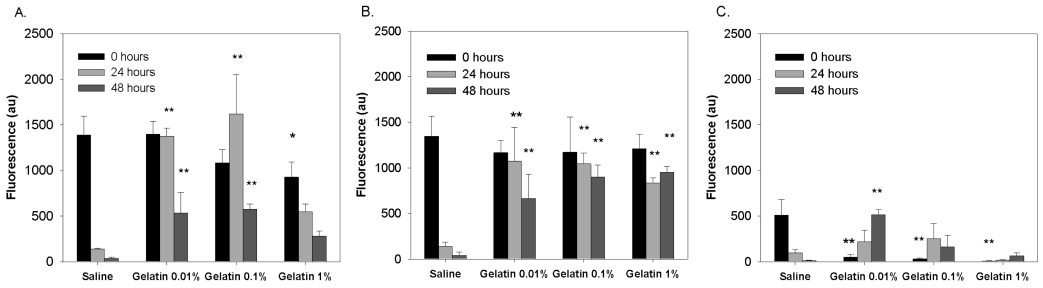

Figure 5-3: Effect of gelatin during monolayer transfections. Transfection efficiencies of PEI-LA (**A**), PEI-LA/PEI (**B**) and PEI-LA/PEI-PEG (**C**) complexes incubated at 37 °C with 0, 0.01, 0.1 and 1% gelatin. After 0, 24 and 48 hours of incubation, the complexes were added to the cells and GFP expression analyzed using flow cytometry. * $p<0.05$ and ** $p<0.01$ compared to complexes in saline for each time point.

We next investigated the stability of complexes formed in the presence of gelatin (rather than gelatin coating). High GFP expression was observed with fresh PEI-LA and PEI-LA/PEI complexes prepared in saline (***Appendix B, Supplemental 5-5***). Complexes made in the presence of gelatin, however, showed only low (PEI-LA and PEI-LA/PEI) or no transfection efficiency (PEI-LA/PEI-PEG). Where some transfection was observed, lower gelatin concentrations during complex formation gave higher GFP expression after transfection, indicating an adverse effect of gelatin when used during the complex preparation. Two further screens on small molecules and polymeric materials were conducted to determine whether the stabilizing properties were unique to gelatin. The small molecule screen showed that incubation with cholesteryl hemisuccinate and glycerol gave improved transfection compared to saline (not shown). The cholesteryl hemisuccinate, however, was not soluble in water while further studies with glycerol showed a limited effectiveness since higher concentrations impeded transfection (***Appendix B, Supplemental 5-7***). The polymeric screen demonstrated that Type B gelatin and free PEG helped to stabilize the particles (***Appendix B, Supplemental 5-6***). Further investigation of Type A and Type B gelatins demonstrated similar stabilizing properties (***Appendix B, Supplemental 5-8***).

The stability of complexes was next evaluated by adding the complexes to absorbable gelatin sponges as a model of implantable delivery of pDNA. Due to the difficulty of recovering cells fully from sponges, a BMP-2 expression plasmid was used for transgene expression and BMP-2 secretion was quantitated for 6

days in an initial study. Both PEI-LA and PEI-LA/PEI, but not PEI/PEI-PEG, led to some BMP-2 secretion from saline incubated complexes (***Figure 5-4A***), but the addition of gelatin (0.01 to 1%) to the complexes increased the BMP-2 expression ($p<0.05$-0.01) by 2.1-5.1 fold. In a longer (12-day) study, gelatin coating increased the BMP-2 secretion ($p<0.01$-0.001) from PEI-LA and PEI-LA/PEI complexes by 1.6 and 2.1-fold, respectively (***Figure 5-4B***). As in ***Figure 5-4A***, PEI-LA/PEI-PEG complexes did not give appreciable BMP-2 secretion with or without gelatin.

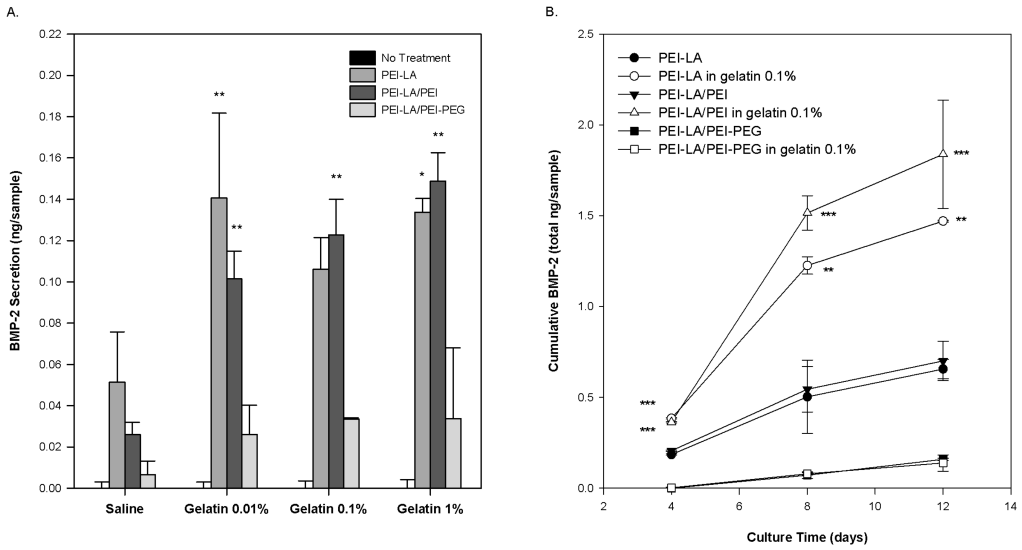

Figure 5-4: Effect of gelatin during sponge transfections. Complexes were prepared with the BMP2-IRES-acGFP plasmid and polymers PEI-LA, PEI-LA/PEI, and PEI-LA/PEI-PEG and loaded onto gelatin sponges. The complexes were prepared in saline or gelatin coating (0.01-1%), added into the sponges after 30 minutes of incubation, followed by the addition of cells. The supernatant was collected for BMP-2 analysis after 6 days (**A**). BMP-2 secretion was assessed over a 12-day period with complexes prepared in saline or 0.1% gelatin (**B**). * $p<0.05$, ** $p<0.01$, and *** $p<0.001$ compared to complexes in saline for each time point.

5.3.3 Effect of gelatin on complex properties

Complex size, dissociation, and cellular uptake were investigated to determine the beneficial effect of gelatin on transfection ability of complexes. The size of complexes incubated without and with gelatin was measured after 24 hours of incubation (***Figure 5-5A***). The PEI-LA complexes in saline were ~9 μm while the PEI-LA/PEI complexes were ~1.5 μm. The PEI-LA/PEI-PEG complexes remained at ~300 nm, consistent with the expected PEG effect. In contrast, all three complexes incubated in 1% gelatin remained at ~300 nm. The size of PEI-LA and PEI-LA/PEI complexes increased with lower gelatin concentrations (0.1% and 0.01%). The zeta-potential of complexes was measured after 0 or 24 hour incubation in either water or 0.1% gelatin (***Figure 5-5B***). Initially, the PEI-LA, PEI-LA/PEI, and PEI-LA/PEI-PEG complexes had zeta potentials of 48, 43, and 42 mV respectively. The addition of gelatin decreased the zeta potential ($p<0.01$) by approximately half to 21, 19, and 16 mV for each of the three complexes. No change in zeta potential for any of PEI-LA, PEI-LA/PEI, PEI-LA/PEI-PEG were observed after 24 hour incubation in either water or gelatin. After heparin-mediated dissociation, complexes prepared with 0.1% gelatin showed improved dissociation after 24 hour incubation for PEI-LA, PEI-LA/PEI, and PEI-LA/PEI-PEG (***Figure 5-5C***). While the PEI-LA and PEI-LA/PEI complexes did not give complete dissociation (but still improved compared to absence of gelatin; see ***Figure 5-2***), the PEI-LA/PEI-PEG complexes showed complete dissociation reminiscent of freshly prepared complexes.

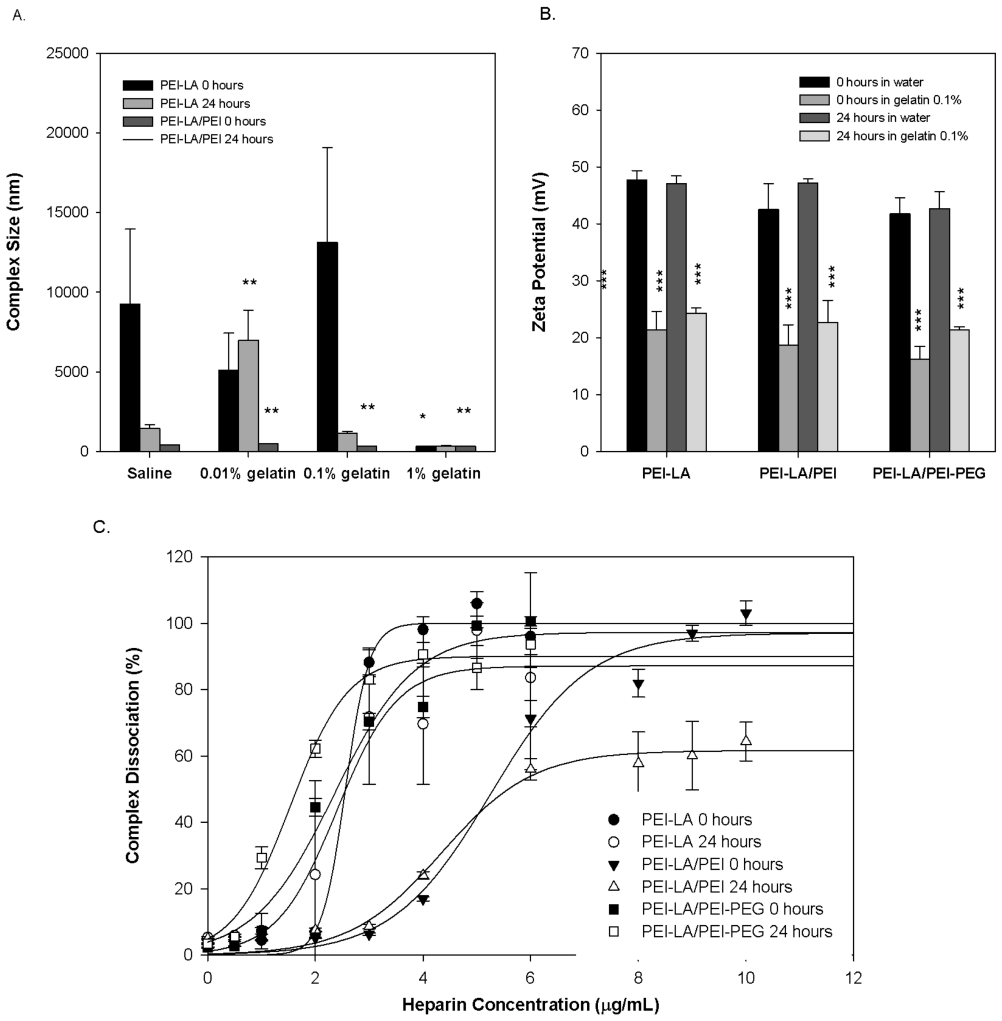

Figure 5-5: Effect of gelatin on complex properties. Complexes were prepared with gWIZ plasmid and polymers PEI-LA, PEI-LA/PEI and PEI-LA/PEI-PEG, and stabilized by gelatin (0.01 to 1%). The complex size was measured after incubation at 37 °C for 24 hours (**A**). The zeta potential of complexes made in water was measured after a 0 or 24 hour incubation in water or gelatin 0.1% (**B**). Dissociation of PEI-LA, PEI-LA/PEI, and PEI-LA/PEI-PEG complexes with heparin after 0 or 24 hours of incubation at 37 °C in 0.1% gelatin (**C**). * $p<0.05$, ** $p<0.01$, and *** $p<0.001$ compared to complexes in saline for each time point.

Finally, pDNA uptake was measured using complexes prepared with gWIZ-Cy3 (***Figure 5-6***). Freshly prepared complexes with all three polymers gave a high uptake (40-70% of cells) in the absence or presence of gelatin (0.01 to 1%). The uptake of PEI-LA and PEI-LA/PEI complexes incubated in the absence of gelatin was reduced after 24 hours incubation (~5% of cells; ***Figure 5-6A***). Gelatin-coated complexes for all three formulations (PEI-LA, PEI-LA/PEI and PEI-LA/PEI-PEG) gave significantly higher uptake ($p<0.05$-0.01), except for PEI-LA/PEI with lowest (0.01%) gelatin coating. The PEI-LA/PEI-PEG complexes gave ~30% pDNA-positive cells, a decrease from 45% for freshly prepared complexes. All three complexes incubated in gelatin for 24 hours displayed uptake profiles reminiscent of freshly prepared complexes.

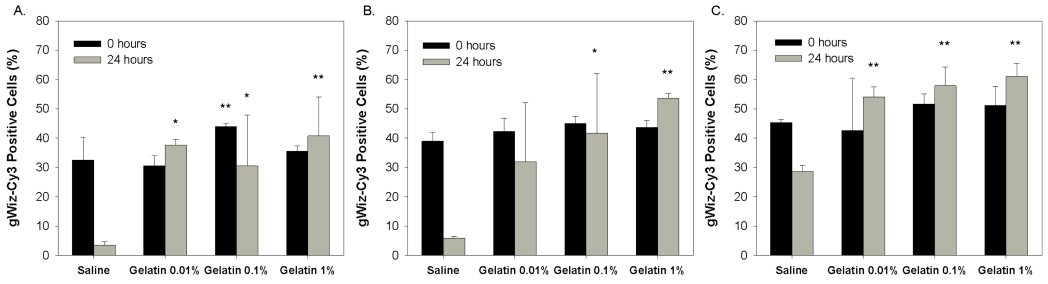

Figure 5-6: Effect of gelatin on complex uptake. Cellular uptake of gWIZ-Cy3 complexes prepared with PEI-LA (**A**), PEI-LA/PEI (**B**) and PEI-LA/PEI-PEG (**C**) and incubated for 0 or 24 hours in saline and 0.01-1% gelatin. The cellular uptakes of complexes were summarized as the percentage of gWIZ-Cy3-positive cell population, as assessed by flow cytometry. * $p<0.05$ and ** $p<0.01$ compared to complexes in saline.

5.3.4 Effect of gelatin coating on siRNA delivery

We next investigated the effect of gelatin coating on the stability of siRNA complexes. A functional siRNA assay was employed, where the effect of KSP-specific siRNA on the viability of breast cancer cells was assessed. Cells treated with siRNA complexes containing scrambled siRNA showed no decrease in viability compared to untreated cells (data not shown). Treatment with fresh complexes containing KSP siRNA led to a ~43% decrease in viability, but after a 24-hour incubation, only a 3% decrease in viability was seen (***Figure 5-7A***). Freshly made complexes with gelatin coating gave 34-55% decrease in cell viability depending on gelatin concentration; this was equivalent to freshly made complexes. The complexes with a gelatin coating were more effective than complexes in saline after 24 hour incubation at 37°C ($p<0.01$), giving a 32-45% decrease in cell viability.

The cellular uptake of siRNA complexes was similarly investigated to determine the beneficial effect of gelatin coating. As expected, cells treated with FAM-labeled siRNA alone (i.e. without a polymeric carrier) showed no uptake. Freshly prepared FAM-labeled complexes with and without gelatin coating all showed 78-92% siRNA-positive cells (***Figure 5-7B***), with no apparent differences among the study groups. The cellular uptake of complexes dropped to ~8% when the FAM-labeled complexes were incubated without gelatin for 24 hours. The FAM-labeled complexes incubated in gelatin for 24 hours, however, gave a robust siRNA uptake ($p<0.01$; 85-90% siRNA-positive cells) reminiscent of freshly prepared complexes.

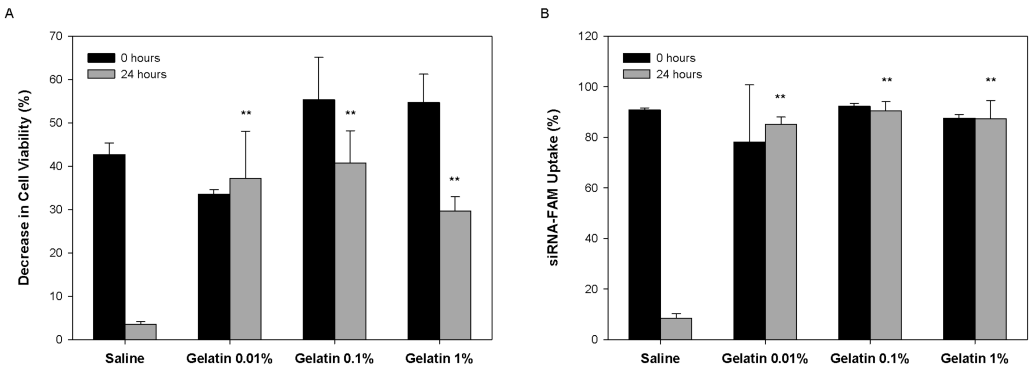

Figure 5-7: Effect of gelatin on siRNA complexes. The viability of MDA-MB-435 cells after treatment with KSP-specific siRNA (**A**). The complexes were formed with PEI-LA in saline and stabilized with gelatin (0.01-1%). Cells were treated with the complexes after 0 and 24 hours of incubation of complexes at 37 ^{o}C. Viability was normalized against the cells treated with control complexes containing scrambled siRNA. Uptake of complexes containing FAM-labeled siRNA (**B**). The siRNA-FAM complexes were formed with PEI-LA in saline and stabilized with gelatin (0.01-1%). The cells were treated with the complexes after 0 and 24 hours of incubation of complexes at 37 ^{o}C. Cellular uptake was assessed by flow cytometry, where untreated cells were set to 1% siRNA-FAM positive population. ** $p<0.01$ compared to complexes in saline.

5.*3.5* *Effect of gelatin on in vivo gene delivery*

To determine whether gelatin coating was effective for *in vivo* gene delivery, gelatin-coated complexes were delivered on an absorbable sponge and implanted subcutaneously. The dsRed2 expression was investigated to confirm the effectiveness of gelatin, since the dsRed2 protein is not secreted and would be localized at the implantation site longer than the secreted protein BMP-2. With implantation of PEI-LA/pCAG-dsRed2 complexes (***Figure 5-8***), none of the sponges harvested after one day showed any increase in dsRed2 fluorescence compared to control (no polymer) sponges. Both uncoated and gelatin-coated PEI-LA complexes ($p<0.05$ and $p<0.01$, respectively) showed significant increases in dsRed2 fluorescence compared to control implants after three days, but only gelatin-coated PEI-LA complexes gave significant fluorescence ($p<0.01$) after 7 days of implantation.

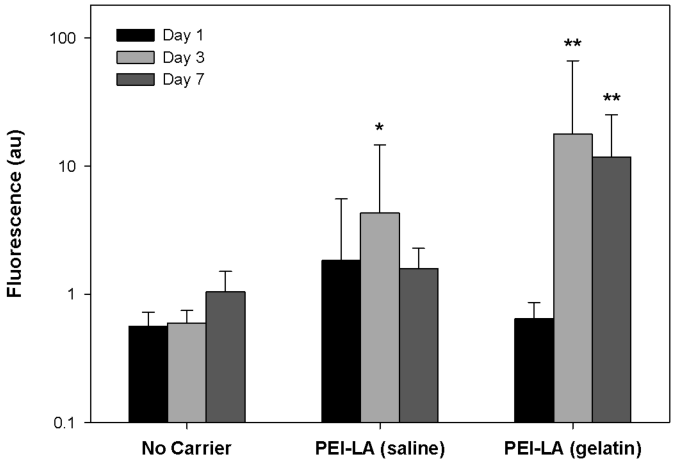

Figure 5-8: *In vivo* application of gelatin-coated complexes. Sponges containing BMP-2 plasmid without a carrier, BMP-2 plasmid in uncoated (saline) PEI-LA complexes, or in gelatin-coated PEI-LA complexes, were implanted for up to 7 days and then assessed for *ex vivo* BMP-2 secretion. DsRed fluorescence was measured and normalized against saline (No Treatment) sponges. * $p<0.05$ and ** $p<0.01$ compared to complexes in saline.

5.4 DISCUSSION

Non-viral carriers are considered to be the safest option for gene delivery. Among various non-viral carriers explored, lipid-substituted polymers are beginning to attract wide interest [9] since they are able to create nucleic-acid containing nanoparticles with optimal balance of cationic charge (essential for nucleic acid binding) and hydrophobicity (needed for cell-membrane compatibility). In line with pharmaceutical studies investigating stability of other non-viral formulations of DNA complexes [5,6,8,28], this study noted a rapid decrease in activity of the complexes prepared with the amphiphilic polymers with extended incubation at the physiological temperature. Complexes loaded onto an absorbable gelatin sponge, which is commonly used to deliver complexes in an implantation format, similarly led to a decrease in transfection. This scaffold, therefore, did not sufficiently stabilize the complexes, and suggests complexes could lose transfection efficiency until cells invade and take up the complexes, a process that usually takes days. We had initially hypothesized that aggregation of hydrophobic complexes in aqueous buffers, given by increasing complex size, was the reason behind the loss in transfection, but PEGylated PEI-LA complexes had a stable size and still lost transfection efficiency as quickly as unmodified complexes. This is a critical finding since PEG is widely used to stabilize nanoparticles for systemic administration [18,23], but it does not seem to maintain the functional stability of nucleic acid-containing complexes despite retention of initial complex size.

A gelatin coating on PEI-LA complexes of nucleic acids did not influence the transfection efficiency of freshly-prepared complexes, but was highly effective at eliminating the decline in transfection activity when incubated at 37 °C. This was demonstrated with vastly different nucleic acids, the 5757 bp gWIZ-GFP, 5507 bp pCAG-dsRed2 and 22 bp KSP siRNA that rely on different intracellular mechanisms of actions. Gelatin also stabilized the transfection ability of complexes delivered onto a sponge: even with fresh complexes, gelatin-coated complexes led to improved transgene expression compared to normal complexes (see ***Figure 5-3***). It is likely that the gelatin was able to stabilize the complexes during the time the trypsinized cells recovered to internalize the complexes, while the complexes in saline show a decrease in activity during this time period. To determine the mechanism of improved stability, we investigated complex size, zeta-potential, dissociation, and uptake of complexes with a gelatin coating. Although 0.01% to 1% gelatin were effective for retaining activity, only the highest concentration stabilized the size of PEI-LA/pDNA complexes, so that size stabilization alone was not the only reason for improved transfection. With respect to delivery, complexes incubated in saline showed a large decrease in the number of cells containing complexes for both pDNA and siRNA complexes. Complexes with a gelatin coating, however, showed minimal difference in cellular uptake in a 24-hour study period. Given that many of the complexes were greater than 1 μm and are therefore prone to sedimentation, it is likely that measurements underestimate the size of complexes, particularly of the complexes in saline or low concentrations of gelatin. It appears that large complexes coated

with low gelatin concentrations were still readily taken up into the cells, in contrast to complexes in saline. This was despite the fact that zeta-potential of the complexes was reduced after gelatin coating. It must be pointed out that the zeta-potentials were determined in water, and the actual measurements in saline could not be performed due high salt concentration. Gelatin was also found to rescue the impaired dissociation of complexes incubated in saline. Both pDNA and siRNA rely on effective dissociation from non-viral carriers to exert their action, so that better retention of this dissociation might provide a secondary mechanism (in addition to cellular uptake) for better functional activity.

To our knowledge, no other studies have reported on gelatin maintaining the transfection efficiency of complexes. Other groups have employed layer-by-layer strategies similar to our coating approach [31], but the purpose of individual layers was to improve physicochemical properties for transfection instead of stabilizing the transfection activity during incubations. Cationized forms of gelatin containing amine groups have also been used as a polymeric carrier for pDNA [12,14] and siRNA [21], but there is no information on whether these complexes can retain their original transfection ability after prolonged incubation at 37 °C. The fact that both Type A gelatin (pI range of 7.0 to 9.0) and Type B gelatin (pI range of 4.7-5.2) were equally effective indicates the possibility of using differently charged macromolecules to stabilize complexes. We assumed that complexes interact with gelatins with electrostatic interactions, but did not control the pH of the medium in this study. It is likely that controlling pH during the coating process

will influence its effectiveness and may further improve the desired outcomes. Further details of this process needs to be elucidated but presumably the hydrophobic groups were retained in the right configuration for this end by gelatin coating. Gelatin has also been modified to act as a hydrogel coating and release polymeric pDNA complexes [3], siRNA complexes [20], or naked pDNA [30]. In these cases, the gelatin is cross-linked to form an intact hydrogel [3,30] or is dried into a thin film [20]. The gelatin in the microspheres and hydrogels have both been extensively processed and modified and it is likely that these are not sufficient to prevent a loss in transfection efficiency. Several methods have been employed to stabilize gene delivery complexes, but most studies only assessed the physicochemical features such as the size. Studies investigating how long the complexes remain active have only been undertaken from a pharmacological perspective, and no solutions to prevent the loss of transfection were proposed.

A gelatin coating offers a practical solution to retain the original transfection efficiency, and was found to be effective at stabilizing PEI-LA/pDNA complexes for *in vivo* implantation. No dsRed expression was observed one day after implantation in any group, and an intense signal was observed only with gelatin-coated particles at later time-points. This strongly suggests that the delay between implantation and cell infiltration is long enough to cause the transfection efficiency of complexes drop such that a robust transfection signal was not observed. The *in vitro* sponge model, furthermore, was a good indicator for testing the use of gelatin coatings, and correlated well with results from *in vivo*

studies. Although earlier harvest time points were chosen in this study to better understand the dynamics of gene expression, the results obtained here agree with our previous *in vivo* gene delivery studies using GFP [27] where transgene expression was observed with (uncoated) PEI-LA complexes after 2 and 3 weeks but not after 7 days. In the present study, no transfection was detected after 7 days with uncoated particles but significant transfection was observed for coated PEI-LA complexes. We hypothesize that the low transfection with uncoated particles may require extended periods of time before sufficient fluorescent protein accumulates to produce a detectable signal, and we further postulate that the higher transfection efficiency of the coated particles at early time-points would be indicative of higher transgene expression at later time-points as well.

Whether gelatin is the most ideal material for functional stabilization remains to be explored, and it might be possible to design more suitable and/or effective polymers for this end. Gelatin, however, is well-characterized as a pharmaceutical excipient, generally regarded as biocompatible, easily obtained and inexpensive; furthermore, it is easily applied to as a stabilizing coat onto the complexes. Considering that gelatin was effective to stabilize both pDNA and siRNA particles, we speculate that gelatin may prove useful for complexes made with other nucleic acids such as anti-sense oligonucleotides and mRNA. Such coatings might prove useful for administration of complexes where the complexes have to retain their transfection activity for a prolonged time.

5.5 REFERENCES

1. Bonadio J, Smiley E, Patil P, Goldstein S. Localized, direct plasmid gene delivery in vivo: prolonged therapy results in reproducible tissue regeneration. Nature Medicine 1999;5(7):753-759.
2. Bright C, Park YS, Sieber AN, Kostuik JP, Leong KW. In vivo evaluation of plasmid DNA encoding OP-1 protein for spine fusion. Spine 2006;31:2163.
3. Brito LA, Chandrasekhar S, Little SR, Amiji MM. In vitro and in vivo studies of local arterial gene delivery and transfection using lipopolyplexes-embedded stents. J Biomed Mater Res A 2010;93(1):325-36.
4. Carter BZ, Mak DH, Woessner R, Gross S, Schober WD, Estrov Z, Kantarjian H, Andreeff M. Inhibition of KSP by ARRY-520 induces cell cycle block and cell death via the mitochondrial pathway in AML cells. Leukemia 2009;23(10):1755-62.
5. Cherng JY, Talsma H, Crommelin DJ, Hennink WE. Long term stability of poly((2-dimethylamino)ethyl methacrylate)-based gene delivery systems. Pharm Res 1999;16(9):1417-23.
6. Del Pozo-Rodriguez A, Solinis MA, Gascon AR, Pedraz JL. Short- and long-term stability study of lyophilized solid lipid nanoparticles for gene therapy. Eur J Pharm Biopharm 2009;71:181-189.
7. Fang J, Zhu YY, Smiley E, Bonadio J, Rouleau J, Goldstein S, et al. Stimulation of new bone formation by direct transfer of osteogenic plasmid genes. Proc Natl Acad Sci USA 1996;93:5753.
8. Hobel S, Prinz R, Malek A, Urban-Klein B, Sitterberg J, Bakowsky U, Czubayko F, Aigner A. Polyethylenimine PEI F25-LMW allows the long-term storage of frozen complexes as fully active reagents in siRNA-mediated gene targeting and DNA delivery. Eur J Pharm Biopharm 2008;70:29-41.

9. Incani V, Lavasanifar A, Uludag H. Lipid and hydrophobic modification of cationic carriers on route to superior gene vectors. Soft Matter 2010;6(10):2124-38.
10. Kaihara S, Dessho K, Okubo Y, Sonobe J, Kawai M, IIzuka T. Simple and effective osteoinductive gene therapy by local injection of a bone morphogenetic protein-2-expressing recombinant adenoviral vector and FK506 in rats. Gene Therapy 2004;11:439-447.
11. Kang Q, Sun M, Cheng H, Peng Y, Montag A, Deyrup A, et al. Characterization of the distinct orthotopic bone forming activity of 14 BMPs using recombinant adenovirus-mediated gene delivery. Gene Ther 2004;11(17):1312–20.
12. Kim SW, Ogawa T, Tabata Y, Nishimura I. Efficacy and cytotoxicity of cationic-agent- mediated nonviral gene transfer into osteoblasts. J Biomed. Mat. Res. (2004) 71: 308-315.
13. Kohn DS, Sadelain M, Glorioso JC. Occurrence of leukaemia following gene therapy of X-linked SCID. Nat Rev Cancer 2003;3(7):477-88.
14. Konat Zorzi G, Contreras-Ruiz L, Parraga JE, Lopez-Garcia A, Romero Bello R, Diebold Y, Seijo B, Sanchez A. Expression of MUC5AC in ocular surface epithelial cells using cationized gelatin microspheres. Mol Pharm 2011;8(5):1783-8.
15. Li J, Li H, Sasaki T, Holman D, Beres B, Dumont J, Pittman D, Hankins G, Helm G. Osteogenic potential of five different recombinant human bone morphogenetic protein adenoviral vectors in rat. Gene Therapy 2003;10:1735-1743.
16. Luo X, Pan S, Feng M, Wen Y, Zhang W. Stability of poly(ethylene glycol)-graft-polyethylenimine copolymer/DNA complexes: influences of PEG molecular weight and PEGylation degree. J Mater Sci: Mater Med 2010;21:597-607.
17. Merdan T, Kunath K, Petersen H, Bakowsky U, Voigt KH, Kopecek J, Kissel T. PEGylation of poly(ethylene imine) affects stability of complex with plasmid DNA under in vivo conditions in a dose-dependent

manner after intravenous injection into mice. Bioconjugate Chem 2005;16:785-792.

18. Messerschmidt SK, Musyanovych A, Alvater M, Scheurich P, Pfizenmaier K, Landfester K, Kontermann RE. Targeted lipid-coated nanoparticles: delivery of tumor necrosis factor-functionalized particles to tumor cells. J Control Release 2009;137(1):69-77.
19. Neamnark A, Suwantong O, KC Remant, Hsu C, Supaphol P, Uludag H. Aliphatic lipid substitution on 2 kDa polyethylenimine improves plasmid delivery and transgene expression. Mol Pharm 2009;6(6):1798-1815.
20. Nolte A, Walker T, Schneider M, Kray O, Avci-Adali M, Zeimer G, Wendel HP. Small-interfering RNA-eluting surfaces as a novel concept for intravascular local gene silencing. Mol Med 2011;17(11-12):1213-1222.
21. Obata Y, Nishino T, Kushibiki T, Tomoshige R, Xia Z, Miyazaki M, Abe K, Koji T, Tabata Y, Kohno S. HSP47 siRNA conjuageted with cationized gelatin microspheres suppresses peritoneal fibrosis in mice. Acta Biomater 2012; 8(7):2688-96.
22. Okubo Y, Bessho K, Fujimura K, Iizuka T, Miyatake S. Osteoinduction by bone morphogenetic protein-2 via adenoviral vector under transient immunosuppression. Biochem Biophys Res Commun 2000;267(1):382-7.
23. Parveen S, Sahoo SK. Long circulating chitosan/PEG blended PLGA nanoparticle for tumor drug delivery. Eur J Pharmacol 2011;670(2-3):372-83.
24. Ping Y, Liu C, Zhang Z, Liu KL, Chen J, Li J. Chitosan-*graft*-(PEI-beta-cyclodextrin) copolymers and their supramolecular PEGylation for DNA and siRNA delivery. Biomaterials 2011;32(32):8328-8341.
25. Remaut K, Lucas B, Raemdonck K, Braeckmans K, Demeester J, De Smedt SC. Protection of oligonucleotides against enzymatic degradation by PEGylated and NonPEGylated branched polyethyleneimine. Biomacromolecules 2007;8:1333-1340.

26. Roesler S, Koch FPV, Schmehl T, Weissmann N, Seeger W, Gessler T, Kissel T. Amphiphilic, low molecular weight poly(ethylene imine) derivatives with enhanced stability for efficient pulmonary gene delivery. J Gene Med 2011;13(2):123-133.
27. Rose L, Kucharski C, Uludag H. Protein expression following non-viral delivery of plasmid DNA coding for basic FGF and BMP-2 in a rat ectopic model. Biomaterials 2012;33(11):3363-74.
28. Sharma VK, Thomas M, Klibanov AM. Mechanistic studies on aggregation of polyethylenimine-DNA complexes and its prevention. Biotech Bioeng 2005;90(5):614-620.
29. Sonobe J, OkuboY, Kaihara S, Miyatake S, Bessho K. Osteoinduction by bone morphogenetic protein 2-expressing adenoviral vector: application of biomaterial to mask the host immune response. Hum Gene Ther 2004;15:659-668.
30. Takemoto Y, Kawata H, Soeda T, Imagawa K, Somekawa S, Takeda Y, Uemura S, Matsumoto M, Fujimura Y, Jo JI, Kimura Y, Tabata Y, Saito Y. Human placental ectonucleoside triphosphate diphosphohydrolase gene transfer via gelatin-coated stents prevents in-stent thrombosis. Atherioscler Thromb Vasc Biol 2009;29(6):857-62.
31. Wang C, Luo X, Zhao Y, Han L, Zeng X, Feng M, Pan S, Peng H, Wu C. Infuence of the polyanion on the physic-chemical properties and biological activities of polyanion/DNA/polycation tertiary polyplexes. Acta Biomaterialia 2012;8(8):3014-3026.
32. Wickersham IR, Lyon DC, Barnard RJ, Mori T, Finke S, Conzelmann KK, Young JA, Callaway EM. Monosynaptic restriction of transsynaptic tracing from single, genetically targeted neurons. Neuron 2007;53(5):639-47.
33. Zhang S, Kucharski C, Doschak MR, Sebald W, Uludag H. Polyethylenimine-PEG coated albumin nanoparticles for BMP-2 delivery. Biomaterials 2010;31(5):952-63.

6 Pharmacokinetics and transgene expression of implanted polyethylenimine-based pDNA complexes

A version of this chapter was published in: L Rose, P Mahdipoor, C Kucharski, H Uludag. Biomaterials Sciences 2013.

6.1 INTRODUCTION

Gene delivery is an exciting prospect for regenerative medicine especially for bone tissue repair [27], based on its ability to deliver a continuous supply of a therapeutic protein, in place of protein delivery schemes where high protein doses are associated with undesirable and serious side effects [6]. The envisioned paradigm is that a biomaterial scaffold impregnated with either naked plasmid DNA (pDNA) or a carrier/pDNA complex is implanted at the desired repair site. Infiltrating host cells take up the administered pDNA, leading to local production of a protein to induce effective bone formation. This approach has been previously demonstrated for bone regeneration with both viral [7, 11] and non-viral carriers [4,13], although many virus-based vectors show reduced or abolished efficacy in immunocompetent animals [1, 14, 17]. Several studies have employed pDNA without a carrier [4, 5, 8, 9, 23], but higher doses of pDNA (500-1000 μg) were required in this case, indicating the low efficiency of naked pDNA delivery. More tailored non-viral carriers have been successfully applied to ectopic and intraosseous models, and resulted in significant bone regeneration [12, 13, 20, 22]. The development of new non-viral carriers, however, is impeded by an uncertain correlation between *in vitro* and *in vivo* performance characteristics of the delivery systems [13, 16, 26]. This is further compounded by a lack of important information on pharmacokinetics of locally administered pDNA and corresponding transgene expression in these gene-activated matrix models. Although the

classical definition of pharmacokinetics has been limited to drug concentrations over time in the blood, new therapies and delivery modes have required expansion the expansion of pharmacokinetics. For this paper, we have considered the definition of pharmacokinetics to include the change in drug at a local site (i.e. subcutaneously implanted plasmid DNA).

The pharmacokinetics and pharmacodynamics of current gene delivery systems have been recently reviewed, but with a focus on intravenous administration of delivery systems [24]. Only a few studies reported *in situ* gene expression following pDNA delivery [4, 13, 25] but pharmacokinetics of the implanted pDNA was missing in these studies. There is a fairly poor understanding of specific events once the complexes are locally delivered in implants, including how long the pDNA remains at the local implant site, how long the pDNA is expressed, and the role of a delivery system on transgene expression. More detailed studies on the onset and duration of mRNA expression would be helpful to understand differences in functional response. Such information might also allow investigations into correlations between *in vitro* and *in vivo* performance of carriers, especially in light of conflicting efficacy results from similar carriers in bone regeneration models [12, 13]. The pharmacokinetic studies for intravenous delivery have typically employed modified pDNA to allow for tracking of both complexes and naked pDNA using either fluorescent [10] or radioactive labels [33]. The presence of such a label, however, does not guarantee the presence of pDNA or whether the pDNA is still intact. Other options include

Southern blots [15] or agarose gels [29], but these approaches are likely to detect only naked pDNA that is not bound to a carrier, which is usually impermeable into electrophoretic gels. Real-time PCR is a more precise was to quantify pDNA, but challenges remain in the amplification of pDNA bound to non-viral carriers, since this technique is incapable of amplifying polymer-bound pDNA. A recent method described an extraction method with an anionic polymer to allow amplification of bound pDNA in circulation [34], which could provide a more reliable assessment of *in situ* levels of total pDNA, including the bound pDNA fraction.

This study was conducted to determine the local kinetics of pDNA delivered with polymeric carriers. A low molecular weight (2 kDa) polyethylenimine modified with linoleic acid (PEI-LA) was employed for *in vivo* pDNA delivery, given its superior performance over the native 2 kDa PEI [26]. Unlike high molecular weight (25 kDa) PEI, which is highly effective but also toxic, unmodified PEI of this low molecular weight is considered ineffective for *in vitro* delivery of pDNA [19] and siRNA [2, 3] alike. We set out to conduct thorough gene expression studies following *in vivo* pDNA delivery using PEI and PEI-LA, and present studies in this paper on the pharmacokinetics of pDNA, including a method of extracting pDNA from complexes to allow PCR amplification of polymer-bound pDNA. We specifically sought to identify the role of the carrier, duration of pDNA retention at local implant sites and the onset and length of mRNA expression.

6.2 MATERIALS & METHODS

6.2.1 *Materials*

Dulbecco's Modified Eagle Media (DMEM), fetal bovine serum (FBS), penicillin/streptomycin, trypsin/EDTA, and DNase/RNase free water were obtained from Life Technologies (Grand Island, NY). Absorbable gelatin sponges (Gelfoam) were obtained from Pharmacia & Upjohn (Walkersville, MD). The pCAG-DsRed plasmid was purchased from Addgene (Cambridge, MA), while the gWiz plasmid was purchased from Aldevron (Fargo, ND). The Cy5 pDNA labelling kit was from Mirus (Madison, WI). Branched PEI (2 kDa), Poly-aspartic acid (2 kDa), poly-acrylic acid (2 kDa), Tris-HCl, Proteinase K, Hoechst 33258, heparin sodium salt, and sucrose were purchased from Sigma (St Louis, MO). Poly-L-aspartic acid sodium salt was from Alamanda Polymers (Huntsville, AL). Phenylmethanesulphonylfluoride (PMSF) was from BioShop (Burlington, ON). DNeasy Blood & Tissue kit, RNeasy kit, RNA Later RNA stabilization reagent, and DNase I were all obtained from Qiagen (Hilden, Germany). Ketamine was obtained from Bayer HealthCare (Toronto, ON), while Xylazine was obtained from Wyeth (Guelph, ON). Tris-hydroxypropylphosine (THP) was from EMD Millipore (San Diego, CA). Shandon Cryomatrix was from Thermo Scientific (Pittsburgh, PA), Hank's Balanced Salt Solution (HBSS) from BioWhittaker (Walkersville, MD). Primers and FAM-labelled probes with Zen and Iowa fluorescent black quenchers were obtained from IDT Technologies (Ottawa, ON). 2 kDa PEI

modified with linoleic acid (PEI-LA; 4 LA substitutions per PEI) was prepared as previously described [19].

6.2.2 *Methods*

6.2.2.1 Complex formation

DNA in DNase/RNase free water (2.5 mg/mL) was diluted in 150 mM NaCl, to which the desired polymer solutions were added and gently mixed at room temperature. The weight ratio of polymer to pDNA was controlled at 10/2 [25]. Complexes for *in vitro* studies were allowed to incubate for 30 minutes in microcentrifuge tubes at room temperature, whereas the complexes for sponges used *in vivo* were incubated for 15 minutes in microcentrifuge tubes and 15 minutes after absorbing onto a 1 cm x 1 cm sponge. The Cy5-labeled gWIZ (i.e., a control plasmid that gives no transgene expression) was prepared for uptake studies using a commercial labelling kit according to the manufacturer's instructions. The labelling protocol included a spin column to purify the labelled pDNA and remove any unreacted free dye. The gWiz-Cy5 was diluted 1:12 with unlabelled gWiz for use in *in vitro* and *in vivo* delivery studies. The DsRed expressing plasmid pCAG-DsRed2 was used for transfection [31]. Sponges for animal studies were loaded with either gWiz, gWiz-Cy5 or pCAG-DsRed. The plasmids were loaded with PEI or PEI-LA in a total volume of 150 µL with the pDNA dose described in each of the studies (see Figure Legends). Blank sponges loaded with saline alone were included as controls.

6.2.2.2 In vitro transfections

In vitro transfections were performed in the 293T cell line grown in DMEM supplemented with 10% FBS and 1% penicillin/streptomycin. Cells were seeded the day before transfection in 24-well plates. Complexes were added at a final concentration of 1 μg/mL pDNA. Complexes for uptake experiments contained either gWiz or Cy5-gWiz, while the complexes for transfection experiments contained either gWiz or pCAG-DsRed. Control cells were treated with saline (designated as No Treatment). The cells for uptake studies were harvested after a 24 hour exposure to complexes, whereas cells for transfection studies were harvested 2 days after exposure to complexes. The cells were washed with HBSS, trypsinized with 0.05% trypsin, and fixed in 3.7% formalin in HBSS. The cells were stained with Hoechst 33258 at a final concentration of 1 μM and then analysed using an LSR-Fortessa flow cytometer (BD Biosciences). A total of 10,000 cells were counted for each sample, and analysed for Cy5 fluorescence (λ_{ex} 640 nm, λ_{em} 670 nm) or DsRed fluorescence (λ_{ex} 561 nm, λ_{em} 586 nm) using Hoechst (λ_{ex} 355 nm, λ_{em} 450 nm) to distinguish cells from debris. Each study group contained three replicates.

6.2.2.3 Animal care and implantations

Female Sprague-Dawley rats (4-6 weeks) were obtained from Biosciences (Edmonton, AB). All procedures involving rats were approved in advance by the Animal Welfare Committee at the University of Alberta

(Edmonton, AB). Animals were kept under standard laboratory conditions (12h light/dark, 23 °C) with free access to water and rat chow, and allowed to acclimate for one week prior to procedures. Rats were anesthetized with Ketamine/Xylazine (80 and 8 mg/kg, respectively), and their abdomens shaved and prepared with an antiseptic iodine solution. Bilateral ventral pouches were made and a sponge containing pDNA with or without a polymeric carrier as described above was implanted in each pouch with rats receiving replicates of the same group. Each group contained 3-4 rats to give 6-8 implants, with the dose of pDNA described in figure legends. Rats were sacrificed with CO_2 at pre-determined time points and sponges were harvested and taken for analysis as described in the following sections.

6.2.2.4 Assessment of Cy5 and DsRed fluorescence in implants

After harvest, whole explants were imaged with an MF SX ProImager (Carestream) for either Cy5 (λ_{ex} 630 nm, λ_{em} 700 nm) or DsRed fluorescence (λ_{ex} 550 nm, λ_{em} 600 nm). For pharmacokinetics studies, gWIZ-Cy5 retention in explants was calculated based on the fluorescence of un-implanted sponges. These sponges were incubated at 37 °C, and were loaded with an additional 50 µL of either 150 mM NaCl or FBS to prevent drying. The un-implanted sponges with unlabelled gWiz or saline were set to 0% pDNA, and sponges containing the same dose of implanted gWiz-Cy5 were set to 100% retention. After imaging, the harvested sponges were cut into smaller sections for various assays. To analyse the cell-associated fluorescence in

sponges, half of the sponge was trypsinized with 0.05% trypsin, fixed with 3.7% formalin, and stained with Hoechst (1 μM). The extracted cells were analysed by flow cytometry. A total of 10,000 cells were counted for each sample and analysed for Cy5 fluorescence (λ_{ex} 640 nm, λ_{em} 670 nm) using Hoechst (λ_{ex} 355 nm, λ_{em} 450 nm) to distinguish cells from debris. Cells were also imaged with a Zeiss LSM 710 laser scanning confocal microscope to investigate intracellular presence of the complexes. The other half of the explants was used for histological analysis; the explant was fixed for 24 hours in 3.7% formalin at 4°C and then for another 24 hours in 30% sucrose as a cryoprotectant. The samples were then frozen at -20°C in Shandon Cryomatrix, sections and stained with DAPI. The cryosections were imaged with the fluorescent microscope FSX100 (Olympus).

6.2.2.5 RNA extraction, cDNA synthesis, and qPCR

RNA was extracted from an ~30 mg sections of harvested explants using the RNeasy Kit following homogenization with a Qiashredder kit. The manufacturer's instructions for RNA extraction were followed including the optional treatment with DNAse I to remove possibly contaminating pDNA or genomic DNA. The DNase I treatment was found to be sufficient to remove contaminating plasmid or genomic DNA despite the large amount of pDNA remaining on the sponge. Complementary DNA (cDNA) was synthesized from the RNA as previously described [2]. In brief, 0.5 μg of RNA was reverse transcribed using M-MLV reverse transcriptase in a reaction mixture

containing 5x synthesis buffer, random hexamer primers, dNTPs, dithiothreitol, and RNase Out Ribonuclease Inhibitors. The reaction mixture was incubated at 25 °C for 10 minutes, 37 °C for 50 minutes, and then 70 °C for 15 minutes. The cDNA was then analysed with quantitative PCR (q-PCR) on the Applied Biosystems StepOne Plus (Burlington, ON) with SYBR green chemistries. Each reaction contained 2.5 µL of cDNA, 2.5 µL of 3.2 µM forward and reverse primers, and 5.0 µL of a PCR master mix containing SYBR green, with added ROX as a passive reference. Sample was run with rat beta-actin (Forward: 5'-CCACCCCACTTCTCTCTAAGGA-3', Reverse: 5'-AATTTACACGAAAGCAATGCT-3') and DsRed (Forward: 5'-CACTACCTGGTGGAGTTC AAG-3', Reverse: 5'- GATGGTGTAGTCCTCGTTGTG-3') primers. Each sample was performed in triplicate. The cycle threshold (C_T; number of cycles to reach a pre-determined threshold) was determined using the Applied Biosystems StepOne Plus software to find the most linear section of the curve suitable for all samples. A $\Delta\Delta C_T$ analysis was performed, where the difference between the housekeeping (beta-actin) C_T and target (DsRed) C_T of the control and treatment group are compared. Treatment groups were normalized against the average of the blank control sponges for each time point to obtain a relative quantitation.

6.2.2.6 DNA extractions and qPCR

pDNA was extracted from explant samples using two extraction methods: a commercially-available Blood & Tissue Kit (Qiagen) and a

modified protocol originally described by Zhou *et al* [34]. Extractions using the Blood & Tissue Kit were extracted according to the manufacturer's instructions, including an optional step where a second aliquot of buffer was employed to increase pDNA yield from the column. The two aliquots were combined and used for further q-PCR analysis. Samples were extracted either with or without a 60 minute incubation with heparin dissociation. For the second extraction method, explant samples were incubated a lysis buffer (0.5 mg/mL Proteinase K, 2.0 mg/mL 2 kDa poly-L-acrylic acid, and 10 mM tris-hydroxypropylphosine) at ~50 mg of tissue/mL of buffer overnight at 37 °C. Afterwards, 25 µL of the lysed tissue was added to 375 µL of TB buffer (1 mM EDTA, 183 mM KCl, 47 mM NaCl, 1 mM PMSF, 10 mM Tris-HCl; pH 6.8), and samples were heated at 95 °C for 10 minutes. The extracted samples were analysed with q-PCR on the Applied Biosystems StepOne Plus (Burlington, ON) using probe based chemistry. For each reaction, 2.5 µL of sample was added to 1.25 µL of 3.2 µM DsRed primers described above, 1.25 µL of DsRed probe (5'-/56-FAM/TCC ATC TAC/ZEN/ATG GCC AAG AAG CCC/IABkFQ/-3'), and 5 µL of master mix without SYBR green. ROX was used as a passive reference for the reaction. The C_T was determined with the Applied Biosystems StepOne Plus software, and standard curves were constructed relating C_T to pDNA concentration by spiking blank (saline) implanted sponge with either pDNA or polymer/pDNA complexes. The C_T of unknown samples were compared against the standard curve to determine the concentration of the DsRed plasmid DNA (standard curves for pDNA in

solution and pDNA soaked in sponges were equivalent under *in vitro* settings). Each 96-well plate for q-PCR included a standard curve. Treatment groups containing pDNA were compared with the pDNA standard curve, whereas treatment groups with polymer/pDNA complexes were compared with the appropriate polymer/pDNA complex standard curve. The total pDNA content in the whole sponge was extrapolated from the amount of pDNA in the tissue section, based on the known mass of total explants and the fraction used for pDNA extraction.

6.2.2.7 Statistical Analysis

Results were analysed with an analysis of variance (ANOVA). For groups that did not follow a Gaussian distributions, a Kruskal-Wallis non-parametric ANOVA was used to determine significant differences of treatment groups from control. The relationship between gene expression and pDNA retention in sponges was determined by testing the significance of the Pearson Product-Moment Correlation Coefficient.

6.3 RESULTS

6.3.1 *In vitro pDNA uptake and transfection*

The pDNA uptake was investigated in 293T cells by using gWiz-Cy5. Cells exposed to PEI-LA/gWiz-Cy5 complexes gave high fluorescence (***Figure 6-1A***) whereas the background from PEI-LA/gWiz complexes and naked

gWiz-Cy5 was much lower as expected. In a follow-up study, non-treated cells and cells treated with unlabelled gWIZ complexes (PEI/gWiz and PEI-LA/gWiz) gave low levels of autofluorescence, whereas cells treated with PEI/gWiz-Cy5 and PEI-LA/gWiz-Cy5 gave high levels of fluorescence (***Figure 6-1B-i***). Approximately 63 and 68% of the cells were positive for gWiz-Cy5 in the case of PEI and PEI-LA, respectively (not shown). A DsRed expressing plasmid (pCAG-DsRed) was used to evaluate transfection efficiency (***Figure 6-1B-ii***). Cells transfected with PEI/gWiz and PEI-LA/gWIZ complexes gave no DsRed expression as expected. Some DsRed positive cells were observed (~2%, not shown) leading to a small increase in DsRed fluorescence for PEI/pCAG-DsRed transfected cells (433 au for PEI/pCAG-DsRed vs. 107 au for PEI/gWiz). For PEI-LA/pCAG-DsRed transfected cells, however, the fluorescence increased to 2.6×10^4 au (***Figure 1B-ii***), corresponding to ~65% DsRed-positive cell population (not shown).

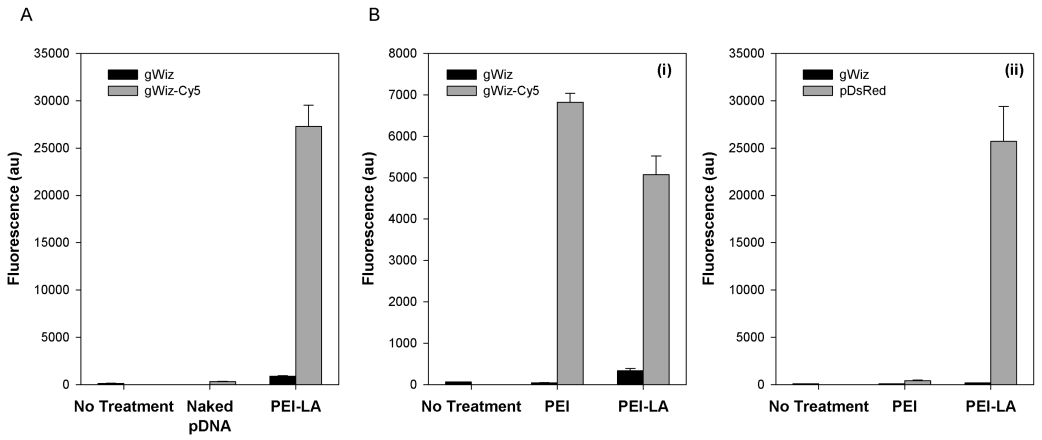

Figure 6-1: pDNA uptake and transfection *in vitro*. 293T cells were used to investigate pDNA uptake with naked and PEI-LA complexes (**A**) and to compare PEI and PEI-LA for uptake (**B-i**) and transfection (**B-ii**). For the uptake, cells were exposed to the indicated pDNA or complexes for 24 hours, and then analysed for Cy5 content using flow cytometry. For transfection, cells were exposed to the indicated complexes for 24 hours, and then harvested for flow cytometry after two days for analysis of DsRed expression.

6.3.2 *Pharmacokinetics of Cy5-labelled pDNA*

6.3.2.1pDNA retention on sponges

The retention of pDNA in sponges was next investigated in a rat subcutaneous implant model using gWiz-Cy5. The fluorescence of sponges harvested from rats was normalized against the fluorescence of un-implanted sponges. For the latter sponges, minimal changes in fluorescence were observed from Day 1 to Day 7, indicating stability of the label at 37 ^{o}C. A decrease in Cy5 fluorescence was observed when gWiz-Cy5 was bound to PEI, but not to PEI-LA, and the fluorescence was not affected by the presence of serum under *in vitro* incubation conditions (***Appendix C, Supplemental 6-1***). For implanted sponges, there was no autofluorescence in the case of saline, PEI/gWiz and PEI-LA/gWiz soaked sponges (***Figure 6-2A***), as expected. Sponges soaked with gWiz-Cy5, PEI/gWiz-Cy5, and PEI-LA/gWiz-Cy5 all had high Cy5 fluorescence on both Day 1 and Day 7. The gWiz-Cy5 group had lowest levels at 9.4±1.6 % and 3.6±1.8% retention of the implanted dose for Days 1 and 7, respectively. While PEI/gWiz-Cy5 gave 28.1±4.1% and 45.1±8.3% retention, whereas PEI-LA/gWiz-Cy5 gave 17.9±10.1% and 11.3±2.9% retention for Day 1 and 7 respectively.

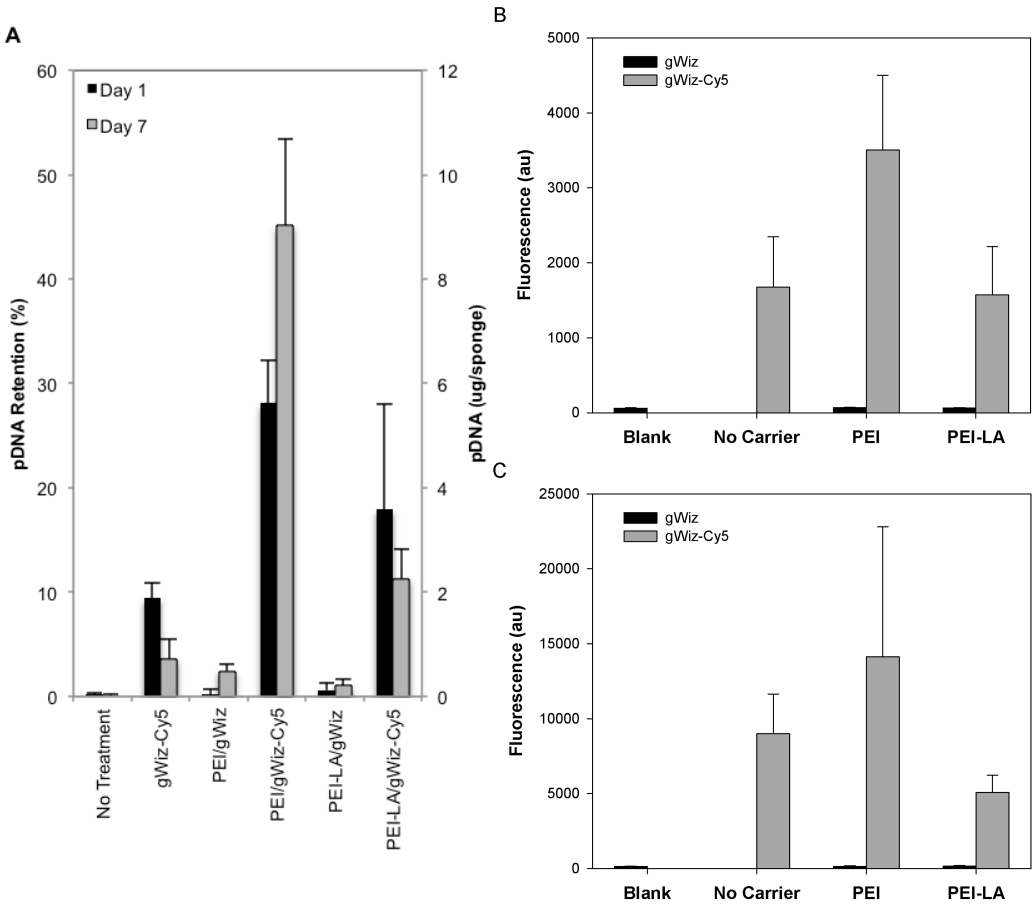

Figure 6-2: Pharmacokinetics of pDNA assessed with gWiz-Cy5. Sponges were loaded with indicated gWIZ and gWIZ-Cy5 complexes of PEI and PEI-LA, and implanted subcutaneously in rats. Harvested sponges were assessed for Cy5 fluorescence 1 and 7 days after implantation (**A**). Cells extracted from the Day 1 (**B**) and Day 7 (**C**) harvested sponges were analysed for Cy5 fluorescence with flow cytometry and the mean (±SD) fluorescence/cell are shown.

6.3.2.2 Cellular uptake of Cy5-labelled pDNA

To differentiate between the pDNA residing in the extracellular space of sponges and the cell internalized pDNA, cells were harvested from the implants and analysed for Cy5 fluorescence using flow cytometry. Cells harvested from blank, PEI/gWiz, and PEI-LA/gWiz sponges all had low autofluorescence for both Day 1 (***Figure 6-2B***) and Day 7 (***Figure 6-2C***). Cells harvested from naked gWiz-Cy5, PEI/gWiz-Cy5, and PEI-LA/gWiz-Cy5 soaked sponges all gave high fluorescence for both time points. The harvested cells were further analysed by confocal microscopy for gWiz-Cy5 particles (***Figure 6-3***). The blank and gWiz containing groups gave no Cy5 fluorescence under confocal analysis as expected (data not shown). Both PEI/gWiz-Cy5 and PEI-LA/gWiz-Cy5 implants contained cells with distinct particles internalized (***Figure 6-3B, C, E, F***). The naked gWiz-Cy5 also gave some cell-associated Cy5 fluorescence, but was less bright and more diffuse without any particulate appearance. In confocal microscopy images, there were no obvious differences between PEI/gWiz-Cy5 and PEI-LA/gWiz-Cy5 particles.

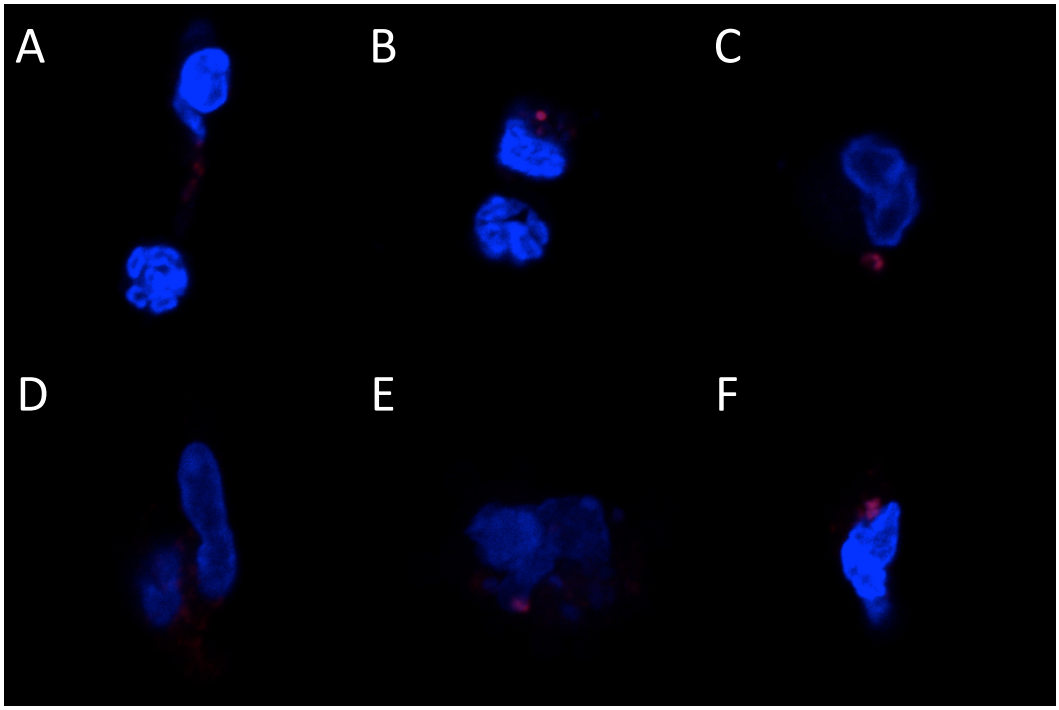

Figure 6-3: Confocal microscopy of cells recovered from implants. Cells were harvested from sponges explanted on Day 1 (**A-C**) or Day 7 (**D-F**) and fixed cells were analysed with confocal microscopy (representative pictures shown). Sponges were loaded with naked gWiz-Cy5 (**A** and **D**), PEI/gWiz-Cy5 complexes (**B** and **E**), or PEI-LA/gWiz-Cy5 complexes (**C** and **F**). Blue: Hoechst, Red: gWIZ-Cy5.

6.3.3 *Method development for PCR based detection of pDNA in sponges*

A qPCR-based method was investigated in order to determine intact amount of pDNA in implants. Standard curves were constructed from naked pCAG-DsRed and PEI-LA/pCAG-DsRed complexes either in solution or absorbed onto sponges. Using a commercial kit designed for pDNA extraction from blood and tissue, a linear standard curve was obtained for naked pDNA but no relationship was obtained for the PEI-LA/pDNA complexes (***Appendix C, Supplemental 6-2A***). For the PEI-LA complexes, the cycle thresholds for all points of the standard curve were 23-24 in our set-up, which was similar to the background levels (i.e., no pDNA). Polymer binding therefore seems to abolish the feasibility of amplification by PCR. To allow amplification in PEI-LA/pDNA complexes, heparin was used to dissociate the complex [32], but this did not also allow amplification of the PEI-LA/pDNA complexes (***Appendix C, Supplemental 6-3***) and even interfered with the amplification of naked pDNA.

A second extraction method was undertaken where samples are incubated with the anionic poly-acrylic acid. We used poly-acrylic acid in place of poly-L-aspartic acid employed in the original procedure [34] since PCR amplification with poly-L-aspartic acid interfered with the ROX dye used as a passive reference (data not shown). Linear standard curves were obtained for both naked and PEI-LA-bound pDNA in this method (***Appendix C, Supplemental 6-2B***). Separate calibration curves were generated for

naked and polymer bound pDNA, and due to the slight divergence of the curves at higher pDNA doses, treatment groups were run with a standard curve containing the same type of pDNA (i.e. either naked or specific polymer bound pDNA).

Finally, to account for the possibility of aberrant amplification from implanted sponge contents, standard curves were generated in a background of explanted sponges. Standard curves from 1-day implanted sponges had higher C_T compared to un-implanted sponges (***Supplemental 4***). Sponges implanted for 7 days also gave higher C_T compared to sponges implanted for 1 day. To determine the reason for this shift, pDNA standard curves were spiked with blood components. The addition of serum had minimal effect on the amplification of pDNA (***Supplemental 5A***) while the addition of clotted blood exhibited a dose-dependence shift in C_T (***Supplemental 5B***). Based on this shift, we estimate that, an implant with ~50% whole blood would lead to approximately 1 C_T decrease, giving an apparent reduction of half pDNA dose. The total error for explanted sponges, however, is likely less than this value since the bloodiest implants had an estimated ~30% blood content.

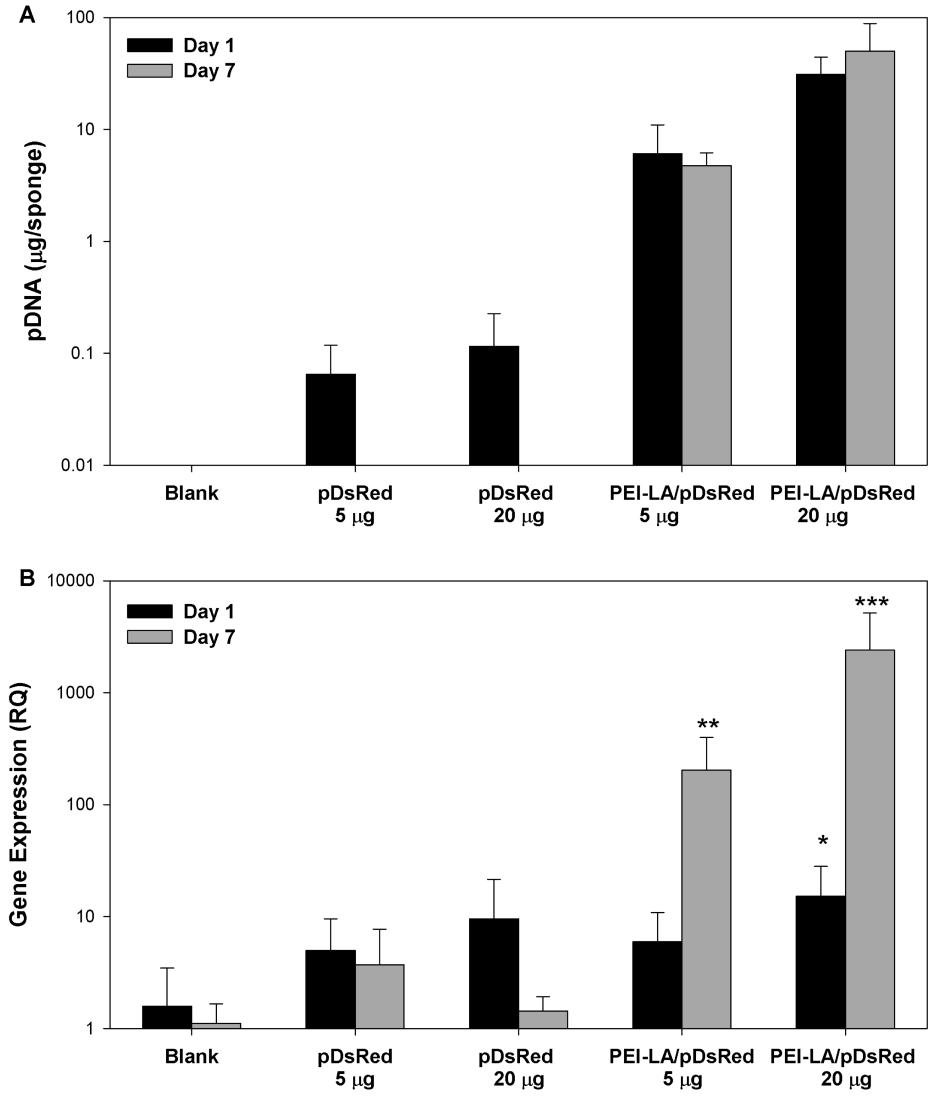

Figure 6-4: Retention and expression of naked and PEI-LA-bound pCAG-DsRED. The plasmid retention was quantitated by qPCR and using blank implants spiked with either free pCAG-DsRED or PEI-LA/pCAG-DsRED complexes to create standard curves (**A**). qPCR was used to measure mRNA expression of DsRed relative to beta-actin in explants harvested after 1 or 7 days (**B**). The mRNA results were analysed with Kruskal-Wallis test. * $p<0.05$, ** $p<0.01$, *** $p<0.001$ compared to blank implants for each time point

6.3.4 *Comparison of pDNA pharmacokinetics and expression by qPCR*

Sponges implanted with naked pCAG-DsRed or PEI-LA/pCAG-DsRed, complexes were harvested after 1 or 7 days to measure pDNA retention with qPCR (***Figure 6-4A***). No pDNA was detected in blank sponges (i.e., the signal below the detection limit of 0.01 μg/sponge on Day 1 and 0.3 μg/sponge on Day 7). A minimal amount of pDNA was detected in both naked pDNA groups on Day 1: 0.06 μg of pCAG-DsRed left from the 5 μg implant dose and 0.1 μg from the 20 μg implant dose. This represents 1.3% and 0.6% retention for the corresponding groups. All explants from 5 μg and 20 μg naked pCAG-DsRed groups on day 7 gave signals below the detection limit of the PCR assay (~0.3 μg per explant). For the 5 μg dose of PEI-LA/pCAG-DsRed, an average of 6 μg of pDNA/sponge were detected after a 1 day implantation and an average of 5 μg after 7 days. For the 20 μg dose of PEI-LA/pCAG-DsRed, PCR calibration curves indicated ~31 and 39 μg of pDNA/sponge were detected after 1 and 7 days respectively. These values were seemingly equivalent or higher than the implant dose (see Discussion on this issue).

Sponges implanted with naked pCAG-DsRed and PEI-LA/pCAG-DsRed complexes were investigated for DsRed mRNA expression. Low levels of DsRed mRNA were found 1 day after implantation when the most pDNA was present. Only the high (20 μg) dose of PEI-LA/pCAG-DsRed complexes led to significant ($p<0.05$ vs. Blank) levels of DsRed mRNA on day 1 (***Figure 6-4B***).

At 7 days, both the 5 μg ($p<0.01$) and 20 μg ($p<0.001$) dose of PEI-LA/pCAG-DsRed complexes led to high, dose-dependent DsRed mRNA expression.

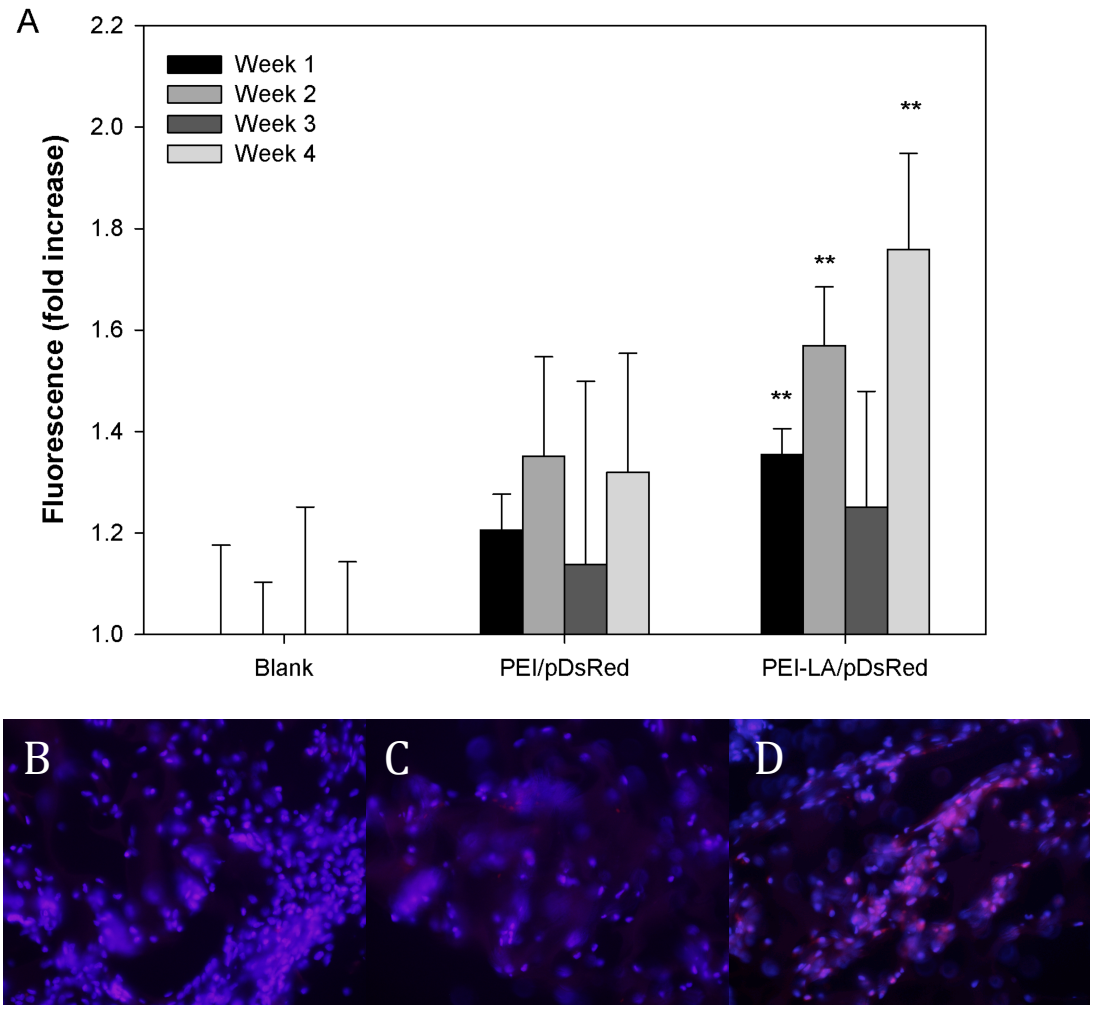

Figure 6-5: DsRed quantitation by *ex vivo* fluorescence imaging. Sponges were harvested after 1 to 4 weeks for DsRed imaging and the measured fluorescence was normalized against the mean fluorescence of blank sponges from the same harvest time (**A**). PEI/pDsRed and PEI-LA/pDsRed sponges were compared against blank sponges for each time point using a Kruskall-Wallis test, followed by the Dunn post-hoc test. **p<0.01 compared to the No Treatment for each time point. Sponges harvested after one week were frozen in cryomatrix and sectioned. Images show blank sponges (**B**), PEI/pCAG-DsRed soaked sponges (**C**), and PEI-LA/pCAG-DsRed soaked sponges (**D**) from week 1. Blue: DAPI, Pink: DsRed

6.3.5 *Long-term pCAG-DsRED delivery by PEI and PEI-LA*

No significant increase in DsRed fluorescence was observed for PEI/pCAG-DsRED at any time point. For PEI-LA/pCAG-DsRED implants, increased fluorescence ($p<0.01$) was observed for sponges harvested at 1, 2, and 4 weeks. Although PEI-LA/pCAG-DsRED sponges on week 3 had comparable fluorescence to PEI-LA/pCAG-DsRED sponges from other time points, the background fluorescence for blank sponges was higher for this time point. The measured fluorescence is likely an underestimation of the DsRed content of the sponges, since the presence of blood significantly attenuated the DsRed fluorescence (***Figure 6-5A***). No significant increase in DsRed fluorescence was observed for PEI/pCAG-DsRED at any time point. For PEI-LA/pCAG-DsRED implants, increased fluorescence ($p<0.01$) was observed for sponges harvested at 1, 2, and 4 weeks. Although PEI-LA/pCAG-DsRED sponges on week 3 had comparable fluorescence to PEI-LA/pCAG-DsRED sponges from other time points, the background fluorescence for blank sponges was higher for this time point, leading to a lack of significant difference. The measured fluorescence is likely an underestimation of DsRed content in sponges, since the presence of blood significantly attenuated the DsRed fluorescence (***Appendix C, Supplemental 6-7***). Sponges were processed for histology to confirm the presence of transfected cells. No DsRed was observed in the DAPI-stained sections of blank (***Figure 6-5B***) or PEI/pCAG-DsRED (***Figure 6-5C***). Regions of DsRed fluorescence, however, were observed with PEI-LA/pCAG-DsRed samples (***Figure 6-5D***).

Using the qPCR methodology, no pDNA was detected in any of the blank implants again (***Figure 6-7A***). The pDNA was detected in both the PEI and PEI-LA delivered pCAG-DsRed groups after 1 week, with 14 and 3 μg pDNA/sponge respectively. The PEI/pCAG-DsRed group had only ~0.06 μg pDNA/sponge after 2 weeks, with pDNA being below the limit of detection after 3 and 4 weeks. The amount of pDNA in PEI-LA/pCAG-DsRed sponges was significantly higher; 4, 0.6, and 0.1 μg/sponge for week 2, 3, and 4, respectively. As before, there was no DsRed mRNA in any of the blank sponges, and no differences were found between blank sponges and PEI/pCAG-DsRed sponges (***Figure 6-7B***). The PEI-LA/pCAG-DsRed containing sponges, however, gave increased DsRed expression at all four weekly time points ($p<0.01$ for week 1, 3 and 4; $p<0.05$ for week 2), with maximal expression appearing at 2 and 4 weeks. A relationship between mRNA expression and pDNA retention was investigated by pooling implants containing PEI-LA and PEI complexes from all time points; a significant correlation between mRNA expression and pCAG-DsRED retention was found for PEI-LA implants ($p<0.01$), but not for PEI implants (***Figure 6-7***).

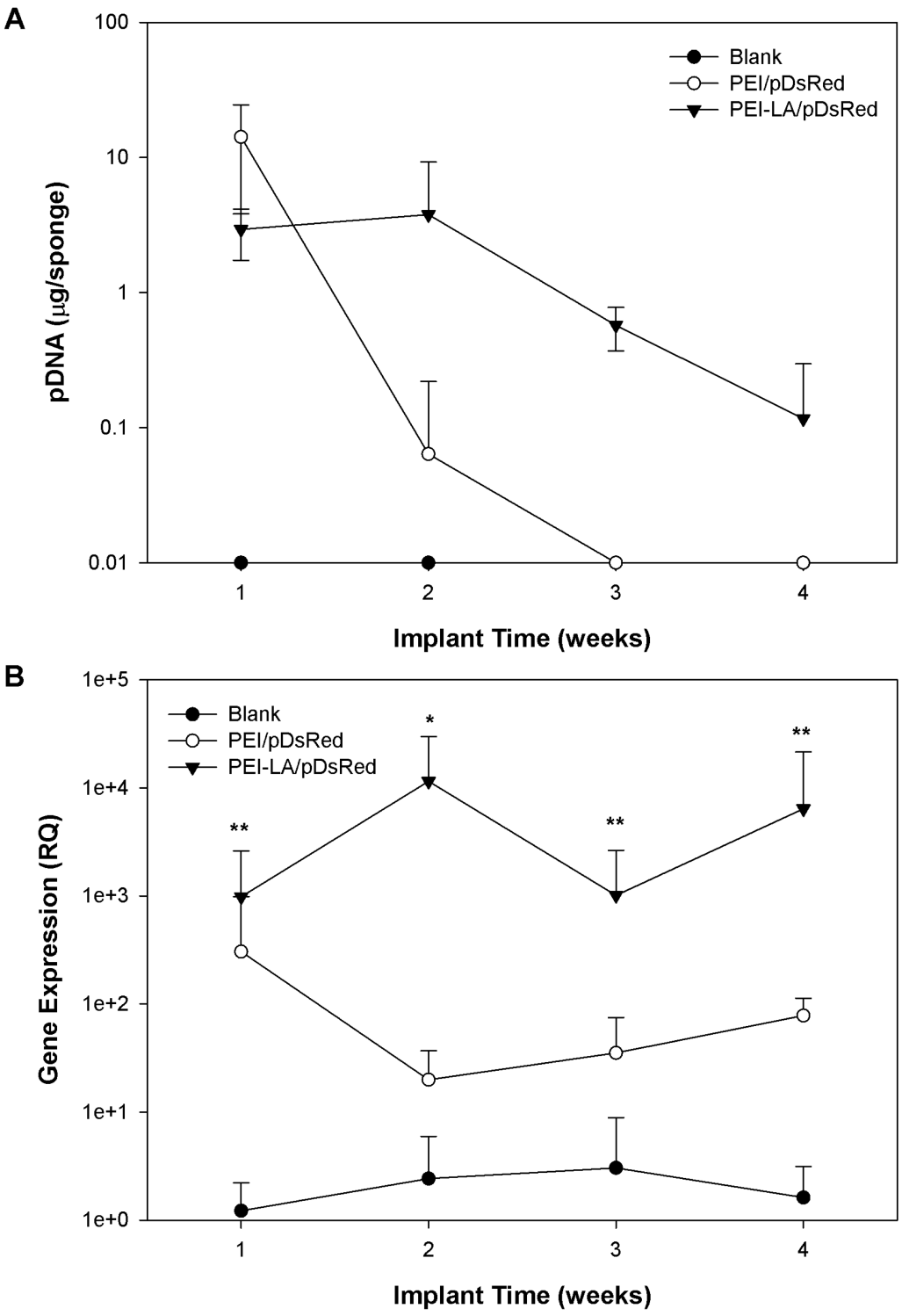

Figure 6-6: Long-term pDNA pharmacokinetics and mRNA expression. The amount of pDNA remaining on sponges was quantified with qPCR (**A**). The mRNA expression was also analysed by using qPCR (**B**). The mRNA levels

at each time point were compared against blank sponges with a Kruskal-Wallis test at each time point. * $p<0.05$ and ** $p<0.01$.

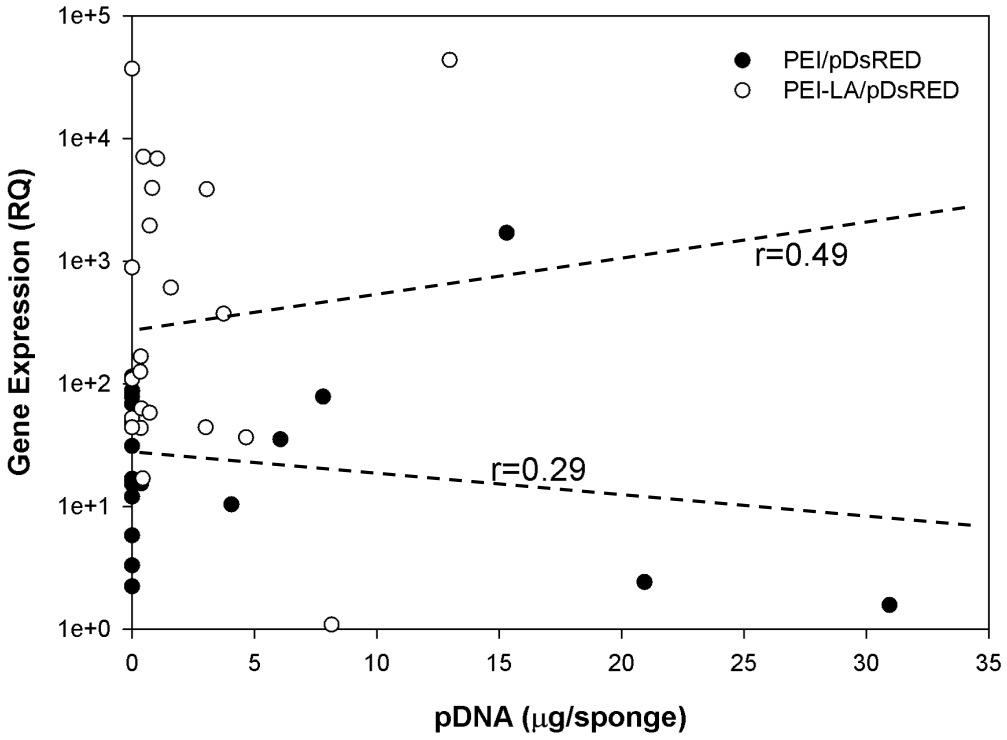

Figure 6-7: Correlation between gene expression and pDNA retention. Graph shows the correlation between dsRED mRNA expression (in relative quantity) and pDNA retention (in μg/sponge) for each individual implant. PEI/pCAG-DsRED and PEI-LA/pCAG-DsRED implants were pooled from all harvest points between week 1 and week 4.

6.4 DISCUSSION

Investigations into pDNA pharmacokinetics and mRNA expression dynamics are paramount to provide information for development of biomaterial carriers intended for *in vivo* use. Such studies will depend on a reliable method to quantitate pDNA and mRNA levels in implants. Commercially available kits are usually designed for extraction of naked pDNA and, although low concentrations of heparin were compatible with PCR [32], the high amount required to fully dissociate polymeric complexes impeded PCR amplification in this study. Besides the method described in this paper, only one other competitive qPCR-based method has been described where pDNA was quantitatively detected in polymeric complexes using an internal standard (IS) as a competitor molecule [21]. In this method, a second plasmid template (IS) that produced a different size PCR product is amplified alongside the target plasmid. Standard curves with varying amounts of IS can be constructed to provide a relationship between concentration of target pDNA and the ratio of amplification between the target and IS. In the study that compared uptake and intracellular trafficking of naked to that of PEI-bound pDNA [21], the generated standard curves allowed the authors to perform pharmacokinetics of pDNA bound to complexes, but the curves for naked and bound pDNAs were very different. This method would therefore be error-prone in biological samples: pDNA is eventually released from the complex during transfection, and therefore a portion of the pDNA in a sponge sample would be naked pDNA. This

contrasts our method where the standard curves for naked and bound pDNA are similar, so that we could generate a total quantity of the pDNA in implants.

Our qPCR-based method, which was modified from a previous report [34], was found to be suitable for quantifying pDNA on the sponge, but not differentiating between the naked and bound pDNA. Although qPCR does not guarantee that the entire pDNA is undamaged, the primer set amplifies the DsRed section so that detection ensures that the coding region of interest is at least intact. The qPCR method, however, might still be associated with error due to dynamic nature of tissue in sponges, where cell invasion and vascularization occurred as a function of time. There was a range of hematomas in sponges harvested at different times, whether they were blank or pDNA-containing sponges. The variability was evident within each study group (i.e., same type of implant) so that this variability might reflect differences in the physiology of individual rats. Blood clots impeded the qPCR reaction in our hands and other studies have also reported qPCR interference due to both heme and leukocytes in blood [18, 32]. The original extraction protocol from Zhou *et al.* [34] were applied to complexes in blood samples but it was possible that a systematic error was introduced to all samples given the same 'background' interference. The immune response to our complexes was investigated to ensure that blood in our studies was not enriched with activated leukocytes. Levels of tumor necrosis factor-α, interleukin-6, and interleukin-2 in implants showed no increase with

implantation of complexes (***Appendix C, Supplemental 6-8***), ruling out the activated leukocytes as a source of error for qPCR. Another source of error may be due to a lack of uniform distribution of pDNA in sponges, particularly for the PEI-LA and PEI complexes. This variability might be due to initial loading differences or due to release from implants, which was expected to deplete the pDNA from the periphery. Since we sample only a small fraction of sponges (15-50% depending on implant mass), it is possible to erroneously calculate the retained dose due to heterogeneous sampling. Despite these unresolved issues, the qPCR method remains a promising way to measure the amount of pDNA in sponge.

There was a good agreement between the Cy5- and qPCR-based assessments of pDNA pharmacokinetics for polymer complexes. Retention studies using gWIZ-Cy5 and qPCR gave similar results with respect to initial ability of PEI and PEI-LA to retain pDNA in implants. Both PEI and PEI-LA complexes showed similar retention after 1 and 7 days of implantation with both methods, even though PEI appeared to provide higher localization initially. Assessment by gWIZ-Cy5, however, gave results that were not in agreement with the qPCR-based methodology specifically for naked pDNA implants. Due to lack of DsRed mRNA expression, we hypothesize that the majority of naked pDNA implanted was degraded (or lost) within one day, as indicated by the qPCR method. It was considered likely that the gWIZ-Cy5 assessment was obscured by the liberated Cy5 label, which highlights the benefit of qPCR to ensure detection of intact pDNA. This finding is in

agreement with previous systemic delivery studies that found naked pDNA to be rapidly degraded with a half-life on the scale of minutes [10]. While some bone regeneration studies found a beneficial effect due to locally delivered pDNA without a carrier, the dose required for this effect was generally high [4, 5, 8, 9] or multiple smaller doses were required for an effect [23]. Unlike our study, naked pDNA and mRNA expression was detected after 6 weeks in one study [4], but that study used a 1000 μg pDNA dose as compared to our 5 and 20 μg doses (i.e., such excessive doses may exceed the amount of pDNA that can be degraded in a short period of time). It is also possible that difference in biomaterial scaffold used as a vehicle for pDNA implantation may alter the half-life of the pDNA payload, with changes in scaffold's integrity possibly altering the clearance of pDNA, either naked or polymer-bound, from the site. The sponges in our study showed a gradual decrease in size over the course of the four-week implantation period (size ultimately reducing to <half). It is likely that this is indicative of sponge degradation, which may have accelerated release or clearance of DNA from the implantation site. It remains unclear whether the therapeutic effect reported with different scaffolds was due to production of the protein or the foreign body/immune response to the implanted pDNA. The beneficial effect of the naked pDNA may be due to a general immunogenic response, since unmethylated cytosine-guanine dinucleotides (CpG motifs) of pDNA are known to be immunogenic [28].

The pDNA delivered with PEI and PEI-LA both showed prolonged retention in implants. The pDNA delivered by PEI was detected for up to 2 weeks and pDNA from PEI-LA complexes remained in implants for at least 4 weeks. This difference in retention could be due to a difference in intracellular fate of pDNA. Both *in vitro* and *in vivo*, this low molecular weight PEI gave comparable cellular uptake of pDNA but negligible transfection as compared to PEI-LA delivery. The rate-limiting step for 2 kDa PEI complexes appeared to be endosomal escape [30], and so that the pDNA contained within PEI complexes might be eventually destroyed and no longer detectable. In contrast, the PEI-LA complexes led to effective transgene expression, so that pDNA was likely in the nucleus where it was less likely to be destroyed. The agreement between the transfection results from an immortalized cell line and animal model is particularly encouraging. Although the absolute transfection efficiency observed here *in vitro* and *in vivo* is likely different, intracellular traficking appears to be a limited factor for unmodified PEI.

A correlation was found between the mRNA expression and pDNA retention for PEI-LA implants, but not for PEI implants. This is in line with the lack of expression from the PEI complexes. An even stronger correlation would be expected with a better sampling strategy, as there should be a delay between pDNA presence and mRNA expression, and implants that retained higher pDNA at initial time points would have led to higher mRNA expression at a later time point. This, however, would have required multiple samplings

from the same sponge while still being implanted, which was not possible with our current methodology. Nevertheless, the observed correlation is a testament to the stronger mRNA expression by the PEI-LA/pCAG-DsRed complexes during the study period. In addition to long duration of expression, mRNA was also expressed very quickly: with a 20 μg dose of pDNA in PEI-LA complexes, increased levels of DsRed mRNA were detected within 24 hours of implantation. The lower 5 μg dose was also effective, but increased mRNA expression was not observed until the second time point (7 days post-implantation). The subcutaneous model employed for these studies may be less biologically active than an intraosseous site, but these studies are intended to provide preliminary information about pDNA retention and mRNA expression for non-viral delivery systems. This length and onset of transgene expression is especially encouraging for bone regeneration therapies, where weeks of expression and fast onset would be beneficial. Since transgene expression was possible at four weeks, future studies will investigate when transgene expression diminishes, as extended production of bone inducing proteins is eventually unneeded. The correlation between the presence of pDNA and mRNA expression also calls for gene delivery approaches that maximize pDNA retention in implants as a means to enhance transgene expression. With the availability of the current qPCR-based methodology, we envision more detailed investigations of pDNA pharmacokinetics in implanted sponges to be pursued in the future.

6.5 CONCLUSIONS

A polymeric carrier for gene delivery is expected to display two important functions, namely to protect the pDNA from degradation in the extracellular environment and to navigate cellular barriers to allow protein expression. We distinguished between the pDNA uptake and successful intracellular trafficking with the comparison of PEI and PEI-LA carriers in this study. While both carriers appeared to protect the pDNA in implants initially, the delivered pDNA remained detectable for a prolonged time (up to 4 weeks) with the PEI-LA carrier. Similarly, expression of a DsRED reporter gene was observed within 24 hours of implantation with the more effective PEI-LA, whose pharmacokinetics profile corresponded closely to the transgene expression profile up to 4 weeks. A relatively weak but nevertheless significant correlation between pDNA retention of transgene expression was observed. The methodology described here and the unique carriers characterized should facilitate gene delivery efforts in tissue regeneration and repair.

6.6 REFERENCES

1. Alden T, Pittman D, Hankins F, Beres E, Engh J, Das S, Hudson S, Kerns K, Kallmes D, Helm G. In vivo endochondral bone formation using a bone morphogenetic protein 2 adenoviral vector. Hum Gene Ther 1999;10(13):2245-53.
2. Aliabadi HM, Mahdipoor P, Uludag H. Polymeric delivery of siRNA for dual silencing of Mcl-1 and P-glycoprotein and apoptosis induction in drug-resistant breast cancer cells. Cancer Gene Ther 2013;20(3):169-77.
3. Aliabadi HM, Landry B, Mahdipoor P, Hsu CY, Uludag H. Effective down-regulation of breast cancer resistance protein (BCRP) by siRNA delivery using lipid-substituted aliphatic polymers. Eur J Pharm Biopharm 2012;81(1):33-42.
4. Bonadio J, Smiley E, Patil P, Goldstein S. Localized, direct plasmid gene delivery in vivo: prolonged therapy results in reproducible tissue regeneration. Nature Medicine 1999;5(7):753-759.
5. Bright C, Park YS, Sieber AN, Kostuik JP, Leong KW. In vivo evaluation of plasmid DNA encoding OP-1 for spine fusion. Spine 2006;31(19):2163-72.
6. Carragee EJ, Hurwitz EL, Weiner BK. A critical review of recombinant human bone morphogenetic protein-2 trials in spinal surgery: emerging safety concerns and lessons learned. Spine J 2011;11(6):471-91.
7. Chen Y, Luk K, Cheung K, Xu R, Lin M, Lu W, Leong J, Kung H. Gene therapy for new bone formation using adeno-associated viral bone morphogenetic protein-2 vectors. Gene Therapy 2003;10:1345-1353.
8. Fang J, Zhu YY, Smiley E, Bonadio J, Rouleau J, Goldstein S, McCauley L, Davidson B, Roessler B. Stimulation of new bone formation by direct transfer of osteogenic plasmid genes. Proc Natl Acad Sci USA 1996;93:5753.

9. Geiger F, Betram H, Berger I, Lorenz H, Wall O, Eckhardt C, Simank HG, Richter W. Vascular endothelial growth factor gene-activated matrix (VEGF165-GAM) enhances osteogenesis and engiogenesis in large segmental bone defects. J Bone Miner Res 2005;20:2028.
10. Houk BE, Martin R, Hochhaus G, Hughes JA. Pharmacokinetics of plasmid DNA in the rat. Pharm Res 2001;18:67-74.
11. Hu WW, Wang Z, Hollister SJ, Krebsbach PH. Localized viral vector delivery to enhance in situ regenerative gene therapy. Gene Ther 2007;14(11):891-901.
12. Huang YC, Simmons C, Kaigler D, Rice KG, Mooney DJ. Bone regeneration in a rat cranial defect with delivery of PEI-condensed plasmid DNA encoding for bone morphogenetic protein-4 (BMP-4). Gene Therapy 2005; 12:418.
13. Itaka K, Ohba S, Miyata K, Kawaguchi H, Nakamura K, Takato T, Chung U, Kataoka K. Bone regeneration by regulated in vivo gene transfer using biocompatible polyplex nanomicelles. Molecular Therapy 2007;15(9):1655.
14. Kang Q, Sun M, Cheng H, Peng Y, Montag A, Deyrup A, Jiang W, Luu H, Luo J, Szatkowski J, Vanichakarn P, Park J, Li Y, Haydon R, He T. Characterization of the distinct orthotopic bone forming activity of 14 BMPs using recombinant adenovirus-mediated gene delivery. Gene Ther 2004;11(17):1312-20.
15. Lew D, Parker SE, Latimer T, Abai AM, Kuwahararundell A, Doh SG, et al. Cancer gene-therapy using plasmid DNA-Pharmacokinetic study of DNA following injection in mice. Human Gene Ther 1995;6:553-64.
16. Li D, Wang W, Guo R, Qi YY, Gou ZR, Gao CY. Restoration of rat calvarial defects by poly(lactide-co-glycolide)/hydroxyapatite scaffolds loaded with bone mesenchymal stem cells and DNA complexes. Chin Sci Bull 2012;57:435-444.
17. Li J, Li H, Sasaki T, Holman D, Beres B, Dumont J, Pittman D, Hankins G, Helm G. Osteogenic potential of five different recombinant human bone

morphogenetic protein adenoviral vectors in rat. Gene Therapy 2003;10:1735-1743.

18. Morata P, Queipo-Ortuno MI, de Dios Colmenero J. Strategy for optimizing DMA amplification in a peripheral blood PCR assay used for diagnotsis of human brucellosis. J Clin Microbiol 1998;36(9)):2443-6.
19. Neamnark A, Suwantong O, Bahadur RK, Hsu CY, Supaphol P, Uludag H. Aliphatic lipid substitution on 2 kDa polyethylenimine improves plasmid delivery and transgene expression. Mol Pharm 2009;6(6):1798-815.
20. Oda M, Kuroda S, Kondo H, Kasugai S. Hydroxyapatite fiber material with BMP-2 gene induces ectopic bone formation. J Biomed Mat Res Part B 2009;90(1): 101.
21. Oh YK, Suh D, Kim JM, Choi HG, Shin K, Ko JJ. Polyethylenimine-mediated cellular uptake, nucleus trafficking and expression of cytokine plasmid DNA. Gene Therapy 2002;9(23):1627-32.
22. Ono I, Yamashita T, Jin HY, Ito Y, Hamada H, Akasaka Y, Nakasu M, Ogawa T, Jombow K. Combination of porous hydroxyapatite and cationic liposomes as a vector for BMP-2 gene therapy. Biomaterials 2004;25:4709-4718.
23. Osawa K, Okubo Y, Nakao K, Koyama N, Bessho K. Osteoinduction by repeat plasmid injection of human bone morphogenetic protein-2. J Gene Med 2010;12(12):937-44.
24. Parra-Guillen ZP, Gonzales-Aseguinolaza G, Berraondo P, Troconiz IF. Gene Therapy: A Pharmacokinetic/Pharmacodynamic modelling overview. Pharm Res 2010;27:1487-1497.
25. Rose L, Aliabadi HM, Uludag H. Gelatin coating to stabilize the transfection ability of nucleic acid polyplexes. Acta Biomater 2013;9(7):7429-38.
26. Rose LC, Kucharski C, Uludag H. Protein expression following non-viral delivery of plasmid DNA for basic FGF and BMP-2 in a rat ectopic model. Biomaterials 2012;33(11):3363-74.

27. Rose L, Uludag H. Realizing the potential of gene-based molecular therapies in bone repair. J Bone Miner Res 2013. Doi: 10.1002/jmbr.1944
28. Takahashi Y, Nishikawa M, Takakura Y. Development of safe and effective nonviral gene therapy by eliminating CpG motifs from plasmid DNA vector. Front Biosci 2012;4:133-41.
29. Thierry AR, Rabinovish P, Peng B, Mahan LC, Bryant JL, Gallo RC. Characterization of liposome-mediated gene delivery:expression, stability and pharmacokinetics of plasmid DNA. Gene Ther 1997;4:226-37.
30. Varga CM, Tedford NC, Thomas M, Klibanov AM, Griffith LG, Lauffenburger DA. Quantitative comparison of polyethylenimine formulations and adenoviral vectors in terms of intracellular gene delivery processes. Gene Ther 2005;12(13):1023-32.
31. Wickersham IR, Lyon DC, Barnard RJ, Mori T, Finke S, Conzelmann KK, Young JA. 2007. Monosynaptic restriction of transsynaptic tracing from single, genetically targeted neurons. Neuron 53:639-47.
32. Yokota M, Tatsumi N, Nathalang O, Yamada T, Tsuda I. Effects of heparin on polymerase chain reaction for blood white cells. J Clin Lab Anal 1999;13(3):133-40.
33. Yu L, Suh H, Koh JJ, Kim SW. Systemic administration of TerplexDNA system: pharmacokinetics and gene expression. Pharm Res 200;18:1277-83.
34. Zhou QH, Wu C, Manickam DS, Oupicky D. Evaluation of pharmacokinetics of bioreducible gene delivery vectors by real-time PCR. Pharm Res 2009;26(7):1581-9.

7 General Discussion, Conclusions, and Future Directions

The research work in this thesis sought to develop strategies for bone formation using gene-based therapies. We implanted *in vivo* plasmid DNA (pDNA) complexes for transgene expression ultimately to be used in tissue regeneration. The complexes are loaded in a biomaterial scaffold for implantation, and the host's cells infiltrate the scaffold and become transfected. This approach has previously been used for bone regeneration by others [4, 7, 8], among other regeneration approaches. An advantage of this system is that it transfects the host's own cells, bypassing potentially immunogenic foreign cells. This type of *in vivo* gene delivery, however, still requires an understanding of many fundamental questions in order to improve pDNA delivery and provide a better therapeutic response. Many fundamental questions, such as transfection efficiency, remained unanswered due in part to the difficulty in measuring transgene expression. The fourth and sixth chapters demonstrate the difficulty in measuring transgene expression and transfection efficiency. The use of fluorescent reporter genes, as frequently employed *in vitro*, allow easy detection by flow cytometry but autofluorescence from complex toxicity can lead to false positives as found in Chapter 4, especially in primary cells [20]. The low level of expression *in vivo* found in Chapter 4 5, 6, combined with the high autofluorescence due to high complex dose hampered our efforts. Imaging

the fluorescence of entire sponges with a red fluorescent protein allowed a quantitative measure of expression, but this is likely an underestimation due to the quenching effect of blood on the fluorescence signal as found in Chapter 6. The fluorescent reporter genes, however, do allow histological confirmation of transfection, since the expression transgene ends up getting concentrated inside the transfected cells.

Secreted reporter gene, such as bFGF and BMP-2, ultimately provided the best measure of transfection for our purposes. Since these proteins are secreted, they could be detected in supernatant of sponges with enzyme-linked immunoassays (ELISAs). Sponges were loaded with complexes containing a BMP-2 expressing plasmid, and then implanted. The harvested sponges were cultured *ex vivo* in tissue culture media to allow sufficient accumulation of BMP-2. This allowed us to obtain expression rates (on the order of 0.3 ng/sponge/day) and compare our delivery system with others. This method is limited in its use because the ELISA was particularly prone to background interference in blank sponges that had been implanted for extended periods of time as observed in Chapter 4, preventing clear detection of protein expression at later time points. This problem is exasberated since the obtained secretion rates were barely above the background levels. The combination of fluorescent and secreted reporter genes along with mRNA expression has allowed us to determine that expression is observed for at least four weeks, and that the expression level is comparable to viral vectors [1, 16].

The gene delivery studies reported in Chapter four, five, and six were all performed in a subcutaneous implant model because there are no endogenous bone-related proteins to interfere with detection of recombination growth factors. While less invasive and easier to analyse, a subcutaneous implantation may not represent the best site to investigate bone formation. Since the end purpose of our gene delivery studies is to induce bone regeneration, evaluating the gene delivery system in an osteogenic defect might be more suitable, since a better biological response is expected in a more dynamic injury environment [12]. The protein secretion rate [14] and length of transgene expression [15] found in our studies with PEI-LA in the subcutaneous model are similar to those found with viral systems in an osteo or osteochondral defect model [1, 16, 19], all of which resulted in bone formation. Based on the performance of PEI-LA, and that comparable viral-based transfections resulted in bone regeneration, we conducted a preliminary testing of our gene delivery system in an animal model comparable to the indicated condition. A skull defect model was chosen [8], where a 5 mm circular defect was filled with the biomaterial sponge containing the complexes. PEI-LA was used to deliver plasmid DNA expressing either bFGF or BMP-2. The details of this study have been included in **Appendix D**. Ultimately we found no increase in bone regeneration when the therapeutic plasmid was delivered compared to control plasmid. The reasons for this remain unclear, since the expression of

BMP-2 (as measured in a subcutaneous model) was comparable to other systems that resulted in bone regeneration.

The majority of presented studies used absorbable gelatin sponges (Gelfoam™) to deliver the pDNA complexes, with the exception of one study in Chapter 4 that used collagen sponges. Although the collagen sponges are closer to material found in bone, the gelatin sponges were previsouly found to be suitable to support bone formation following gene delivery [5, 9]. We therefore hypothesize that one reason for lack of regeneration may be due to the toxicity of treatment (i.e., complexes). In our skull defect study, 10 μg of pDNA and 50 μg of PEI-LA were implanted in a circular 5 mm defect. Previous studies have found that the toxicity from ~32 μg of 25 kDa PEI was enough to interfere with bone formation at subcutaneous site following delivery of BMP-2 [22]. The toxicity of 2 kDa PEI-LA is lower than 25 kDa PEI [11], but the dose required for *in vivo* transfection may still be sufficient to interfere with cellular processes for differentiation. Now that we have robust methods to detect transgene expression, it may be easier to develop new carrier systems that have similar transfection efficiencies but lower toxicity. It may also be possible to use a lower polymer to pDNA weight ratio. Chapter 5 shows that complete binding is obtained at approximately 1:1 weight ratio [13], and so there is excess free polymer at 10:2. Free polymer *in vitro* has been previously shown in increase uptake [21], possibly through preventing undesireable interactions of cationic complexes with anionic glycosaminoglycans [6]. It remains to be investigated whether free polymer

in vivo is similarly beneficial. If not, it might be possible to reduce polymer concentrations in order to reduce any undesirable effect on local tissues and invading cells. Another option for improving the outcome of transfection is the use of novel polymers that are more efficient such that either a lower dose of pDNA or less polymer can be employed.

Another reason for the lack of bone formation could be the different cells transfected in the subcutaneous versus intraosseous defect. The PEI-LA employed for *in vivo* gene delivery is not designed to target specific cell populations. One reason for this is that it remains unclear which cells should be targeted. For bone regeneration purpose, mesenchymal stem cells or cells harvested from bone marrow [2, 20] are often the target of modification *in vitro* as preliminary studies for *in vivo*. It remains unclear, however, whether bone marrow, specifically the mesenchymal stem cell population, would (a) infiltrate the sponge implant and (b) get transfected by the complexes. It is, therefore, not logical to target this cell population. In our subcutaneous model, a homogenous population of cells is observed one day after transfection. After one week of implantation, the cells harvested from the population were heterogeneous and in some cases contained multiple populations (based on flow cytometry profiles obtained on extracted cells). A similar gene activated matrix for spinal cord regeneration showed that Schwann cells, fibroblasts, and macrophages were the most prominent type of transfected cells [3]. It is unlikely that Schwann cells are present in our implants but it is likely that fibroblasts and macrophages are primarily

transfected both in the subcutaneous model and the intraosseous model. It is likely that there will be more red and white blood cells (including macrophages) in an intraosseous defect compared to subcutaneous due to the increased injury of creating a defect. It remains unclear whether shifting the variety of infiltrating cells changes the transfection efficiency and transgene expression.

One of the challenges of gene delivery, especially in clinically relevant primary cells and *in vivo*, is the low transfection efficiency. In many transfection models, the rate-limiting step is intracellular trafficking, including endosomal escape and nuclear targeting. In an effort to better understand the obstacles to transfection, we screened a library of siRNA against kinases and identified kinases whose knockdown led to increased transfection of pDNA. Use of a small molecule kinase inhibitor led to an increase in pDNA transfection [17], and a screen allows identification of multiple targets for further use. A summary of these studies is included in **Appendix E**. The top three kinases found to be positive for two different statistical tests were activin A receptor type II-like 1 (ACVRL1; Gene ID 94), LOC391295 (locus with an unnamed gene product; Gene ID 391295), and phosphatidylinositol-4-phosphate 5-kinase, type II α (PIP4K2A, also known as PIP5K2A; Gene ID 5305). In validation studies, knockdown with any of these siRNAs led to increased transfection, compared treatment with scrambled control siRNA. Inconsistent results were subsequently observed during the validation studies, where some studies demonstrated the efficacy

of target siRNAs and other studies showed no effect or no baseline transfection. These studies were therefore not continued due to the unstable nature of the cord blood cells, but still provided method development that may prove useful for future screens.

Future Directions

Our ultimate goal remains the development of a non-viral gene therapy for bone regeneration. I propose several areas of future study to improve gene delivery specifically *in vivo* for the purpose of inducing bone formation.

- **Extent of transgene expression**. I have determined that pDNA is retained on the implant and mRNA is expressed for four weeks with PEI-LA as a carrier, an encouraging result. The pDNA retention in non-viral complexes we used is near the baseline of detection by the end and so will likely not be detected for longer than 5-6 weeks. The mRNA expression, however, remained similar to the previous three weeks and is likely to continue for some time. Determining when transgene expression ceases provides a better understanding of the dynamics of *in vivo* gene delivery.
- **Role of free polymer and naked pDNA *in vivo***. Although free polymer is beneficial for uptake in cell culture, it is unclear to what extent it is needed *in vivo*. High weight ratios currently used may be responsible for toxicity, but if free polymer is less useful then lower weight ratios may be employed. With better methods to measure

transgene expression, the effect of different weight ratios on transfection efficiency can be more accurately measured. Alongside the role of free polymer, it would be interesting to determine the proportion of polymer-bound pDNA. The commercial kits are designed to extract naked pDNA whereas the polymer extraction allows amplification of naked and bound pDNA. A more thorough comparison of these two extraction methods may allow a better distinction between naked and bound pDNA.

- **Identification of cell populations transfected *in vivo***. A better understanding of the cells that infiltrate and become transfection would help select an appropriate polymer. Different cells transfect differently [10], and if we can identify a prominent population that becomes transfected, it may be possible to screen polymer candidates for improved transfection efficiency. Such a screen may even be able to be performed *in vitro* and allow us to short-list polymers to be tested in *in vivo*. It is also likely that the infiltrating populations are different in subcutaneous and intraosseous, but there may be some some overlap that may allow continued use of the subcutaneous model.
- **Gelatin-coated complexes in bone regeneration**. The stabilized gelatin-coated complexes proved successful for increasing transgene expression in a subcutaneous model. A similar approach should be

beneficial for an intraosseous model and may increase transgene output sufficiently to increase regeneration.

REFERENCES

1. Betz O, Betz V, Abdulazim A, Penzkofer R, Schmitt B, Schroder C, et al. The repair of critical-sized bone defects using expedited autologous BMP-2 gene activated fat implants. Tiss Eng Part A 2010;16:1093-1101.
2. Clements BA, Hsu CY, Kucharski C, Lin X, Rose L, Uludag H. Nonviral delivery of basic fibroblast growth factor gene to bne marrow stromal cells. Clin Orthop Relat Res 2009;467(12):3129-37.
3. De Laporte L, Yang Y, Zelivyanskaya ML, Cummings BJ, Anderson AJ, Shea LD. Plasmid releasing multiple channel bridges for transgene expression after spinal cord injury. Mol Ther 2009;17(2):318-26.
4. Fang J, Zhu YY, Smiley E, Bonadio J, Rouleau J, Goldstein S, McCauley L, Davidson B, Roessler B. Stimulation of new bone formation by direct transfer of osteogenic plasmid genes. Proc Natl Acad Sci USA 1996;93:5753.
5. Fujita N, Matsushita T, Ishida K, Sasaki K, Kubo S, Matsumoto T, et al. An analysis of bone regeneration at a segmental bone defect by controlled release of bone morphogenetic protein 2 from a biodegradable sponge composed of gelatin and tricalcium phosphate. J Tissue Eng Regen Med 2011;6(4):291-8.
6. Hanzlikova M, Ruponen M, Galli E, Raasmaja A, Aseyev V, Tenhu H, et al. Mechanisms of polyethylenimine-mediated DNA delivery: free carrier helps to overcome the barrier of cell-surface glycosaminoglycans. J Gene Med 2011;13(7-8):402-9.
7. Huang YC, Simmons C, Kaigler D, Rice KG, Mooney DJ. Bone regeneration in a rat cranial defect with delivery of PEI-condensed plasmid DNA encoding for bone morphogenetic protein-4 (BMP-4). Gene Therapy 2005; 12:418.
8. Itaka K, Ohba S, Miyata K, Kawaguchi H, Nakamura K, Takato T, Chung U, Kataoka K. Bone regeneration by regulated in vivo gene transfer

using biocompatible polyplex nanomicelles. Molecular Therapy 2007;15(9):1655.

9. Kohara H, Tabata Y. Enhancement of ectopic osteoid formation following the dual release of bone morphogenetic protein 2 and Wnt1 inducible signalling pathway protein 1 from gelatin sponges. Biomaterials 2011;32(24):5726-32.
10. Landry B, Aliabdi HM, Samuel A, Gul-Uludag H, Jiang X, Kutsch O, Uludag H. Effective non-viral delivery of siRNA to acute myeloid leukemia cells with lipid-substituted polyethylenimines. PLoS One 2012;7(8):e44197.
11. Neamnark A, Suwantong O, Bahadur RK, Hsu CY, Supaphol P, Uludag H. Aliphatic lipid substitution on 2 kDa polyethylenimine improves plasmid delivery and transgene expression. Mol Pharm 2009;6(6):1798-815.
12. Park J, Jung I, Yun J, Choi S, Cho K, Kim C. Induction of bone formation by Escherichia coli-expressed recombinant human bone morphogenetic protein-2 using block-type macroporous biphasic calcium phosphate in orthotopic and ectopic rat models. J Periodontal Res 2011;46(6):682-90.
13. Rose L, Aliabadi H, Uludag H. Gelatin coating to stabilize the transfection ability of nucleic acid polyplexes. Acta Biomater 2013;9(7):7429-38.
14. Rose LC, Kucharski C, Uludag H. Protein expression following non-viral delivery of plasmid DNA for basic FGF and BMP-2 in a rat ectopic model. Biomaterials 2012;33(11):3363-74.
15. Rose L, Mahdipoor P, Kucharski C, Uludag H. Pharmacokinetics and transgene expression by polyethylenimine-based pDNA complexes after *in vivo* gene delivery.
16. Rundle C, Miyakoshi N, Kasukawa Y, Chen S, Sheng M, Wergedal J, Lau K, Baylink D. In vivo bone formation in fracture repair induced by direct retroviral-based gene therapy with bone morphogenetic protein-4. Bone 2003;32(6):591-601.

17. Ur Rehman Z, Hoekstra D, Zuhorn IS. Protein kinase A inhibition modulates the intracelluluar routing of gene delivery vehicles in HeLa cells, leading to productive transfection. J Control Release 2011;156(1):76-84.
18. Varga CM, Tedford NC, Thomas M, Klibanov AM, Griffith LG, Lauffenburger DA. Quantitative comparison of polyethylenimine formulations and adenoviral vectors in terms of intracellular gene delivery processes. Gene Ther 2005;12(13):1023-32.
19. Vogt S, Wexel G, Tischer T, Schillinger U, Ueblacker P, Wagner B, et al. The influence of the stable expression of BMP2 in fibrin clots on the remodeling and repair of osteochondral defects. Biomaterials 2009;30:2385-2392
20. Wang Y, Mostafa NZ, Hsu CY, Rose L, Kucharski C, Yan J, Jiang H, Uludag H. Modification of human BMSC with nanoparticles of polymeric biomaterials and plasmid DNA for BMP-2 secretion. J Surg Res 2013;183(1):8-17.
21. Yue Y, Jin F, Deng R, Cai J, Dai Z, Lin MC et al. Revisit complexation between DNA and polyethylenimine-effect of length of free polycationic chains on gene transfection. J Control Release 2011;152(1):143-51.
22. Zhang S, Kucharski C, Doschak MR, Sebald W, Uludag H. Polyethylenimine-PEG coated albumin nanoparticles for BMP-2 delivery. Biomaterials 2010;31(5):952-63.

8 Appendix A

SUPPLEMENTARY INFORMATION

For

PROTEIN EXPRESSION FOLLOWING NON-VIRAL DELIVERY OF PLASMID DNA CODING FOR BASIC FGF AND BMP-2 IN A RAT ECTOPIC MODEL

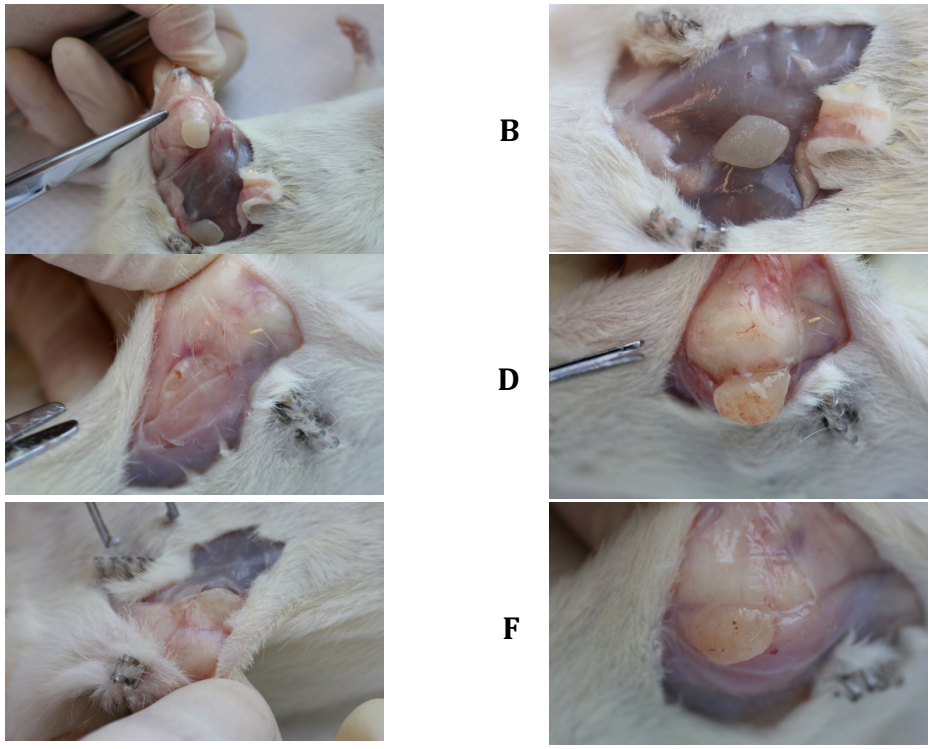

***In situ* images of gelatin sponges following 1 week of implantation**. Sponges contained PEI-LA complexes with either (**A,B**) gWiz, (**C,D**) bFGF-IRES-AcGFP or (**E,F**) BMP2-IRES-AcGFP plasmids. Implants were imaged either immediately following opening of the implant site (**A,C,E**) or during excision from the implant site (**B,D,F**) in order to better reveal angiogenesis. Note the hematoma formation in **D** and **F** that received the expression vector for growth factors, but not in **B** that received the control plasmid.

9 Appendix B

SUPPLEMENTARY INFORMATION

For

GELATIN COATING TO STABILIZE THE TRANSFECTION ABILITY OF NUCLEIC ACID POLYPLEXES

A. MATERIALS AND METHODS

S1. Materials. Dextrose (D-glucose), L-glutamine, β-alanine, L-leucine, L-methionine, tricine, polyoxyethylene (20) sorbitan monolaurate (Tween 20), polyoxyethylene (80) sorbitan monooleate (Tween 80), polyoxyethylene (40) monostearate, cholesteryl hemisuccinate, glycerol, gelatin Type B (catalogue number G9391), bovine serum albumin, 2 kDa polyacrylic acid, and poly-L-lysine (70-150 kDa) were obtained from Sigma (St Louis, MO). Tri-sodium orthophosphate was obtained from British Drug House (Poole, UK) and polyethyleneglycol (PEG; 3.4 kDa) was obtained from Polysciences (Warrington, PA).

S2. Complex Formation. Polymer/pDNA complexes were formed as described in section 2.2. To determine the effect of temperature on transfection efficiency, complexes were incubated in eppendorfs at 37 °C, 23 °C, or 4 °C for 0, 24, or 48 hours prior to addition to cell cultures. To determine the effect of serum, complexes in eppendorfs were mixed in media

containing 0-50% serum and incubated for 0, 24, or 48 hours at 37 °C prior to addition to cell cultures. For screens, 0.1% (w/v) solutions containing various compounds were added to complexes in eppendorfs during the 8 hour incubation at 37 °C. To determine the effect of gelatin during formation, pDNA was diluted in gelatin solution prior to mixing with polymer. Complexes were incubated for 0 or 24 hours at 37 °C prior to addition to cell cultures.

S3. Assessment of GFP Expression. Large screens were performed in 48-well plates, and GFP expression was analyzed with a fluorescent plate reader (λ_{ex}: 485 nm, λ_{em}: 527 nm). For more detailed analysis of GFP expression, cell were transfected in 24-well plates and GFP expression was assessed using Beckman Coulter Cell Lab Quanta SC flow cytometer.

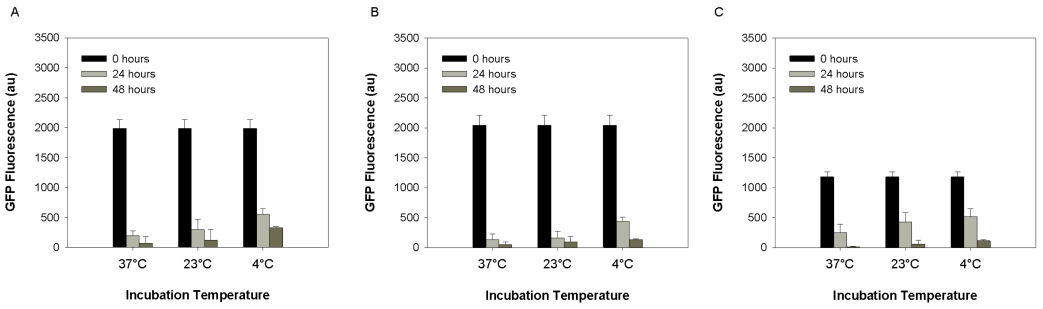

Supplemental 5-1: Transfection with complexes incubated at different temperatures. PEI-LA (**A**), PEI-LA/PEI (**B**), or PEI-LA/PEI-PEG (**C**) complexes were incubated at 37 °C, 23 °C (room temperature), or 4 °C for 0, 24 or 48 hours before exposure to 293T cells. GFP expression was analyzed with flow cytometry and the results were summarized as the mean GFP-fluorescence of cell population.

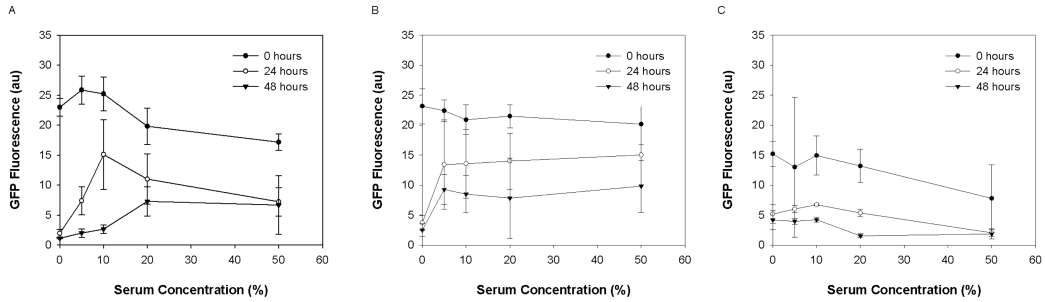

Supplemental 5-2: Transfection with complexes incubated in serum. PEI-LA (**A**), PEI-LA/PEI (**B**), or PEI-LA/PEI-PEG (**C**) complexes were incubated at 37 °C for 0, 24 or 48 hours in 0-50% serum before exposure to 293T cells. GFP expression was analyzed with a plate reader after 48 hours.

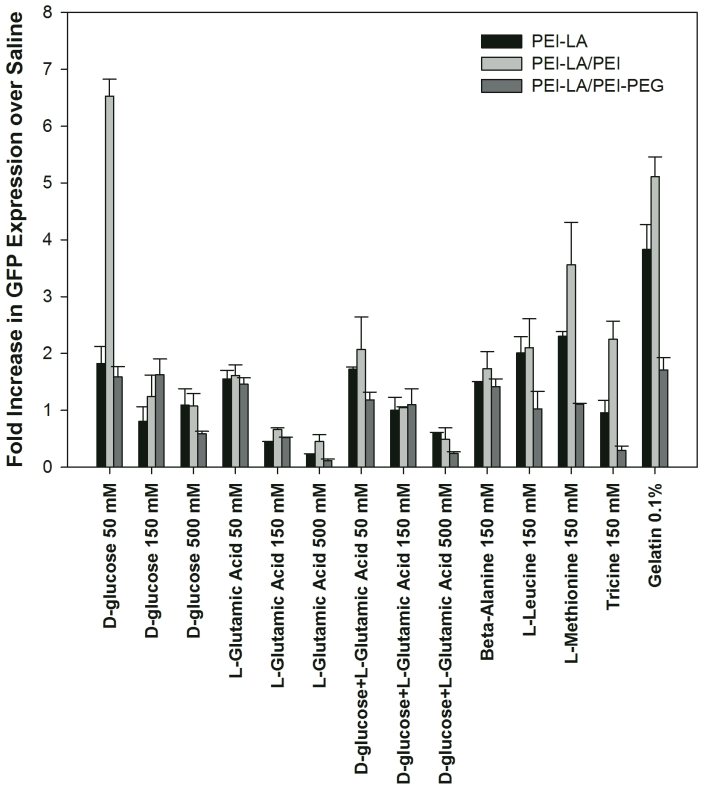

Supplemental 5-3: Screening of various additives to stabilize the complexes. PEI-LA, PEI-LA/PEI and PEI-LA/PEI-PEG complexes were prepared with gWIZ-GFP in saline and incubated at 37 °C for 8 hours in various additives (dissolved at indicated concentrations in water). GFP expression in 293T cells was measured with a plate reader 48 hours after complex exposure, and normalized to complexes incubated in saline without any additive.

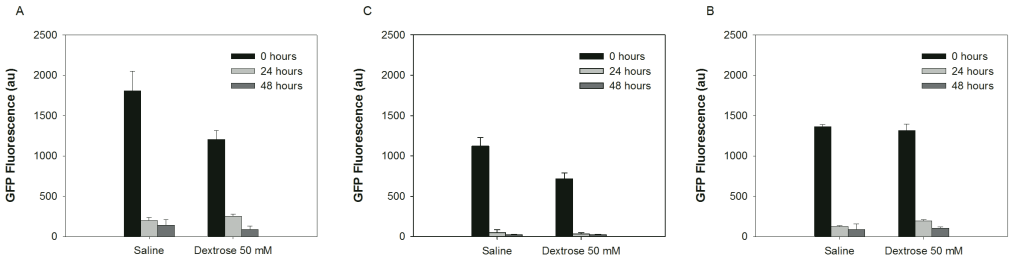

Supplemental 5-4: Transfection with complexes incubated in dextrose. PEI-LA (**A**), PEI-LA/PEI (**B**), or PEI-LA/PEI-PEG (**C**) complexes were incubated in either saline or 50 mM dextrose for 0, 24 and 48 hours at 37 °C. GFP expression was analyzed with flow cytometry and the results were summarized as mean GFP fluorescence of the cell population.

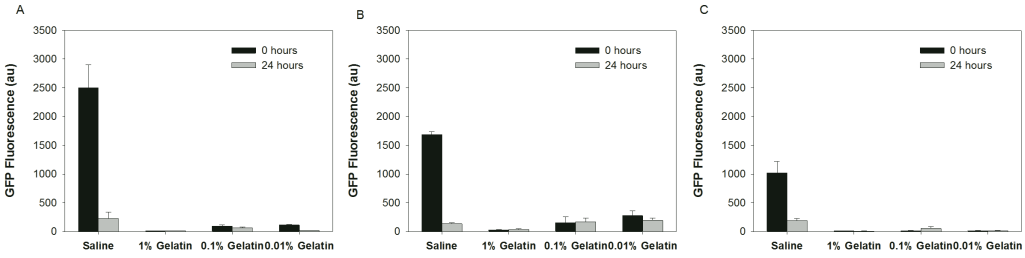

Supplemental 5-5: Transfection with complexes made in gelatin. PEI-LA (**A**), PEI-LA/PEI (**B**), or PEI-LA/PEI-PEG (**C**) complexes were prepared in saline with the indicated concentrations of gelatin (0.01-1%). After a 0 or 24-hour incubation, cells were transfected. GFP expression was analyzed with flow cytometry. The results were summarized as the mean GFP-fluorescence of cell population.

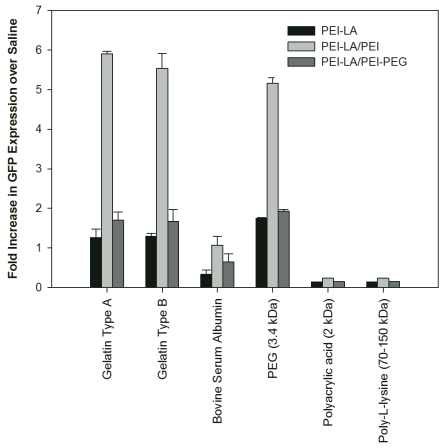

Supplemental 5-6: Screening of various additives to stabilize the complexes. PEI-LA, PEI-LA/PEI and PEI-LA/PEI-PEG complexes were prepared with gWIZ-GFP in saline and incubated at 37 °C for 24 hours with polymeric compounds dissolved in at 0.1%. GFP expression in 293T cells was measured with a plate reader 48 hours after complex exposure, and normalized to complexes incubated in saline without any additive.

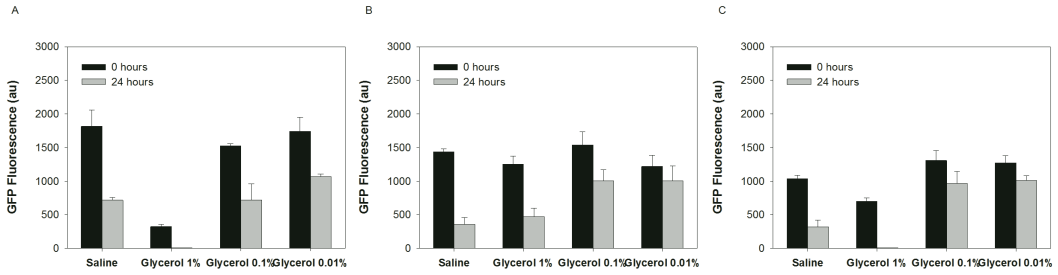

Supplemental 5-7: Complexes incubated in glycerol. PEI-LA (A), PEI-LA/PEI (**B**), or PEI-LA/PEI-PEG (**C**) complexes were incubated at 37 °C in either saline or glycerol (0.01-1%) for 0 or 24 hours before transfection. GFP expression was measured after 48 hours with flow cytometry, which is summarized as mean GFP fluorescence of the cell population.

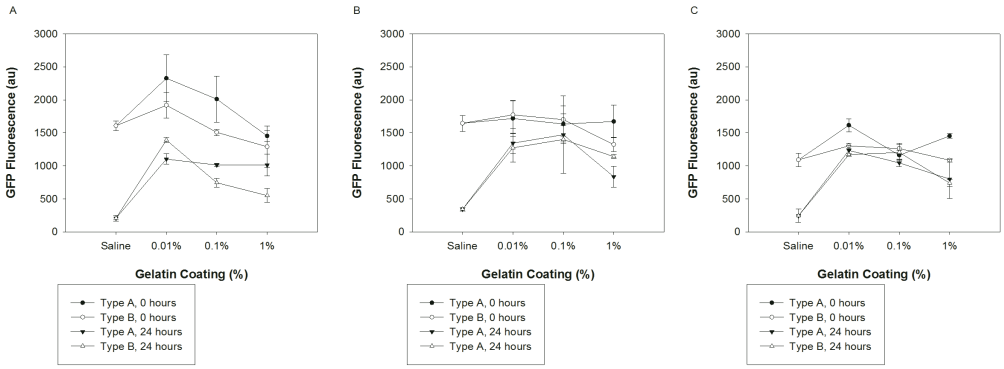

Supplemental 5-8: Comparison of Type A and Type B Gelatin. PEI-LA (**A**), PEI-LA/PEI (**B**), or PEI-LA/PEI-PEG (**C**) complexes were incubated in Type A or Type B gelatin (0.01-1%) or saline for 0 or 24 hours. GFP expression was analyzed with flow cytometry and results were summarized as mean GFP-fluorescence of the cell population.

10 Appendix C

SUPPLEMENTARY INFORMATION

For

PHARMACOKINETICS AND TRANSGENE EXPRESSION BY POLYETHYLENIMINE-BASED PDNA COMPLEXES AFTER *IN VIVO* GENE DELIVERY

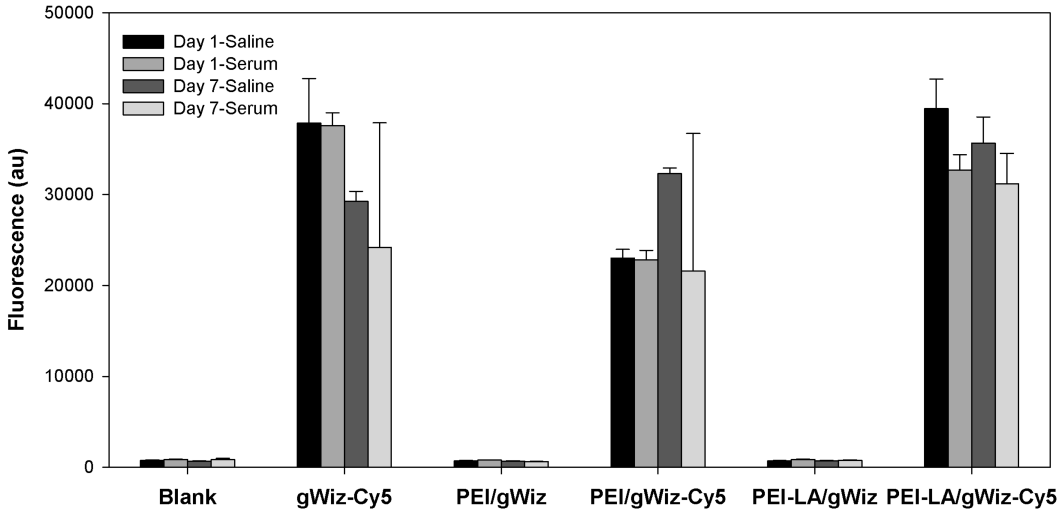

Supplemental 6- 1: Changes in mean Cy5 fluorescence over time *in vitro*. Sponges were loaded with saline (blank sponges), naked gWiz-Cy5, and PEI and PEI-LA complexes of gWiz or gWiz-Cy5, and incubated at 37 °C in either saline or full serum. The Cy5 fluorescence in sponges was imaged after 1 or 7 days and expressed as mean + SD.

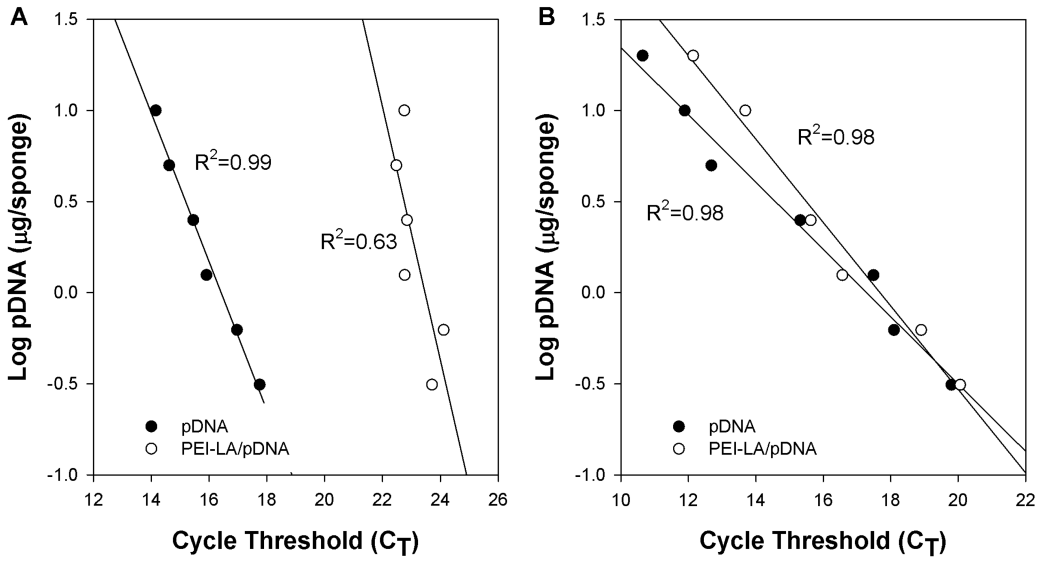

Supplemental 6-2: Comparison of pDNA extraction methods. Sponges were loaded with pDNA (pCAG-dsRED) alone or pDNA bound to PEI-LA at a range of concentrations to give standard curves. pDNA was extracted from the sponges using either a column-based commercial kit (**A**) or a protocol using poly-acrylic acid to dissociate the complexes (**B**). The qPCR was run similarly in both protocols.

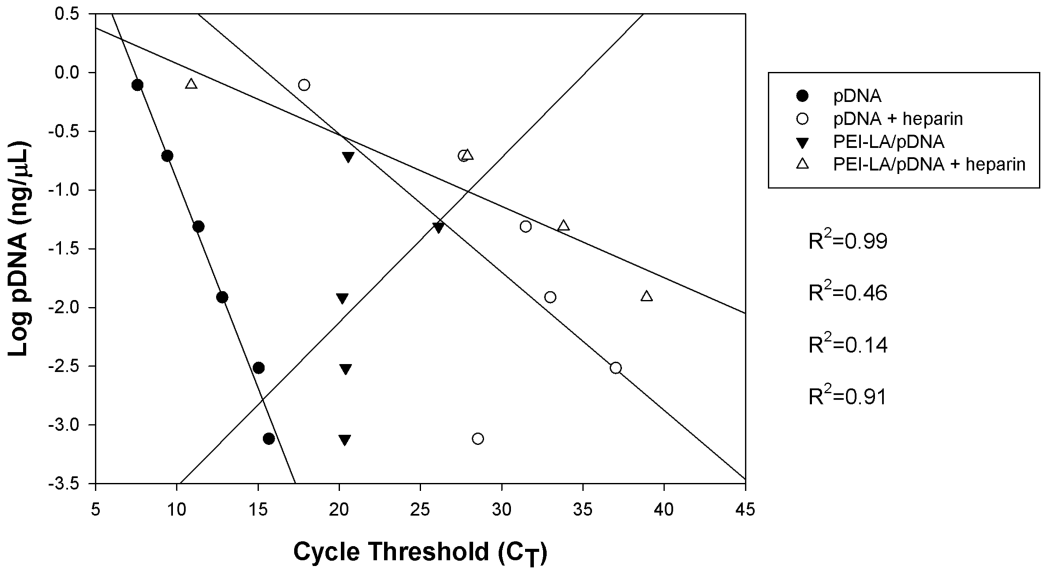

Supplemental 6- 3: qPCR of heparin-dissociated complexes. pDNA (pCAG-dsRED) with or without PEI-LA was incubated with or without heparin to dissociate the pDNA from the PEI-LA. The qPCR was then run to determine the C_T for each preparation.

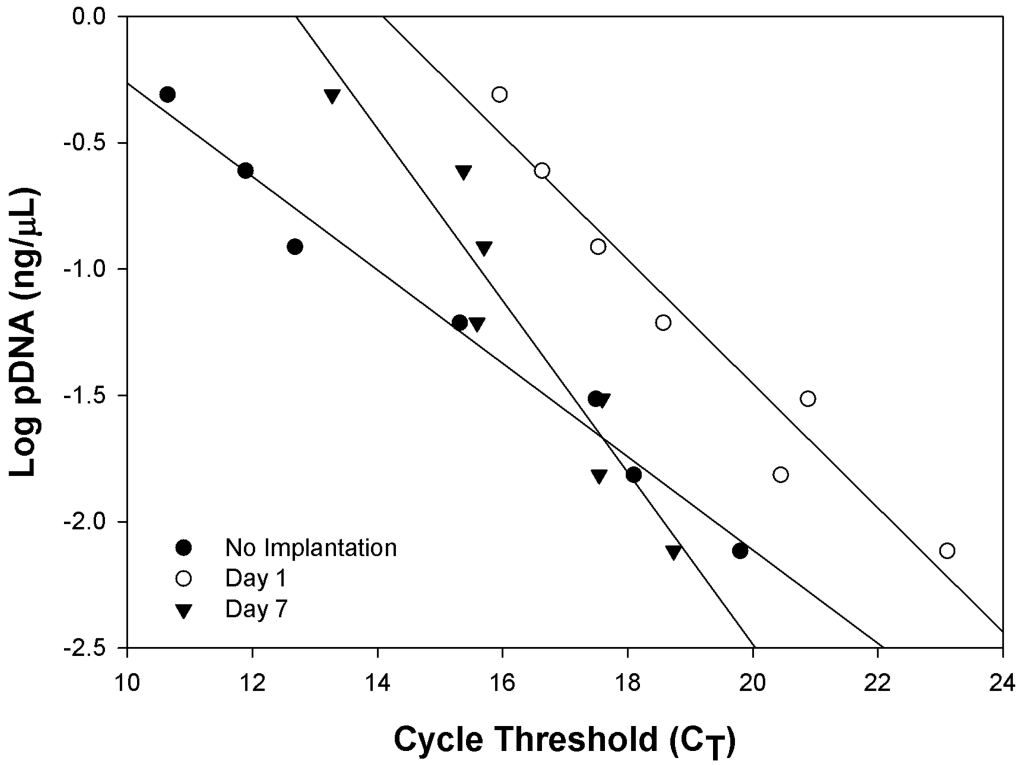

Supplemental 6-4: qPCR standard curves as a function of explant time point. Naked pDNA (pCAG-dsRED) was soaked onto sponges that were either not implanted, or onto homogenates of blank sponges that were implanted for 1 and 7 days.

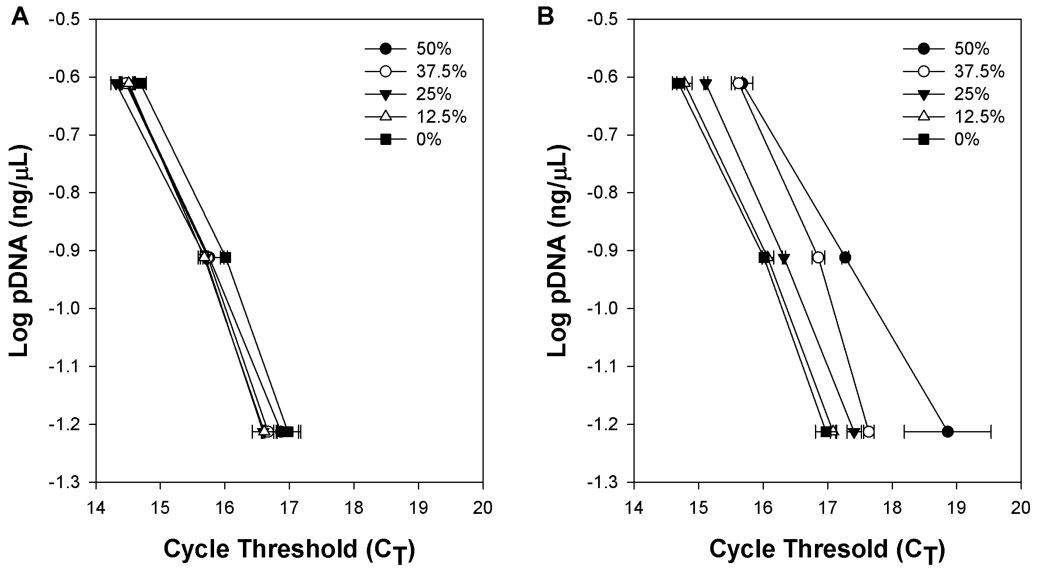

Supplemental 6-5: Blood spiked qPCR analysis. Standard curves of naked pCAG-DsReRED were spiked with varying amounts of blood components (0 to 50% by volume). An equal amount of either rat serum (**A**) or rat blood clot (**B**) was extracted, diluted, and then added to the pDNA standard curve. Addition of extraction buffer alone (0% sample) served as the reference.

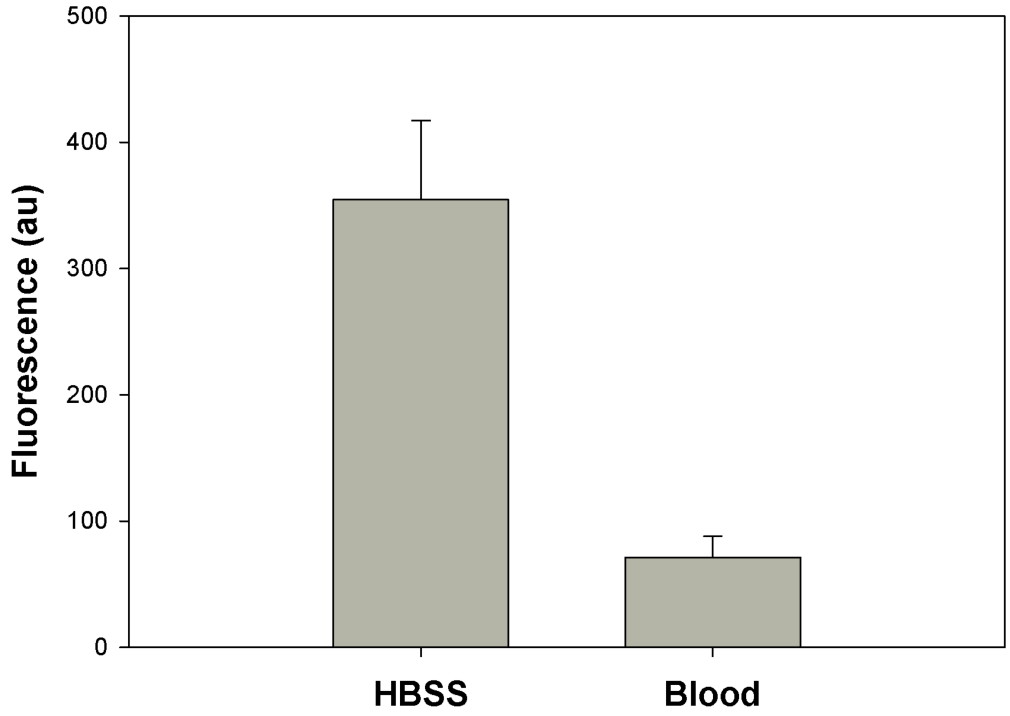

Supplemental 6-6: Imaging DsRed fluorescence with blood. 293T cells expressing DsRed were trypsinized and then diluted with either HBSS or rat blood before being added to sponges. The DsRed fluorescence signal was measured from the sponges and normalized to a sample of HBSS-soaked sponge alone.

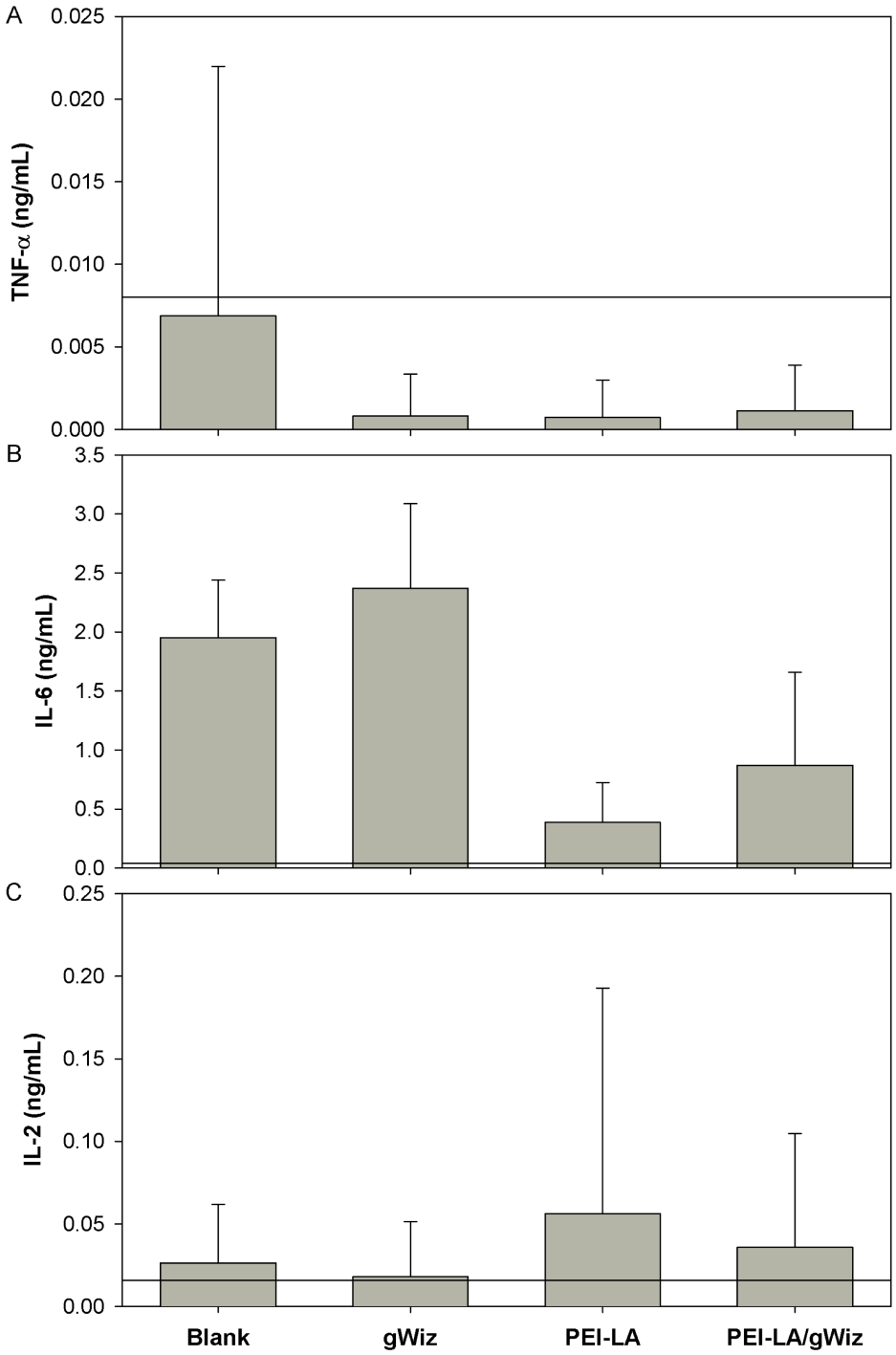

Supplemental 6-7: Levels of cytokines TNF-α, IL-6 and IL-2 in implanted sponges. Sponges loaded with saline (blank), gWIZ (25 μg), PEI-LA (125 μg) and PEI-LA/gWIZ complexes (25/125 μg) were implanted subcutaneously

for 10 days and then harvested and cultured in cell culture media for 5 days. The supernatant was collected and assessed for tumor necrosis factor-α (**A**), interleukin-6 (**B**), and interleukin-2 (**C**) levels by commercially avalaible ELISA kits (R&D Systems).

11 Appendix D

DELIVERY OF POLYMER/PDNA COMPLEXES TO A RAT SKULL DEFECT FOR BONE REGENTATION[1]

11.1 INTRODUCTION

Gene delivery has been investigated for bone regeneration using both viral [4, 6] and non-viral carriers [3, 8], but viral carriers show attenuated or abolished bone regeneration [19]. Although very high doses of plasmid DNA (pDNA) resulted in bone formation [3], we have previously shown that naked plasmid DNA delivered *in vivo* is quickly destroyed and that no transgene is expressed [12]. Various carriers have been employed to deliver pDNA for bone formation, including high molecular weight (25 kDa) polyethylenimine (PEI) [7], but we have found that this carrier does not lead to transgene expression *in vivo* [11]. We have recently demonstrated that low molecular weight PEI (2 kDa) modified with linoleic acid (PEI-LA) is an effective carrier *in vivo* [11]. We have also found that pDNA delivered with PEI-LA gave mRNA and transgene expression for up to four weeks. Since bone healing would require weeks of transgene expression [14], we hypothesized that delivery of pDNA with this carrier would provide sufficient transgene expression to

[1] This study was made possible with surgical help of Dr. Ahmed Hussain, Mr. Cezary Kuckarski and Dr. Hasan Uludağ

promote regeneration. Here, we deliver pDNA with PEI-LA to a skull defect to test whether this gene-based therapy is sufficient for bone regeneration in a clinically relevant model.

11.2 MATERIALS & METHODS

11.2.1 Materials

Absorbable gelatin sponges (Gelfoam) was obtained from Pharmacia & Upjohn (Kalamazoo, MI). The 2 kDa polyethylenimine (PEI) was modified with linoleic acid (1.6 LA per PEI2) as previously described [10]. The plasmids used (bFGF-IRES-AcGFP and gWiz-BMP2) were constructed as previously described [5, 17]. Hank's Balanced Salt Solution (HBSS) was from BioWhittaker (Walkersville, MD), and formalin solution was obtained from Sigma (St Louis, MO).

11.2.2 Skull defect and complex implantation

Rats were anesthetized with Ketamine/Xylazine (80 and 8 mg/kg, respectively), and a 5 mm circular defect was made in approximately in the center of the parietal bone. Gelatin sponges, loaded with PEI-LA/pDNA complexes as previously described [12], were implanted into the defect. Control groups with no implant and blank implant (saline alone) were also included. The details of the study are included in Supplemental Table D-1.

After three weeks, the rats were sacrificed, and the skulls harvested for analysis. The skulls were fixed in 3.7% formalin in HBSS.

11.2.3 Analysis of bone density

Skulls were imaged with x-ray and μ-computer tomography (μ-CT) to assess new bone formation. The μ-CT analysis was conducted at the laboratory of Dr. Steven Boyd (U. of Calgary, Calgary, Alberta). For x-rays, the extent of regeneration (%) was calculated with the contral-lateral (no defect) intact side set to 100% bone and the background (i.e. empty defect) set to 0%. A circular region of interest (ROI) was selected to encompass the majority of the defect. Each rat was used as its own control since there were significant variations among the rats for native bone density, as measured by x-ray densitometry. For μ-CT, a threshold of 180 per 1000 was set to segment the image. The ROI was the entire 5 mm defect.

Supplemental Table D-1: Study Groups for Bone Defect Study

No	Description	Rats	PEI-LA	pDNA	w/w
1	No Implant	5	0	0	N/A
2	Saline	5	0	0	N/A
3	PEI-LA/gWiz-BMP2	5	50 μg	10 ug	10/2
4	PEI-LA/bFGF-IRES-AcGFP	5	50 μg	10 ug	10/2
5	PEI-LA/gWiz-BMP2+bFGF-IRES-AcGFP	5	100 μg	10+10 ug	10/2
6	PEI-LA/gWiz	5	50 μg	10 ug	10/2
7	gWiz-BMP2 (No Carrier) *	5	0	10 ug	10/2

*24 μg was implanted instead of 10 μg

11.3 RESULTS

A 5 mm defect was made in the skulls of male rats, and were treated with sponges as described in ***Supplemental Table D-1***. After a three week implantation, the skulls were harvested and fixed in formalin. The skulls were first analyzed with x-ray to measure mineralized tissue regeneration at the defect site (***Supplemental Table D-2, Supplemental Figure D-1***). The baseline regeneration observed in empty defects without sponge was high at 65%. Treatment of the defect with the sponge alone gave regeneration around 82%. The groups with therapeutic pDNA expressing BMP-2, bFGF or a combination of BMP-2 and bFGF delivered either in a PEI-LA complexes or as naked pDNA gave 78-88% regeneration. Sponges delivering PEI-LA containing control pDNA (i.e. that does not express a therapeutic protein) gave 87% regeneration.

The skulls were next analyzed with μ-CT to measure new bone formation in the defect. Defects left untreated or treated with a blank (saline) sponge both gave 2 mm^3 of new bone within the 5 mm defect (considered as background). Rats treated with PEI-LA/pDNA complexes expressing therapeutic proteins gave 0.7-1.0 mm^3 of new bone, whereas rats treated with control complexes and naked pDNA gave 0.8-1.0 mm^3 of new bone. Large SDs observed in μ-CT was an indication of the significant variation in the regenerative capability, even for untreated defects.

A

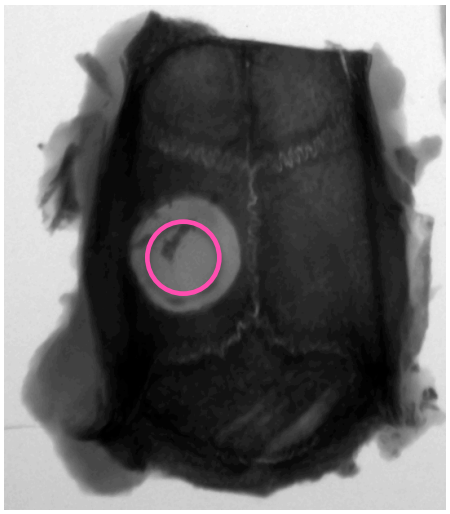

B

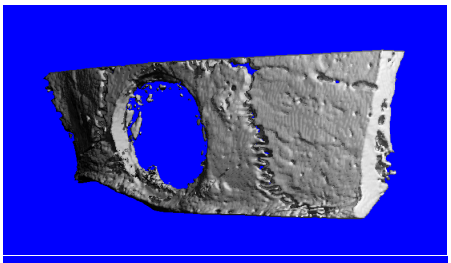

C

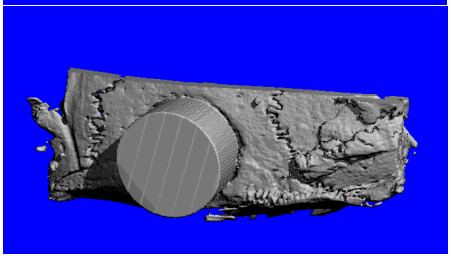

Supplemental Figure D-1: Representative images of skull defect. Sample rat skull with x-ray (**A**) and μ-CT (**B**). Image (**C**) shows the region of interest.

Supplemental Table D-2: Summary of bone analysis

Group	X-Ray (% regeneration)	μ-CT tissue density (mg HA/cm^3)	μ-CT bone volume (mm^3)
1	66.4 ± 14.4	-99.31 ± 19.38	2.07 ± 1.38
2	83.0 ± 5.3	-98.67 ± 14.04	2.02 ±1.63
3	78.2 ± 18.5	-81.56 ± 13.85	0.79 ± 0.30
4	89.3 ± 4.3	-90.70 ± 17.16	1.27 ± 1.73
5	89.8 ± 15.7	-94.10 ± 17.99	0.85 ± 0.55
6	89.5 ± 9.0	-85.02 ± 25.14	1.00 ± 0.52
7	86.1 ± 2.3	-91.68 ± 16.63	1.16 ± 1.19

Supplemental Table D-3: Bone analusis of individual rats

Rat	X-Ray Tissue Density	X-Ray Regeneration (%)	μ-CT tissue density (mg HA/cm^3)	μ-CT bone volume (mm^3)
Group 1				
1	8467.0	78.3	-100.09	3.13
2	9046.4	73.0	-117.58	2.72
3	11723.7	41.4	-111.29	0.87
4	8295.7	70.7	-100.28	3.31
5	8869.4	68.3	-67.32	0.31
Group 2				
6	8226.4	80.0	-112.02	3.62
7	8209.9	86.6	-112.84	1.86
8	7196.0	88.7	-86.53	3.70
9	8505.6	75.6	-99.46	0.08
10	7731.3	84.2	-82.52	0.83

Supplemental Table D-3: Continued				
Group 3				
11	7507.7	86.3	-94.27	0.56
12	9347.2	66.0	-87.98	1.19
13	7535.5	83.4	-58.48	0.42
14	10578.0	54.0	-86.98	0.89
15	5684.0	101.4	-80.06	0.88
Group 4				
16	7336.2	89.4	-116.39	0.01
17	7646.0	85.4	-88.71	4.19
18	7292.8	88.1	-78.79	1.50
19	7296.3	87.0	-97.09	0.35
20	5765.4	96.4	-72.51	0.32
Group 5				
21	6117.3	96.9	-98.82	1.25
22	6892.8	90.5	-94.54	0.05
23	9144.3	62.9	-121.40	0.60
24	5920.2	103.0	-77.70	1.44
25	6394.3	95.7	-78.06	0.91
Group 6				
26	6328.1	86.4	-93.99	1.29
27	7832.4	81.3	-89.81	0.37
28	7743.4	81.4	-108.20	1.50
29	6075.7	97.8	-91.08	0.50
30	6407.0	100.2	-42.00	1.33
Group 7				
31	7270.1	88.4	-71.41	3.17
32	7571.4	85.7	-83.71	0.33
33	7243.6	88.2	-88.35	1.32
34	7798.6	85.5	-115.30	0.66
35	7593.1	82.8	-99.64	0.33

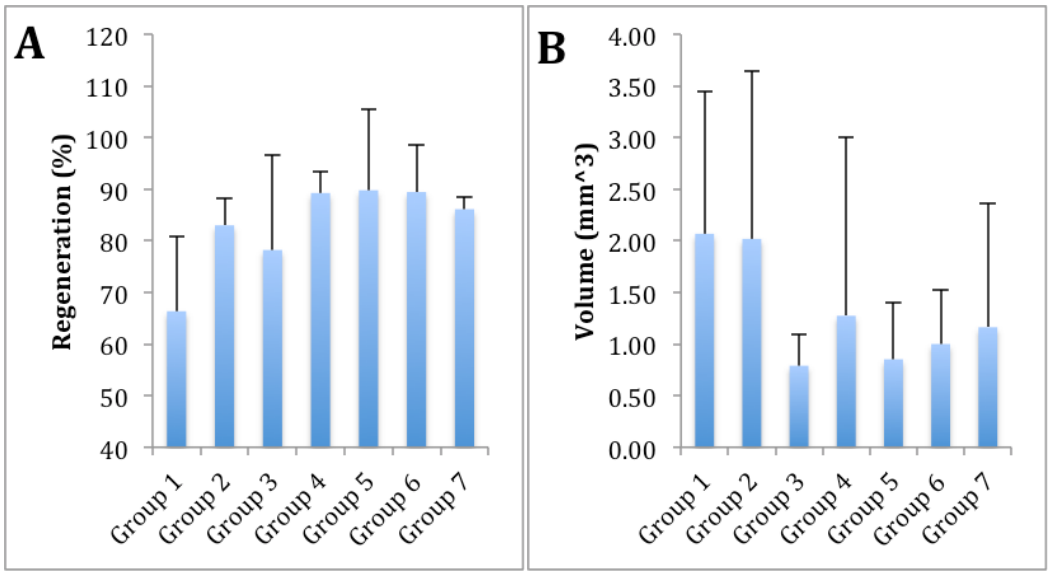

Supplemental Figure D-2: Bone regeneration after gene delivery. Skulls were analyzed with x-rays to measure tissue regneraion in the defect (**A**) and with μ-CT to measure the volume of new bone in the defect (**B**).

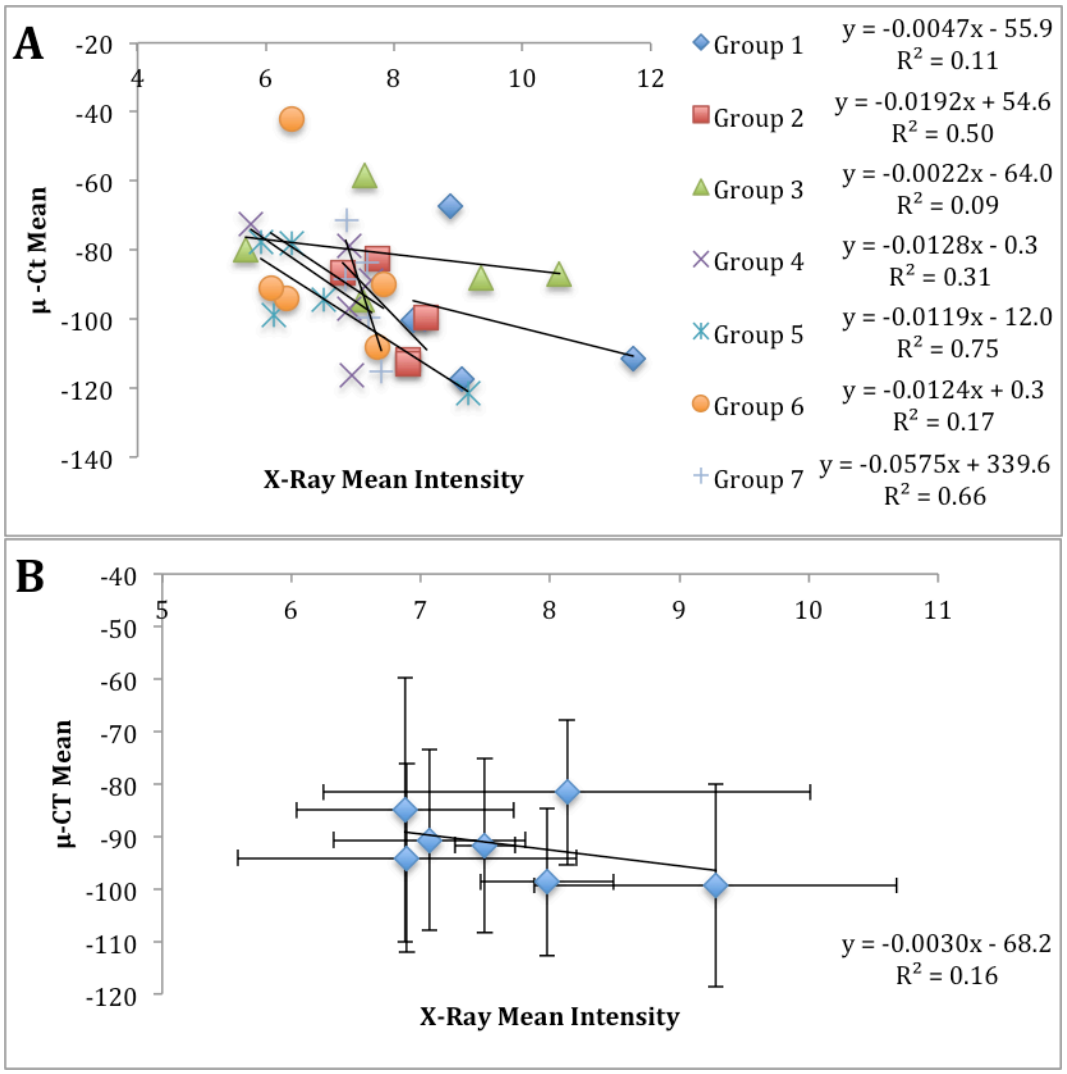

Supplemental Figure D-3: Correlation between mean intensities obtained by µ-CT and x-ray densitometry. Correlation for individual implants is shown for individual rats in each group (**A**) and the group averages (**B**).

11.4 DISCUSSION

Therapeutic pDNA expressing bFGF or BMP-2 proteins were delivered to a skull defect to test the efficacy of PEI-LA gene delivery system. No effect, however, as measured by mineralized tissure regeneration or bone volume was observed as compared to control groups with no implant, a blank (saline) implant or an implant with control complexes that expressed no therapeutic protein. This was surprising, since in Chapter 6 mRNA expression was previously found to begin 24 hours of implantation at a subcutaneous site and continued beyond the time point when these rats were sacrificed. Furthermore, the rate of protein expression observed with PEI-LA was found to be similar to virus-based delivery systems that resulted in bone regeneration [2, 15]. The lower dose employed in this study at 10 μg compared to 20 μg [13] and 25 μg [11] in previous studies may partially explain the lack of regeneration, but we have found similar kinetics for the lower 5 μg dose and the higher 20 μg dose at subcutaneous sites.

One feature of this specific animal model that may be responsible for the lack of effect is that the control groups show robust regeneration. This may indicate that the defect is not large enough to be considered a critical size, which is generally considered to be 8 mm for rat calvarial defects [16]. With our 5 mm defect, it is possible that complete and spontaneous healing may be observed without external influence. In that case, the animal model is suitable to measure acceleration of bone healing and not necessarily

assurance of healing. A similar gene delivery studies using a rat model employed 9 mm [7] and showed no new bone growth after 15 weeks when a blank scaffold was inserted. In contrast, we observed that empty defects showed 60% regeneration and 80% regeneration when a blank scaffold was implanted into the defect after three weeks. In our current model, it therefore may be difficult to show a therapeutic effect where a vigorous response is already observed. A more suitable animal model may better assess the potential of our gene delivery system.

11.5 REFERENCES

1. Alden T, Pittman D, Hank ins F, Beres E, Engh J, Das S, Hudson S, Kerns K, Kallmes D, Helm G. In vivo endochondral bone formation using a bone morphogenetic protein 2 adenoviral vector. Hum Gene Ther 1999;10(13):2245-53.
2. Betz O, Betz V, Abdulazim A, Penzkofer R, Schmitt B, Schroder C, et al. The repair of critical-sized bone defects using expedited autologous BMP-2 gene activated fat implants. Tiss Eng Part A 2010;16:1093-1101.
3. Bonadio J, Smiley E, Patil P, Goldstein S. Localized, direct plasmid gene delivery in vivo: prolonged therapy results in reproducible tissue regeneration. Nature Medicine 1999;5(7):753-759.
4. Chen Y, Luk K, Cheung K, Xu R, Lin M, Lu W, Leong J, Kung H. Gene therapy for new bone formation using adeno-associated viral bone morphogenetic protein-2 vectors. Gene Therapy 2003;10:1345-1353.
5. Clement B, Hsu C, Kucharski C, Lin X, Rose L, Uludag H. Nonviral delivery of basic fibroblast growth factor gene to bone marrow stromal cells. Clin Orthop Relat Res 2009;467(12):1329-37.

6. Hu WW, Wang Z, Hollister SJ, Krebsbach PH. Localized viral vector delivery to enhance in situ regenerative gene therapy. Gene Ther 2007;14(11):891-901.
7. Huang YC, Simmons C, Kaigler D, Rice KG, Mooney DJ. Bone regeneration in a rat cranial defect with delivery of PEI-condensed plasmid DNA encoding for bone morphogenetic protein-4 (BMP-4). Gene Therapy 2005; 12:418.
8. Itaka K, Ohba S, Miyata K, Kawaguchi H, Nakamura K, Takato T, Chung U, Kataoka K. Bone regeneration by regulated in vivo gene transfer using biocompatible polyplex nanomicelles. Molecular Therapy 2007;15(9):1655.
9. Kang Q, Sun M, Cheng H, Peng Y, Montag A, Deyrup A, Jiang W, Luu H, Luo J, Szatkowski J, Vanichakarn P, Park J, Li Y, Haydon R, He T. Characterization of the distinct orthotopic bone forming activity of 14 BMPs using recombinant adenovirus-mediated gene delivery. Gene Ther 2004;11(17):1312-20.
10. Neamnark A, Suwantong O, Bahadur R, Hsu C, Supaphol P, Uludag H. Aliphatic lipid substitution on 2 kDa polyethylenimine improves plasmid delivery and transgene expression. Mol Pharm 2009;6(6):1798-815.
11. Rose LC, Kucharski C, Uludag H. Protein expression following non-viral delivery of plasmid DNA for basic FGF and BMP-2 in a rat ectopic model. Biomaterials 2012;33(11):3363-74.
12. Rose L, Aliabadi HM, Uludag H. Gelatin coating to stabilize the transfection ability of nucleic acid polyplexes. Acta Biomater 2013;9(7):7429-38.
13. Rose L, Mahdipoor P, Kucharski C, Uludag H. Pharmacokinetics and transgene expression of implanted polyethylenimine-based pDNA complexes. Submitted to Biomaterials Science, August 23 2013. BM-ART-08-2013-060200.

14. Rose L, Uludag H. Realizing the potential of gene-based molecular therapies in bone repair. J Bon Miner Res. E-published on April 2, 2013.
15. Rundle C, Miyakoshi N, Kasukawa Y, Chen S, Sheng M, Wergedal J, Lau K, Baylink D. In vivo bone formation in fracture repair induced by direct retroviral-based gene therapy with bone morphogenetic protein-4. Bone 2003;32(6):591-601.
16. Spicer PP, Kretlow JD, Young S, Jansen JA, Kasper FK, Mikos AG. Evaluation of bone regeneration using the rat critical size calvarial defect. Nat Protoc 2012;7(10):1918-29.
17. Wang Y, Mostafa NZ, Hsu CY, Rose L, Kucharski C, Yan J, Jiang H, Uludag H. Modification of human BMSC with nanoparticles of polymeric biomaterials and plasmid DNA for BMP-2 secretion. J Surg Res 2013;183(1):8-17.

12 Appendix E

IDENTIFICATION AND KNOCKDOWN OF KINASE TARGETS WITH SIRNA FOR IMPROVED PDNA TRANSFECTION IN CORD BLOOD CELLS[2]

12.1 INTRODUCTION

Delivery of plasmid DNA to primary cells is tightly controlled, and as a result transfection efficiency in primary cells is generally lower compared to cell lines [1, 5]. Despite this, genetic manipulation of primary cell is desirable due to their clinical utility. To this end, improving gene delivery to clinically relevant primary cells remains an active area of investigation. Although viral vectors can be more efficient, the undesirable effects associated with such delivery may impede their clinical use [3]. Non-viral methods such as synthetic carriers and physical delivery methods have therefore been investigated as means to yield high efficiency gene transfer. A small molecule inhibitor has previously been found to increase transfection of a cell line in a carrier-dependent manner [4]. Since it remains unclear which kinases are responsible to interfering with transfection, we set out to identify kinases whose knockdown increases transfection or transgene expression. From lead candidates, we chose three kinases for further study.

---

[2] This study was made possible with cell culture and kinase screening help from Mr. Robert Maranchuk, Mr. Cezary Kucharski, and Dr. Hasan Uludag.

12.2 MATERIALS AND METHODS

12.2.1 MATERIALS

Trypsin-EDTA, DMEM, fetal bovine serum (FBS), and penicillin/streptomycin (P/S) were purchased from Life Technologies (formerly Invitrogen; Grand Island, NY). Hank's Balanced Salt Solution (HBSS) was from BioWhittaker (Walkersville, MD) and formalin solution was obtained from Sigma (St Louis, MO). The Silencer Human Kinase siRNA Library and FAM-labelled scrambled siRNA was obtained from Ambion. The gWiz and gWiz-GFP plasmids were obtained from Aldevron (Fargo, ND). The fluorescence maker Cy3 was used to label the gWiz pDNA using the Label-It Tracker kit from Mirus (Piscataway, NJ). Polyethylenimine 2 kDa modified with linoleic acid (PEI-LA) was modified as previously described [2].

12.2.2 KINASE SCREEN

The Ambion Silencer Human Kinase siRNA Library was used to screen kinases whose knockdown was beneficial for transfection or transgene expression. Cord blood MSC were seeded in 96-well plates in 100 uL of media. The day after seeding, cells were transfected with either siRNA from the kinase library or scrambled (non-silencing control) siRNA. The weight ratio of PEI-LA to siRNA was 2:1 and the final concentration was 72 nM. The day after knockdown, cells were transfected with gWiz-GFP pDNA. The

weight ratio of PEI-LA to plasmid DNA was 10:2 with a final pDNA concentration of 2 μg per mL of media. Three days after the pDNA transfection, cells were washed with HBSS, detached with 0.05% trypsin-EDTA, and fixed in 3.7% formalin in HBSS. The mean fluorescence of cells was analysed with a Beckman Coulter Cell Lab Quanta SC flow cytometer. Each transfection was performed in triplicate. Target kinases were categorized as soft hits, potential hits, or hard hits. Soft hits were kinases that have a positive t-test or z-score, whereas solid hits were kinases that were positive for both statistical tests. Potential hits were kinases where one sample was lost during flow cytometry, and therefore gave a positive z-score but the lack of sufficient replicated gave a t-test inadequate to be considered a solid hit.

12.2.3 SIRNA AND PDNA CO-DELIVERY AND KINASE VALIDATION

Binding of siRNA and pDNA to PEI-LA was investigated with an electropheric mobility shift assay (EMSA), where PEI-LA was added to a mixture of siRNA and pDNA with weight ratios of PEI-LA:nucleic acid of 0:1 to 1:1. The complexes were run on a gel containing ethidium bromide. The amount of free nucleic acid remaining was used to calculate the binding to polymer. These complexes were also tested in 293T cells to ensure that both the pDNA and siRNA were as functional in the combination complexes as individual pDNA and siRNA complexes. The 293T cells were transfected with GFP, along with either control siRNA or siRNA against the GFP. The three hits

from the kinase screen were selected for further validation in 24-well plates using the combination siRNA/pDNA complexes at the doses described in the figures. The cells were harvested at Day 3 and 6 for GFP fluorescence. Cells were analyzed with flow cytometry.

12.3 RESULTS

Cord blood cells were screened to determine which siRNA against kinases resulted in higher GFP fluorescence. Hits from the screens were classified as either soft hits or hard hits, depending on whether they were positive with one or both z-score and t-test statistical tests. Of the 719 kinases tested, 53 potential hits were identified with 35 were positive for the t-test and 18 were positive for the z-score (***Table SE-1, Supplemental Figure E-1***). Six kinases were deemed potential hits because a sample was lost during flow cytometry such that the t-test did not give a positive result even though the z-score did. Four kinases led to increased transfection by both the t-test and z-scorewere identified as hard hits (***Table SE-2***). Although positive, one of these hard hit kinases (nuclear receptor binding protein (NRBP); Gene ID 29959) had a z-score (2.23) lower than the other three hard hits (2.96-3.14). This indicated that although an increase was observed, the effect size was small and so this hit was not taken for further evaluation. The three hard hits identified were activin A receptor type II-like 1 (ACVRL1; Gene ID 94), LOC391295 (locus with an unnamed gene product; Gene ID 391295), and

phosphatidylinositol-4-phosphate 5-kinase, type II α (PIP4K2A, also known as PIP5K2A; Gene ID 5305).

Soft Hits: T-test			
No	Name	z-score	t-test
1	mitogen-activated protein kinase kinase kinase 9	1.85	5.55
2	polo-like kinase 3 (Drosophila)	0.74	3.16
3	protein kinase C, epsilon	0.18	3.38
4	serum/glucocorticoid regulated kinase 2	0.74	4.31
5	mitogen-activated protein kinase 13	0.57	5.23
6	spleen tyrosine kinase	0.59	4.92
7	glutamate receptor interacting protein 2	1.18	8.53
8	integrin beta 1 binding protein 3	0.68	5.30
9	ribosomal protein S6 kinase, 90kDa, polypeptide 6	1.17	7.87
10	DKFZp434B1231	0.28	2.91
11	plexin B2	0.51	3.09
12	TNNI3 interacting kinase	0.71	3.56
13	serine/threonine kinase 40	0.56	5.00
14	riboflavin kinase	0.05	4.04
15	LOC91807	0.48	4.82
16	calcium/calmodulin-dependent protein kinase II inhibitor 1	0.38	3.03
17	protein kinase C, delta binding protein	0.62	3.49
18	membrane protein, palmitoylated 6 (MAGUK p55 subfamily member 6)	0.34	3.23
19	BMP2 inducible kinase-like	0.86	7.12
20	nuclear receptor binding protein 2	0.43	4.49
21	membrane associated guanylate kinase interacting protein-like 1	0.62	5.05
22	NIMA (never in mitosis gene a)-related kinase 5	1.22	3.68
23	membrane associated guanylate kinase, WW and PDZ domain containing 3	0.41	6.04
24	adenylate kinase 3 like 1	1.53	4.64
25	PI4K2B	1.45	4.20
26	eukaryotic translation initiation factor 2-alpha kinase 3	0.21	4.46
27	mitogen-activated protein kinase kinase 3	0.26	3.05
28	3-phosphoinositide dependent protein kinase-1	0.40	3.21
29	ribosomal protein S6 kinase, 70kDa, polypeptide 1	1.76	5.84
30	inositol 1,4,5-trisphosphate 3-kinase B	1.18	4.07
31	adenylate kinase 3	1.73	4.51
32	MAP/microtubule affinity-regulating kinase 1	0.97	4.03
33	eukaryotic translation initiation factor 2-alpha kinase 1	1.52	3.09
34	ribosomal protein S6 kinase, 90kDa, polypeptide 3	1.96	2.98
35	ribosomal protein S6 kinase, 90kDa, polypeptide 3	1.90	4.09
Soft Hits: Z-Score			
36	neurotrophic tyrosine kinase, receptor, type 2	3.58	2.05
37	membrane protein, palmitoylated 2 (MAGUK p55 subfamily member 2)	3.10	1.30
38	feline sarcoma oncogene	2.23	1.89
39	fibroblast growth factor receptor 3 (achondroplasia, thanatophoric dwarfism)	2.65	1.95
40	mitogen-activated protein kinase kinase 1 interacting protein 1	2.27	1.71

41	LATS, large tumor suppressor, homolog 1 (Drosophila)	3.44	1.43
42	tyrosine kinase with immunoglobulin-like and EGF-like domains 1	2.62	1.10
43	zinc finger, C3HC type 1	3.74	1.40
44	inositol 1,4,5-trisphosphate 3-kinase A	2.54	2.61
45	protein kinase D3	2.78	2.12
46	v-yes-1 Yamaguchi sarcoma viral oncogene homolog 1	2.26	2.24
47	CDC42 binding protein kinase alpha (DMPK-like)	2.65	0.69
48	carbohydrate kinase-like	4.39	1.15
49	ZAK	2.96	1.79
50	cell division cycle 2, G1 to S and G2 to M	2.05	1.58
51	mitogen-activated protein kinase kinase 1	2.18	1.82
52	v-akt murine thymoma viral oncogene homolog 2	2.08	0.65
53	OSRF	2.14	1.11
Potential Hits			
54	protein kinase, cGMP-dependent, type I	4.82	1.26
55	interleukin-1 receptor-associated kinase 3	2.125	1.65
56	KIAA1639	2.81	1.26
57	myosin light chain kinase 2, skeletal muscle	3.17	1.35
58	serine/threonine kinase 32A	2.76	1.44
59	serine/threonine kinase 19	2.27	0.78

Supplemental Table E-1: Soft and potential hits from kinase screen.

No	Name	z-score	t-test
1	Activin A receptor type II-like 1	3.07	3.00
2	LOC391295	3.13	4.29
3	Phosphatidylinositol-4-phosphate 5-kinase, type II, alpha	2.96	4.78
4*	Nuclear receptor binding protein	2.23	4.78

Supplemental Table E-2: Hits from kinase screen. * not further evaluated)

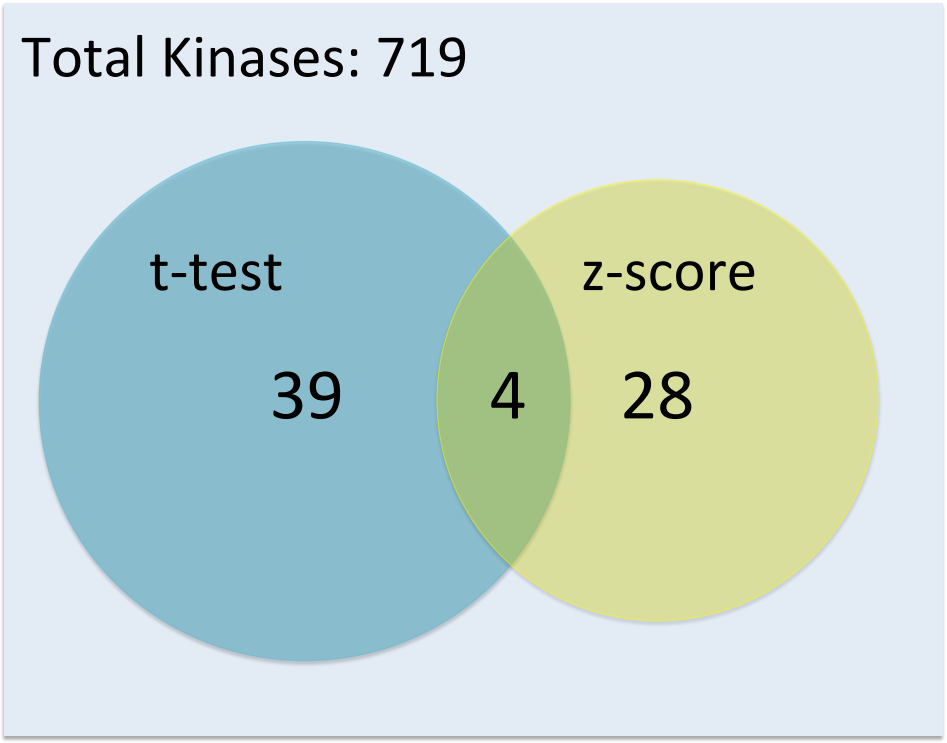

Supplemental E-1: Hits from kinase screen with t-test and z-score. Figure shows the proportion of hits based on the t-test or z-score.

Since only cells receiving the pDNA would need to have the target kinase knocked down, a combination PEI-LA complex containing both the pDNA and siRNA was formed. Complete binding of both the siRNA and pDNA was obtained by a weight ratio of PEI-LA to nucleic acid of 1:1 (***Supplemental E-2A***). To test the function of siRNA and pDNA in these combination complexes were used to transfect 293-T cells. The pDNA expressed GFP, while the siRNA was either a scrambled control or against the GFP (***Supplemental E-2B***). As expected, transfection with the GFP plasmid alone led to high levels of fluorescence. Addition of control siRNA, either as a separate siRNA complex or in a combination complex, led to no change in GFP fluorescence. The siRNA against GFP, however, led to a decrease in fluorescence, with equal knockdown performance observed with the individual and combination complexes. The combination complexes were therefore employed for the validation study.

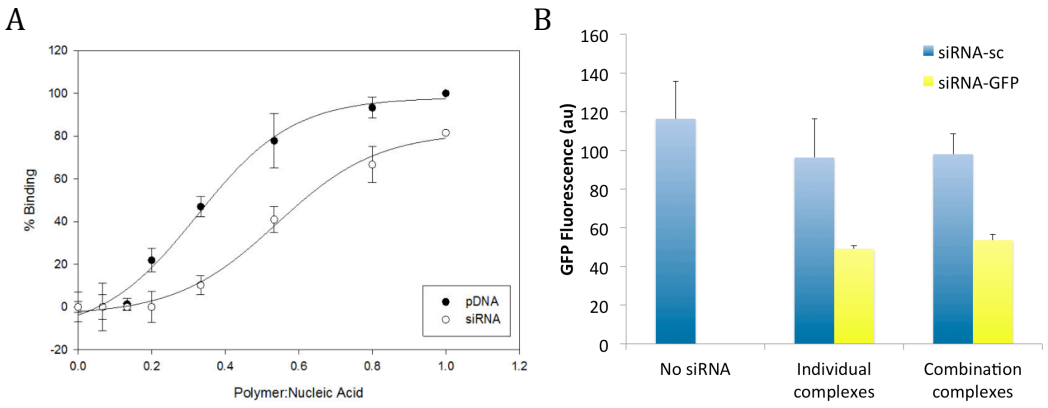

Supplemental E-2: Formation of combination siRNA/pDNA complexes. The binding of siRNA and pDNA to PEI-LA was investigated with an EMSA (**A**). The function of the siRNA and pDNA of combination complexes was compared against individual siRNA and pDNA complexes in 293T cells transfected with a GFP plasmid and either control siRNA or siRNA against GFP (**B**).

Next, the siRNA against the three hits ACVRL1, LOC391295, or PIP4K2A were tested for their abibility to increase GFP output in cord blood cells. Cells were transfected with GFP pDNA and either scrambled control siRNA or siRNA against one of the three hits (***Supplemental E-3***). An increase in GFP fluorescence compared to cells treated with the control gWiz plasmid was observed for the 2.0 and 1.0 μg/mL pDNA doses, with only neglible transfection observed for the 0.5 μg/mL. Cells treated with the kinase siRNA led to increased GFP fluorescence ($p<0.05$-0.01) only for the highest 72 nM dose. At the lower 36 and 18 nM siRNA dose, the kinase siRNAs gave GFP

fluorescence comparable to GFP pDNA delivered with control siRNA. By Day 6, GFP fluorescence was no longer detected (data not shown).

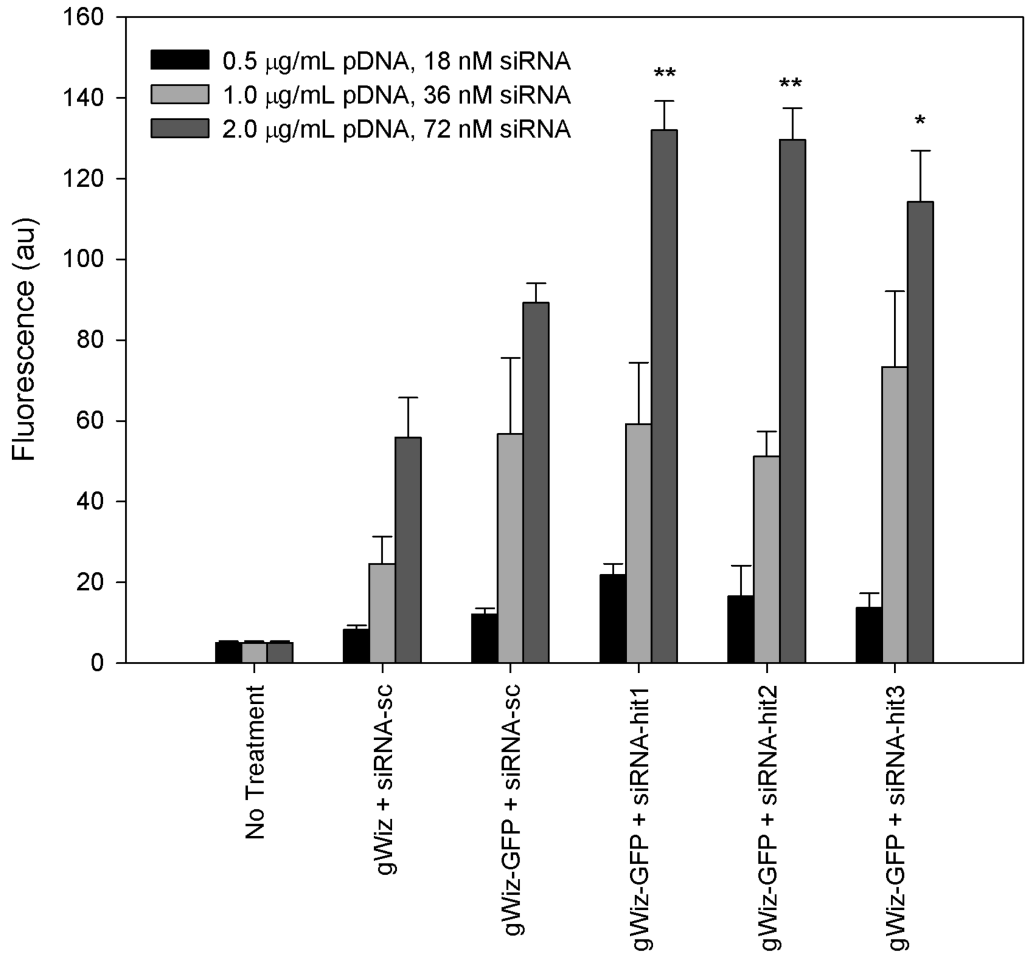

Supplemental E-3 Validation of selected hits from kinase screen. Cells were transfected with complexes containing pDNA and siRNA, with DNA expressing GFP and siRNA against a hit from the kinase screen or non-silencing control siRNA. The GFP fluorescence of cells was measured with flow cyotmetry thee days after transfection. *$p<0.05$, **$p<0.01$ against gWiz-GFP+siRNA-sc.

12.4 DISCUSSION

The transfection efficiency of primary cells remains low (<20%) despite their clinical utility. We aimed to screen primary cord blood cells with siRNA against kinases to find targets to improve transfection. Our goal was to begin with cord blood cells and then test the lead candidates in other cell types to find multi-purpose kinases that could be employed for several different cells. The cord blood cells were chosen for these initial studies because of their growth and baseline transfection. Cord blood cells grow rapidly in culture, enabling us to obtain 4 × 75 cm^2 flasks of low passage (P4-6) required to seed the 27 96-well plates. These cells also show sufficient control transfection rate to allow dose-dependent detection of GFP, allowing us to see increases in transfection. With the cord blood cells, three lead kinases were validated for their ability to increase GFP fluorescence. After this initial success, subsequent attempts to understand the mechanism of increased transfection were impeded by the stability of the cord blood cells. In other transfections, no baseline GFP expression was detected, and the presence of the kinase siRNA had no beneficial effect (data not shown). The reasons for the instability remain unclear. The top three kinases were also tested in the immortalized 293T human cell line and human bone marrow stromal cells, but no beneficial effect was found (data not shown). Although tests in cell types are limited, it is possible that the three top hits were specific to cord blood cells. The screen, however, did identify several soft hits that would likely be beneficial across a broad spectrum of cell types. Six

ribosomal and translation factors were soft hits, with positive t-test scores. Although the effect size (i.e. the increase in fluorescence) may be limited, the benefit to these kinases is their utility in multiple cell types. Cummutavely, these studies provide methodology on co-delivery of siRNA and pDNA to enable screens of transfection inhibitors.

12.5 REFERENCES

1. Clements BA, Hsu CY, Kucharski C, Lin X, Rose L, Uludag H. Nonviral delivery of basic fibroblast growth factor gene to bone marrow stromal cells. Clin Orthop Relat Res 2009;467(12):3129-37.
2. Neamnark A, Suwantong O, Bahadur R, Hsu C, Supaphol P, Uludag H. Aliphatic lipid substitution on 2 kDa polyethylenimine improves plasmid delivery and transgene expression. Mol Pharm 2009;6(6):1798-815.
3. Trobridge G. Genotoxicity of retroviral hemaotopoietic stem cell gene therapy. Expert Opin Biol Ther 2011;11(5):581-93.
4. Ur Rehman Z, Hoekstra D, Zuhorn IS. Protein kinase A inhibition modulates the intracelluluar routing of gene delivery vehicles in HeLa cells, leading to productive transfection. J Control Release 2011;156(1):76-84.
5. Wang Y, Mostafa NZ, Hsu CY, Rose L, Kucharski C, Yan J, Jiang H, Uludag H. Modification of human BMSC with nanoparticles of polymeric biomaterials and plasmid DNA for BMP-2 secretion. J Surg Res 2013;183(1):8-17.